U.PORTO

DOUTORAMENTO

CIÊNCIAS BIOMÉDICAS

Phenotypic Variability in Familial Amyloid Polyneuropathy: TTR modifiers in *Caenorhabditis Elegans* and Human Models.

Miguel Alves Ferreira

D

2019

U.PORTO

Miguel Alves Ferreira. Phenotypic Variability in Familial Amyloid Polyneuropathy: TTR modifiers in *Caenorhabditis Elegans* and Human Models.

Phenotypic Variability in Familial Amyloid Polyneuropathy: TTR modifiers in *Caenorhabditis Elegans* and Human Models.

Miguel Alves Ferreira

D.ICBAS **2019**

INSTITUTO DE CIÊNCIAS BIOMÉDICAS ABEL SALAZAR

D 2019

U.PORTO

INSTITUTO DE CIÊNCIAS BIOMÉDICAS ABEL SALAZAR
UNIVERSIDADE DO PORTO

PHENOTYPIC VARIABILITY IN FAMILIAL AMYLOID POLYNEUROPATHY: TTR MODIFIERS IN *CAENORHABDITIS ELEGANS* AND HUMAN MODELS.

Doctoral program in Biomedical Sciences

IBMC INSTITUTO DE BIOLOGIA MOLECULAR E CELULAR
INSTITUTE FOR MOLECULAR AND CELL BIOLOGY

3S

UniGENe IBMC

The Scripps Research Institute

centro hospitalar do Porto

ICBAS

U.PORTO

MIGUEL FERNANDO ALVES FERREIRA

PHENOTYPIC VARIABILITY IN FAMILIAL AMYLOID POLYNEUROPATHY: TTR MODIFIERS IN *CAENORHABDITIS ELEGANS* AND HUMAN MODELS.

Tese de Candidatura ao grau de Doutor em Ciências Biomédicas submetida ao Instituto de Ciências Biomédicas Abel Salazar da Universidade do Porto.

Orientador – Prof. Doutora Carolina Luísa Cardoso Lemos

Categoria – Professora Auxiliar Convidada

Afiliação – Instituto de Ciências Biomédicas Abel Salazar da Universidade do Porto.

Co-orientadora – Prof. Doutora Alda Maria Botelho Correia de Sousa

Categoria – Professora Associada com Agregação

Afiliação – Instituto de Ciências Biomédicas Abel Salazar da Universidade do Porto.

Co-orientadora – Prof. Doutora Sandra Encalada

Categoria – Assistant Professor

Afiliação – The Scripps Research Institute (TSRI)

Porto, 2019

Financial support

This study was supported by Fundação para a Ciência e Tecnologia, FCT, (PTDC/SAU-GMG/100240/2008) and PEsT, co-supported by ERDF and COMPETE, and by Financiamento Plurianual de Unidades de Investigação and through a PhD grant (SFRH/BD/101352/2014) financed by Programa Operacional and União Europeia.

"Sou incapaz de dar respostas
às minhas interrogações,
exatamente porque sou
um homem de interrogações."

Corino de Andrade

ACKNOWLEDGMENTS/AGRADECIMENTOS

"*Se vi mais longe foi por estar de pé sobre ombros de gigantes.*" (Isaac Newton)

Quero agradecer a todas as pessoas que cientificamente e/ou pessoalmente me ajudaram a ver mais longe.

À Prof. Doutora Carolina Lemos, por desde sempre ter confiado em mim e apoiado todos aqueles momentos em que eu surgia com “Tive uma ideia! Acho que podíamos…”. Pela orientação, incentivo e por mostrar o quão prazeroso é trabalhar em equipa. Gratidão!

À Prof. Doutora Alda Sousa, um agradecimento muito especial, por toda a dedicação, racionalidade e partilha de conhecimentos demonstrada ao longo destes anos. Pelos conselhos tão imparciais e assertivos, sempre na altura certa.

Ao Professor Jorge Sequeiros, por me ter aceitado desde início no seu grupo e continuar a apoiar os meus projetos. Pelas sábias correções e questões pertinentes que tem feito aos meus trabalhos.

To Professor Sandra Encalada, thank you for welcoming me in your great lab and for everything you taught me about *C. elegans*. Your advice and support were very helpful to complete part of my graduate work.

To Professor Jeffery Kelly, for the valuable collaboration, and for many insightful discussions and suggestions about amyloidosis. I also immensely appreciated the very kind and warm welcome to San Diego.

À Dra. Teresa Coelho, por ter proporcionado as colaborações e fornecido muito do material que ajudaram a que esta tese fosse possível. Obrigado pelas interessantes e motivadoras reuniões e por ter partilhado tanto do seu excecional conhecimento sobre a PAF.

À Prof. Doutora Isabel Alonso, pela disponibilidade e apoio neste projeto e por me ter transmitido muitas das minhas bases científicas.

À Doutora Diana Santos, pela constante disponibilidade e ajuda. Pelo companheirismo neste mundo da PAF em que tantas histórias hilariantes partilhámos.

À Dra. Ana Azevedo, pela estima, dedicação e contributo neste trabalho.

Aos meus colegas da UnIGENe, Conceição, João, Sara, Marlene, Mariana, Joana, Cátia e Andreia, por todos os conselhos, amizade, pela prontidão em ajudar, boa disposição, e essencialmente por criarem um bom ambiente no laboratório.

Aos meus colegas do CGPP, Ana Brandão, Ana Margarida, Rita, Patrícia, Susana, Paulo, Milena, Andreia e Victor, pela colaboração e ajuda ao longo destes anos.

To Encalada Lab: Diana, Phil, Romain, George, Kayal and Shirley for their excellent team spirit and for making me feeling comfortable. I would like to specially mention Erin and Nirvan for your tremendously help, support and friendship.

À Doutora Cecília Monteiro, por toda a amizade, encorajamento e constante cuidado.

To everyone in Petrascheck, Wiseman and Kelly laboratories, for their support and assistance.

À equipa da Unidade Corino de Andrade – CHP, pela disponibilidade e auxílio na recolha dos dados/amostras. Um especial agradecimento à Marta e à Vanessa, pela boa disposição e recetividade aos meus pedidos.

Aos doentes e familiares, que foram imprescindíveis neste projeto.

Aos meus Amigos, que durante estes anos compreenderam as minhas ausências e pelos desabafos e pelas tantas conversas não-científicas que me ajudavam a “desligar”.

À Bárbara e Família, pelas palavras de ânimo, carinho, cuidado constante e motivação. Bem hajam!

Aos meus Pais, pelo amor, alegria e apoio incondicional em tudo o que faço. Grato pela educação que também permitiu que esta tese fosse possível.

Agradeço também à Fundação para a Ciência e a Tecnologia (FCT) a atribuição da bolsa de doutoramento SFRH/BD/101352/2014 e à Amyloidosis Foundation e à Pfizer o apoio nos projetos.

Agradeço ao Instituto de Ciências Biomédicas de Abel Salazar (ICBAS); ao Instituto de Biologia Molecular e Celular (IBMC) - Instituto de Investigação e Inovação em Saúde (i3S) e ao The Scripps Research Institute por terem proporcionado as condições essenciais ao desenvolvimento desta tese.

TABLE OF CONTENTS

Publications I
Abbreviations II
Abstract VI
Sumário VIII
INTRODUCTION 1
Transthyretin familial amyloid polyneuropathy (TTR-FAP) 5
History of FAP: Major Milestones 5
Genetic Scenario 6
Epidemiology 8
Transthyretin Biochemistry 9
Transthyretin Aggregation 10
TTR Partners 11
Symptomatology 13
Age-at-onset (AO) 15
Genetic Modifiers 17
Origin 19
Misdiagnosed/ Mimicking neuropathies 19
Treatment 19
Animal Models 22
MAIN OBJECTIVES 25
Specific Objectives 27
GENERAL METHODS 29
RESULTS 35
Article 1: Beyond TTR Val30Met: potential regulatory variants associated with age-at-onset in familial amyloid polyneuropathy 38
Article 2: A *trans*-acting factor may modify age-at-onset in familial amyloid polyneuropathy ATTRV30M in Portugal 56
Article 3: Large anticipation of genetic TTR Familial Amyloid Polyneuropathy Val30Met: *MYH11* gene as a putative modulator 80
Article 4: Cellular Clearance of Circulating Transthyretin Decreases Cell Non-Autonomous Proteotoxicity in *Caenorhabditis elegans* 100
Article 5: Genetic Modulators of Transthyretin Amyloid Disease Toxicity in *Caenorhabditis elegans* models of Familial Amyloid Polyneuropathy (FAP). 164
DISCUSSION 185
TTR gene sequencing - At the heart of the matter 187
From alleles to haplotypes - Broadening the field of view 190

TTR (post-) transcriptional regulation – *In silico* Analysis 191
MYH11 - Thinking outside the (TTR) box 196
C. elegans models of TTR-FAP 198
R193.2 a suppressor of TTR 201
Intertwining these approaches 203
Future Relevance 204
CONCLUSION 205
FUTURE PERSPECTIVES 209
REFERENCES 213

PUBLICATIONS

Results already published or in preparation were used in this thesis, as described below:

Article 1: **Alves-Ferreira M**, Azevedo A., Coelho T, Santos D, Sequeiros J, Alonso I, Sousa A, Lemos C. Beyond TTR Val30Met: potential regulatory variants associated with age-at-onset in familial amyloid polyneuropathy. (Submitted)

Article 2: **Alves-Ferreira M**, Coelho T, Santos D, Sequeiros J, Alonso I, Sousa A, Lemos C. A *Trans*-acting Factor May Modify Age at Onset in Familial Amyloid Polyneuropathy ATTRV30M in Portugal. Mol Neurobiol. 2018 May;55(5):3676-3683. doi: 10.1007/s12035-017-0593-4. Epub 2017 May 19. PMID: 28527106

Article 3: **Alves-Ferreira M**, Coelho T, Sequeiros J, Sousa A, Lemos C. Large anticipation of genetic TTR Familial Amyloid Polyneuropathy Val30Met: *MYH11* gene as a putative modulator. (in preparation)

Article 4: Madhivanan K, Greiner ER, **Alves-Ferreira M**, Soriano-Castell D, Rouzbeh N, Aguirre CA, Paulsson JF, Chapman J, Jian X, Ooi FK, Lemos C, Dillin A, Prahlad V, Kelly JW, Encalada SE. Cellular Clearance of Circulating Transthyretin Decreases Cell Non-Autonomous Proteotoxicity in *Caenorhabditis elegans*. Proc Natl Acad Sci U S A. 2018 Jul 30. pii: 201801117. doi: 10.1073/pnas.1801117115. Epub ahead of print PMID:30061394.

Article 5: **Alves-Ferreira M**, Lowry J., Bowerman B., Encalada SE. Genetic Modulators of Transthyretin Amyloid Disease Toxicity in *Caenorhabditis elegans* models of Familial Amyloid Polyneuropathy (FAP). (in preparation)

ABBREVIATIONS

AD	Alzheimer's disease
ALS	Amyotrophic lateral sclerosis
AO	Age-at-onset
ApoA-I	Apolipoprotein A-1
APOE	Apolipoprotein E
APP	Amyloid precursor protein
ASO	Antisense oligonucleotide
ATTRm	Mutant transthyretin amyloidosis
ATXN2	Ataxin-2
Aβ	Amyloid-β
BLAST	Basic Local Alignment Search Tool
bp	Base pairs
BWA	Burrows-Wheeler Aligner software
C1Q	Complement, serum
CADD	Combined Annotation Dependent Depletion
CGC	Caenorhabditis Gene Center
CGPP	Centro de Genética Preditiva e Preventiva
CHP	Centro Hospitalar do Porto
CI	Confidence Intervals
CIDP	Chronic inflammatory demyelinating polyneuropathy
CMPD5	Compound 5
CMT1	Chronic idiopathic axonal polyneuropathy
CNPD	National Commission for Data Protection
CSF	Cerebrospinal fluid
DIC	Differential Interference Contrast microscopy
dNTPs	Deoxynucleotides
DPD	3,3-diphosphono-1,2-propanodicarboxylic acid
dsRNA	double-stranded RNA
DT-A	Diphtheria toxin
ECM	Extracellular matrix
EGFP	Enhanced green fluorescent protein
EMA	European Medicines Agency
EMS	Ethyl Methanesulfonate
ER	Endoplasmic reticulum
ERAD	Endoplasmic Reticulum-Associated Degradation
ESSE	Exonic splicing enhancer
et al.	*et alii*
EV	Empty Vector
ExAC	Exome Aggregation Consortium
FAC	Familial amyloid cardiomyopathy
FAP	Familial amyloid polyneuropathy

FCT	Fundação para a Ciência e Tecnologia
FUDR	5-fluoro- 2´-deoxyuridine
GEE	Generalized estimating equations
GI	Gastro-intestinal
gnomAD	Genome Aggregation Database
GTEx	Genotype-Tissue Expression database
HD	Huntington's disease
HDL	High-density lipoprotein
HGVS	Human Genome Variation Society
HNF	Hepatocyte nuclear factor
HNF4G	Hepatocyte nuclear factor 4 gamma
HSA	Hospital Santo António
HSF1	Heat shock transcription factor 1
HSPB1 or HSP27	Heat shock protein family B (small) member 1
HSR	Heat-Shock Response
hTTR	human Transthyretin
IF	Immunofluorescence
IGV	Integrative Genomics Viewer
IRIDA	Iron-Refractory Iron Deficiency Anemia
kb	Kilobases
kDa	Kilodalton
LB	Luria-Bertani
LD	Linkage Disequilibrium
LDL	Low-density lipoprotein
M	Monomeric
MAF	Minor Allele Frequency
MEK1/2	ERK1/2 kinases
MIDAS	metal ion-dependent adhesion site
mRNA	Messenger RNA
mtDNA	Mitochondrial DNA
NGAL	Neutrophil gelatinase-associated lipocalin
NGM	Nematode Growth Media
NN	Non-Native
OR	Odds Ratios
PCR	Polymerase Chain Reaction
PD	Parkinson's disease
pmp-3	plasma membrane protein 3
PPI	Protein-protein interaction
RBP	Retinol binding protein
RBPA	Retinol Binding Pre-Albumin
rec	Recombinant
RFLP	Restriction fragment length polymorphism
RNAi	RNA interference

ROCK2	Rho activated coiled Coil protein Kinase 2
rpl-6	ribosomal protein L6
RT-PCR	Reverse Transcriptase - Polymerase Chain Reaction
SAP	Shrimp Alkaline Phosphatase
SC35	Serine/arginine-rich splicing factor
SD	Standard deviation
SF2/ASF	pre-mRNA-splicing factor SF2/alternative splicing factor
SIFT	Sorting Intolerant from Tolerant
siRNA	Small interfering RNA
SMMHC	Smooth muscle myosin heavy chain
SNP	Single Nucleotide Polymorphim
SR	Serine and arginine-rich
SRp40	Splicing factor, arginine/serine rich 40 kDa
Srp55	Splicing factor, arginine/serine rich 55 kDa
SS	Signal Sequence
STRING	Search Tool for the Retrieval of Interacting Genes/Proteins
sttr	suppressors of TTR
SUMO	Small Ubiquitin-related MOdifier
T4	Thyroxine
TAAD	Thoracic Aortic Aneurysm
TBPA	Thyroxine Binds Pre-Albumin
TF	Transcription factor
TFBS	Transcription factor binding site
TTR	Transthyretin
TTR-FAP	Transthyretin-familial amyloid polyneuropathy
TUDCA	Tauroursodeoxycholic acid
UCA	Unidade Corino de Andrade
Unc	Uncoordinated
UPLC	Ultra-Performance Liquid Chromatography
UTR	Untranslated region
V30M	Val30Met
VUS	Variant of uncertain/unknown significance
VWA	von Willebrand A domain
WES	Whole-exome sequencing
WGS	Whole-genome sequencing
WT	Wild-type
ΔSS	without the Signal Sequence

ABSTRACT

Transthyretin- (TTR) Familial amyloid polyneuropathy (FAP) is an autosomal dominant amyloidosis that presents as a progressive sensorimotor and autonomic polyneuropathy, due to a Val30Met disease-causing variant in *TTR* gene with death occurring within a decade of symptom onset.

Variability in age-at-onset (AO) and in clinical presentation is present in Val30Met TTR-FAP, showing a remarkably wide variation in AO (19-82 years) in Portuguese patients. However, early (AO <40 years) and late-onset cases (AO ≥50) are not separate entities and coexist in the same family. In a recent study, our group confirmed anticipation as a true biological phenomenon in these families, where late-onset cases often had offspring with early-onset, but the reverse never occurred: that 'protection' may be lost in just one generation. This raised the hypothesis of a closely linked modifier. Furthermore, it is not still clear whether TTR interactions with other proteins play a significant role in proteotoxicity, or whether such interactions could also provide protective effects in neurons.

The central idea of this thesis was to identify molecular mechanisms intertwined with genetic modifiers in human and animal models that are associated with phenotypic variability. This thesis focused on two principal strategies: (I) to understand the mechanisms that influence AO, concentrating the study in families; and (II) to identify modifiers of TTR proteotoxicity using a Val30Met TTR-FAP animal model.

Resorting to the largest cohort of Val30Met TTR-FAP patients worldwide, first, several variants were identified associated with AO variability in the promoter, coding and intron / exon boundaries of the *TTR* gene. Their putative effect was then studied through an extensive *in silico* study which disclosed significant alterations in the mechanism of splicing, transcription factors binding and miRNAs binding.

Second, by a haplotype study, a possible modulatory effect on AO was unraveled, exerted by a significant *trans*-factor more frequent in early than in late-onset cases, reinforcing the genetic role of the non-carrier parent in AO modulation.

Third, whole-genome sequencing was applied in two nuclear families with 3 generations where the decrease in AO is evident between parents-offspring pairs, showing a large anticipation (>10 years), resulting in a difference of ≈ 40 years in AO of the grandmother to the grandchild. *MYH11* was identified as a modifier candidate gene. *MYH11* gene encodes a component of a

myosin protein, which was undoubtedly found to be involved in a protein-protein interaction network with TTR.

In addition, *Caenorhabditis elegans* models of FAP were generated and characterized, which expressed different human *TTR* variants that recapitulate critical features of human FAP disease, including impairment in locomotion and nociception impairment.

Then, using this TTR-FAP animal model, a suppressor of TTR toxicity was uncovered from a forward genetic screen followed by whole-genome sequencing. The phenotypes that were modulated from this candidate gene and the pathways involved in TTR toxicity were investigated *in vivo* in the Val30Met TTR-FAP model.

The results obtained with this thesis revealed new genetic modulators and pathways of TTR proteotoxicity, including those that might regulate AO mechanisms in TTR amyloidosis. In conclusion, with this work we have shown that TTR-FAP is affected by numerous genomic factors that are either nearby or physically separated from the disease-causing variant. Some of these factors are located in the TTR *locus* and may affect the expression levels and/or TTR function; other genes directly or indirectly cross the TTR-related pathways.

Elucidating TTR proteotoxic pathways and mechanisms of AO variability in FAP may have clear clinical implications, helping clinicians in identifying early-onset families at risk and to diagnose them early, when modifying treatments can be implemented with greater success. FAP patients with this rare and debilitating genetic disease urgently need more effective therapies. Importantly, an increased awareness of the factors that impact AO in FAP patients may well contribute to a better understanding of the pathogenic mechanisms of more common neurodegenerative states such as Alzheimer’s and Parkinson’s disease, with which FAP shares some common features.

SUMÁRIO

A Polineuropatia Amiloidótica Familiar (PAF) associada à Transtirretina (TTR), vulgarmente conhecida como “Doença dos pezinhos” ou paramiloidose, é uma amiloidose autossómica dominante que apresenta uma polineuropatia progressiva sensitivo-motora e autonómica devido a uma variante-causal no gene da *TTR*, levando à morte numa década após o início dos sintomas.

A variabilidade na idade de início dos sintomas (ii) e na apresentação clínica está bem presente na TTR-PAF Val30Met, ocorrendo numa grande amplitude de idades (19-82 anos) em doentes portugueses.

Contudo, casos precoces (ii <40 anos) e tardios (ii ≥50) não são entidades separadas e coexistem na mesma família. Num estudo recente, o nosso grupo confirmou a antecipação como um verdadeiro fenómeno biológico nestas famílias, onde os casos de início-tardio frequentemente tiveram filhos com início-precoce, mas o inverso nunca ocorreu: a “proteção” pode ter sido perdida em apenas uma geração; o que levantou a hipótese da existência de um modificador ligado ao gene. Além disso, não está ainda claro se as interações da TTR com outras proteínas desempenham um papel significativo na proteotoxicidade ou se essas interações também podem providenciar efeitos protetores nos neurónios.

A ideia central desta tese foi identificar mecanismos moleculares interligados com modificadores genéticos, em modelos humanos e animais, que estão associados à variabilidade fenotípica. Esta dissertação focou-se em duas estratégias principais: (I) compreender os mecanismos que influenciam a ii, concentrando o estudo em famílias, e (II) identificar modificadores da proteotoxicidade da TTR, usando um modelo animal TTR-PAF Val30Met.

Recorrendo à maior coorte mundial de doentes TTR-PAF Val30Met:

Primeiro, foram identificadas diversas variantes no promotor associadas à variabilidade na ii, nas regiões codificantes e nos limites intrão/exão no gene da TTR. Os seus efeitos putativos foram então estudados através de um extenso estudo *in silico* que revelou alterações significativas nos mecanismos de *splicing*, ligação de fatores de transcrição e miRNAs.

Segundo, num estudo haplotípico foi revelado um possível efeito modulador na ii, exercido por um factor em *trans* significativo, mais frequente nos casos precoces que nos tardios, reforçando o papel genético do progenitor não-afetado na modulação da ii.

Em terceiro lugar, procedeu-se a um *whole-genome sequencing* em duas famílias nucleares com 3 gerações, onde o decréscimo na ii é evidente entre os pares pais-filhos, mostrando uma grande antecipação (>10 anos), resultado numa diferença de ≈ 40 anos na ii da avó para os netos. O gene *MYH11* foi identificado como um gene candidato modificador, codificando uma componente da proteína miosina, estando indubitavelmente envolvido na rede de interações proteína-proteína com a TTR.

Além disso, foram gerados e caracterizados modelos de PAF em *Caenorhabditis elegans* que expressam diferentes variantes da TTR humana e sintetizam características fundamentais da PAF humana, incluindo alterações na locomoção e na nocicepção.

Posteriormente, usando este modelo animal TTR-PAF, foi identificado um supressor da toxicidade da TTR num *forward genetic screen*, seguido de *whole-genome sequencing*. Foram investigados em modelos TTR-PAF Val30Met *in vivo* os fenótipos que foram modulados por este gene candidato e as vias envolvidas.

Os resultados obtidos com esta tese revelaram novos genes moduladores e vias da proteotoxicidade da TTR, incluindo aqueles que podem regular os mecanismos da ii na amiloidose da TTR. Em conclusão, com este trabalho demonstrámos que a TTR-PAF é afetada por inúmeros fatores genéticos que estão próximos ou fisicamente separados da variante-causal da doença. Alguns desses fatores estão localizados no *locus* da TTR e podem afetar os níveis de expressão e/ou a função da TTR; outros genes diretamente ou indiretamente cruzam as vias relacionadas com a TTR.

Clarificar as vias de preotoxicidade da TTR e os mecanismos da variabilidade da ii na PAF pode ter claras implicações clínicas, ajudar os clínicos na identificação de famílias em risco de início precoce e a diagnosticá-las precocemente, quando os tratamentos modificadores podem ser implementados com maior sucesso. Os doentes PAF com esta doença genética rara e debilitante necessitam urgentemente de terapias mais eficazes. É importante realçar que uma maior consciencialização dos fatores que afetam a ii em doentes PAF pode contribuir para um melhor conhecimento dos mecanismos patogénicos dos estados neurodegenerativos mais comuns, como a doença de Alzheimer e de Parkinson, com os quais a PAF partilha algumas características semelhantes.

INTRODUCTION

In the past decades, with access to DNA information, a large number of genetic variants have been discovered. These variants affect the coding region of a single gene, are mostly responsible for a genetic disease – monogenic disorders. These disease-causing genetic variants (formerly known as mutations) are transmitted over the generations and, in cases of dominance, one copy of the altered gene pair is sufficient to manifest the disease. The traditional process of linking monogenic disease phenotypes to a genotype is an oversimplification. Nowadays it has been clear that the genotype at a single *locus* rarely predicts the full phenotype, where variations in different genes can lead to similar phenotype defects and, also on the contrary, a single gene has been implicated in different phenotypes. Thus, other genetic factors may exist and exert an effect on the primary genotype on phenotype expression.

Multifactorial phenotypes are caused by a combination of *de novo* and inherited variants in multiple *loci*, often acting together with environmental factors (e.g. diet, climate). However, there is still a substantial gap in the factors known to contribute to phenotypic heterogeneity and disease presentation. Monogenic diseases provide an excellent opportunity to study phenotypic variability as they have, in many cases, uniform etiology (same affected gene and the same disease-causing variant), familial clustering and detailed and recognized phenotyping of affected individuals.

Familial Amyloid Polyneuropathy (FAP)

An example of a monogenic disorder is Familial Amyloid Polyneuropathy (FAP). FAP is an umbrella of familial diseases that present amyloid forms deposition mainly in the peripheral nerves. Subtypes are categorized depending on the type of protein composing the amyloid: apolipoprotein A-1 (ApoA-I), gelsolin and transthyretin (TTR).

Apolipoprotein A-I amyloidosis

Apolipoprotein A-I amyloidosis is a rare, autosomal dominant disorder caused by disease-causing variants in the *APOA1* gene. Approximately 20 disease-causing variants are associated with the hereditary form, 13 are missense, and the others are insertions/deletions[1]. *APOA1* gene encodes ApoA-I, a plasma protein synthesized by the liver and the small intestine that transports cholesterol from peripheral cells to the liver[2]. Clinically, is characterized by polysystemic manifestations with predominance in kidney and hepatic disease with onset in the fourth decade of life. However, there is a strong association of protein regions where disease-causing variants lie: if it is in the residues

1–75 the patients mainly suffer from hepatic and renal amyloidosis, whereas disease-causing variants that are located in codons 173–178 cause amyloidosis of the heart, larynx, and skin[3]. Currently, the available treatments are limited to hemodialysis and hepatorenal transplantation.

Gelsolin amyloidosis

Gelsolin amyloidosis also known as Familial amyloid neuropathy type IV is a rare, autosomal dominant disorder cause by G654A (p.Asp187Asn) or G654T (p.Asp187Tyr) variants in gelsolin gene[4]. The substitution of aspartate at position 187 in the gelsolin protein to an asparagine or tyrosine, respectively, lead to gelsolin fragment formation and amyloidogenesis. The extracellular amyloid deposits occur at ocular, neural, and cutaneous level. The age-at-onset (AO) is usually after the third decade of life with secondary lattice lines in corneal stroma, progressive cranial and peripheral neuropathy, and cutis laxa[5]. Finland has the highest prevalence of the disease, often known as the Finnish type. Although a specific treatment it is not yet available, solutions for these patients undergo symptomatic treatment and good ophthalmological care[4].

Transthyretin (TTR)-FAP

Transthyretin familial amyloid polyneuropathy (TTR-FAP) is an autosomal dominant amyloidosis that presents as a progressive sensorimotor and autonomic polyneuropathy, due to disease-causing variants in the *TTR* gene with death occurring within a decade of symptom onset. It is by far the most common and life-threatening type of amyloidosis, which was the main focus of this thesis and which will be described in more detail below.

Transthyretin familial amyloid polyneuropathy (TTR-FAP)

Although the "amyloid" term was brought in the scientific literature in 1838 to describe "a normal amylaceous constituent in plants"[6], it was in 1854 the first time applied it in the medical literature[7] to describe small round deposits in the nervous system.

About one century later, TTR-FAP was first recognised as a disease by Professor Corino de Andrade[8], opening a new field of medical and laboratory research and discoveries until the present day.

In the last 60 years much has been discovered about this new clinical entity, from gene to the causal variant. However, in these last few years there was a major interest for new treatments as this disease still has no cure and many of the phenotypic manifestations continue to be explained.

History of FAP: Major Milestones

1838 – Matthias Schleiden coined the term "amyloid".

1842 – von Rokitansky wrote the first pathological descriptions of amyloid.

1875 - André-Victor Cornil, Richard Heschl and Rudolph Jürgens independently reported the use of aniline dyes in the recognition of amyloid.

In 1906 - Alois Alzheimer described "senile" plaques and neurofibrillary tangles in a demented patient, later named Alzheimer's disease.

1922 – Hermann Bennhold introduced the use of Congo red as a specific stain for the detection of amyloid.

1929 – De Bruyn and Stern described the first clinical picture of what would come to be known as familial amyloid polyneuropathy.

1938 – De Navasquez and Treble reported one of the earliest descriptions of amyloid neuropathy.

1939 – Américo Graça, a physician from Póvoa de Varzim, sent a woman to Dr. Corino with a disease known in the region by "Doença dos pézinhos" (foot disease).

1942 – Kabat et al, discovered for the first time transthyretin (formerly Prealbumin) in human cerebrospinal fluid (CSF) and Siebert and Nielson, found thransthyretin in human serum.

1943 – João Resende, Jorge Silva Horta e Corino de Andrade identified amyloid substance in tissues of a patient with FAP.

1952 – Corino de Andrade published for the first time the definition of the disease in the journal Brain, entitled: "A Peculiar Form of Peripheral Neuropathy; familiar atypical generalized

amyloidosis with special involvement of the peripheral nerves", which is until the present day the most cited Portuguese reference in international medical literature.

1958- Ingbar determined the TTR molecular mass of 55kDa and discovered TTR bind thyroid hormones.

1964 – P. E. Becker established the autosomal dominant inheritance.

1968 - Shukuro Araki described FAP in Japan and Kanai *et al.* characterized transthyretin as a retinol binding protein.

1969 – van Allen described Apolipoprotein A-1 amyloidosis and Jouko Meretoja described Hereditary Gelsolin Amyloidosis.

1970 – Rune Andersson described FAP in Umeå (northern Sweden).

1978 – Pedro Pinho Costa reported prealbumin (later called transthyretin) as the protein component of the amyloid fibrils that accumulate in tissues of patients with FAP.

1981 – Nomenclature Committee of the International Union of Biochemistry accepted Transthyretin as the official name.

1984 – Maria João Saraiva and Shukuro Araki identified an abnormal transthyretin caused by Val30Met mutation in Portuguese and Japanese FAP patients.

1988 – Alda Sousa and Luisa Lobato showed the familial aggregation of late-onset cases.

1991 – Gösta Holmgren introduced in Umeå (Sweden) liver transplantation as a therapy for FAP.

1992 – João Pena started at the Hospital Curry Cabral the liver transplantation for FAP in Portugal.

2003 – Jeffery W. Kelly published the chemical structure of Tafamidis, the first drug for FAP.

2011 – Tafamidis (Vyndaqel®; Pfizer Inc.) approved in Europe.

2013 – Diflunisal is repurposed for familial amyloid polyneuropathy.

2014 – Carolina Lemos *et al.* confirmed anticipation as a true biological phenomenon in TTR-FAP.

2018 – Novel therapeutic drugs were approved for the treatment of FAP: Patisiran (Onpattro™), the first small interfering RNA-based drug approved by the US Food and Drug Administration (FDA) and Inotersen (*TEGSEDI*™), an antisense oligonucleotide (ASO).

Genetic Scenario

The *TTR* gene is located on the long arm of chromosome 18 in the region 11.2-q12.1. This gene is approximately 6.9 Kb in length and contains a promoter, four exons and three introns[9]. Exon 1 encodes 23 amino acids of which 20 relate to the signal peptide.

Most of the TTR protein annotations in the literature are in accordance with the old nomenclature, which considered the mature protein after signal peptide cleavage[10]. Nowadays, we have to shift 20 amino acids in the TTR protein annotations that correspond to the TTR-signal sequence.

Until now, there are 140 non-synonymous variants in the coding regions of the *TTR* gene registered in "Mutations in hereditary amyloidosis" database[11]. Furthermore, The Genome Aggregation Database (gnomAD), which collects genetic data from 125,748 exome sequences and 15,708 whole-genome sequences, comprises more than 250 genetic variants in the *TTR* gene (including the non-coding regions).

The most frequent amino acid substitution variant in gnomAD is p.Gly26Ser (also known as Serine6)[12]. Although it causes an amino acid change in TTR protein, this variant is not disease-causing[13]. As the variant arose in a CpG hotspot it may have arisen on multiple occasions[14].

The substitution of a threonine for methionine at position 139 (Thr119Met) is another non disease-causing change. However, this substitution seems to stabilize the TTR tetramer and, thereby confer a greater resistance to amyloid formation[15; 16]. Similarly, TTR Arg104His seems to be a non-causing change and with a protective role in TTR amyloidosis[17-19].

On the other hand, more than 120 variants are reported as amyloidogenic and have an associated phenotype (Figure 1)[11]. TTR Val30Met (NP_000362.1:p.Val50Met) is the most common disease-causing variant worldwide associated with hereditary TTR-FAP with polyneuropathy[20-22]. Identified in 1984 for the first time in Portuguese patients, this variant results from a guanine to an adenine substitution (rs28933979, c.148G>A) in the exon 2 of the *TTR* gene[23]. This substitution has serious consequences on the protein, notably it makes the TTR tetramer very unstable which results in the formation of amyloid deposits (mechanism described below)[24; 25].

The variants Asp18Gly (D18G) and Ala25Thr (A25T) are even more TTR destabilizing[26; 27]. These variants are associated to a central nervous system amyloidosis and both showed low or absence levels of TTR in serum and CSF of central nervous system amyloidosis patients, suggesting that there is an increased clearance within the cell[26; 27].

The Val122Ile variant leads to the vast majority of hereditary TTR amyloidosis with cardiomyopathy (also known as Familial amyloid cardiomyopathy (FAC))[21; 28]. This is the most common variant in United States and is strongly associated with African American individuals[28]. This variant has nearly equivalent tetramer stabilities as wild-type (WT) form (also responsible for a cardiac phenotype)[25; 29].

In addition to the compound heterozygosity (e.g. Thr119Met/Val30Met), there are also variants in homozygosity (e.g. Val30Met[30-32] and Val122Ile[33]). Interestingly, the double genetic dosage of TTR Val30Met homozygous carriers does not appear to make them clinically different from those in heterozygosity, nor is it sufficient to trigger the disease[30; 31].

It is important to understand the role of WT TTR which, despite not suffering any alteration in the amino acid structure of the protein, is responsible for a cardiac form of TTR disease known as Wild-type ATTR (formerly as Senile Systemic Amyloidosis or senile cardiac amyloidosis)[34; 35]. Typically occurs in elderly men (over 60 years) with TTR amyloid deposits commonly in heart, albeit can be found throughout the body[34; 35].

Epidemiology

TTR Val30Met is the most common and almost the only TTR-FAP causing variant found in Portugal and represent 20-50% of the variants worldwide[3; 36]. Recently, the global prevalence of TTR-FAP was estimated to be around 10,000 persons (range 5,526–38,468)[37].

In Portugal, more than 99% of the affected families carry the TTR Val30Met variant, while other families carry the TTR Ser50Arg; TTR Ser52Pro and TTR Val28Met. These non-Val30Met variants are represented in 5 families in the inland of mainland Portugal, 1 family in central coast and seven families are from Madeira island[22].

Andrade looked for patients with the same clinical picture, examined their relatives and thus described the first cluster of the disease, an area in Northern Portugal centred and around the districts of Póvoa do Varzim and Vila do Conde, which remains the largest concentration of patients worldwide[38]. In 2018, Schmidt *et al.* estimated that the highest global prevalence of TTR-FAP is in Northern Portugal (1,631.20/1M) and Northern Sweden (1,040.00/1M)[37]. Moreover, in 2016 Inês *et al*., using the reference centers databases in Portugal as a source for prevalence estimates, reported that Portugal has the highest country estimate of 22.93/100,000 adult inhabitants, where 71 new patients yearly are diagnosed[36]. Importantly, the prevalence for Póvoa de Varzim/Vila do Conde is currently 176.01/100,000 adult inhabitants which represents an increase of 16% over the last 25 years[36; 38].

Thus, although TTR-FAP it is considered a rare disease, it is very prevalent in some clusters, as in 19 municipalities in Portugal (in Europe the threshold is established in <5/10,000 persons)[36].

Transthyretin Biochemistry

TTR gene encodes the transthyretin protein of 127 amino acids, originally named pre-albumin because it migrates faster than albumin on agarose gel electrophoresis. However, it has no structural relationship to albumin. It is mainly synthesized in liver but also in the choroid plexus[39], retinal pigment epithelium[40], kidney[41] and pancreas [42; 43].

TTR is a homotetramer with 55kDa comprising four identical monomeric subunits. Each monomer contains eight β-strands and a helix between them; and in association with another monomer, it forms a dimer. When two dimers associate the final tetrameric conformation is formed, becoming fully functional[44]. TTR contains two identical T4-binding sites where T4 is attached and transported T4 and four binding sites for retinol binding protein (RBP), forming itself a complex with retinol (vitamin A). This is how transthyretin gained its name*:* transports thyroxine and retinol[45]. T4 is a major form of thyroid hormone primarily responsible for regulation of metabolism and brain development[46]. In the plasma, where TTR is a relatively abundant protein (secreted by liver), most of TTR does not bind to RBP and only transports 15-20% of T4[47; 48]. On the other hand, in the CSF (secreted by choroid plexus) TTR transport 80% of T4[49]. But, the absence of TTR does not prevent the transport of T4 in the brain, suggesting that there are other compensatory mechanisms[50]. TTR is also involved in nerve physiology, namely in the process of peripheral nerve regeneration, after injury[51]; in the biology of lipoproteins (LDL and HDL), through the binding to ApoA-I[52]; as a neuroprotective molecule in Alzheimer's disease (AD)[53] and cerebral ischemia[54]; in the maintenance of memory capacities and normal cognitive process during aging, through its ability to regulate brain retinoid availability and[55]; as an assessment protein in nutrition status, inflammation and bacterial infection, since plasma TTR levels are altered under these clinical conditions settings[56].

Another important role of TTR is in the pathogenesis of AD and it has been for some time the study of many researchers. In 1982, TTR were identified in the neurofibrillary tangles as well as in neuritic plaques and in the microangiopathy in AD patients' brains [57]. Afterwards, TTR was found to be one of the major amyloid-*β* (Aβ) peptide binding protein in the CSF (jointly with ApoE and clusterin), forming stable complexes with Aβ thus preventing the formation of amyloid - the AD hallmark[58; 59]. It was also found that the mean TTR levels in AD patients were reduced in CSF and plasma[60; 61]. These facts, have led several researchers to study TTR as modulator of the mechanisms of AD, developing several transgenic animal models, such as rodent, flies and worm models [62].

Transthyretin Aggregation

Aggregation of TTR causes TTR amyloidosis. Under the amyloid-forming conditions, native TTR tetramer (a dimer of dimers) dissociates into monomers which misfold and eventually grow into insoluble fibrillar structures, amyloid[63-66] (Figure 4). Distinct patterns of amyloid fibrils have been reported: a full-length TTR form and C-terminal TTR fragments ranging from residues 46–127 to 55–127[67; 68]. The residue 49–127 C-terminal fragment is a major component of *ex vivo* TTR amyloid fibrils[68; 69]. When amyloid fibrils contain a mixture of fragmented and full-lenght forms, it is termed Type A; and if are composed only by the full-length form, it is termed Type B[70]. The correlation between the types of TTR fibrils and phenotype has been proposed[70]. In the following Table 1 is shown the most common phenotype for each type of fiber.

Table 1- Main characteristics of type A and B fibrils.

Fibrils Type	A	B
Composition	Full-Length + C-terminal fragments	Only Full-Length
Val30Met	Late-onset mixed phenotype	Early-onset neuropathic
Other Variants	Majority of non-Val30Met; only in TTR WT	Few Non-Val30Met
DPD scintigraphy	Uptake	No uptake
Congo red staining	Low affinity	High affinity

DPD: 3,3-diphosphono-1,2-propanodicarboxylic acid

It is a fact that, amyloid fibrils themselves induce tissue damage, albeit we cannot forget the cytotoxic role of other lower molecular mass oligomeric species and with these aggregation-prone species extensive native-like structures are retained with them[71-73].

The quality control machinery of the cell protects more from forms of amyloid, with highly destabilized TTR variants being detected and degraded by the endoplasmic reticulum (ER) quality control system before secretion, while others are secreted and escape the clearance mechanisms[74].

Although the WT form itself destabilize the native TTR tetramer and forms amyloid, some amino acid changes in the protein were shown to energetically (kinetically or thermodynamically) accelerate the dissociation of the tetramers into partially unfolded species, which is the rate-determining step in TTR amyloid formation process[25]. These forms of amyloid deposit extracellularly and impair organ function.

Amyloid deposits in peripheral and autonomic nerves; cardiac tissue and leptomeninges, result in the cardinal signals that are denominated as the major clinical syndromes: FAP, FAC and leptomeningeal amyloidosis, respectively[75]. But amyloid deposits are usually multisystemic, not specific to a disease-causing variant or clinical syndrome. For instance, TTR Val30Met patients besides the deposits in peripheral and autonomic nerves also have prominent deposits in the heart, thyroid gland, gastrointestinal tract, pancreas, adrenal gland, kidney, skin and eyes (Figure 1)[76-78].

Likewise, WT TTR aggregates are not organ specific, although they primarily deposit in the heart, lungs, blood vessels, kidneys and carpal tunnel are affected too[79; 80].

Despite the tremendous advances to unravel the process of TTR misfolding and amyloid formation, detailed molecular mechanisms and tissue-specific deposition pathways remain partially unknown[81].

TTR Partners

While TTR amyloid cascade and symptomatology have been well characterized, the molecular interacting partners are not fully defined. Since TTR discovery that its name has been modified according to its partners. More than a decade later, Ingbar *et al.* discovered for the first time that Thyroxine Binds Pre-Albumin, starting to call the TTR as TBPA[46]. In 1968, Kanai *et al.* characterized TTR as a retinol binding protein and TTR became Retinol Binding Pre-Albumin (RBPA) [82]. RBP and retinol exist in the circulation bound as a ternary complex to TTR; TTR-RBP complex if formed within the ER of hepatocytes prior to secretion[83]. Later based on this interaction, Transthyretin became its official name. Furthermore, Sousa *et al.*, showed that TTR binds to megalin (a multiligand receptor) which is important for TTR renal uptake and the thyroid hormone homeostasis[84]. In the same way, sensory neurons also express megalin and TTR depends on its internalization for neuritogenic activity[85].

For years, scientists explored the role of TTR in AD after finding that TTR is the major Aβ binding protein[53; 86]. This binding is affected by the interaction of TTR with human metallothioneins, namely TTR-MT-2 decrease and TTR-MT-3 increase TTR-Aβ binding[**87; 88**]. In the plasma, around 1-2% of the TTR is carried in HDL, through binding to ApoA-I, forming the TTR-ApoA-I complex[52].

In addition to the aforementioned functions, it has been shown that TTR has a proteolytic activity[89]. Liz *et al.*, showed that TTR was able to cleave ApoA-I and neuropeptide Y (the major neuropeptide present in the mammalian brain) and that its proteolytic activity affects axonal growth[89; 90]. In contrast, TTR was identified as a substrate for DJ-1 protease and an inactive form of DJ-1 was secreted into the serum of FAP patients[91].

Recently, it was proposed that TTR interacts with δ subunit of GABAA receptors (expressed abundantly in the brain) and regulates their expression and function[92].

Additionally, several nonsteroidal anti-inflammatory drugs and natural polyphenols, such as curcumin[93]; genistein[94-96], epigallocatechin-3-gallate (the most abundant catechin of green tea)[97] and; resveratrol[98] have been found to bind TTR and inhibit the formation of amyloid fibrils[99].

Symptomatology

In general, Dr. Corino described this clinical entity as a "*Peculiar form of peripheral neuropathy; familiar atypical generalized amyloidosis with special involvement of the peripheral nerves*"[8]. Throughout the detailed and meticulous description, Dr. Corino characterized this multisystemic disease with paresis and early impairment of thermal and painful sensibilities (predominantly and beginning in the lower extremities), and gastro-intestinal; sexual and sphincter dysfunction[8]. Nowadays these characteristics remain a pathognomonic signs. illustrates the

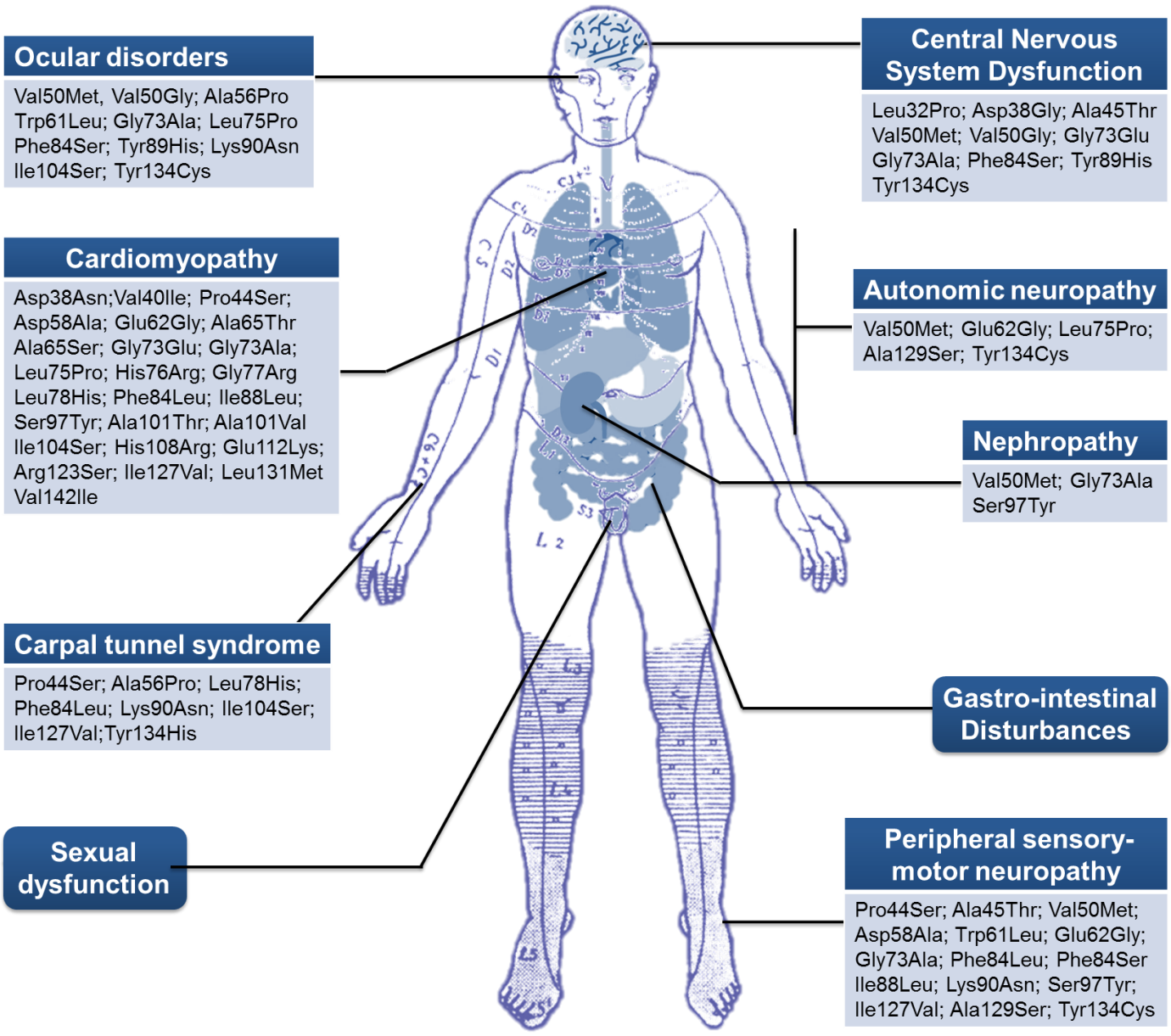

Figure 1 - TTR-FAP is a multisystemic disease in which different disease-causing variants contribute to the phenotype heterogeneity. Adapted from [75; 97; 98].

The Neuromuscular System

The main neurologic feature in TTR-FAP is a progressive sensorimotor and autonomic polyneuropathy with involvement of the small myelinated and unmyelinated nerve fibers[8; 100].

Usually, the loss of sensation begins in the feet and extends to proximal lower limbs, including numbness and spontaneous pain. Later, the sensory neuropathy spreads to the upper limbs and even the trunk as the disease progresses[101; 102]. Carpal tunnel syndrome may also arise in initial disease presentation[103]. Subsequently, larger myelinated sensory and motor nerve fibers become affected and symptoms of motor neuropathy appears leading to difficulties in walking and weakness[104].

Regarding patients' locomotion, the progression of the disease was divided into 3 stages according to Coutinho *et al.*[105]. In stage 1 symptomatic patients walk unassisted, and by stage 2 they can no longer walk unassisted (one or two sticks or crutches). Patients in stage 3 are confined to wheelchair or bedridden, which occurs after a mean of 10,4 years.

Autonomic Neuropathy

Autonomic neuropathy emerges at the beginning of the clinical manifestations, concomitantly with the sensory and motor deficits. Autonomic dysfunction presents as erectile dysfunction; neurogenic bladder; orthostatic hypotension and sweat abnormalities[102].

Patients also have a high prevalence of gastro-intestinal complaints, most commonly alternating between constipation and diarrhea, nausea, vomiting and delayed gastric emptying. These disturbances of gastro-intestinal motility leads to a severe loss of weight (a hallmark of this disease) and ultimately in cachexia[102]. Not as frequent is the involvement of the central nervous system which includes ataxia, spastic paralysis, dementia, stroke-like and focal neurological episodes[106; 107].

Cardiomyopathy

Cardiomyopathy is the result of TTR amyloid fibrils infiltration in myocardium, often with rhythm and conduction disturbances[102]. Heart failure with preserved ejection fraction is also characteristic for some forms of the disease[108]. Cardiac involvement is typical for older patients or may develop after the onset of neuropathy[108].

Other organs and systems

Albeit renal involvement being quite rare for some TTR variants, in TTR Val30Met Portuguese patients is not uncommon and all presented renal amyloid deposition, even in the absence of urinary abnormalities[109]. Microalbuminuria can be the first sign of clinical kidney

involvement and is premonitory of neuropathy[110]. Late-onset females' patients, low penetrance in the family, and cardiac dysrhythmias were shown to be risk factors for nephropathy[111].

Ocular manifestation represents another TTR-FAP clinical features, are associated with vitreous opacities derived from amyloid, and may lead to visual impairment. Abnormal conjunctival vessels, dry eye, pupillary abnormalities and glaucoma are equally common as ophthalmological manifestations and their prevalence increases with disease duration[77; 112-114]. Must be point out that this clinical picture is influenced by several factors as AO and gender[20].

Generally, complications such as cachexia, renal failure, infections or cardiac problems, lead to death 10 to 20 years after AO, without treatment[22].

With the increasing knowledge and as clinicians become more aware of this disease, several atypical phenotypes have been reported, especially for sporadic cases of non-clusters areas (i.e. scattered, frequently without family history, and late-onset)[115].

Age-at-onset (AO)

In 1952, Andrade first described TTR-FAP in Northern Portugal as a disease of the young adult ("*It begins insidiously in the second or third decade of life.*")[8]. Variation in AO between clusters and within the same focus has been described[38; 116-121]. Specifically, the differences in mean AO among the world's major TTR Val30Met clusters are: Portugal: 35,1; Brazil: 34,5; Sweden: 56,7; Balearic Islands: 45,7years; Japan: 35,3 years[38; 106]. Though the mean and shape distribution is considerable different among populations, the range is similar and very wide. In Portuguese Val30Met TTR-FAP families, AO shows a remarkable wide variation [19-82 years], and an increasing number of late-onset cases (AO ≥50 years), as well as asymptomatic carriers aged up to 95 years, have being ascertained[38].

Families where the proband (usually with a late-onset) had no affected parent at diagnosis have been increasingly ascertained (≈ 60 families in last decade)[122]. The portion of Portuguese late-onset cases incident increased 22%, increasing the proportion of late-onset cases to 28.7%[36]. Typically, these late-onset probands aggregate in families, often descending from parents who had died at old age with no signs of the disease or in some cases, these parents showed to be TTR Val30Met carriers with no symptoms as late as at 95 years of age[109; 122]. These families often come from geographical areas distinct from the typical clusters described. Although late-onset and aged asymptomatic carriers aggregate in families, it was also observed that in many families, "protective" factor(s) associated with late-onset may be lost in one generation, and offspring of late-onset cases often have an early-onset (AO <40 years).

Most importantly, it was found that early- and late-onset cases are not separate entities, they may coexist in the same family[38; 123]. Anticipation of AO (an early-onset in the offspring when compared to their affected late-onset parents) was found in Val30Met TTR-FAP families from Portugal (Figure 2), Sweden and Japan[116; 124-126]. Our group analysed 926 parent-offspring pairs with well-established AO and found that women had a statistically significant higher AO than men, either for daughters *vs.* sons or mothers *vs.* fathers. Furthermore, mother-son pairs showed a larger anticipation (>10 years) while the father-daughter pairs showed only residual anticipation[127].

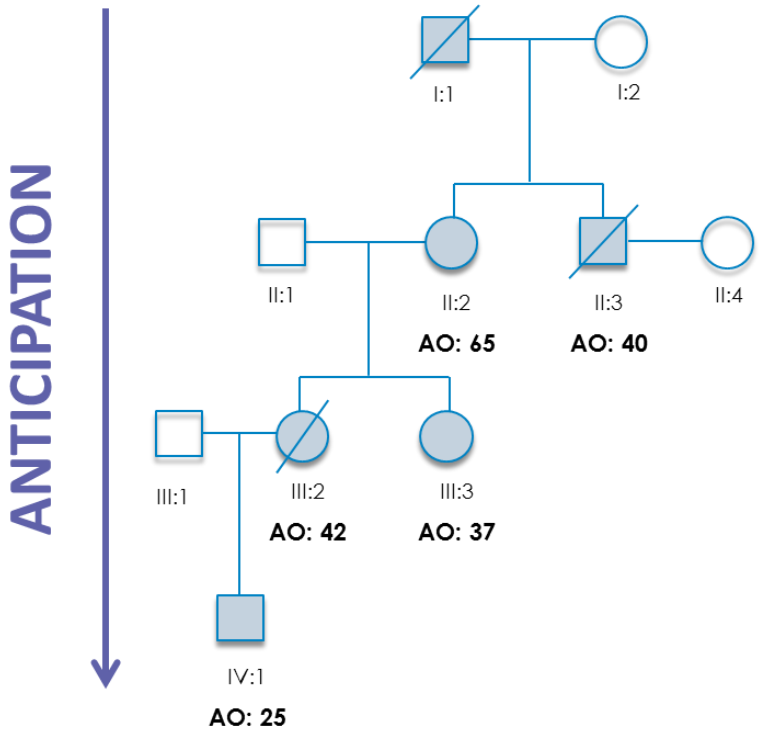

Figure 2- Example of a Portuguese Val30Met TTR-FAP pedigree showing anticipation. Val30Met TTR individuals are indicated by filled symbols. AO, Age-at-onset.

The following Table 2 summarizes the background and the main clinical features between early- and late-onset Portuguese Val30Met TTR patients accordingly to Conceição *et al.*, 2007 and 2016[104; 128].

Table 2 - Background and the main clinical features of Portuguese Val30Met TTR patients, adapted from Conceição et al., 2007 [128]; 2016 [78].

	Early-onset	Late-onset
N	43	43
Mean AO (SD), years	33.1 (5.4)	59.5 (6.8)
Gender (Male/Female)	20/23	21/22
Presence of family history, %	86%	32%
Symptoms, % of patients		
Sensory-motor symptoms	35%	84%
Autonomic and GI symptoms	65%	16%
Neuropathic pain	2%	47%
Cardiac signs	0%	14%
Renal dysfunction	0%	7%
Ocular symptoms	0%	2%

SD, standard deviation; GI, gastro-intestinal. Some patients may have more than one first symptom.

Genetic Modifiers

Searching for genetic modifiers in FAP is a very promising avenue. Few studies have been published aiming to disentangle possible genetic modifiers involved in AO variability[129; 130] Some of the hypothesis proposed that a small part of the phenotypic heterogeneity may be explained by non-coding variant in potentially regulatory regions *in cis*[131-134]. Polimanti *et al.* 2013, suggested that non-coding *TTR* variants have a role in determining phenotypic presentation in African patients, suggesting a contribution to a phenotype with increased cardiac achievement. The analysis of extended haplotypes within and surrounding the *TTR* gene using microsatellites suggested a possible modulatory effect on AO, exerted by a *trans* factor more frequent in late than in early-onset cases[134]. However, it failed to reach significance, possibly due to the multiple factors involved and/or to a small sample size.

Candidate genes were also studied, looking for common variants that could be associated with Val30Met and AO[129] (Figure 3). Possible interactions between *loci* seemed to contribute more to the observed differences in AO, than a single-*locus* effect.

Our group published several studies, using a family-centred approach, where diverse candidate-genes associated with TTR pathways were investigated as they might act as genetic modifiers of AO in TTR-FAP Val30Met[135; 136]. Namely, some variants in candidate-genes related with TTR-FAP signaling pathways (*APCS*, *RBP4, NGAL*, *BGN*, *MEK1*, *MEK2*, *HSP27*, *YWHAZ)* are significantly associated with AO variation in Portuguese population, reinforcing the effect also found in previous studies[135; 136]. Also, sex hormones may have a modifier effect in the disease onset, as it was shown for the first time the contribution of AR gene as an AO modifier[135]. Soares

et al. screened 9 parent-offspring pairs with large anticipation and no trinucleotide-repeats were found associated with anticipation[126]. In contrast, using a larger sample of 123 Val30Met TTR-FAP families, Santos *et al.* 2019 found an association of large normal alleles of a trinucleotide-repeat in *ATXN2* and a decrease in AO. Moreover, based on the co-localization of chaperones proteins in TTR deposits, Dardiotis *et al.*, found association of variants in *C1Q* complement and *APOE* genes with AO in a Greek-Cypriot TTR-FAP sample, although family structure was not taken into account[130]. In our Portuguese families we also found similar results, as rare *APOE* variants lead to an earlier-onset and variants in *C1QA* and *C1QC* were associated with an earlier or later AO of TTR-FAP[137; 138].

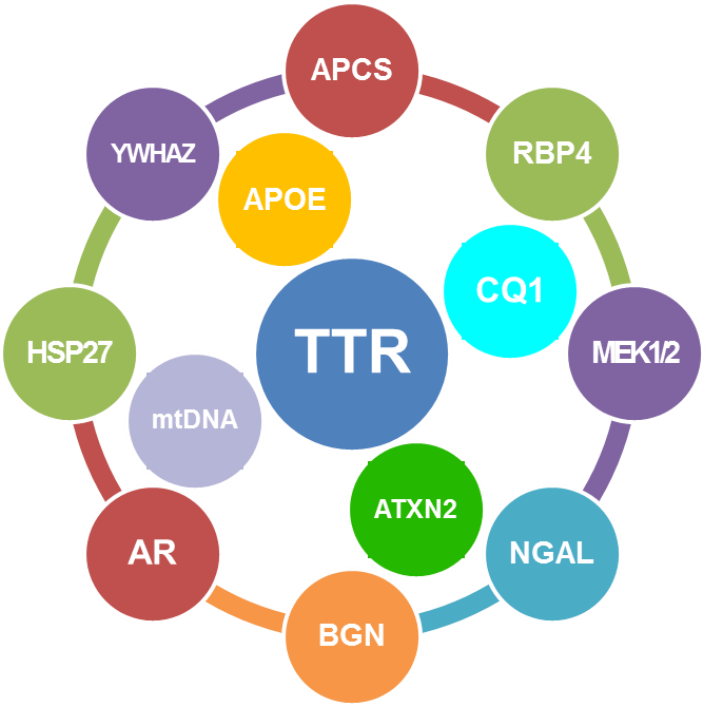

Figure 3- Scheme of candidate-genes associated as potential AO genetic modifiers.

Mitochondrial DNA (mtDNA) variation may also contribute to AO variability. The presence of a mtDNA variant may explain the observed differences in penetrance according to the transmitting parent gender[139] and different mtDNA haplogroups were associated with AO variation in TTR-FAP Swedish and French patients[140]. Our group explored the mtDNA copy number variations and we found that TTR Val30Met carriers have a significantly higher mean mtDNA copy number than controls. This variation was also observed in particular in early-onset offspring that showed a significant increase in the mtDNA copy number, when compared with their late AO parents[141].

Origin

It is still an open question whether the worldwide spread of Val30Met variant results from a single founder and what is the genetic relation between different clusters of the disease. It was hypothesized that the disease originated from Portugal, and then spread throughout the world, with the Portuguese travellers of the 16th century: to Sweden during the salt trade and, to Japan where the Portuguese are supposed to have introduced cartography, astronomy, the art of navigation, printing, a new vocabulary and rifles[6].

On the other hand, other authors suggested that population differences in AO could be explained by different mutation origins[142]. Thus, it was suggested that an independent founder effect might have arisen in Swedish patients[134; 143] and the gene may have travelled with Vikings from Sweden who visited Western Europe in the beginning of the 8th century. Additionally, a study suggested that the Italian Val30Met variant may have originated before the Portuguese and Swedish Val30Met variant[142], but this is still an open question. This Italian study suggested that non-coding regions of *TTR* can influence the genetic diversity found in the three populations, which will have implications, for example, in AO variability[**142**]. In Portugal, the differences in AO are also observed in two main disease clusters: Northern Coast and Inland region. Recently, our group found robust insights indicating that Val30Met arose in the Northern Coast and probably the dispersion occurred from Northern Coast to Inland region[144].

Misdiagnosed/ Mimicking neuropathies

There are other diseases that due to its symptomatology similar to TTR-FAP or uncommon signs (elderly patients and no family history, biopsy without amyloid substance), are often confused and misdiagnosed. Consequently, this fact leads to a delay of diagnosis in average of 4 years, post onset[145].

Chronic inflammatory demyelinating polyneuropathy (CIDP), immunoglobulin light chain, diabetic neuropathy and leprosy are some of the common examples of misdiagnosis. CIDP is the commonest misdiagnosis especially in individuals with slightly or no autonomic dysfunction[146; 147].

The difficulties of clinical diagnosis of TTR-PAF are a current reality that clinicians tend to face. Their awareness is fundamental to reduce the long delay in diagnosis.

Treatment

The multiplicity of affected systems in this disease poses serious problems in the therapeutic approach. As first-line treatment is the symptoms relief of the affected systems not only to control them but also to prevent complications. However, this does not affect the course of the disease[20].

In a broad sense, there are different stages to prevent the disease progression: (A) a really early stage is the suppression of TTR expression; (B) an intermediate stage is the TTR stabilization and; (C) at the end of the cascade is the clearance of amyloid deposits (Figure 4).

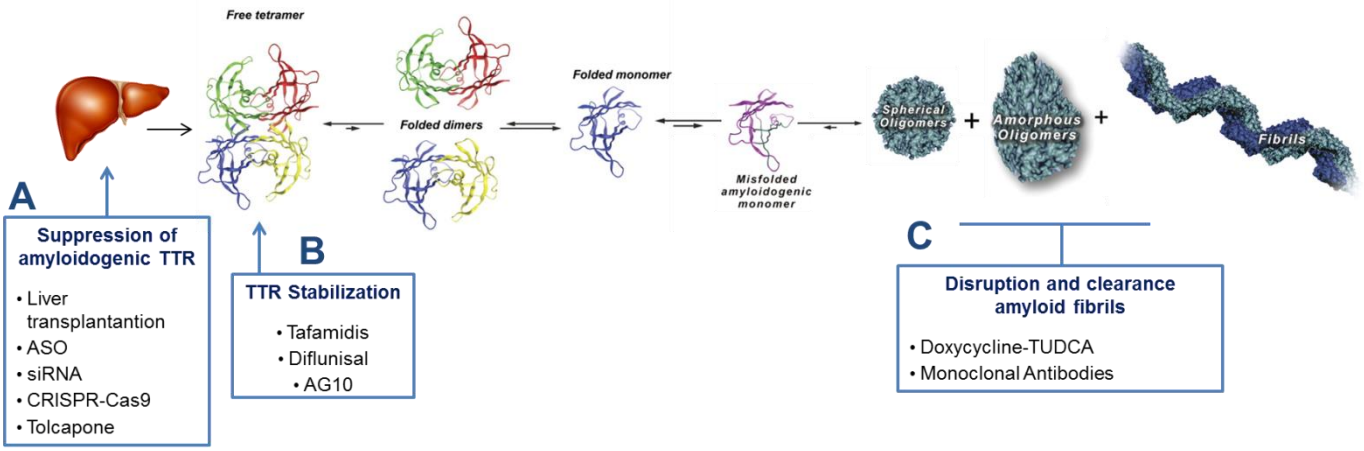

Figure 4- The TTR amyloid cascade showing the therapeutic options and their targets in TTR-FAP. Modified with permission from Jeffery Kelly, TSRI.

(A) Liver Transplantation

As TTR is predominantly produced by the liver (>90%), if the TTR Val30Met liver is replaced by a TTR WT liver, it is expected that no progression of the disease could occur[148]. In 1995 in Portugal, the first sequential liver transplant was performed, later denominated internationally as "domino"[149]. The domino liver transplantation, the liver excised from the patient with TTR-FAP, anatomically normal and with no other functional abnormalities than the Val30Met TTR production, serves as a graft for transplantation hepatic with terminal liver disease (for example: viral or tumoral patients). This method has achieved good results and apparently does not imposes risk to donors' lives since the symptoms were expected to take as long as it takes in a TTR-FAP patient (about 20-30 years) to start at the liver receptor[149]. However, after a few years some cases began to appear where *de novo* amyloidosis was detected in domino receivers in 8-10 years[150].

Until recently the only effective therapy known was liver transplantation, improving the general state and stabilization of neuropathy, in most cases; however encompasses some limitations: (1) availability of organs, which is not sufficient for all patients leading to a growing number of deaths in patients on the waiting list; (2) lifelong treatment with immunosuppressors; and (3) older patients cannot be submitted to a liver transplant, due to the increased probability of complications during surgery[106].

(A) Therapeutic Oligonucleotides: Patisiran e Inotersen

By 2018, two similar approaches for silencing WT and disease-causing variants TTR expression in the liver were approved: Patisiran e Inotersen. The two therapeutic oligonucleotides resulted in a high serum TTR knockdown of ~80% in patients over several months of treatment. Clinical trial data have demonstrated that are equally well tolerated and improve the quality of life and neuropathy impairment[151]. Both bind to RNA in a sequence specific manner but exploit different mechanisms[152].

Patisiran, is a lipid nanoparticle-formulated small interfering RNA (siRNA) that mediated RNA interference (RNAi) via binding to 3'UTR of TTR mRNA in the cytoplasm for TTR mRNA cleavage[153; 154]. Patisiran is administered by intravenous infusion every 3 weeks[153].

Inotersen, is antisense oligonucleotide (ASO) with a complementary sequence to target TTR pre-mRNA in the nucleus via RNaseH. The complex ASO/TTR mRNA induces the RNaseH activity resulting in TTR RNA degradation[152; 155]. TTR-FAP patients receive Inotersen weekly by subcutaneously injection[155].

(B) Tafamidis

A promising alternative to liver transplant has emerged through Tafamidis. In 2011, Tafamidis became the first drug to be approved for the treatment of TTR-FAP by European Medicines Agency (EMA) for stage 1 TTR-FAP patients (symptomatic patient walking unassisted)[156; 157]. Tafamidis is an oral-administered novel small molecule that binds to hydrophobic T4-binding sites of the TTR and stabilizes the TTR tetramer, consequently, prevents TTR tetramer dissociation and aggregation[156]. Patients treated with tafamidis have shown a significant slowdown in the progression of peripheral neuropathy, cardiomyopathy and improvements in the nutritional status[156]. Regarding the mortality risk, tafamidis reduced this risk in early- and late-onset patients by 91% and 63%, respectively[158]. However, Tafamidis only showed efficacy in 60% of patients, while in 40% disease has progressed normally[156]. In addition to this problem, we must take into account that a significant proportion of patients do not meet the necessary criteria to use Tafamidis.

(B) Diflunisal

Another stabilizer of TTR tetramer is Diflunisal. Unlike Tafamidis, this drug was not designed specifically for TTR, is a repurpose of a non-steroidal anti-inflammatory agent which also bind T4-binding site of the TTR[159]. This old drug also proved a delay in the rate of progression of neurological impairment and preserved quality of life[159].

(B) AG10

AG10 is also an orally-administered small molecule designed to potently bind and stabilizes TTR in the blood[160]. This is currently in clinical trials, but so far has been well tolerated and demonstrated >90% average TTR stabilization[160].

(C) Disruption of insoluble amyloid fibrils

Another therapeutic strategy for ameliorating the hereditary TTR amyloidosis involves the degradation of the substance amyloid already deposited. For example:

- A humanized monoclonal antibody was designed specifically against TTR epitopes in order to target and clear the TTR misfolded forms[161]. The similar strategy has already shown positive results in AD[162].
- Doxycycline + tauroursodeoxycholic acid (TUDCA), is a synergetic effect of two agents that in the open-label phase II study demonstrated to be well tolerated and stabilized the neuropathy and cardiac disease[163]. Doxycyline is an antibiotic that might be capable to disrupt TTR fibrils *in vitro* and in mice and TUDCA is a biliary acid that reduces non-fibrillar TTR aggregates[164].

So far, these therapeutic options are in pre-clinical studies.

Animal Models

Much of what is known today about many disorders derives from *in vivo* studies. Several TTR animal models have been created, including rodents, fruit flies, *C. elegans* and non-human primates. They have revealed important TTR pathophysiological mechanisms and have assisted to test potential therapeutic options[62].

Several groups have generated transgenic murine with valuable insight into the mechanisms underlying TTR-mediated amyloid aggregation. These TTR mouse models including WT and disease-causing variants showing TTR deposition in some tissues, but they never afforded a neuropathy or cardiomyopathy degenerative phenotypes[165; 166].

Mouse models

A mouse strain transgenic for WT human *TTR* genes demonstrated that these animals over 18-months of age had both nonfibrillar and to a lesser extent amyloid fibril TTR deposits in the heart and kidney[165]. FAP mice expressing human *TTR* Val30Met gene [167-171], and the more aggressive human Leu55Pro variant were previously generated, but these models failed to present nonfibrillar or fibrillar TTR amyloid deposits in the peripheral and/or autonomic nervous

system to recapitulate the full spectrum of human disease features[172]. On the other hand, Santos *et al.*, found fibrillar TTR deposition in the peripheral nervous system in a human TTR Val30Met transgenic mouse but only in a heat shock transcription factor 1 (*Hsf1*) null background and yet the development of neuropathy was not observed[173]. These transgenic mice show more prominently amyloid deposition in the gastrointestinal tract than in TTR amyloidosis patients[174]. Moreover, a drug doxycycline was demonstrated that might be capable of disrupting TTR amyloid deposits in a transgenic mice expressing human TTR Val30Met gene in a mouse Ttr gene knockout[175].

Another key point in these type of studies is that the different strains may lead to different phenotypes for the same variant. Panayioyou *et al.*, using two lines of transgenic mice bearing the same TTR Val30Met transgene concluded that the genetic background modulates TTR amyloid deposition and affects pathogenic cascades involved in amyloidogenesis, as it had been reported for other diseases[176]. Recently, a double-humanized mice where the mouse *Ttr* and *Rbp4* were replaced with the human *TTR* and *RBP4* gene observed amyloid deposition more pronounced than in conventional transgenic mouse strains and, importantly were the first mice model to observe amyloid deposition in the sciatic nerve without additional genetic change[177].

Drosophila melanogaster models

Drosophila melanogaster models of TTR amyloidoses have previously been reported, also expressing human WT TTR[178; 179], two amyloidogenic variants in TTR β-strand regions[180; 181] and the destabilizing TTR-FAP TTR variants Leu55Pro[178] and Val30Met[179; 181; 182]. In these studies, the TTR variants were expressed in the eye, nervous system or fat body and were associated with neurodegeneration, shortened lifespan, and reduced climbing activity when compared to the wildtype TTR flies that demonstrate a milder phenotype[178-182].

C. elegans models

A *C. elegans* expressing human WT TTR was previously generated, yet the model exhibited neither toxic phenotypes nor mechanism of toxicity[183]. Recently, Tsuda *et al.*, generated a *C. elegans* model expressing in the body wall muscle full-length WT and TTR Val30Met and various WT TTR fragments fused to enhanced green fluorescent protein (EGFP)[184]. The authors proposed that epigallocatechin-3-gallate, a major polyphenol in green tea, significantly inhibited the phenotype caused by residues 81-127 of TTR[184]. Nonetheless, as these fusion proteins do not contain the TTR signal peptide, as a result, they are localized in the cytoplasm of the body wall muscle.

Non-human primates' models

So far, only three studies have emerged with non-human primates. All are about aged vervet monkeys showing cardiac dysfunction and positive TTR amyloid deposits in several organs, including the heart[185-187]. Without genetic confirmation, two studies suspect of senile systemic amyloidoses based on the pathological relationship between TTR amyloidosis found and the disease in humans[186; 187], while the other study identified the TTR Val122Ile variant[185]. In addition to humans, spontaneously developed systemic TTR amyloidosis in animals has not been reported.

Thus, there is a pressing need to generate a good model system that mimic the disease phenotype in order to unravel important disease-related mechanisms and ultimately the development of new drugs and treatments.

Taking into account this state-of-the-art, there was still room available, which led us to explore and identify the molecular mechanisms intertwined with genetic modifiers in human and animal models that are associated with phenotypic variability of TTR-FAP Val30Met.

MAIN OBJECTIVES

Our research hypotheses were:

(1) why do some patients start the disease very early (AO <30 years), while their ascendants start the disease much later (AO >50 years)?; (2) what causes differences in AO between generations in some families?; (3) what are the proteins that interact with TTR and contribute to neuronal proteotoxicity? and (4) can the function of these proteins reverse the neuronal dysfunction in FAP models?

This project focused on two main aims:

(I) to identify and characterize genetic variations that can explain the disease phenotypes reported, by concentrating the study on families; and

(II) to characterize the role of TTR in FAP neurodegeneration using a Val30Met TTR FAP animal model.

Therefore, the core of this thesis was to identify molecular mechanisms and/or genetic modifiers associated with phenotypic variability as evidenced by age-of-onset variation.

Specific Objectives

To elucidate the relevant questions mentioned above, our aim was to identify modifiers closely linked to the TTR *locus* that may in part explain the wide variability in AO. We proposed to explore genetic mechanisms that may act as modifiers for AO in FAP including: *cis*- and *trans*-acting factors and whole-genome sequencing in TTR-FAP families with large anticipation.

Furthermore, we also aimed to identify TTR modulators in a forward genetic screen using *Caenorhabditis elegans,* to further elucidate genetic pathways that might correlate with AO variability and severity of human FAP disease phenotypes.

The possibility of anticipating or understanding the diverse and complex mechanisms that influence AO can help in the prediction of disease onset.

GENERAL METHODS

Two major methodologies were applied: I) in human DNA (Article 1-3) and; II) in *C. elegans* TTR- FAP models (Article 4 and 5).

All individuals' data were collected from Unidade Corino de Andrade (Centro Hospitalar do Porto), the largest dataset on Val30Met TTR-FAP worldwide collected for 70 years now. The availability of such a large sample of patients, clinically well characterized by the same small group of neurologists, is a unique opportunity for this research. Moreover, family members, unrelated controls and some asymptomatic carriers were also collected from the bio bank at Centro de Genética Preditiva e Preventiva (Instituto de Investigação e Inovação em Saúde). This bio bank already has permission of CNPDP (National Commission for Personal Data Protection) for collection and storage of diagnostic and research samples and associated data. All samples were coded, and personal data kept separately from clinical and genetic information. All procedures were done in accordance with Law 12/2005 (genetic information) and Law 67/98 (data protection). Written informed consent was requested from selected individuals, for collection of DNA and to take part in this study.

DNA was extracted from blood or saliva samples and quantified by spectrophotometry. Genotyping was performed according to the specific objectives of each article: Sanger sequencing; Multiplex PCR following SNaPshot approach and Whole-genome sequencing (WGS).

After genotyping, the functional impact was evaluated *in silico* by a plethora of bioinformatics tools. Results were analyzed using standard statistical and to account for non-independency of AO between members of the same family approaches as described specifically in each Chapter/article. Corrections for multiple comparisons were also taken into account.

For *C. elegans* ' experiments, standard nematode culture methods and genetics were used to maintain the nematodes on nematode growth medium (NGM) plates seeded with E. coli strain OP50, unless otherwise specified.

Germline transformation was performed to generate *C. elegans* integrated strains expressing human WT-, D18G-, V30M-, T119M- TTR under the body wall muscle-specific promoter.

All strains were tested by quantitative RT-PCR and western blot to quantitate mRNA and TTR protein levels, respectively.

In vitro TTR tetramer levels were measured by Ultra Performance Liquid Chromatography (UPLC) employing validated fluorogenic TTR folding probes A2 that are dark until they selectively

bind and reacts to TTR tetramers. Non-native TTR oligomer levels were quantified by Native-PAGE and by ELISA sandwich assays, using non-native TTR polyclonal MDX114 antibody, and monoclonal MDX102 and MDX108 antibodies. The antibodies are specific to misfolded forms of TTR and do not recognize tetrameric native form of TTR.

The in vivo localization of TTR was visualized by immunofluorescence (IF) microscopy using specific antibody against TTR or compound 5 for TTR tetramer. Coelomocyte uptake assay were performed injecting worms with dextran and coelomocytes were selectively ablated in our TTR models by expressing a variant diphtheria toxin (DT-A). Imaging of coelomocytes was done on live animals with simultaneous differential interference contrast microscopy (DIC) and epifluorescence modalities.

C. elegans were fed with RNA interference to reduce of TTR transgene activity and R193.2 gene.

Three TTR-dependent phenotypes were characterized by: Thermal avoidance assay for nociception; analysis of FLP dendritic branching for neuronal morphology and worm tracking analysis for locomotion. These phenotypes were ameliorated by treatment of TTR strains with tafamidis and RNAi against TTR.

Forward genetic screen was conducted by chemically mutagenize V30M TTR *C. elegans* to identify F2 generation homozygous mutants that suppress the defects in locomotion. Candidate suppressors were placed in complementation groups and identified individual mutations by WGS.

The following scheme give us a general overview of the methods used in these thesis which are detailed described in each article.

TTR-FAP

HUMANS

Phenotype	• Age-at-Onset	• Family Anticipation			
DNA	• Sanger Sequencing	• Multiplex PCR + SNaPshot	• Whole-Genome Sequencing		
In Silico Tools	• is-rSNP	• Alamut	• GTEx	• ESE Finder	• PITA algorithm
	• FuncPred	• Polyphen-2	• JASPAR	• Human Splicing Finder	• miRWalk

C. ELEGANS

Phenotype	• Thermal avoidance assay	• Locomotion assay	• Neuronal morphology
DNA	• Mutagenesis	• Whole-Genome Sequencing	
mRNA	• RT-PCR		
Protein	• SDS-PAGE	• ELISA	• Western Blot
	• UPLC	• Native PAGE gel	• IF microscopy

RESULTS

The aim of **Article 1** was to identify genetic alterations and regulatory factors at *TTR locus* in addition to TTR Val30Met variant and to understand how they may contribute as genetic modifiers in TTR-FAP.

We reported common and rare variants that were identified in the promoter, coding and intron / exon boundaries of the *TTR* gene in 330 TTR Val30Met patients from Portugal. Their putative effect was then studied through an extensive *in silico* study.

Eight variants were identified in the coding and flanking region of the TTR gene, including 2 new ones. In addition, 15 variants were found 2.1kb upstream of *TTR* (in the promoter region) including a novel one and a CA repeat. The frequency of variants was compared between the early and intermediate/ late onset groups.

The *in silico* study suggested the presence of 3 non-coding variants that possibly modulate the mechanism of splicing and 2 variants in the promoter interacting with transcription factors binding sites. Also, it was shown that 2 variants might interfere with miRNA binding sites in the 3'UTR of *TTR*.

The current data suggest possible mechanisms that may account for expression of *TTR* as a modulator of the course of FAP. Genetic testing could go beyond screening for the disease-causing variant and our results could improve efficacy of current therapies or allow to identify new biomarkers of disease-onset for this disabling disease.

Article 1: Beyond TTR Val30Met: potential regulatory variants associated with age-at-onset in familial amyloid polyneuropathy

Miguel Alves-Ferreira, MSc[1,2]; Ana Azevedo, MSc[2]; Teresa Coelho, MD[3]; Diana Santos, PhD[1,2]; Jorge Sequeiros, MD, PhD[1,2]; Isabel Alonso, PhD[1,2]; Alda Sousa, PhD[1,2]; Carolina Lemos, PhD[1,2]

[1] UnIGENe, IBMC - Institute for Molecular and Cell Biology; i3S – Instituto de Investigação e Inovação em Saúde, Universidade do Porto, Portugal;

[2] ICBAS - Instituto Ciências Biomédicas Abel Salazar, Universidade do Porto, Portugal;

[3] Unidade Corino de Andrade (UCA), Centro Hospitalar do Porto (CHP), Largo Prof. Abel Salazar, Porto, Portugal.

Corresponding Author:
Carolina Lemos, PhD
Invited Auxiliary Professor, ICBAS
UnIGENe, IBMC-i3S
Rua Jorge Viterbo Ferreira, 228
4050-313 Porto
Telephone: +351 22 042 80 02
E-mail: clclemos@ibmc.up.pt

Submitted

ABSTRACT

Objectives: Val30Met in transthyretin (*TTR*) gene is causative for familial amyloid polyneuropathy (FAP). FAP shows a wide variation in age-at-onset (AO) between clusters, families, and among generations. We aim at identifying genetic modifiers of disease onset that may contribute to this clinical variability in Portuguese patients.

We hypothesized that other variants in *TTR* locus, beyond the TTR-FAP causing variant, could play a regulatory role in its expression level and modify disease expressivity.

Methods: We analyzed DNA samples of 330 Val30Met carriers (300 patients, 30 aged-asymptomatic carriers) from 120 families currently under follow-up. A generalized estimating equation analysis (GEE) was used to take into account non-independency of AO between relatives. In these individuals an intensive *in silico* analysis was performed in order to understand a possible regulation of gene expression.

Results: We found variants in the promoter, coding and intron/exon boundaries of the *TTR* gene associated with the onset of symptoms before and after age 40 years, namely rare variants and a tandem CA-dinucleotide repeat. *In silico* analysis disclosed significant alterations in the mechanism of splicing, transcription factors and miRNAs binding.

Interpretation: Variants within the promoter region may modify disease expressivity and variants in the 3'UTR can impact the efficacy of novel therapeutic interventions. Importantly, the putative mechanisms of regulation of gene expression within the TTR gene deserve to be better explored in order to useful in the future as potential therapeutical targets.

Keywords: Age-at-onset, familial amyloid polyneuropathy, *TTR* gene

INTRODUCTION

Transthyretin-related familial amyloid polyneuropathy (TTR-FAP) is an autosomal dominant neurodegenerative disease that presents as a progressive sensorimotor and autonomic polyneuropathy with involvement of the small myelinated and unmyelinated nerve fibers[1,2]. It is characterized by mutated protein deposition in the form of amyloid substance (ATTRm). Without treatment, it leads to death within 10-20 years[1]. The Val30Met variant (p.Val50Met) in the transthyretin gene (*TTR*) is the commonest causative variant for TTR-FAP[3]. Significant phenotypic heterogeneity, namely in age-at-onset (AO), has been described in Val30Met patients. Variation between clusters has been widely documented, with Portuguese, Brazilian and Japanese patients showing mostly an early-onset, whereas Swedish patients are known for their late-onset[4,5]. However, variation is equally large within each cluster, with range in AO being quite similar. In Portuguese patients clinical symptoms typically occur before age 40 years (early-onset), but a wide variation in AO (19-82 years), has been identified[6]. The most intriguing feature is variation within the same family and the fact that late-onset patients often have very early-onset offspring, while the reverse was never observed[7].

This intra-generational variability led us to explore the role of common variants in different candidate genes, taking into account the family structure and the non-independency of AO among members of the same family[8-10].

However, due to the main role of TTR in FAP, another approach consisted on identifying modifiers closely linked to the *TTR locus*.

A small part of this variability may be explained by non-coding genetic variants in *cis*[11] and a *trans*-acting factor[12], but additional factors clearly remain to be discovered.

We speculated that variants within the regulatory regions of the *TTR* gene may account for the changed gene expression and ultimately culminate in phenotypic heterogeneity. The aim of this study was then to identify other variants and regulatory factors at *TTR locus* and understand how they may contribute as genetic modifiers in TTR-FAP.

SUBJECTS AND METHODS

Subjects and families

Unidade Corino de Andrade do Centro Hospitalar Universitário do Porto (UCA-CHUP, Porto) has the largest TTR-FAP Val30Met registry worldwide (more than 3000 patients), collected over 80 years and clinically well characterized. We selected 120 families currently under follow-up, with at least 2 generations affected and coming from all geographical areas of Portugal. Our study sample consists of 330 Val30Met carriers (299 patients, 31 asymptomatic carriers).

Diagnostic criteria and age-at-onset (AO) were defined as previously[7]. Briefly, AO was defined of each patient by the same team of neurologists specialized in Val30Met TTR-FAP, considering the presence of a whole set of symptoms characteristic of small fibers' neuropathy and not isolated and unspecific symptoms. In what concerns AO, it has long been accepted to classify patients in three groups: early (≤40), intermediate (40-49) and late (≥ 50)[13]. In this study, patients were divided in two groups only: early (≤40) and intermediate/late-onset (>40 years), in order to include also the intermediate AO patients (40-49). Asymptomatic carriers aged 50 years or more were also included in the intermediate/late-onset group. The presence of Val30Met variant was confirmed in all subjects. DNA samples were collected at UCA-CHUP and stored at Centro de Genética Preditiva e Preventiva (CGPP-IBMC, Porto) biobank, authorized by CNPD (National Commission for Data Protection). The study was approved by the Ethics Committee of CHP. Written informed consent was obtained from all patients.

Genotyping

Genomic DNA was extracted either from peripheral blood leucocytes or saliva, using the QIAamp® DNA Blood Mini Kit (QIAGEN™) and Oragene DNA Self Collection Kits (DNA Genotek, Ottowa, Canada) according to manufacturer's instructions, respectively.

The promoter, coding and all intron/exon boundaries of the TTR gene were amplified by polymerase chain reaction (PCR) using HotStarTaq DNA Polymerase® (Qiagen™) and primers forward and reverse for each amplicon (sequences available upon request).

Then the PCR products were examined by direct Sanger sequencing using dye terminator chemistry approach from Applied Biosystems™, with the same set of primers as for

amplification, and samples loaded on an ABI-PRISM 3130 XL genetic analyzer (Applied Biosystems).

Statistical analysis

Association of genetic variants with AO (as a dichotomous variable), as in the case of the tandem repeat and the two variants together, was explored using Chi-Square. When AO analyzed as a continuous variable, and to account for non-independency of AO between members of the same family, we used generalized estimating equations (GEE); to correct for multiple testing, we applied a Bonferroni correction, dividing by the number of GEE tests performed. Statistical significance was set at $\alpha<0.05$. All statistical analyses were performed using IBM SPSS Statistics software (v.24).

In silico analysis

To predict the impact of sequence variants on TTR function, bioinformatics tools included in the Alamut Mutation Interpretation Software (Interactive Biosoftware, Rouen France) and Polyphen-2 were applied.

Also, we ran a comprehensive bioinformatics package, FuncPred[14], organized by NIH and one of the most reliable and popular function-prediction tools.

In order to predict potential consequences of variants on splicing events, we used two prediction programs (ESEfinder and Human Splicing Finder) in Alamut Software.

The JASPAR[15] database was utilized to explore the transcription factors binding (TFB) capacity. Transcription factors were filtered by expression in liver with an expression level greater than 1 Transcripts per Million (TPM) using Genotype-Tissue Expression (GTEx) project.

miRNA target sites in the 3'UTR *TTR*-wild type (WT) were predicted by miRWalk[16] and we used PITA algorithm, taking in account the conservation and the differences in the alignment scores[17].

RESULTS

Study group demographic characteristics

This study included individuals Val30Met carriers (174 females, 156 males). In the AO ≤40 group (n=202), mean (SD) AO was 31.2 (4.5) years, whereas the AO >40 group (n=128) presented a mean (SD) AO of 56.2 (10.6) years, which includes 30 late asymptomatic carriers aged 40 years or more, who might be considered similar to late-onset patients.
We sequenced 2.1kb upstream *TTR* to include promoter region and the coding and flanking regions of the *TTR* gene. Location and frequency of the variants found are shown in Table 1.

Common variants identified

We identified four common variants (MAF >10%) as shown in Table 1, 3 in the promoter region and 1 in 3' near gene. None of the common variants presented significant differences when comparing early- and late-onset patients or when analyzing AO as a continuous variable (data not shown). The variants rs3764479 and rs3794885 were the most common alterations in the promoter region (43.5% and 42.8%, respectively).
Noteworthy, in the AO ≤40 group, more patients carried simultaneously the minor allele of rs3764479 and rs3764478 (p=0.03), with a 2.22-fold susceptibility for symptoms to start before age 40 (OR=2.22, 95% CI=1.05 to 4.70).
Interestingly one variant is a tandem repeat composed by a CA-dinucleotide (rs71383038) in the promoter region (Table 1). While the most common allele in the Portuguese population was CA_{10}, followed by the minor allele CA_9, we found an unreported allele with seven CA-repeats (CA_7). When we compared CA_9 carriers with CA_{10}, the only two CA_9 homozygotes for the tandem repeat rs71383038 showed onset after 60 years (p=0.066); 56.1% of the patients presented the common genotype (CA_{10}/CA_{10}) and 42.7% the CA_9/CA_{10} genotype. Noteworthy, the only patient with a deletion of 3 CA-repeats (CA_7) showed a very early-onset (30 years).

Rare Variants

In the promoter region, 12 rare variants were found, including one novel (c. -1993 G>T). Seven rare variants in the coding and flanking regions of the *TTR* gene were identified, including two novel ones: c.105A>G, in exon 2 (p.Lys35Lys), a synonymous variant and

c.200+107 T>C, in intron 2. Variants already reported included 2 intronic, two at the 3' UTR and 2 exonic ones. Importantly, rare variants: c. -1993 G>T; rs13381522; rs546878244; rs3764477; rs540872876; rs58616646; 146750662 and rs996949357 in the promoter region and c.200+107 T>C; rs28933981; and rs1053907197 in the coding and flaking regions of *TTR* gene showed an association with AO ($p<0.0125$), significant after multiple-testing correction (Table 2).

Regarding the coding variant, TTR Ser6 (rs1800458, p.Gly26Ser), ten patients showed an early-onset and eight patients a late-onset, ($p>0.05$), showing that TTR Ser6 is not associated with early or late-onset. All compound heterozygotes for TTR Val30Met/Thr119Met (p.Val50Met/Thr139Met) showed a later-onset, as previously described[18].

Putative effects of the rare genetic variants

Using JASPAR database and GTEx project, we predicted that the combination of rs3764479/rs3764478 variants (as they were found to be present mostly together) create 69 new potential transcription-factor binding sites and may disrupt another 18, all expressed in the liver, where TTR is synthetized (Supplementary Table 1).

We also assess how likely a splicing change would occur as a result of the presence of DNA variants. Table 3 shows the variants that may alter splicing significantly (consensus value (CV) higher than 70). We found a new acceptor site, 2 nucleotides downstream rs1800458, probably an active splice site. A branch point, probably inactive in the wild-type sequence, is predicted to become a strongly active splice site in the presence of rs1791228. Also, presence of rs36204272 leads to loss of a donor site probably inactive in wild-type TTR. Disruption of four exonic splicing enhancers was observed in rs28933981, while creation of three new ones was seen in rs1800458.

Using miRNA-target prediction programs, we detected two miRNAs: mir-200a and mir-141, which are predicted target-sites for the TTR 3'UTR. Presence of rs62093482 or rs1053907197 (located in TTR 3'UTR) does not interfere with miRNA binding. rs62093482 creates a putative target site to mir-622. The rare allele of rs1053907197 is a putative target site to mir-138 and mir-622.

DISCUSSION

TTR-FAP phenotypic variability is evident not only between different disease-associated variants but also for patients with the same disease-causing variant that display different clinical manifestations. The main focus of this study was on the phenotypic variability of the TTR-FAP Val30Met individuals regarding AO.

Phenotypic effect of variant

Using a parametric test (GEE), which is a quite powerful statistical method, we found interesting results regarding the association of some of these variants with AO, which showed that rare variants in fact seem to modulate AO variability. We found significant results for some rare variants that despite the heterozygous genotype appeared only once, this is in accordance with the genotypic frequencies described for European (Non-Finnish) in Genome Aggregation Database (GnomAD). We consider that these rare variants results are equally important and should be reported, because their identification may have implications for genetic screening and personalized treatment.

The protective role of rs1800458 (p.Gly26Ser) has already been hypothesized[11,19]; however, results do not allow us to state that this coding variant was protective in our Val30Met patients, since it did not significantly associate with late-onset.

Both Thr119Met carriers found had a very late AO (61 and 63 years), though they belonged to an early-onset family. This supports the theory that stability of the TTR molecule may be an important factor to prevent amyloidogenesis, offering a protection from the Val30Met effects[18,20].

Interestingly, the double genetic dosage of TTR Val30Met homozygous carriers does not appear to be related to the onset of symptoms, nor it appears to trigger the disease onset, as we found late-onset carriers of Val30Met/Val30Met.

Interestingly, it is very promising that the combination of the minor alleles of rs3764479 and rs3764478 (which appear mostly together) showed a high risk for an early-AO. This approach deserves our future attention, as clusters of patient-specific variant combinations have already been found[21].

Putative effect on splicing activity, TFBSs and miRNA target sites

Analysis of non-coding regions suggests the presence of three non-coding variants, possibly *cis*-regulatory elements of the *TTR* gene that modulate the effect of Val30Met on the disease phenotype.

To the best of our knowledge, no other studies about genetic alterations in splicing activity on *TTR* gene have been performed, except for a recent association study for variants in the *TTR* gene in Han Chinese patients with Alzheimer disease[22]. It is important to emphasize that some of the differences between WT and variant sequences could alter splicing either by re-directing the spliceosome or by altering the binding of auxiliary factors, such as SR proteins, exonic and intronic splicing enhancers and silencers[23].

The *TTR* gene is regulated by the promoter at the transcriptional level in liver cells[24]. In this study, we identified two variants in the promoter region that together reduce significantly AO. *In silico*, these variants not only disrupt potential binding sites once occupied by transcription factors, but also create new ones. Human transcription factors were predicted with a relative profile score threshold >80% and filtered by expression in liver.

miRNA mir-200a and mir-141 inhibit TTR expression, by directly binding to the 3′UTR of TTR, which is reversed by variants in the miRNA binding site[25]. rs62093482 and rs1053907197 variants do not affect the 3'UTR miRNA binding sites, but they create new ones. Two novel therapeutic drugs recently approved for treatment of FAP modulate TTR expression at the RNA level: patisiran, the first small interfering RNA-based drug approved by the FDA[26]; and inotersen, an antisense oligonucleotide[27]. Since both drugs prevent the production of TTR by targeting its 3' UTR, we hypothesized that variants in this region could modify their efficacy.

To the extent of our knowledge, this is the largest screening study of *TTR* variants in Val30Met TTR-FAP. Our data suggest possible mechanisms that may account for expression of TTR as a potential modulator of the course of FAP. This suggests even more the idea that molecular diagnosis should go beyond simply screening for the disease-causing variant.

ACKNOWLEDGMENTS

We thank all the patients and families for participating in this study and Joana Silva for all the help with the optimization of protocol for sequencing. We would like to thank FEDER funds, through the Programa Operacional Factores de Competitividade – COMPETE 2020

and by Nacional funds through the FCT – Fundação para a Ciência e a Tecnologia [COMPETE: POCI-01-0145-FEDER-007440]. This work was supported by grants of Fundação para a Ciência e Tecnologia, FCT [PTDC/SAU-GMG/100240/2008 and PEsT], co-funded by ERDF and COMPETE; and by Financiamento Plurianual de Unidades de Investigação (FCT). MAF is recipient of a FCT fellowship [SFRH/BD/101352/2014]. The funders had no role in the design and conduct of the study; collection, management, analysis, or interpretation of the data; preparation, review, or approval of the manuscript; or decision to submit the manuscript for publication.

Author Contributions

Conception and the study design: M.A.F., A.A., A.S. and C.L. Data acquisition and analysis: M.A.F., A.A., T.C., D.S., A.S. and C.L. Drafting the manuscript and figures: M.A.F., A.A., A.S. and C.L. Critical revisions to the manuscript: all authors.

Conflict of Interest Disclosures: T.C.'s institution has received support from FoldRx Pharmaceuticals, which was acquired by Pfizer Inc in October 2010; T.C. has served on the scientific advisory board of Pfizer Inc and received funding from Pfizer Inc for scientific meeting expenses (travel, accommodations, and registration). T.C. currently serves on the THAOS (natural history disease registry) scientific advisory board.
The other authors have no conflicts of interest.

Table 1: Variants found in the TTR *locus*: dbSNP ID, location, frequency in AO ≤40 and >40 onset patients, and minor allele frequency in Val30Met patients and in the Genome Aggregation Database (GnomAD)

TTR Region		dbSNP ID	Location NM_000371.3 (HGVS)	N	Variant frequency		Allele Frequency	
					AO ≤40	AO >40	Val30Met	European (Non-Finish)
PROMOTER		rs3764479	c.-2041A>G	111	64	47	0.222	0.328
			c. -1993 G>T	1	1	0	0.002	-
		rs13381522	c.-1933C>T	7	3	4	0.014	0.046
		rs546878244	c.-1700G>A	1	1	0	0.002	0.000
		rs3764478	c.-1383G>T	39	27	12	0.078	0.111
		rs71383038	c.-1232_-1231delCA	112	64	48	0.220	-
		rs72922940	c.-1168A>G	35	18	17	0.069	0.116
		rs3764477	c.-1157G>A	9	4	5	0.018	0.045
		rs540872876	c.-1156G>A	1	0	1	0.002	0.000
		rs58616646	c.-1136C>T	8	4	4	0.016	0.046
		rs146750662	c.-950C>T	2	2	0	0.004	0.004
		rs116409170	c.-833C>T	6	3	3	0.012	0.025
		rs3794885	c.-743A>T	109	63	46	0.218	0.296
		rs79748512	c.-682G>A	6	2	4	0.012	0.039
		rs996949357	c.-543T>C	1	0	1	0.002	-
Coding and flanking regions	In 2		c.200+107 T>C	1	0	1	0.002	-
	Ex 2	rs1800458	c.76G>A, p.Gly26Ser	18	10	8	0.027	0.074
	In 3	rs36204272	c.337-18G>C	7	3	4	0.011	0.037
	Ex 3		c.105A>G, p.Lys35Lys	1	0	1	0.002	-
	Ex 4	rs28933981	c.416C>T, p.Thr139Met	2	0	2	0.003	0.003
	3'UTR	rs62093482	c.*261C>T	6	3	3	0.009	0.028
	3'UTR	rs1053907197	c.*75A>C	1	1	0	0.002	-
	3' near gene	rs1791228	c.*402C>T	127	87	40	0.194	0.463

AO, age-at-onset

Table 2: Statistically significant results for rare variants associated with AO variation, using GGE analysis, after Bonferroni correction

TTR Region	Rare variant	Genotypes	B	95% CI	P-value
Promoter	Intercept	-	40.1	[36.7; 43.6]	<0.001
	c. -1993 G>T	GG (Ref)	-	-	-
		GT	-6.1	[-9.6; -2.7]	<0.001
	rs13381522	CC (Ref)	-	-	-
		CT	21.4	[8.5; 34.3]	0.001
	rs546878244	GG (Ref)	-	-	-
		GA	-8.1	[-11.6; -4.7]	<0.001
	rs3764477	GG (Ref)	-	-	-
		GA	-15.5	[-18.2; -12.9]	<0.001
	rs540872876	GG (Ref)	-	-	-
		GA	18.4	[14.8; 21.9]	<0.001
	rs58616646	CC (Ref)	-	-	-
		CT	-18.4	[-21.9; -14.8]	<0.001
	rs146750662	CC (Ref)	-	-	-
		CT	-8.1	[-11.6; -4.7]	<0.001
	rs996949357	TT (Ref)	-	-	-
		TC	11.9	[8.4; 15.3]	<0.001
Coding and flanking regions	Intercept	-	42.0	[39.5; 44.5]	<0.001
	c.200+107 T>C	TT (Ref)	-	-	-
		TC	8.19	[5.3; 11.1]	<0.001
	rs28933981	CC (Ref)	-	-	-
		CT	21.59	[17.3; 25.9]	<0.001
	rs1053907197	AA (Ref)	-	-	-
		AC	-7.81	[-10.7; -4.9]	<0.001

Ref, Reference genotype; B, unstandardized coefficient (estimated quantitative effect of each genotype on mean AO variation according to the intercept, compared with the reference genotype); CI, confidence interval; significance level set to 0.0125

Table 3: Prediction of splice sites and splicing enhancers (ESE) alterations by HSF and the ESEfinder software

Variant	Splice sites	Wild-type CV	Val30Met CV	CV variation	Distance from variant
rs1800458	acceptor site	0	77	77	2 nt downstream
rs36204272	donor site	68.6	0	-68.6	-
rs1791228	branch point	60.2	85	24.8	2 nt downstream
Variant	**SR protein**	**Wild-type MS**	**Val30Met MS**	**MS variation**	**Distance from variant**
rs1800458	SC35	0	2.73	2.73	6 nt upstream
	SC35	0	2.67	2.67	2 nt upstream
	SC35	3.02	2.57	-0.45	7 nt upstream
	SF2/ASF site	0	1.99	1.99	6 nt upstream
	SF2/ASF site	4.64	2.73	-1.91	4 nt upstream
	SF2/ASF (IgM-BRCA1) site	4.56	2.86	-1.70	4 nt upstream
rs28933981	*SRp40*	2.81	0	-2.81	6 nt upstream
	SRp55	3.89	0	-3.89	2 nt upstream
	SF2/ASF site	2.03	0	-2.03	-
	SF2/ASF (IgM-BRCA1) site	2.87	0	-2.87	-
rs62093482	SC35	3.73	3.5	-0.23	3 nt upstream
rs1791228	SRp40	3.05	3.71	0.66	3 nt upstream
	SF2/ASF (IgM-BRCA1) site	2.33	2.58	0.25	1 nt upstream

CV, Consensus value; MS, Matrix score; nt, nucleotides; SR protein: Serine and arginine-rich (SR) proteins; SC35, Serine/arginine-rich splicing factor; SF2/ASF, pre-mRNA-splicing factor SF2/alternative splicing factor; SRp40, Splicing factor, arginine/serine rich 40 kDa; Srp55, Splicing factor, arginine/serine rich 55 kDa.

REFERENCES

1. Andrade C. A peculiar form of peripheral neuropathy; familiar atypical generalized amyloidosis with special involvement of the peripheral nerves. Brain. Sep 1952;75(3):408-427.
2. Said G, Ropert A, Faux N. Length-dependent degeneration of fibers in Portuguese amyloid polyneuropathy: a clinicopathologic study. Neurology. Aug 1984;34(8):1025-1032.
3. Saraiva MJ, Birken S, Costa PP, Goodman DS. Amyloid fibril protein in familial amyloidotic polyneuropathy, Portuguese type. Definition of molecular abnormality in transthyretin (prealbumin). J Clin Invest. Jul 1984;74(1):104-119.
4. Koike H, Misu K, Sugiura M, et al. Pathology of early- vs late-onset TTR Met30 familial amyloid polyneuropathy. Neurology. Jul 13 2004;63(1):129-138.
5. Sekijima Y, Ueda M, Koike H, Misawa S, Ishii T, Ando Y. Diagnosis and management of transthyretin familial amyloid polyneuropathy in Japan: red-flag symptom clusters and treatment algorithm. Orphanet J Rare Dis. Jan 17 2018;13(1):6.
6. Sousa A, Coelho T, Barros J, Sequeiros J. Genetic epidemiology of familial amyloidotic polyneuropathy (FAP)-type I in Povoa do Varzim and Vila do Conde (north of Portugal). Am J Med Genet. Dec 18 1995;60(6):512-521.
7. Lemos C, Coelho T, Alves-Ferreira M, et al. Overcoming artefact: anticipation in 284 Portuguese kindreds with familial amyloid polyneuropathy (FAP) ATTRV30M. J Neurol Neurosurg Psychiatry. Mar 2014;85(3):326-330.
8. Santos D, Coelho T, Alves-Ferreira M, et al. Variants in RBP4 and AR genes modulate age at onset in familial amyloid polyneuropathy (FAP ATTRV30M). Eur J Hum Genet. May 2016;24(5):756-760.
9. Santos D, Coelho T, Alves-Ferreira M, et al. Familial amyloid polyneuropathy in Portugal: New genes modulating age-at-onset. Ann Clin Transl Neurol. Feb 2017;4(2):98-105.
10. Dias A, Santos D, Coelho T, et al. C1QA and C1QC modify age-at-onset in familial amyloid polyneuropathy patients. Ann Clin Transl Neurol. . 2019.
11. Sikora JL, Logue MW, Chan GG, et al. Genetic variation of the transthyretin gene in wild-type transthyretin amyloidosis (ATTRwt). Hum Genet. Jan 2015;134(1):111-121.
12. Alves-Ferreira M, Coelho T, Santos D, et al. A Trans-acting Factor May Modify Age at Onset in Familial Amyloid Polyneuropathy ATTRV30M in Portugal. Mol Neurobiol. May 19 2017.
13. Coelho T, Sousa A, Lourenco E, Ramalheira J. A study of 159 Portuguese patients with familial amyloidotic polyneuropathy (FAP) whose parents were both unaffected. J Med Genet. Apr 1994;31(4):293-299.
14. Xu Z, Taylor JA. SNPinfo: integrating GWAS and candidate gene information into functional SNP selection for genetic association studies. Nucleic Acids Res. Jul 2009;37(Web Server issue):W600-605.
15. Khan A, Fornes O, Stigliani A, et al. JASPAR 2018: update of the open-access database of transcription factor binding profiles and its web framework. Nucleic Acids Res. Jan 4 2018;46(D1):D260-D266.
16. Dweep H, Sticht C, Pandey P, Gretz N. miRWalk--database: prediction of possible miRNA binding sites by "walking" the genes of three genomes. J Biomed Inform. Oct 2011;44(5):839-847.
17. Kertesz M, Iovino N, Unnerstall U, Gaul U, Segal E. The role of site accessibility in microRNA target recognition. Nature genetics. Oct 2007;39(10):1278-1284.
18. Coelho T, Chorão R, Sousa A, Alves I, Torres MF, Saraiva MJM. Compound heterozygotes of transthyretin Met30 and transthyretin Met119 are protected from the devastating effects of familial amyloid polyneuropathy. Neuromuscular Disorders. 1996;6(Supplement 1):S20.
19. Fitch NJ, Akbari MT, Ramsden DB. An inherited non-amyloidogenic transthyretin variant, [Ser6]-TTR, with increased thyroxine-binding affinity, characterized by DNA sequencing. J Endocrinol. May 1991;129(2):309-313.
20. Hammarstrom P, Wiseman RL, Powers ET, Kelly JW. Prevention of transthyretin amyloid disease by changing protein misfolding energetics. Science. Jan 31 2003;299(5607):713-716.
21. Mellerup E, Moller GL. Combinations of Genetic Variants Occurring Exclusively in Patients. Comput Struct Biotechnol J. 2017;15:286-289.
22. Xiang Q, Bi R, Xu M, et al. Rare Genetic Variants of the Transthyretin Gene Are Associated with Alzheimer's Disease in Han Chinese. Mol Neurobiol. Sep 2017;54(7):5192-5200.
23. Cartegni L, Chew SL, Krainer AR. Listening to silence and understanding nonsense: exonic mutations that affect splicing. Nat Rev Genet. Apr 2002;3(4):285-298.

24. Wang Z, Burke PA. Hepatocyte nuclear factor-4alpha interacts with other hepatocyte nuclear factors in regulating transthyretin gene expression. FEBS J. Oct 2010;277(19):4066-4075.
25. Saha S, Chakraborty S, Bhattacharya A, Biswas A, Ain R. MicroRNA regulation of Transthyretin in trophoblast differentiation and Intra-Uterine Growth Restriction. Sci Rep. Nov 29 2017;7(1):16548.
26. Alnylam PI. Onpattro (patisiran) lipid complex injection, for intravenous use: US prescribing information. . 2018; Accessed 4 Out 2018.
27. EU. EMA-E. Tegsedi International non-proprietary name: inotersen. Assessment report. . 2018, 31 May 2018.

Supplementary Table 1: Predicted transcription factors (TFs) which have lost (disrupted) or gain (new) affinity to bind in the presence of rs3764479/rs3764478variants.

Disrupted TF	New TF		
NR1H4	JUNB	REL	RREB1
MAFG	JUND	NFATC2	CTCF
ATF4	EGR1	AR	HSF1
IRF1	RELA	TCF7L2	HLF
NFIL3	KLF9	MXI1	CEBPG
MLX	HMBOX1	ZBTB7A	RARA
ATF7	NRF1	MYC	HNF4G
NFYA	KLF4	ESRRA	TEAD2
MEF2B	HEY2	ZBTB7B	ZBTB33
TGIF2	NR4A2	JUN	GMEB2
GLIS3	THAP1	USF2	NR3C1
NKX3-1	ZNF263	BHLHE40	RORA
SOX9	ETV6	SREBF1	MAFF
POU6F1	RELB	NR2C2	TFCP2
MSC	TFDP1	ZIC1	GABPA
HSF2	NFKB2	TFAP4	GATA6
FOXP1	SP1	MNT	MTF1
ESR1	SP3	ELK3	HESX1
	TEAD1	TFEB	RUNX1
	ZNF740	CLOCK	
	TBX15	NFATC3	
	SPI1	RUNX3	
	RBPJ	CEBPD	
	ELK4	SREBF2	
	HEY1	HIF1A	

Article 2 focused on a genetic haplotypic study performed in 155 Val30Met TTR-FAP Portuguese families, from a large homogeneous dataset of TTR-FAP Val30Met Portuguese families with invaluable familial and clinical data which represents a worthy opportunity to perform a haplotypic study.

We aimed to unravel genetic modifiers underlying the AO variability by a haplotype analysis and an association study of variants within or closely linked to the *TTR* gene.

Haplotype frequencies were compared in FAP samples and controls and in parent-offspring pairs. We found that a haplotype is over-represented in chromosomes with the Val30Met mutation in the Portuguese population. Importantly, we identified another haplotype that is transmitted by the non-carrier parent with a trans-acting effect, modulating the phenotypic expression of TTR-FAP Val30Met predisposing to early onset.

Article 2: A *trans*-acting factor may modify age-at-onset in familial amyloid polyneuropathy ATTRV30M in Portugal

Miguel Alves-Ferreira, MSc[1,2]; Teresa Coelho, MD[3]; Diana Santos, MSc[1,2]; Jorge Sequeiros, MD PhD[1,2]; Isabel Alonso, PhD[1,2]; Alda Sousa, PhD[1,2]; Carolina Lemos, PhD[1,2]

[1] UnIGENe, IBMC – Institute for Molecular and Cell Biology; Institute for Research and Innovation in Health Sciences (i3S), University of Porto, Porto, 4200-135, Portugal;

[2] ICBAS - Instituto Ciências Biomédicas Abel Salazar, Universidade do Porto, Porto, 4050-313, Portugal;

[3] Unidade Corino de Andrade (UCA), Centro Hospitalar do Porto (CHP), Largo Prof. Abel Salazar, Porto, 4050, Portugal.

Corresponding Author:
Carolina Lemos, PhD
Invited Auxiliary Professor, ICBAS
UnIGENe, IBMC-i3S
Rua Jorge Viterbo Ferreira, 228
4050-313 Porto
Telefone: +351 22 042 80 02
*e-mail: clclemos@ibmc.up.pt

Published in Mol Neurobiol. 2018 May;55(5):3676-3683.
DOI 10.1007/s12035-017-0593-4
Springer Group

ACKNOWLEDGEMENTS

The authors thank all the patients and families for participating in this study and Vanessa Costa (from Unidade Corino de Andrade (UCA), Centro Hospitalar do Porto (CHP)) for all the help in data collection. This work was supported by grants of Fundação para a Ciência e Tecnologia, FCT [PTDC/SAU-GMG/100240/2008 and PEsT], co-funded by ERDF and COMPETE; and by Financiamento Plurianual de Unidades de Investigação (FCT).

ABSTRACT

Although all familial amyloid polyneuropathy (FAP) ATTRV30M patients carry the same causative mutation, early (<40) and late-onset forms (≥50 years) of FAP may coexist in the same family. However, this variability in age-at-onset is still unexplained.
To identify modifiers closely linked to the *TTR locus* that may in part be associated with age-at-onset of FAP ATTRV30M, in particular in a group of very-early onset patients (≤30 years) when compared with late-onset individuals.

A clinical genetic study at a referral center comprising a sample of 910 Portuguese individuals (including 589 Val30Met carriers, 102 spouses and 189 controls from the general population). Haplotype analysis was performed, using eight intragenic single nucleotide polymorphisms (SNPs) at the *TTR locus*. We compared haplotypes frequency in FAP samples and controls and in parent-offspring pairs using appropriated statistical analysis.

Haplotype A was the most common in the general population. Noteworthy, haplotype C was more frequent in early-onset (<40) than in late-onset patients (≥50 years) (p=0.012). When comparing allelic frequencies of each SNP within haplotype C between “very early” (≤30yrs) and late-onset (≥50yrs) cases, the A allele of rs72922947 was associated with an earlier onset (p=0.009); this remained significant after a permutation-based correction. Also, the heterozygous genotype (GA) for this SNP was associated with a decrease in mean age-at-onset of 8.6 years (p=0.014).

We found a more common haplotype (A) linked to the Val30Met variant and a possible modulatory *trans* effect on age-at-onset. These findings may lead to potential therapeutical targets.

Keywords

Familial amyloid polyneuropathy (FAP); transthyretin-related amyloidosis; *trans* effect; transthyretin (TTR); age-at-onset; haplotype;

INTRODUCTION

Familial amyloid polyneuropathy (FAP [MIM: 105210]) ATTRV30M is a severe autosomal dominant (AD) systemic amyloidosis, first described by Andrade in Portugal in 1952 [1] as occurring mainly between the ages of 25 to 35 years. It is due to a sequence variant in the transthyretin (*TTR* [MIM: 176300]) gene (chr18q12.1); more than 100 disease-causing variants have been found in the *TTR* gene, but Val30Met (Val50Met, following HGVS) is by far the commonest, including in Portugal [2].

A wider variability in age-at-onset (AO) has been uncovered along the years, including among Portuguese patients [19-82 yrs] [3,4]. Remarkable differences in the distribution of AO were found among FAP clusters associated to Val30Met (Portugal: 35.1; Brazil: 34.5; Japan: 33.8; Sweden: 56.7; Balearic Islands: 45.7 yrs, in mean AO) [5,3,6-8]. A large variation is found, nevertheless, within a single geographical area and even within the same family.

Early (AO <40 yrs) and late-onset cases (AO ≥50) often coexist in the same family, with offspring often showing an earlier AO than their affected parent (anticipation). We have shown that anticipation is a true biological phenomenon in FAP Portuguese families, some parent-offspring pairs showing ≥10 years of difference in AO [9].

This variability in AO is still unexplained. One of the possible hypotheses is the existence of genetic modifiers within or close to the TTR *locus*. A *cis*-acting effect of closely linked *TTR* gene modifiers has been for long postulated by our group[10,4].

Additionally, Coelho *et al.* found that 40% of the probands had no affected parent at the time of diagnosis: onset in the transmitting parent happened only after the proband's or the transmitting parent may even die at late-age without disease symptoms [11]. These probands, however, had a mean later AO (45.1 yrs) than those with one affected parent (31.2 yrs) [11]. In addition, late-onset cases (≥50 yrs) often had offspring with very early-onset (≤30 yrs), but the reverse was never found: that 'protection' may be lost in just one generation [9]. This raised the hypothesis of a closely linked modifier, and shows we need to concentrate in the differences within the same population and, whenever possible, the same family.

Previous studies with haplotypes have been performed in FAP but most of them focused only on the origin of the mutation [12,13]. Only one major disease haplotype has been found among Portuguese patients [14,15]. Soares *et al* [15] found that onset could be modulated by a region

downstream the TTR *locus* in the non-carrier chromosome. Our aim now was to identify genetic modifiers within or closely linked to the *TTR* gene.

SUBJECTS AND METHODS

Subjects

Unidade Corino de Andrade - UCA (Hospital Santo António, Centro Hospitalar do Porto: HSA, CHP) has the largest dataset of FAP ATTRV30M worldwide, with registries that have been collected and clinically characterized over 75 years (since Andrade's first observation, in 1939), by the same team of neurologists. This dataset has invaluable familial and clinical information (including information on AO), from which we collected 721 samples, belonging to 155 families with DNA available from at least two relatives; from this group, 589 were Val30Met carriers whilst 132 were healthy individuals (spouses and non-carrier siblings) from the same families, that helped in haplotype's reconstruction (Table 1). All spouses were genotyped for Val30Met mutation and found to be non-carriers. Additionally, we evaluated 101 parent-offspring transmissions for haplotypes construction and allelic transmission. We also used 189 controls (63 trios) non-V30M from the general population, previously ascertained at the Centro de Genética Preditiva e Preventiva (CGPP, IBMC-i3S) biobank, authorized by CNPD (National Commission for Data Protection). Written informed consent was obtained for all participants and the Ethics Committee of HSA, CHP, approved this study. Late-asymptomatic carriers (≥50 yrs) were included in the late-onset sample in order to increase the sample power.

Methods

Definition of age-at-onset (AO) and AO groups

AO was defined, as before [3], as the beginning of the first symptoms (either sensitive or dysautonomic), coincident with an abnormal neurological or neurophysiological observation, reported by the neurologist. Although AO is described in the literature as early (<40) and as late-onset (≥50 yrs), in addition, we introduced here a "very early" sub-group for patients with onset ≤30 yrs in order to further explore this high-risk group as described in [9].

Genomic DNA extraction

Genomic DNA was isolated from peripheral blood leucocytes, using a standard salting-out method [16]; or from saliva, using ORAGENE® kits, according to manufacturer's instructions (DNA Genotek Inc. Kanata, ON, Canada).

Selection of single-nucleotide polymorphisms (SNPs)

We selected SNPs based on data available for the Caucasian population in the International HapMap project (Release 24, November 2008, on NCBI B36 assembly, dbSNP build 126) and the 1000 genomes database. Eight SNPs were selected due to their short genetic distance to Val30Met mutation and genotyped, from which 4 were tagging SNPs, selected using Haploview v.4.1 [17], with the following parameters: r2>0.8 (as a measure of linkage disequilibrium, LD) and a minor allele frequency (MAF) ≥0.10. These parameters allowed selecting tagging SNPs covering a total of 57kb of the common variation present in the *TTR* gene (Table 2). The other four SNPs were selected according to previous descriptions of Soares *et al* [15] and Li *et al* [18].

Genotyping

For the selected SNPs, PCR primers were designed using the software Primer3; dimer and hairpin formation were excluded using Autodimer. Primer sequences are available upon request.

The multiplex PCR reaction was performed using the Multiplex PCR Master Mix (Qiagen, Hilden, Germany), and experiments conducted according to the standard protocol. After PCR, unincorporated deoxynucleotides (dNTPs) were removed with ExoSAP-IT (USB Corporation, Cleveland, OH), as recommended by the manufacturer. The SNaPshot technique was used to perform allelic discrimination of SNPs. The probes were also tested in AutoDimer software. Probes sequences are also available upon request. The SNaPshot (Applied Biosystems, Carlsbad, CA) reaction was performed according to manufacturer's instructions. After the mini-sequencing reaction, the excess of ddNTPs was removed by incubating the SNaPshot reaction with SAP (Shrimp Alkaline Phosphatase, USB Corporation), as recommended by the manufacturer. The SNaPshot products were loaded in an ABI-PRISM 3130 XL genetic analyzer (Applied Biosystems) and genotyped with GeneMapper 4.0 software (Applied Biosystems). To confirm uncertain genotypes, some individuals were additionally genotyped by sequencing. Sequencing was performed using the Big Dye Terminator Cycle Sequencing v1.1 Ready Reaction (Applied

Biosystems), according to the manufacturer's instructions, and samples loaded on an ABI-PRISM 3130 XL genetic analyzer (Applied Biosystems).

Haplotypes were constructed in informative families and inferred, using SNPator software, whenever the phase could not be directly determined [19].

Statistical and SNPs analysis

Allelic frequencies were compared in early vs. late cases using Haploview 4.1 with all parameters set at the default values. In order to correct for multiple comparisons, tests were performed using 10,000 permutations [17].

Since we included in the analysis several members of the same family, each patient was 'nested' in his/her family. To account for non-independency of AO between members of the same family, we performed a weighted analysis using generalized estimating equations (GEEs) [20]. Therefore, we assessed any simultaneous association of the different variants with AO (as the dependent variable), using the most common genotype as the reference category. The unstandardized coefficient (B) corresponds to the mean AO variation observed in the individuals carrying a specific genotype when compared with the reference category.

To compare haplotypes frequency in FAP samples and controls and in parent-offspring pairs, a chi-square test was used and odds ratios (OR) estimated, with 95% confidence intervals (CI). These analyses were performed using IBM SPSS Statistics software (v.20; Armonk, NY, USA).

The software is-rSNP (for *in silico* regulatory SNP detection) was used to explore putative changes in the transcription factors binding capacity due to the variants present. We set the significance level for the is-rSNP analysis at 0.05 and the JASPAR database was used as reference [21].

RESULTS

We studied 8 SNPs at the TTR *locus* in a sample of 910 Portuguese individuals, comprising 589 Val30Met carriers, in order to search for genetic modifiers closely linked to the TTR *locus*.

Construction of haplotypes

We surveyed the genetic variation across a 57kb region spanning the TTR *locus* and the haplotypes were reconstructed, using eight SNPs: rs875119, rs3764478, rs1800458, rs72922947, rs7235277, rs62093482, rs1791228 and rs4799586 (Fig. 1).

The estimated haplotype frequencies in FAP patients (just one patient per family) and controls are shown in Table 3. The most common was haplotype A, both in FAP patients (68.7%) and the control group (47.6 %), followed by haplotype D. Haplotype A, however, was relatively more frequent ($p<0.001$) in mutation carriers than in controls (haplotype A against all other haplotypes); there were no significant differences in the relative frequencies of other haplotypes between patients and controls.

Parent-offspring transmissions

When looking at haplotypes' transmission, haplotype D was preferentially transmitted by the non-carrier parent ($p<0.001$). On the other hand, haplotype A was strongly associated with Val30Met: in 97 (96%) of the 101 transmissions, haplotype A co-segregated with the mutation, while haplotype D corresponded to the other 4 families. Presence of haplotypes A and D did not determine anticipation (>10 years) ($p>0.05$). The sex of the transmitting parent did not show any association with the haplotypes transmitted when comparing early to late-onset patients. There was, nevertheless, a trend towards early AO in the offspring when the carrier parent transmitted haplotype D compared to other haplotypes altogether (except haplotype A) ($p=0.055$). Importantly, we found that haplotype C is always transmitted by the non-carrier parent.

Very-early vs. late-onset cases

When we analyzed the haplotype distribution between very early (≤30 yrs) and late-onset (≥50 yrs) patients, haplotype A was clearly the most frequent in both groups (over 50%); but, importantly, haplotype C was more frequent in very early than in late-onset patients ($p=0.009$) (Fig. 2).

Analysis of allele frequencies

Comparing allelic frequencies of each SNP between very early (≤30 yrs) and late-onset (≥50 yrs), we found an association of the A allele of rs72922947 with very early-onset (p=0.009); this remained significant after permutation-based correction (table 4). These results remained significant when we expanded this group to early-onset cases (≤40 yrs); however, this did not remain significant after permutation-based correction (10,000 permutations) (not shown).

Also, the rs72922947 A allele frequency in the control sample did not differ significantly from that found in the 1,000 Genomes project for Utah Residents (CEPH) with northern and western European ancestry (p>0.05). On the other hand, there was a slightly increased frequency of the A allele in very early-onset patients, when compared with 1,000 Genomes database (0.033 and 0.012, respectively) (table 4), although the differences were not significant (p>0.05).

Analysis of genotype frequencies

In a group of 429 patients and in accordance with the results found in the analysis of alleles, the GA genotype of rs72922947 was associated with a significant decrease in AO (p=0.014), a mean difference of 8.58 years, when compared with the GG genotype (the reference class) (B, - 8.58; 95% CI, -15.46 to -1.70) (Fig. 3).

Functional impact*: in silico* analysis

We performed an *in silico* analysis using is-rSNP, with particular attention to rs72922947. The is-rSNP algorithm reported that the DNA binding affinity of three transcription factors is significantly affected by this SNP (LM58, p=0.005; LM56, p=0.01; and LM233, p=0.023).

Additionally, we have also analyzed SNPs in linkage disequilibrium with rs72922947, and found that rs72922938 may alter the TP53 (p=0.001) binding site in the *TTR* gene (Fig. 4).

DISCUSSION

Variability in AO in FAP ATTRV30M has been a most intriguing feature and the object of some previous research. Our strategy now was to identify genetic modifiers within the TTR (FAP) *locus*, or closely linked to it, that might modulate AO, using a haplotype study. We found a haplotype (and a specific variant within it) that confers an increased risk to “very early”-onset patients, which

may partially explain the earlier onset in the offspring, when transmitted by the non-carrier parent (*trans* effect).

Unraveling TTR variants associated with AO modulation

We confirmed a possible *trans* effect on AO, exerted by haplotype C (more frequent in very- early and early than in late-onset cases). All patients with this haplotype received it from the non-carrier parent and the haplotype A from the affected parent, confirming the hypothesis of a *trans*-acting factor within the TTR *locus* associated with AO variability.

The rs72922947 (c.200+795G>A), located within intron 2 of the *TTR* gene, is represented by the minor allele A in haplotype C, distinguishing this from the other haplotypes that carried the common allele G. Both allelic and genotypic analysis showed a significant association with an earlier AO. Accordingly, carriers of the GA genotype tend to show a decrease of AO, on average of nearly 9 years. Furthermore, allele A is a risk factor strongly associated with (at least) very early-onset (≤30 yrs).

In addition, our results show that the A allele is more frequent in the very-early onset cases than expected according to the frequency in Portuguese controls (similar to those on the 1,000 Genomes project data for Utah Residents (CEPH) with Northern and Western European ancestry). This reinforces the findings that the minor allele A of rs72922947 was overrepresented in our FAP cohort.

In silico analysis

The *in silico* analysis of TFBS (transcription factors binding sites) allowed us to estimate the probability of modulation by this SNP of the expression/activity of TTR that could drive the clinical presentation of the disease. Few studies have investigated the role of non-coding SNPs in the *TTR* gene and its possible functional consequences. Polimanti *et al.* identified 59 non-coding variants that may have a functional impact on the *TTR* gene, including rs72922947; however, further studies were required to understand the role of this variant [22]. Three transcription factors binding sites (LM56, LM58 and LM233) were predicted to be disrupted by rs72922947. The minor allele (A) was predicted to have less affinity for all these transcription factors; however, there are scarce data about the role of these TFBS. Additionally, we verified that rs72922938, a SNP that is in linkage disequilibrium with rs72922947 may alter the TP53 binding site. TP53 has been

reported as a genetic modifier of AO in several cancers, as well as in Huntington disease (HD) in which only 30-70% of the variance in AO may be explained by the CAG repeat size alone [23].

These results will enable us to test new hypotheses. Whether this rs72922947 is itself the functional polymorphism responsible for exerting a direct effect on the *TTR* gene expression, or if it is only in linkage disequilibrium with the functional SNP is still an open question.

These hypotheses have also been assessed in other neurodegenerative diseases like HD, where common genetic variants near the mutation site were explored as possibly associated with AO, although no significant results were found [24].

In a previous study, Soares *et al.* focused mainly on comparing extended haplotypes in 18 late-onset (onset ≥50 yrs) and 19 "classic-onset" patients (<40 yrs), versus controls [15]. It was suggested a possible modulatory effect on AO, exerted by a *locus* within or closely linked to the interval between microsatellites D18S457 and D18S456 (but not by the immediately 5' and 3' TTR flanking sequences), and associated with the non-carrier chromosome (i.e., a *trans*-acting effect more frequent in late than in early-onset cases). This failed, however, to reach significance, possibly due to the effect being too small and/or to small sample size. Likewise, the variation within the same family and, particularly, within and among generations was not taken into account. These results still lack validation. Our study showed a similar effect but now within the TTR (FAP) *locus* itself.

Recently, Sikora *et al.* found a nearly significant association between wild-type TTR amyloidosis and rs1800458; a variant in this SNP was predicted to be protector despite the acknowledgment that their results are insufficient to prove this [25]. In our study, this variant showed no statistically significant results that could indicate a putative association with AO. On the other hand, these authors confirmed that this missense variant is non-pathogenic.

In a sample of Swedish patients, which is characterized by low penetrance and high AO, all four TTR exons and flanking regions were sequenced [15]. In that study, rs62093482 was the only SNP which effect was significant after correction for multiple testing; since this is located in the 3' UTR, it was suggested that it could affect TTR expression levels by modifying microRNA binding. Later functional studies, however, did not confirm this [26]. Thus, as reported in this paper, the rs62093482 does not seem to act as a modifier of AO variability.

Conclusions

Haplotype A, followed by haplotype D, is over-represented in chromosomes with the Val30Met mutation in the Portuguese population. Haplotype C is transmitted by the non-carrier parent as described in the Results.

A *trans*-acting effect modulates the phenotypic expression of FAP ATTRV30M, with a sequence variant (A) and genotype (GA) predisposing to early onset. Since we found in a previous study [9] that parents with an AO ≤30 years also have a higher risk of also having offspring with AO ≤30 years, the study of these very-early onset patients helped us to define higher-risk groups where it is important to look for genetic modifiers.

Understanding some of the mechanisms that may influence AO may help predicting AO, which will be of importance for genetic counseling and the follow-up of presymptomatic carriers. These results may prove useful for therapeutic strategies, as the identification of risk genetic modifiers associated with AO (early vs. late-onset, non-penetrance) will have important clinical implications.

Conflict of interest disclosures:

M.A.F. and D.S. have received research support from a FCT fellowship (SFRH/BD/101352/2014 and SFRH/BD/91160/2012, respectively). T. C.'s institution has received support from FoldRx Pharmaceuticals, which was acquired by Pfizer Inc in October 2010; T. C. has served on the scientific advisory board of Pfizer Inc and received funding from Pfizer Inc for scientific meeting expenses (travel, accommodations, and registration). She currently serves on the THAOS (natural history disease registry) scientific advisory board. J. S., I. A., A. S. and C. L. report no disclosures.

REFERENCES

1. Andrade C (1952) A peculiar form of peripheral neuropathy; familiar atypical generalized amyloidosis with special involvement of the peripheral nerves. Brain 75 (3):408-427
2. Benson MD (2012) Pathogenesis of transthyretin amyloidosis. Amyloid 19 Suppl 1:14-15. doi:10.3109/13506129.2012.668501
3. Sousa A, Coelho T, Barros J, Sequeiros J (1995) Genetic epidemiology of familial amyloidotic polyneuropathy (FAP)-type I in Povoa do Varzim and Vila do Conde (north of Portugal). Am J Med Genet 60 (6):512-521. doi:10.1002/ajmg.1320600606
4. Sequeiros J, Saraiva MJ (1987) Onset in the seventh decade and lack of symptoms in heterozygotes for the TTRMet30 mutation in hereditary amyloid neuropathy-type I (Portuguese, Andrade). Am J Med Genet 27 (2):345-357. doi:10.1002/ajmg.1320270213
5. Sousa A, Andersson R, Drugge U, Holmgren G, Sandgren O (1993) Familial amyloidotic polyneuropathy in Sweden: geographical distribution, age of onset, and prevalence. Hum Hered 43 (5):288-294
6. Saporta MA, Zaros C, Cruz MW, Andre C, Misrahi M, Bonaiti-Pellie C, Plante-Bordeneuve V (2009) Penetrance estimation of TTR familial amyloid polyneuropathy (type I) in Brazilian families. Eur J Neurol 16 (3):337-341. doi:10.1111/j.1468-1331.2008.02429.x
7. Munar-Ques M, Saraiva MJ, Viader-Farre C, Zabay-Becerril JM, Mulet-Ferrer J (2005) Genetic epidemiology of familial amyloid polyneuropathy in the Balearic Islands (Spain). Amyloid 12 (1):54-61. doi:Q3K8R92P20M6G7QG
8. Ikeda S, Hanyu N, Hongo M, Yoshioka J, Oguchi H, Yanagisawa N, Kobayashi T, Tsukagoshi H, Ito N, Yokota T (1987) Hereditary generalized amyloidosis with polyneuropathy. Clinicopathological study of 65 Japanese patients. Brain 110 (Pt 2):315-337
9. Lemos C, Coelho T, Alves-Ferreira M, Martins-da-Silva A, Sequeiros J, Mendonca D, Sousa A (2014) Overcoming artefact: anticipation in 284 Portuguese kindreds with familial amyloid polyneuropathy (FAP) ATTRV30M. J Neurol Neurosurg Psychiatry 85 (3):326-330. doi:10.1136/jnnp-2013-305383
10. Sousa A (1995) A Variabilidade Fenotípica da Polineuropatia Amiloidótica Familiar: um estudo de Genética Quantitativa em Portugal e na Suécia. ICBAS, Univ Porto: Porto
11. Coelho T, Sousa A, Lourenco E, Ramalheira J (1994) A study of 159 Portuguese patients with familial amyloidotic polyneuropathy (FAP) whose parents were both unaffected. J Med Genet 31 (4):293-299
12. Zaros C, Genin E, Hellman U, Saporta MA, Languille L, Wadington-Cruz M, Suhr O, Misrahi M, Plante-Bordeneuve V (2008) On the origin of the transthyretin Val30Met familial amyloid polyneuropathy. Ann Hum Genet 72 (Pt 4):478-484. doi:AHG439
13. Yoshioka K, Furuya H, Sasaki H, Saraiva MJ, Costa PP, Sakaki Y (1989) Haplotype analysis of familial amyloidotic polyneuropathy. Evidence for multiple origins of the Val----Met mutation most common to the disease. Hum Genet 82 (1):9-13
14. Almeida MR, Aoyama-Oishi N, Sakaki Y, Holmgren G, Drugge U, Ferlini A, Salvi F, Munar-Quès M, Benson MD, Skinner M, Costa PP, Saraiva MJ (1995) Haplotype analysis of common transthyretin mutations. HumGenet
15. Soares ML, Coelho T, Sousa A, Holmgren G, Saraiva MJ, Kastner DL, Buxbaum JN (2004) Haplotypes and DNA sequence variation within and surrounding the transthyretin gene: genotype-phenotype correlations in familial amyloid polyneuropathy (V30M) in Portugal and Sweden. Eur J Hum Genet 12 (3):225-237. doi:10.1038/sj.ejhg.5201095
16. Miller SA, Dykes DD, Polesky HF (1988) A simple salting out procedure for extracting DNA from human nucleated cells. Nucleic Acids Res 16 (3):1215
17. Barrett JC, Fry B, Maller J, Daly MJ (2005) Haploview: analysis and visualization of LD and haplotype maps. Bioinformatics 21 (2):263-265. doi:10.1093/bioinformatics/bth457

18. Ii S, Sommer SS (1993) The high frequency of TTR M30 in familial amyloidotic polyneuropathy is not due to a founder effect. Hum Mol Genet 2 (8):1303-1305
19. Morcillo-Suarez C, Alegre J, Sangros R, Gazave E, de Cid R, Milne R, Amigo J, Ferrer-Admetlla A, Moreno-Estrada A, Gardner M, Casals F, Perez-Lezaun A, Comas D, Bosch E, Calafell F, Bertranpetit J, Navarro A (2008) SNP analysis to results (SNPator): a web-based environment oriented to statistical genomics analyses upon SNP data. Bioinformatics 24 (14):1643-1644. doi:10.1093/bioinformatics/btn241
20. Zeger SL, Liang KY (1986) Longitudinal data analysis for discrete and continuous outcomes. Biometrics 42 (1):121-130
21. Macintyre G, Bailey J, Haviv I, Kowalczyk A (2010) is-rSNP: a novel technique for in silico regulatory SNP detection. Bioinformatics 26 (18):i524-530. doi:10.1093/bioinformatics/btq378
22. Polimanti R, Di Girolamo M, Manfellotto D, Fuciarelli M (2014) In silico analysis of TTR gene (coding and non-coding regions, and interactive network) and its implications in transthyretin-related amyloidosis. Amyloid 21 (3):154-162. doi:10.3109/13506129.2014.900487
23. Chattopadhyay B, Baksi K, Mukhopadhyay S, Bhattacharyya NP (2005) Modulation of age at onset of Huntington disease patients by variations in TP53 and human caspase activated DNase (hCAD) genes. Neurosci Lett 374 (2):81-86. doi:S0304-3940(04)01270-4
24. Lee JM, Gillis T, Mysore JS, Ramos EM, Myers RH, Hayden MR, Morrison PJ, Nance M, Ross CA, Margolis RL, Squitieri F, Griguoli A, Di Donato S, Gomez-Tortosa E, Ayuso C, Suchowersky O, Trent RJ, McCusker E, Novelletto A, Frontali M, Jones R, Ashizawa T, Frank S, Saint-Hilaire MH, Hersch SM, Rosas HD, Lucente D, Harrison MB, Zanko A, Abramson RK, Marder K, Sequeiros J, MacDonald ME, Gusella JF (2012) Common SNP-based haplotype analysis of the 4p16.3 Huntington disease gene region. Am J Hum Genet 90 (3):434-444.
25. Sikora JL, Logue MW, Chan GG, Spencer BH, Prokaeva TB, Baldwin CT, Seldin DC, Connors LH (2015) Genetic variation of the transthyretin gene in wild-type transthyretin amyloidosis (ATTRwt). Hum Genet 134 (1):111-121. doi:10.1007/s00439-014-1499-0
26. Norgren N, Hellman U, Ericzon BG, Olsson M, Suhr OB (2012) Allele specific expression of the transthyretin gene in swedish patients with hereditary transthyretin amyloidosis (ATTR V30M) is similar between the two alleles. PLoS One 7 (11):e49981. doi:10.1371/journal.pone.0049981

FIGURES

Fig. 1. Structure of the estimated haplotypes and position of the SNPs relatively to *TTR*

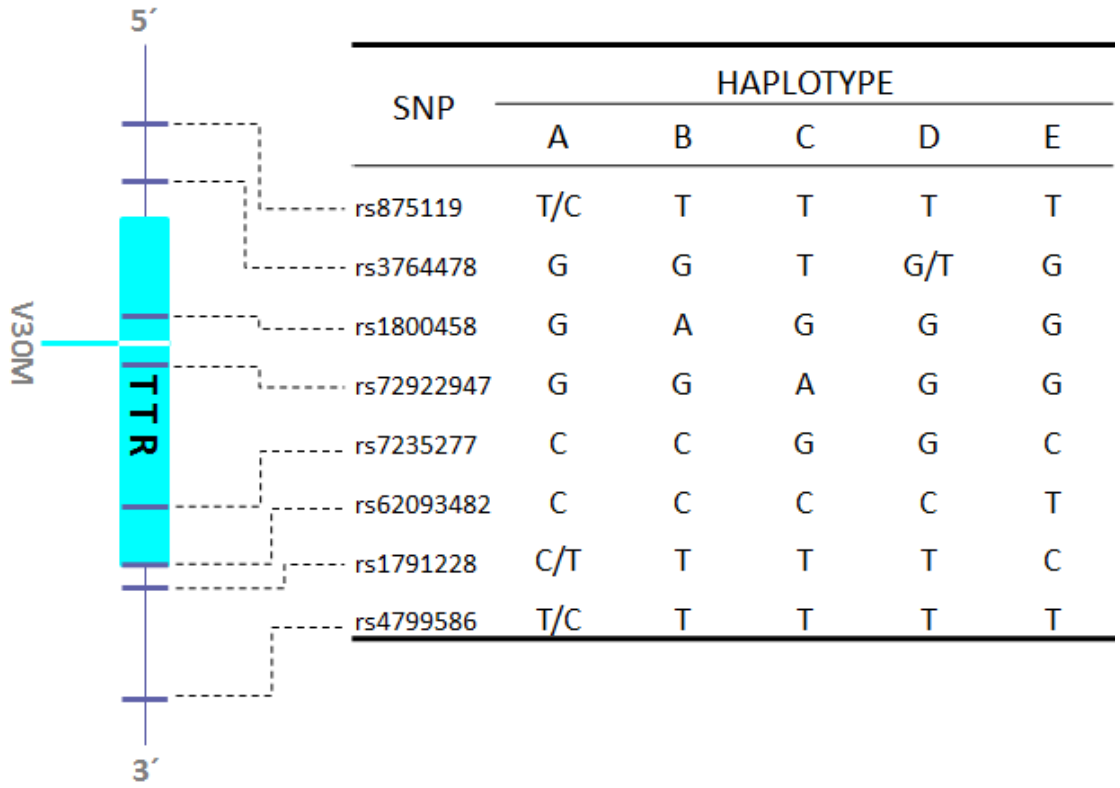

SNP	HAPLOTYPE				
	A	B	C	D	E
rs875119	T/C	T	T	T	T
rs3764478	G	G	T	G/T	G
rs1800458	G	A	G	G	G
rs72922947	G	G	A	G	G
rs7235277	C	C	G	G	C
rs62093482	C	C	C	C	T
rs1791228	C/T	T	T	T	C
rs4799586	T/C	T	T	T	T

The 8 single nucleotide polymorphism (SNP) used for the haplotypes constructed and their location across a 57kb region spanning the *TTR locus*

Fig. 2. Haplotype distribution in Val30Met carriers in very early (≤30 yrs) *vs.* late-onset patients (≥50 yrs)

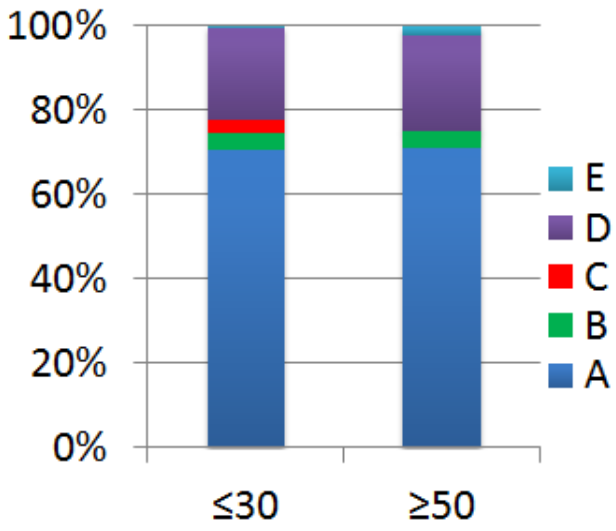

Haplotype	≤30	≥50
A	151	208
B	9	11
C	7	1
D	46	66
E	1	6
Total	214	292

Fig. 3. Genotypic variation in rs72922947 according to age-at-onset

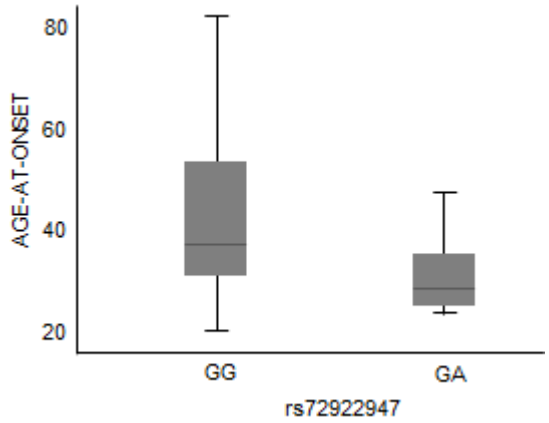

Box-plots showing the association of rs72922947 with age-at-onset, by genotype (GG and GA); none of our subjects carried the rare homozygous genotype (AA)

Fig. 4. The sequence logos of the three TFBS potentially disrupted by rs72922947 and rs72922938

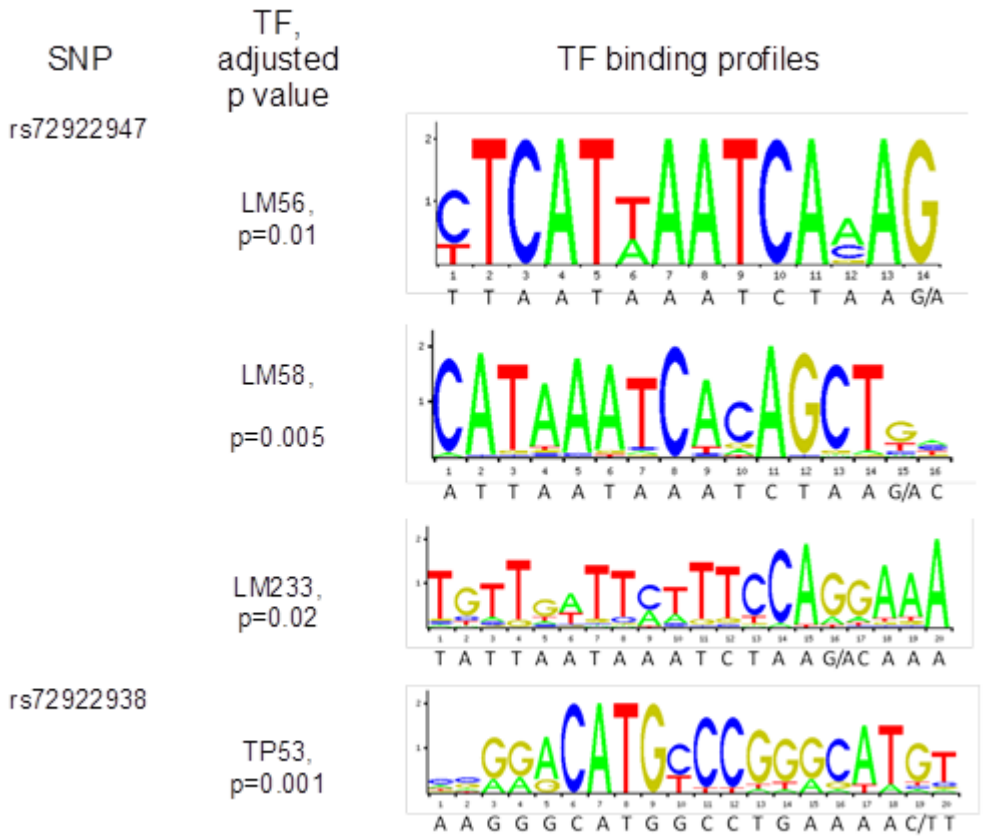

Transcription factor (TF) binding sites (TFBS) potentially disrupted by the TTR single nucleotide polymorphisms (SNPs). The logo plots created by is-rSNP[188] were matched manually to the gene sequence surrounding the marked SNP, as shown below by the transcription factor binding profile (the SNP alleles are shown with the common allele listed first; SNP alleles that differ from taller letters in the binding profile have the largest potential impact)

TABLES

Table 1. Age-at-onset, gender distribution and disease status in the study group

Healthy individuals		**Val30Met carriers**						
Spouses	102		**<=30**	**31-40**	**41-49**	**>=50**	**Assint <50**	**Assint >=50**
Non-carriers siblings	30	**Male**	72	51	12	53	60	12
Male	69	**Female**	35	80	33	60	100	21
Female	63	**Total**	107	131	45	113	160	33

Table 2. SNPs in LD with targeted SNP (threshold for LD is r2 > 0.8)

Targeted SNP	SNPs in LD	Targeted SNP	SNPs in LD
rs875119	rs1791185	rs62093482	rs62093482
	rs875120	rs1791228	rs1791228
	rs875119	rs4799586	rs12458967
rs3764478	rs3764478		rs13381522
rs1800458	rs1800458		rs17740990
rs72922947	rs72922938		rs1791185
	rs72922947		rs1791190
rs7235277	rs1791200		rs1791196
	rs723744		rs1791206
	rs3794884		rs3764477
	rs1080093		rs4799580
	rs1667254		rs4799586
	rs7235277		rs4799587
	rs3764476		rs875119
	rs1791198		rs9948445
	rs3764479		rs4799586
	rs1791199		
	rs1611949		
	rs1667255		
	rs7235277		

SNP, single-nucleotide polymorphism; LD, linkage disequilibrium

Table 3. Haplotype frequency in Val30Met carriers (just one patient per family) and unrelated controls

Haplotype	Val30Met (n=155) *(%)*	Controls (n=189) *(%)*
A[a]	213 *(68.7)*	180 *(47.6)*
B	10 *(3.2)*	23 *(6.1)*
C	4 *(1.3)*	4 *(1.1)*
D	77 *(24.8)*	152 *(40.2)*
E	6 *(2)*	14 *(3.7)*
O	0 *(0)*	5 *(1.3)*

[a] Haplotype A was relatively more frequent ($p<0.001$) in mutation carriers than in controls

Table 4. Allelic analysis comparing very early (≤30) vs. late onset (≥50 yrs) patients

	rs72922947 alleles					
	Very early onset (n=107)	Late onset (n=146)	X^2	OR (95% CI)	p-value	p-value after permutation
A	7	1				
	(3.3%)	*(0.3%)*	6.81	9.84 (1.20-80.59)	0.009*	0.036*
G	207	291				
	(96.7)%	*(99.7)%*				

OR, odds ratio; CI, confidence interval; *p<0.05

During the **Article 3** we focused in the daunting and important task of understanding the complex genetic factors involved in anticipation. Our central idea was that the search for genetic modifiers will be better pursuit concentrating in a family-centered approach and that modifier gene(s) with major effects are more likely to be detected when searching for generational effects within late-onset and incomplete penetrance families with large anticipation of AO in the offspring. We were interested in variants that may act either as a risk factor for early-onset cases or as a protective factor for late-onset patients and to compare the genetic profile of early- and late-onset patients.

For this purpose, we performed a whole-genome sequencing in two TTR-FAP Val30Met families, comprising 3 generations with large anticipation. A variant in *MYH11* (smooth muscle myosin heavy chain) gene was found in patients with early-onset that was inherited from the non-Val30Met parent. This variant possibly has a great functional impact, since it is located in an important region of the myosin protein.

Putative new pathways and protein-protein interaction have been identified that may pinpoint specific components that are modulated during disease course and also might open new research theories into other neurodegenerative diseases that share similar mechanisms.

Article 3: Large anticipation of genetic TTR Familial Amyloid Polyneuropathy Val30Met: *MYH11* gene as a putative modulator

Miguel Alves-Ferreira, MSc[1, 2]; Teresa Coelho, MD[3]; Jorge Sequeiros, MD PhD[1, 2]; Alda Sousa, PhD[1, 2]; Carolina Lemos, PhD[1, 2]

[1] UnIGENe, IBMC – Institute for Molecular and Cell Biology; i3S – Instituto de Investigação e Inovação em Saúde, Universidade do Porto, Portugal;

[2] ICBAS - Instituto Ciências Biomédicas Abel Salazar, Universidade do Porto, Portugal;

[3] Unidade Corino de Andrade (UCA), Centro Hospitalar do Porto (CHP), Largo Prof. Abel Salazar, Porto, Portugal.

Corresponding Author:
Carolina Lemos, PhD
Invited Auxiliary Professor, ICBAS
UnIGENe, IBMC-i3S
Rua Jorge Viterbo Ferreira, 228
4050-313 Porto
Telephone: +351 22 042 80 02
E-mail: clclemos@ibmc.up.pt

In preparation

ABSTRACT

Familial Amyloid Polyneuropathy (FAP) is an autosomal dominant systemic amyloidosis, showing sensorimotor symptoms and progressive incapacity, leading to death 10-15 years after onset. FAP occurs as a result of an inherited point variant in the transthyretin (*TTR*) gene, Val30Met being the commonest. This disorder shows anticipation of age-at-onset (AO) - an earlier-onset in the offspring when compared with the affected late-onset parent. This variation suggests that genetic modifiers, either conferring protection or increasing risk, contribute to clinical manifestation in TTR-FAP.

The aim of this study was to explore other genes and mechanisms that may act as AO modifiers in TTR-FAP. To accomplish this, we collected DNA samples of TTR-FAP Val30Met families with large anticipation. We performed a whole-genome sequencing on six patients from 2 families, comprising 3 generations. Anticipation was obvious in the selected families with a mean decrease in AO of 20 years in each generation, resulting for both families, in a difference of ≈ 40 years in AO between the grandmother and the grandchild. We then compared genetic variants between these extremes (early- and late-onset).

We identified a heterozygous missense variant in *MYH11* (smooth muscle myosin heavy chain) gene, c.4625G>A (p.Arg1542Gln), in the two affected grandsons that is absent in the patients of previous generations. The results were confirmed by Sanger sequencing. This rare variant is evolutionarily conserved in the protein encoded by *MYH11* gene and is located within the coiled coil region. *In silico* tools predicted that Arg1542Gln variant disrupts the structure or function of myosin. We also generated a protein–protein interaction network that allows us to predict functional associations between TTR pathways with several genes of interest such as *APP* and *ROCK2*. These findings collectively point towards a mutual regulatory relationship in AO variability between TTR and MYH11 activity. Functional studies of MYH11 in the pathogenesis of TTR-FAP will be validated in the future regarding phenotype and potential signaling pathways.

Familial-based deep sequencing provides the most robust approach for definition of the genetic determinants of anticipation that can help us to find new mechanisms related with AO variability in TTR-FAP.

Identifying novel genetic modifiers and their pathways may pinpoint specific components that are modulated during disease course, leading to potential druggable targets that ultimately results in new therapeutic strategies. Furthermore, since TTR-related amyloidoses share the main pathogenic mechanism with other neurodegenerative disorders

(as Alzheimer disease), exploring these factors may also have an impact in the understanding of their clinical manifestation.

INTRODUCTION

Clinical heterogeneity is a common characteristic of most neurological diseases. Variability in age-at-onset (AO) is common in Familial Amyloid Polyneuropathy (FAP), an autosomal dominant systemic amyloidosis caused by Val30Met variant in transthyretin (*TTR*) gene. This disease shows sensorimotor symptoms and progressive incapacity, leading to death 10-15 years, after onset, if no therapeutic intervention is undertaken.

There are remarkable differences in age-at-onset (AO), ranging 19-82 years in Portuguese Val30Met TTR-FAP, where late (≥50 years) and early-onset (<40 years) cases can be found within the same family [1]. However, the protective effect observed in patients with late-onset or older asymptomatic carriers may disappear in a single generation, with offspring of late-onset cases unexpectedly showing early-onset, while the reverse pattern has never been observed. Interestingly, all patients carry the same disease-causal variant, TTR Val30Met. In Portuguese kindreds, we observed that offspring may anticipate up to 40 years in respect to their affected parent [2]. Thus, we proved that anticipation is a true biological phenomenon in TTR-FAP, occurring in a disease caused by a point mutation, instead of the typical dynamic expansions [2].

These families are an interesting object of study for protective or risk modifiers' factors that can be therapeutic targets. Having this in mind, it urges to deeply unravel the modifiers mechanisms involved in AO variability.

Our recent work has revealed genetic factors that may play an important role in the disease variability [3-7]. Current consensus is in line with the notion that while each disease-causing variant sensitizes the genome to a primary clinical manifestation, additional variants in the genetic background modulates the phenotype expression. A single etiological mechanism is insufficient to explain the causal origins of phenotypic heterogeneity observed in AO which acts as a complex trait with diverse factors involved.

Our rationale was to search for other genetic modifiers concentrating the study in families, where modifier gene(s) with major effects are more likely to be detected within families with large anticipation of AO.

MATERIALS AND METHODS

Samples' selection

DNA samples were ascertained from Unidade Corino de Andrade - Centro Hospitalar do Porto (UCA-CHP, Porto), which has the largest database of TTR-FAP Val30Met worldwide,

with a registry collected and clinically well characterized over 75 years. Two TTR-FAP Val30Met families, comprising 3 generations with large anticipation of AO (above 10 years) were selected (total 6 samples). These pedigrees are shown in Fig. 1.
AO of each patient has been established by the same team of neurologists, specialized in TTR-FAP Val30Met, considering the presence of a whole set of symptoms characteristic of small fibers' neuropathy and not isolated and unspecific symptoms, reported by the patient and coinciding with an abnormal neurological and/or neurophysiological examination (as described in Dias *et al.*[8]). Presence of amyloid in tissues such as nerve, skin or salivary glands is a requested criterion for diagnosis. In the rare cases of recurrent biopsies without evidence of amyloid deposition the diagnosis was accepted only if objective and unequivocal signs of neuropathy were present and other potential causes had been excluded.
The Ethics Committee of CHP approved the research project and all patients gave written informed consent for collection of DNA. All procedures were conducted in accordance with national and international legislation.

Genomic DNA was extracted from peripheral blood leukocytes, using the standard salting out method [9] or from saliva, using ORAGENE kits according to the manufacturer's instructions (DNA Genotek, Inc.). The quantity of extracted DNA was measured with Qubit HS dsDNA Assay Kit on Qubit 2.0 Fluorometer (Life Technologies, Foster City, CA) following the manufacturer's instructions, and the quality assessed by 1% TAE agarose gel electrophoresis for 40min at 150 V.
The DNA samples of these patients were collected and stored at the Centro de Genética Preditiva e Preventiva (CGPP, Porto) biobank, authorized by CNPD (National Commission for Data Protection).

Whole genome sequencing (WGS)

WGS was performed in three affected individuals in family A (I:2, II:2, and III:1) and in three affected individuals in family B (I:2, II:1, and III:1). All were carriers of Val30Met TTR variant previously determined by Sanger sequencing (Alves-Ferreira M, *et al.*, submitted). Genomic libraries were prepared with average fragment length about 350 bp and sequenced as paired-end reads of 150-bp on either the Illumina HiseqXten or Novaseq platform according to the manufacturer's instructions.

Sanger sequencing

We used Sanger sequencing for validation and to analyze co-segregation in all family members of A and B pedigree, except for the individual III:1 of family A due to DNA unavailability (Fig. 1).

After PCR amplification with 10 ng of genomic DNA template, Sanger sequencing was performed using the Big Dye Terminator Cycle Sequencing v1.1 Ready Reaction (Applied Biosystems), according to the manufacturer's instructions, and samples loaded on an ABI-PRISM 3130 XL genetic analyzer (Applied Biosystems). Primers were designed using the software Primer3; dimer and hairpin formation were excluded using Autodimer. Primer sequences are the following forward and reverse primers, respectively: 5'-GAAGTTTCCACACCAACCATGAGA-3', 5'-AGTCGAGGATGGGTCTGAGTTG-3'.

Bioinformatics analysis

Standard bioinformatics analysis of sequencing data was based on the GeneStack pipeline [10, 11]. An average of 90-Gb sequencing data per subject were generated, and data were subsequently subjected to FastQC [12] for quality checking and Trimmomatic [13] for the trimming and filtering of low quality reads, where reads with a high quality score (average Q≥20) and a minimum length of 15bp after trimming were kept. Low quality bases were removed using seqtk 1.0 tool according to Phred algorithm that encodes the probability that the base is called incorrectly [14]. The sequence reads were aligned to the reference sequence of the human genome (GRCh38) using the Burrows-Wheeler Aligner (BWA v0.7.5) [15]. Duplicate reads were discarded using Picard tools [16]. Prior to variant calling and annotation a post-mapping quality control was performed, based on the BEDtools [17] and the Picard tools [16]. Variants were called and identified using samtools mpileup [18] and BCFtools [19]. Annotation of the discovered variants and their potential effects were analyzed based on SnpEff tool [20].

Variant filtering

First, we subtracted variants that were shared between the late- and early-onset (I:2: vs III:1) pair for each family, thus discarding the "family-specific" variants. Then, we kept variants that overlap between the two families, thus isolating variants present in large anticipation.

Subsequently, we used a series of stringent filters for the variants, in particular: (1) exonic and non-synonymous, or predicted to affect splicing *in silico*; (2) minor allele frequency (MAF)< 0.01 in European (non-Finnish) populations in public variation databases such as

the Genome Aggregation Database (gnomAD), the Exome Aggregation Consortium (ExAC) [21], the 1000Genomes [22] and (3) effect of non-synonymous coding variants on protein function, defined as being predicted as potential pathogenic for all algorithms, including PolyPhen [23], the Sorting Intolerant from Tolerant (SIFT) [24] and Combined Annotation Dependent Depletion (CADD) [25]. Using the online Search Tool for the Retrieval of Interacting Genes/Proteins (STRING v.11) (http://string-db.org/) database [26], which is a biological database to explore and analyse functional interactions between proteins; we constructed protein-protein interaction (PPI). Parameters included a minimum required interaction score>0.4 (medium confidence), with a 40% probability that a predicted link exists between two proteins in the same metabolic map in the KEGG database (genome.jp/kegg/pathway.html).

RESULTS

Families' description

Pedigrees of the two TTR-FAP families in this study are shown in Fig. 1. All patients and family members were sequenced for Val30Met TTR (when DNA was available). In both families, 3 individuals in different generations are confirmed Val30Met carriers and their non-affected spouses are Val30Val. We focused in the family nucleus of 3 generations, in both families, where the decrease in the age-of-onset is evident between parents-offspring pairs, showing a large anticipation (>10 years), resulting in a difference of ≈ 40 years in AO of the grandmother to the grandchild (Fig. 1). All patients analyzed were from the same clinical center and had a similar demographic background.

Identification of *MYH11* a candidate modifier gene and potential pathways

We applied WGS to the three affected individuals in both families and we subtracted the genetic profile in the grandparent-grandson pairs with late- and early-onset. Variants were compared between two families and genomic sequences from the second generation were used to input de novo variants. Relatively to the human reference sequence (GRCh38), the average coverage across all samples was 99.7%, with an average of 32X sequence depth. A combined analysis revealed nine non-synonymous variants, which two were predicted as potential deleterious variants and one of them was excluded for presenting a MAF=0.28 in European non-Finnish population (Table 1). After the selection criteria, we identified a missense variant in exon 34, c.4625G>A, (p.Arg1542Gln) in myosin heavy chain 11 (MYH11), a gene located on chromosome 16, known to be responsible of familial thoracic

aortic aneurysm (Familial TAAD; OMIM: 132900) encoding a smooth muscle myosin protein (SMMHC). The two affected grandsons were heterozygous and their affected parent did not carry the variant. These two grandsons started the symptoms by sensory neuropathy and soon progressed to autonomic neuropathy. This variant, rs137934837, was previously reported and is present in the non-Finnish European gnomAD population with a frequency of 0.003. Arginine at amino acid 1542 is evolutionarily conserved in 12 different vertebrate species and is located within the coiled coil motif (Fig. 2). Therefore, disruption of coiled coil motif of myosin is predicted to disrupt the structure or function of myosin [27]. Both *in silico* tools predicted that this p.Arg1542Gln variant affects the protein function (SIFT: deleterious; PolyPhen: probably damaging), in agreement with CADD algorithm (score of 33). In the PPI analysis, the network demonstrated 9 nodes and 16 edges (Fig. 3), with an average node degree of 3.56 and an average clustering coefficient of 0.741. The PPI enrichment p-value was equal to 0.0014.

Sequencing of Non-affected family members

Sanger sequencing confirmed the CT genotype of MYH11 variant in III:1 individuals for family A and B, and the CC genotype in I:2; II:2 for family A and I:1; I:2; II:1 for family B (Fig. 1 and 2). Importantly, individual II:2 of family B showed the CT genotype of MYH11 variant, thus, indicating that this variant may have been introduced by the Val30Met TTR non-carrier parent.

DISCUSSION

Significant advances in candidate genes studies have helped to identify variants as risk factors for AO in TTR-FAP. Previous work from our group focused mainly in common variants with small effects in candidate genes and found that some variants in *APCS*, *RBP4*, *NGAL*, *BGN*, *MEK1*, *MEK2*, *HSP27*, *YWHAZ*, *APOE*, *ATXN2*, *GBA* and *C1Q* complement genes were significantly associated with AO variation [3, 5, 7, 8, 28]. However, there is a portion of variability that still needs to be unraveled.

As the MYH11 mutation is not inherited through the Val30Met TTR lineage, we aimed to confirm that spouses Val30Val may have introduced susceptibility alleles that suppress the late-onset, or the risk alleles, observed in the younger generations. This result corroborates the role of the *trans*-acting factors, transmitted by the non-carrier parent, raised by us in a previous study [6].

Due to the different clinical aspects of TTR-FAP Val30Met, even within the same family, it is crucial to explore mechanisms that can be either risk or protective factors among patients with early and late-onset and how these variations result in diseases' progression. This family-based deep sequencing strategy provided the most robust approach for delineation of the genetic determinants of the phenotype.

MYH11 was identified as a modifier candidate gene in these two families with large anticipation. rs137934837 variant has a CADD score of 33, meaning that a variant is amongst the top 0.1% of deleterious variants in the human genome, exceeding the pathogenicity threshold >20 [29]. Furthermore, in European non-Finnish population this variant shows a MAF that is below a threshold that most studies would consider as rare (<0.01%) [30]. Thereupon, this variant has the support of reliable data on the potential deleterious effect on the protein function.

Our variant filtering, allowed us to exclude all other weakly pathogenic variants that did not fit in at least one selection criteria, turning the next filtering steps more consistent. Nevertheless, we cannot rule out the role of other variants on disease mechanisms.
MYH11 gene encodes a smooth muscle myosin heavy chain (SMMHC), a major component of the contractile unit in smooth muscle cells. Mutations in MYH11 are associated with familial thoracic aortic aneurysm, patent ductus arteriosus and, recently, moyamoya-like occlusive cerebrovascular disease [27, 31]. Variants in the SMMHC protein structure lead to reduced myosin motor elasticity, aberrant interactions with actin filaments, smooth muscle cells shortening, and contractile force generation followed by upregulation of tumor growth factor–β activity [31].

We identified a PPI network between TTR/MYH11 with a significantly PPI enrichment p-value, indicating that the nodes are not random and the observed number of edges is significant. Thus, we hypothesize that MYH11 modulates TTR-FAP disease expressivity through the mechanism involving rho activated coiled coil protein kinase 2 (ROCK2) and amyloid precursors protein (APP).
A strong pathological overlap has long been recognized between TTR and amyloid-beta (Aβ) peptide (which comes from processing APP). TTR was found to be capable of clearance of Aβ peptide and also can rescue phenotype and pathology-associated in Aβ

animal models [32-35]. In the same way, modulating the expression of ROCK2 will lead to a decrease in Aβ levels [36]. ROCK2 affects Aβ production by regulating the intracellular trafficking of APP as well as the secretion of Aβ [37]. On the other hand, MYH11 and ROCK2 played an important role in vascular smooth muscle contraction, a pathway that is remodeling in response to Aβ [38, 39]. Such biological evidences indicate that these proteins are at least partially biologically connected, as a group.

As in all genetic studies, robust phenotyping and family-based genetic studies are far superior to studies in isolated cases or in a cohort of sporadic cases. Since, early and late-onset patients are found within the same families, we focused on the modifier factors found in the WGS, to confirm the role of those factors in a family-based approach. WGS can provide uniform coverage along the whole genome as well as in coding regions, more than WES. Furthermore, our coverage allowed us to detect coding-variants with a detection power similar to 100x coverage in the WES, reducing the sensitivity and lower false-positive rate [40]. At the same time, filtering tens of thousands of variants to identify a significant gene relevant to a specific phenotype like AO is still a complex exercise.

The effect size of the variants found could be small, which can be a limitation in order to achieve a significant association with AO, due to statistical power. Also, this can be overcome in a future study to replicate these findings in additional families. Likewise, how to point out rare variants as a causative effect on AO remains challenging, as they may not be shared by all affected individuals. Although the role of environmental factors cannot be excluded, even as, the contribution of other genetic factors (common or rare) and a global role of them in modulation of specific phenotypes in the presence of the same disease-causing variant. Recently, exome and genome sequencing studies have reported an increased burden of rare deleterious variants toward risk for neurodevelopmental disorders [41-43], as well as, the presence of other variants in addition to the disease-associated variant explain the atypical clinical presentations [44-47].

The patients included in this first analysis were selected due to the fact that they represent the extreme phenotypes: grandsons with early-onset (24 years and 25years) and later-onset grandparents (65 years and 66 years). We intent to expand this study in order to: (1) include more families with large anticipation; (2) prioritize genes and pathways involved in disease mechanisms and (3) proceed to a functional validation.

In conclusion, as far as we know, this was the first study to show crosstalk mechanisms between *MYH11* gene and *TTR* pathways. The identification of new genes and their correlations with age-at-onset variability do allow us not only to understand the mechanisms involved in the TTR-FAP genesis, but also may well be helpful to understand the pathophysiology and finding valuable diagnosis biomarkers and therapy drugs for diseases portrayed in this study, like Alzheimer disease.

Fig. 1 Pedigrees of Family A and B with large anticipation (>10 years).
Val30Met TTR individuals are indicated by filled symbols. Spouses were confirmed as Val30Val

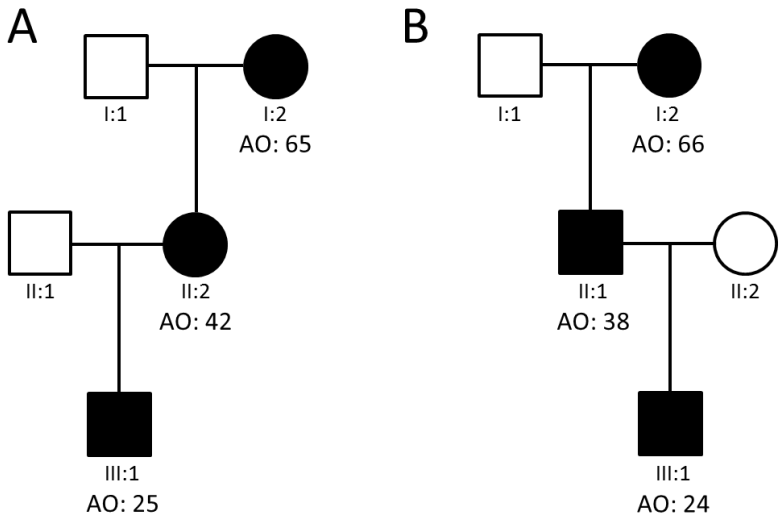

TTR. Whole-genome sequencing was performed on all affected individuals. AO: Age-at-onset (years).

Fig. 2 Human MYH11 protein domains and the analysis of evolutionary conservation for the sequence around the variant site.

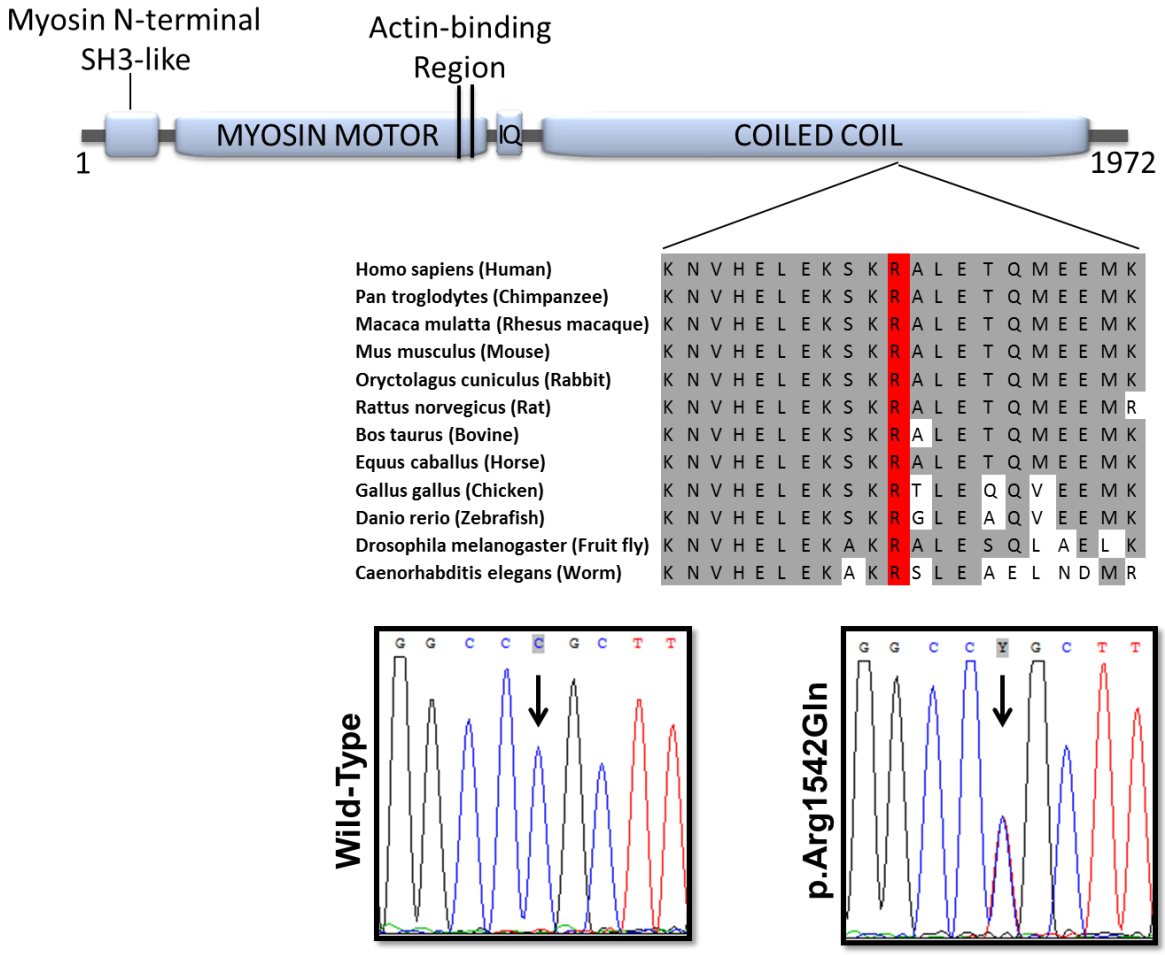

The MYH11 protein consists of 1972 amino acids and contains a Myosin N-terminal SH3-like domain, two Actin-binding regions, an IQ domain, and a coiled coil motif. Multiple protein alignment shows the conservation of residues (in grey). The Arginine 1542 (in red) in the coiled coil motif, which is changed to Glutamine, is highly conserved in all species. Example of Sanger sequencing chromatograms for individual I.2 (WT) and III.1 (p.Arg1542Gln), family A. Sanger sequencing confirmed the missense variant c.4625C>T, (p.Arg1542Gln) in exon 34 of the *MYH11* gene. Variant position is indicated by a black arrow.

Fig. 3 The PPI network for human MYH11 and predicted proteins encoded by genes proposed as candidates for TTR-FAP modulation.

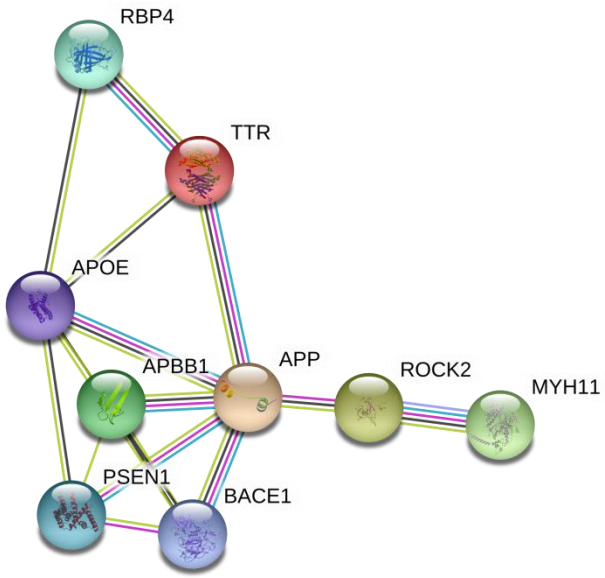

The network was constructed with String (version 11.0). It contains 9 nodes and 16 edges, with an average node degree of 3.56 and an average clustering coefficient of 0.741. The PPI enrichment *p*-value was equal to 0.0014.

Table 1 List of all non-synonymous variants after filtering of whole-genome sequencing data.

Gene	Chromosomal Position	dbSNP	cDNA Change	Protein Change	Prediction algorithms			MAF
					PolyPhen2 (score)	SIFT (score)	CADD	
C1orf159	1:1087150	rs144168476	c.299C>G	p.Arg100Pro	Benign (0.159)	Tolerated (0.4)	6.000	0
CFAP57	1:43183663	rs6663799	c.547G>T	p.Ala183Ser	Benign (0.012)	Tolerated (1)	6.836	0.005698
MOGS	2:74461951	rs142032474	c.1838G>A	p.Arg613Gln	Benign (0.005)	Tolerated (0.62)	7.756	0.009493
HLA-DRB5	6:32519438	rs148933006	c.584G>A	p.Arg195Gln	Benign (0.009)	Tolerated (1)	12.78	0.00955
HLA-DRB5	6:32519432	rs189435670	c.590G>C	p.Gly197Ala	Possibly Damaging (0.722)	Deleterious (0)	23.9	0.2836
HLA-DRB5	6:32519435	rs201372521	c.587G>A	p.Ser196Asn	Benign (0.263)	Deleterious (0.03)	22.0	0
TRBV6-7	7:142487869	rs565744849	c.7C>A	p.Leu3Ile	Benign (0)	Tolerated (0.43)	0.038	0
TRBV7-6	7:142492603	rs73742284	c.277A>G	p.Ile93Val	Benign (0)	Tolerated (0.49)	0.029	0.9978
MYH11	16:15721026	rs137934837	c.4625G>A	p.Arg1542Gln	Probably Damaging (0.984)	Deleterious (0.01)	33	0.003051

PolyPhen scores between 0.85 and 1.00 were interpreted as “Probably damaging”, scores between 0.5 and 0.85 were “Possibly damaging”, and scores between 0 and 0.5 were “Benign”. SIFT scores:≤0.05 were interpreted as “Deleterious” and scores>0.05 were “Tolerated”. MAF, minor allele frequency according to the non-Finnish European gnomAD population. Combined Annotation Dependent Depletion (CADD) score>20 is recommended as pathogenic.

REFERENCES

1. Sousa, A., et al., *Genetic epidemiology of familial amyloidotic polyneuropathy (FAP)-type I in Povoa do Varzim and Vila do Conde (north of Portugal).* Am J Med Genet, 1995. **60**(6): p. 512-21.
2. Lemos, C., et al., *Overcoming artefact: anticipation in 284 Portuguese kindreds with familial amyloid polyneuropathy (FAP) ATTRV30M.* J Neurol Neurosurg Psychiatry, 2014. **85**(3): p. 326-30.
3. Santos, D., et al., *Variants in RBP4 and AR genes modulate age at onset in familial amyloid polyneuropathy (FAP ATTRV30M).* Eur J Hum Genet, 2016. **24**(5): p. 756-60.
4. Santos, D., et al., *mtDNA copy number associated with age of onset in familial amyloid polyneuropathy.* J Neurol Neurosurg Psychiatry, 2017.
5. Santos, D., et al., *Familial amyloid polyneuropathy in Portugal: New genes modulating age-at-onset.* Ann Clin Transl Neurol, 2017. **4**(2): p. 98-105.
6. Alves-Ferreira, M., et al., *A Trans-acting Factor May Modify Age at Onset in Familial Amyloid Polyneuropathy ATTRV30M in Portugal.* Mol Neurobiol, 2017.
7. Santos, D., et al., *Large normal alleles of ATXN2 decrease age at onset in transthyretin familial amyloid polyneuropathy Val30Met patients.* Ann Neurol, 2019. **85**(2): p. 251-258.
8. Dias, A., et al., *C1QA and C1QC modify age-at-onset in familial amyloid polyneuropathy patients.* Ann Clin Transl Neurol. , 2019.
9. Miller, S.A., D.D. Dykes, and H.F. Polesky, *A simple salting out procedure for extracting DNA from human nucleated cells.* Nucleic Acids Res, 1988. **16**(3): p. 1215.
10. GeneStack. 2018; Available from: https://genestack.com.
11. Dogan, H., H. Can, and H.H. Otu, *Whole genome sequence of a Turkish individual.* PLoS One, 2014. **9**(1): p. e85233.
12. Andrews, S. *FastQC A Quality Control tool for High Throughput Sequence Data*. 2014; Available from: https://.
13. Bolger, A.M., M. Lohse, and B. Usadel, *Trimmomatic: a flexible trimmer for Illumina sequence data.* Bioinformatics, 2014. **30**(15): p. 2114-20.
14. Li, H. *Seqtk is a fast and lightweight tool for processing sequences in the fasta or fastq format*. 2016; Available from: https://github.com/lh3/seqtk.
15. Li, H. and R. Durbin, *Fast and accurate long-read alignment with Burrows-Wheeler transform.* Bioinformatics, 2010. **26**(5): p. 589-95.
16. *Picard Tools*. 2018; Available from: http://broadinstitute.github.io/picard.
17. Quinlan, A.R. and I.M. Hall, *BEDTools: a flexible suite of utilities for comparing genomic features.* Bioinformatics, 2010. **26**(6): p. 841-2.
18. Li, H., et al., *The Sequence Alignment/Map format and SAMtools.* Bioinformatics, 2009. **25**(16): p. 2078-9.
19. *BCFtools*. Available from: https://samtools.github.io/bcftools/.
20. Cingolani, P., et al., *A program for annotating and predicting the effects of single nucleotide polymorphisms, SnpEff: SNPs in the genome of Drosophila melanogaster strain w1118; iso-2; iso-3.* Fly (Austin), 2012. **6**(2): p. 80-92.
21. Lek, M., et al., *Analysis of protein-coding genetic variation in 60,706 humans.* Nature, 2016. **536**(7616): p. 285-91.
22. Auton, A., et al., *A global reference for human genetic variation.* Nature, 2015. **526**(7571): p. 68-74.
23. Adzhubei, I.A., et al., *A method and server for predicting damaging missense mutations.* Nat Methods, 2010. **7**(4): p. 248-9.

24. Kumar, P., S. Henikoff, and P.C. Ng, *Predicting the effects of coding non-synonymous variants on protein function using the SIFT algorithm.* Nat Protoc, 2009. **4**(7): p. 1073-81.
25. Kircher, M., et al., *A general framework for estimating the relative pathogenicity of human genetic variants.* Nat Genet, 2014. **46**(3): p. 310-5.
26. Szklarczyk, D., et al., *STRING v11: protein-protein association networks with increased coverage, supporting functional discovery in genome-wide experimental datasets.* Nucleic Acids Res, 2019. **47**(D1): p. D607-D613.
27. Milewicz, D.M., et al., *Genetic basis of thoracic aortic aneurysms and dissections: focus on smooth muscle cell contractile dysfunction.* Annu Rev Genomics Hum Genet, 2008. **9**: p. 283-302.
28. Abreu-Silva, J., *Modulators of phenotypic variability in Familial Amyloid Polyneuropathy (TTR-FAP Val30Met)*, in *Public Health Master Thesis* 2017, University of Porto.
29. Jagadeesh, K.A., et al., *M-CAP eliminates a majority of variants of uncertain significance in clinical exomes at high sensitivity.* Nat Genet, 2016. **48**(12): p. 1581-1586.
30. Panoutsopoulou, K., I. Tachmazidou, and E. Zeggini, *In search of low-frequency and rare variants affecting complex traits.* Hum Mol Genet, 2013. **22**(R1): p. R16-21.
31. Keylock, A., et al., *Moyamoya-like cerebrovascular disease in a child with a novel mutation in myosin heavy chain 11.* Neurology, 2018. **90**(3): p. 136-138.
32. Link, C.D., *Expression of human beta-amyloid peptide in transgenic Caenorhabditis elegans.* Proc Natl Acad Sci U S A, 1995. **92**(20): p. 9368-72.
33. Choi, S.H., et al., *Accelerated Abeta deposition in APPswe/PS1deltaE9 mice with hemizygous deletions of TTR (transthyretin).* J Neurosci, 2007. **27**(26): p. 7006-10.
34. Buxbaum, J.N., et al., *Transthyretin protects Alzheimer's mice from the behavioral and biochemical effects of Abeta toxicity.* Proc Natl Acad Sci U S A, 2008. **105**(7): p. 2681-6.
35. Kerridge, C., et al., *The Abeta-clearance protein transthyretin, like neprilysin, is epigenetically regulated by the amyloid precursor protein intracellular domain.* J Neurochem, 2014. **130**(3): p. 419-31.
36. Herskowitz, J.H., et al., *Pharmacologic inhibition of ROCK2 suppresses amyloid-beta production in an Alzheimer's disease mouse model.* J Neurosci, 2013. **33**(49): p. 19086-98.
37. Lai, A.Y. and J. McLaurin, *Rho-associated protein kinases as therapeutic targets for both vascular and parenchymal pathologies in Alzheimer's disease.* J Neurochem, 2018. **144**(5): p. 659-668.
38. Wan, L., et al., *Screening key genes for abdominal aortic aneurysm based on gene expression omnibus dataset.* BMC Cardiovasc Disord, 2018. **18**(1): p. 34.
39. Hald, E.S., C.D. Timm, and P.W. Alford, *Amyloid Beta Influences Vascular Smooth Muscle Contractility and Mechanoadaptation.* J Biomech Eng, 2016. **138**(11).
40. Barbitoff, Y.A., et al., *Systematic dissection of biases in whole-exome and whole-genome sequencing reveals major determinants of coding sequence coverage.* bioRxiv, 2018.
41. Krumm, N., et al., *Excess of rare, inherited truncating mutations in autism.* Nat Genet, 2015. **47**(6): p. 582-8.
42. Singh, T., et al., *The contribution of rare variants to risk of schizophrenia in individuals with and without intellectual disability.* Nat Genet, 2017. **49**(8): p. 1167-1173.
43. Turner, T.N., et al., *Genomic Patterns of De Novo Mutation in Simplex Autism.* Cell, 2017. **171**(3): p. 710-722 e12.
44. Karaca, E., et al., *Phenotypic expansion illuminates multilocus pathogenic variation.* Genet Med, 2018. **20**(12): p. 1528-1537.
45. Posey, J.E., et al., *Resolution of Disease Phenotypes Resulting from Multilocus Genomic Variation.* N Engl J Med, 2017. **376**(1): p. 21-31.
46. Schaaf, C.P., et al., *Oligogenic heterozygosity in individuals with high-functioning autism spectrum disorders.* Hum Mol Genet, 2011. **20**(17): p. 3366-75.

47. Pizzo, L., et al., *Rare variants in the genetic background modulate cognitive and developmental phenotypes in individuals carrying disease-associated variants.* Genet Med, 2018.

In **Article 4**, we developed and characterized the first TTR amyloidosis animal model that recapitulates cell-nonautonomous neuronal phenotypes. In our *C. elegans* transgenic lines, expressing human WT TTR or the destabilizing TTR variants, we verified that TTR follows the mammalian secretion profile and is suitable to study cell-nonautonomous phenotypes.

Disease proteins induce several neural phenotypes including impaired nociception and locomotion, as well as late onset branching of nociceptive neurons. Phenotypes are dependent upon the expression of the TTR, since RNAi knockdown abolished phenotypes.

To scrutinize putative FAP-directed therapeutic mechanisms, we used three different approaches to test the hypothesis that modulating TTR would affect the severity of the above phenotypes. First, we genetically ablated coelomocytes (macrophage-like cells that degrade TTR) resulting in higher TTR protein levels and this significantly worsened nociceptive response in Val30Met TTR animals. Second, we used RNAi to reduce TTR protein levels, and this rescued the Unc phenotype in the Val30Met TTR animals. Third, to test if TTR tetramer stabilization reduced proteotoxicity by decreasing oligomer formation, we treated Val30Met TTR worms with tafamidis, a TTR stabilizer approved for FAP treatment, and observed a significant rescue of the Unc phenotype.

Article 4: Cellular Clearance of Circulating Transthyretin Decreases Cell Non-Autonomous Proteotoxicity in *Caenorhabditis elegans*

Kayalvizhi Madhivanan[a,b,c], Erin R. Greiner[a,b,c,1], Miguel Alves-Ferreira[a,b,c,d,e,f], David Soriano-Castell[a,b,c], Nirvan Rouzbeh[a,b,c,2], Carlos A. Aguirre[a,b,c], Johan F. Paulsson[a,3], Justin Chapman[g], Xin Jiang[g], Felicia K. Ooi[h], Carolina Lemos[d,e,f], Andrew Dillin[i,j], Veena Prahlad[h], Jeffery W. Kelly[a,k,l], and Sandra E. Encalada[a,b,c,4]

[a]Department of Molecular Medicine, The Scripps Research Institute, La Jolla, CA 92037;

[b]Department of Molecular and Cellular Neuroscience, The Scripps Research Institute, La Jolla, CA 92037;

[c]Dorris Neuroscience Center, The Scripps Research Institute, La Jolla, CA 92037;

[d]Instituto de Biologia Molecular e Celular, Universidade do Porto, 4150-171 Porto, Portugal;

[e]Instituto de Investigação e Inovação em Saúde, Universidade do Porto, 4150-171 Porto, Portugal;

[f]Instituto de Ciências Biomédicas de Abel Salazar, Universidade do Porto, 4150-171 Porto, Portugal;

[g]Misfolding Diagnostics, San Diego, CA 92121;

[h]Department of Biology, Aging Mind and Brain Initiative, University of Iowa, Iowa City, IA 52242;

[i]Department of Molecular and Cell Biology, University of California, Berkeley, CA 94720;

[j]Howard Hughes Medical Institute, University of California, Berkeley, CA 94720;

[k]Department of Chemistry, The Scripps Research Institute, La Jolla, CA 92037; and

[l]The Skaggs Institute for Chemical Biology, The Scripps Research Institute, La Jolla, CA 92037

[1]Present address: Illumina, San Diego, CA 92122.

[2]Present address: Department of Biomedical and Pharmaceutical Sciences, University of Montana, Missoula, MT 59812.

[3]Present address: Department of Obesity Biology, Global Research, Novo Nordisk A/S, 2760 Måløv, Denmark.

[4]To whom correspondence should be addressed. Email: encalada@scripps.edu.

Published in Proc Natl Acad Sci U S A. 2018 Aug 14;115(33):E7710-E7719.
DOI: 10.1073/pnas.1801117115.
National Academy of Sciences

SIGNIFICANCE

Evidence suggests that transthyretin (TTR) amyloid diseases result from rate-limiting dissociation of TTR tetramers secreted from the liver into monomers, followed by monomer misfolding and misassembly into a spectrum of aggregates that compromise postmitotic tissue function, including peripheral nerve function. It is unknown how TTR aggregation leads to the demise of neurons cell nonautonomously. Herein we introduce transgenic *Caenorhabditis elegans* models of TTR amyloidosis that exhibit aggregation and quantifiable cell nonautonomous neuronal phenotypes, including impaired pain sensation, as seen in humans, and altered neuronal morphology. Neuronal dysfunction can be exacerbated by eliminating distal macrophage-like cells that degrade TTR and ameliorated by treating the transgenic worms with TTR RNAi or a TTR kinetic stabilizer, strategies that also delay human polyneuropathy.

Keywords: aggregation, cell-nonautonomous, neurodegeneration, nonnative oligomers, polyneuropathy

ABSTRACT

Cell-autonomous and cell-nonautonomous mechanisms of neurodegeneration appear to occur in the proteinopathies, including Alzheimer's and Parkinson's diseases. However, how neuronal toxicity is generated from misfolding-prone proteins secreted by nonneuronal tissues and whether modulating protein aggregate levels at distal locales affects the degeneration of postmitotic neurons remains unknown. We generated and characterized animal models of the transthyretin (TTR) amyloidoses that faithfully recapitulate cell-nonautonomous neuronal proteotoxicity by expressing human TTR in the *Caenorhabditis elegans* muscle. We identified sensory neurons with affected morphological and behavioral nociception-sensing impairments. Nonnative TTR oligomer load and neurotoxicity increased following inhibition of TTR degradation in distal macrophage-like nonaffected cells. Moreover, reducing TTR levels by RNAi or by kinetically stabilizing natively folded TTR pharmacologically decreased TTR aggregate load and attenuated neuronal dysfunction. These findings reveal a critical role for *in trans* modulation of aggregation-prone degradation that directly affects postmitotic tissue degeneration observed in the proteinopathies.

INTRODUCTION

In protein-aggregation disorders, cell-autonomous and cell-nonautonomous mechanisms of neurodegeneration appear to occur, the latter associated with the propagation of protein aggregates and/or pathologies throughout the nervous system (1, 2). Elucidating these degenerative pathways is often confounded by the fact that affected tissues express the misfolding-prone protein(s). Moreover, it is unclear whether modulating levels of native aggregation-prone proteins or of protein aggregates in distal tissues would change cell-nonautonomous proteotoxicity. Knowledge of these features is important for further understanding neurodegenerative diseases and for envisioning new therapeutic strategies.

In the transthyretin (TTR) systemic amyloidoses, the unaffected liver secretes tetrameric TTR into the blood stream, where TTR dissociates, misfolds and aggregates, compromising organ systems such as the heart and the autonomic and peripheral nervous systems, tissues that do not synthesize TTR (3). Thus, cell-nonautonomous proteotoxic pathways are clearly distinguished in the TTR amyloidoses, allowing the mechanism(s) to be carefully studied. Native TTR exists as a β-sheet–rich tetramer (4), whose established function is to transport holo-retinol–binding protein in the plasma and to serve as a back-up carrier for thyroxine (T_4) (5, 6). Strong genetic, pathologic, biochemical, and pharmacologic evidence suggests that TTR amyloid diseases result from TTR aggregation, compromising the function of various tissues (7–10). A central unanswered question is how TTR aggregation leads to the cell-nonautonomous demise of postmitotic tissues, including neurons (11). This key question remains unanswered for all human amyloid diseases (12–14). Moreover, it is unclear whether nonnative (NN) TTR oligomers contribute to neurodegeneration and, if so, whether their levels can be modulated at distal sites to diminish neuronal proteotoxicity (9, 15).

Over 115 different TTR mutations associated with human disease render the tetramer less stable and more aggregation prone (16, 17). The most common TTR variant is V30M (10), which leads to familial amyloid polyneuropathy (FAP), affecting the peripheral and autonomic nervous systems and resulting in the degeneration of thermo- and pain-sensing neurons (18). The highly unstable D18G TTR variant is not readily secreted by the liver but instead is targeted for endoplasmic reticulum (ER)-associated degradation (ERAD) (16, 19). Partial secretion of D18G TTR from the choroid plexus results in aggregation that leads to familial meningocerebrovascular amyloidosis characterized by dementia and cerebrovascular bleeding (20). The aggregation of circulating WT TTR leads to senile systemic amyloidosis, a cardiomyopathy that is the most common TTR amyloid disease affecting ~10% of elderly adults, leading to congestive heart failure (21).

Interestingly, mutations also exist that are protective against disease. For example, T119M TTR when present in hetero-allelic combination with V30M TTR results in the formation of highly kinetically stable, nonamyloidogenic T119M/V30M heterotetramers that stop or delay FAP pathology (7).

Numerous attempts to model human neuronal TTR proteotoxicity in transgenic mice have failed to recapitulate cell-nonautonomous disease phenotypes, including degeneration of postmitotic tissue, despite the presence of extracellular TTR aggregates (22). In *Drosophila*, expression of TTR in the cytosol of neurons resulted in neuronally related phenotypes, but in humans TTR is not significantly expressed in the cytosol of neurons (23, 24). Therefore, there is a pressing need to develop an animal model relevant to human pathology wherein the mechanism of TTR aggregation-associated toxicity occurs cell nonautonomously. Successful models become even more relevant if the existing regulatory agency-approved drugs that slow the progression of human FAP, such as tafamidis and patisiran (an RNAi therapeutic targeting TTR) (8), also ameliorate disease phenotypes in the animal model, thus contributing to the identification of mechanisms by which TTR is toxic as well as the means by which toxicity can be ameliorated.

Herein we report animal models in the nematode *Caenorhabditis elegans* that generate TTR aggregates including NN oligomers analogous to those in humans (9, 25). Critically, expression of human TTR (hTTR) uniquely in the body-wall muscle resulted in TTR secretion and aggregation and in cell-nonautonomous structural and functional impairments of sensory nociceptive neurons not expressing TTR. Decreasing TTR levels cell nonautonomously resulted in a reduced NN TTR oligomeric load and a significant amelioration of cell-nonautonomous proteotoxicity. These data suggest that TTR oligomers are likely proteotoxic, as it is hypothesized to be the case in humans (9, 25, 26). Notably, the degenerative phenotypes in *C. elegans* linked to TTR proteotoxicity were exacerbated by impairing the turnover of TTR tetramers and oligomers in distal cells, suggesting that increased TTR oligomer levels correlate with enhanced proteotoxicity and that enhancing TTR degradation could be a viable therapeutic strategy. These *C. elegans* models provide a platform to study the mechanism(s) of *in trans* neurodegeneration as well as the influence of cell-nonautonomous TTR degradation and have the potential to provide insights into the etiology of other aging-associated protein-aggregation disorders linked to neurodegeneration such as Alzheimer's disease (AD) and Parkinson's disease (PD).

RESULTS

Generation of *C. elegans* Models Expressing Human TTR Variants.

To model TTR proteotoxicity in *C. elegans*, we expressed human WT TTR, V30M TTR, or D18G TTR in the body-wall muscle under the control of the *unc-54* promoter (Fig. 1*A*). We modeled these disease-promoting TTR sequences because earlier work showed that they have diverse stabilities and secretion efficiencies that could allow us to investigate the range of cell-nonautonomous versus cell-autonomous effects (16). We also made a transgenic strain with the protective, non–aggregation-prone T119M mutation (7) that allowed us to scrutinize the hypothesis that the proteotoxic phenotypes observed in the pathogenic strains (see below) were not simply the result of the overexpression of an hTTR sequence. In each model strain, the hTTR signal sequence (SS) (Fig. 1*A*) was included to enable TTR to be inserted into the ER and to target it for secretion (see below). As TTR is a small protein and fusions to GFP or other large fluorescent proteins could significantly impact its folding, assembly, and/or trafficking in the early secretory pathway, the TTR transgenes were not tagged.

To test whether the *C. elegans* strains expressed comparable TTR levels, *TTR* mRNA and TTR protein levels were assessed. *TTR* mRNA levels quantitated from age-synchronized animals peaked at day 1 of adulthood and declined by day 8 for all strains (*SI Appendix*, Fig. S1*A*). Soluble and insoluble TTR protein levels were quantified by Western blot (Fig. 1 *B* and *C*) using antibodies that recognized all four hTTR variants equally (*SI Appendix*, Fig. S1*B*) but did not recognize endogenous *C. elegans* TTR-like proteins in the non-TTR control or TTR strains. Animals expressing stable human variants (i.e., WT TTR, V30M TTR, and T119M TTR) generated comparable levels of soluble TTR protein that peaked in day-1 adult animals in all strains (Fig. 1*B*). TTR was not detected in the insoluble pellet except for V30M TTR, which is the most amyloidogenic of these three sequences (Fig. 1*C*). In contrast, animals expressing the highly unstable and, as shown in humans, poorly secreted D18G TTR displayed very low levels of soluble protein but notably higher levels of insoluble TTR that increased with aging (Fig. 1*C*) (16, 20). Collectively, these data show that the strains generated had comparable levels of *TTR* mRNA and TTR protein and that the solubility profile of TTR sequences is consistent with that observed in humans, which had not been previously modeled (16).

Differential Secretion of Tetrameric TTR Variants in *C. elegans* Recapitulates hTTR Secretion Profiles.

In humans, WT TTR, V30M TTR, and T119M TTR are efficiently secreted from the liver, while D18G TTR is not (16, 19). To test the hypothesis that hTTR variants expressed in *C. elegans* were

secreted from the body-wall muscle with differential secretion efficiencies, we first performed immunofluorescence (IF) with a polyclonal antibody against hTTR to visualize total TTR expression and localization in day-1 adult animals. The TTR signal was observed in the periphery of individual body-wall muscle cells and in colocalization with phalloidin, suggesting that TTR reached the plasma membrane for possible secretion and deposited at myofilament striations of sarcomeres (Fig. 2*A*). In addition, we observed WT, V30M, and T119M TTR signal in the body cavity, demonstrating secretion of TTR from muscle cells. In contrast, the D18G TTR signal was absent from the body cavity, suggesting that this highly unstable variant was not secreted efficiently. Instead, we observed pronounced D18G TTR intracellular aggregates, likely a result of its retention inside muscle cells (Fig. 2*A*). We confirmed these observations by repeating the IF (*SI Appendix*, Fig. S2) using fit-for-purpose antibodies that uniquely and selectively recognized NN TTR (monomers and/or oligomers) but not native TTR tetramers (*SI Appendix*, *SI Materials and Methods* and Fig. S3 *A* and *B*). Whether NN TTR was also present inside other tissues is not clear at this time.

To further scrutinize the hypothesis that natively folded TTR tetramers were secreted from the *C. elegans* body-wall muscle (16), we analyzed their *in vivo* subcellular localization by feeding animals compound 5 (**CMPD5**) (Fig. 2*B*). This small molecule is a validated fluorogenic probe for natively folded TTR that binds to the T_4-binding sites in TTR and remains dark until it selectively reacts with the Lys-15 ε-amino groups of TTR to render the TTR–(**CMPD5**)$_2$ conjugates fluorescent (27). Pronounced TTR–(**CMPD5**)$_2$conjugate fluorescence was detected in WT TTR, V30M TTR, and T119M TTR strains in all six coelomocytes, macrophage-like cells that endocytose soluble material from the body cavity for degradation (28) (Fig. 2 *C*, *d–l*). These data demonstrate that TTR tetramers were secreted from the muscle. We and others previously observed TTR localization to coelomocytes in independently generated WT TTR *C. elegans* strains (29, 30). Neither the non-TTR control nor the D18G TTR animals showed a TTR–(**CMPD5**)$_2$ conjugate-positive signal in coelomocytes (Fig. 2 *C*, *a–c* and *m–o*, respectively), suggesting that D18G TTR was not secreted out of muscle cells. Thus, the various TTR sequences expressed in the *C. elegans* body-wall muscle showed secretion profiles comparable to those exhibited by humans, rendering these models suitable for studying TTR cell-nonautonomous proteotoxicity.

Expression of TTR in *C. elegans* Results in the Generation of Native TTR Tetramers and Oligomeric TTR Aggregates.

Since soluble and secreted hTTR can remain natively tetrameric or can dissociate, misfold, and aggregate into a variety of aggregate structures, including NN TTR oligomers that we hypothesize

are toxic (9, 25), we next characterized the age-dependent profile of tetrameric and oligomeric TTR in the *C. elegans* transgenic TTR strains (25, 31). Natively folded TTR tetramers were quantified in the soluble fractions from lysates of age-synchronized day-1, day-5, and day-8 animals by incubating the lysates with the fluorogenic small molecule **A2** (31). Similar to **CMPD5**, **A2** binds strongly to both T_4-binding pockets of the folded TTR tetramer and reacts with Lys-15 residues to create a fluorescent TTR tetramer–(**A2**)$_2$conjugate that is quantified by ultra-performance liquid chromatography (UPLC) (31). Fluorescent TTR tetramer–(**A2**)$_2$ conjugate levels from *C. elegans* lysates, as measured by UPLC, were compared with a calibrated standard curve generated by the addition of increasing amounts of purified recombinant WT TTR into day-1 control lysates (Fig. 3*A* and *SI Appendix*, Fig. S3*C*). We found that native TTR tetramer levels decreased with aging (Fig. 3*B*). The decrease is consistent with expression of the *unc-54* promoter (32), but message instability, tetramer degradation, or tetramer-to-monomer-to-aggregate conversion could also contribute (16). Notably, the most stable TTR variant (T119M TTR) had the highest TTR tetramer levels from day 1 through day 8 of adulthood, whereas the least stable variant (D18G TTR) yielded the lowest native TTR tetramer levels (Fig. 3*B*), consistent with observations in humans showing that these are highly stable and unstable variants, respectively (16). Thus, the *C. elegans* transgenic strains expressing stable TTR variants generated measurable levels of TTR tetramers.

We next evaluated whether NN oligomeric or aggregated TTR was being generated in the transgenic TTR strains. NN TTR oligomer levels from soluble and insoluble fractions of lysates from all *C. elegans* strains were assessed by Native-PAGE and by a sandwich ELISA using the same antibodies against NN TTR that were used for IF (Fig. 2*A*). Native-PAGE showed the presence of high-molecular-weight aggregates primarily in the soluble and insoluble lysate fractions of the V30M TTR and D18G TTR strains but not in the WT TTR or T119M TTR strains (Fig. 3*C* and *SI Appendix*, Fig. S3*D*). To test whether we could more quantitatively assess NN TTR oligomer levels, soluble and insoluble lysate fractions of day-1 and day-5 age-synchronized animals were analyzed by a sandwich ELISA (*Materials and Methods*) (25). Consistent with the observations from the Native-PAGE analysis (Fig. 3*C*), NN TTR levels were detected primarily in insoluble lysates of D18G TTR strains, but not in lysates from V30M TTR animals (Fig. 3*D*). As with Native-PAGE, the ELISA was unable to detect NN WT TTR or T119M TTR, likely because of the conformational stability of these sequences. The presence of NN oligomers in the transgenic strains expressing V30M TTR and D18G TTR is consistent with the higher amyloidogenicity of these sequences (16). Taken together, these data show that expression of the TTR variants in

the *C. elegans* body-wall muscle resulted in the generation of differential native tetramer and NN oligomeric TTR concentrations, as observed in human patients.

TTR FAP Variant Impairs Sensory Nociception Cell Nonautonomously.

In FAP patients, the aggregation of V30M TTR and its deposition around peripheral and autonomic neurons is associated with the loss of nociception and temperature perception in the extremities (18). To test whether the expression of V30M TTR in the body-wall muscle leads to the impairment of nociception in *C. elegans*, we measured the reflex-like escape reaction of V30M TTR animals with a thermal-avoidance assay developed previously to measure pain responses (Fig. 4*A*) (33). Individual animal responses were scored into four categories (classes I–IV), as previously established (*SI Appendix*, *SI Materials and Methods*) (33). As controls, we scored thermal avoidance in *eat-4(n2474)* and *unc-86(n846)* 1-d-old mutant animals, shown previously to have attenuated and unaltered responses, respectively (Fig. 4*B*) (33). A significantly higher percentage of V30M TTR animals (10 ± 0.6%) than non-TTR control animals (0%) or T119M TTR animals (0%) were unresponsive to noxious heat (class IV) (Fig. 4*B* and *SI Appendix*, Table S1). The T119M TTR data demonstrate that the nociceptive defect was not due simply to the overexpression of an hTTR sequence. To ascertain that the V30M TTR-dependent defect was not the result of locomotion-related impairments that would prevent the animals from backing up, we tested reversal movement in each class IV animal with a soft touch to the nose. All class IV animals (100%; n = 41) backed in response to this stimulus. To test whether the nociception defects were TTR dependent, we repeated the noxious heat assay in V30M TTR animals treated with TTR RNAi, which afforded a protein knockdown of >90% (*SI Appendix*, Fig. S4). The nociception defect was rescued in RNAi-treated V30M TTR animals (Fig. 4*C* and *SI Appendix*, Table S2). These results are consistent with cell-nonautonomous V30M TTR neuronal toxicity.

To further test whether defects in nociception exhibited by V30M TTR animals were cell nonautonomous, we generated transgenic animals expressing V30M TTR in the body-wall muscle but lacking the SS (V30MΔSS TTR, *SI Appendix*, Fig. S6 *A* and *B*) to prevent its secretion (*SI Appendix*, Fig. S6*C*). V30M ΔSS animals did not exhibit a defective thermal-avoidance response (2.6 ± 0.5% class IV) compared with V30M animals with TTR fused to an SS (10 ± 0.6%) (Fig. 4*B* and *SI Appendix*, Table S1). Furthermore, we tested for thermal avoidance in day-1 D18G TTR animals in which we did not find evidence for TTR secretion (Fig. 2 *A* and *C*). D18G TTR animals did not exhibit defective nociception (Fig. 4*B*). Taken together our data show that secretion of V30M TTR from the muscle results in proteotoxicity to sensory pain-sensing neurons in a cell-

nonautonomous manner, likely owing to V30M TTR's ability to dissociate, misfold, and misassemble (16).

Impaired Dendritic Morphology of Somatosensory Neurons in V30M TTR Animals.

The neural circuitry for the nociceptive thermal-avoidance responses in *C. elegans* tested here was previously mapped to the AFD and FLP head sensory neurons (33, 34). The FLP neurons are polymodal cells that extend elaborate dendritic branches enveloping the head of the animal (Fig. 5 *A* and *B*) (35). To probe whether the nociceptive defects observed in V30M TTR animals (Fig. 4) correlated with morphological neuronal defects, we quantified the dendritic morphology of their FLP neurons. Day-1 adult V30M TTR animals had a significantly higher number of quaternary branches than age-matched non-TTR control or T119M TTR animals, suggesting that the expression of V30M TTR affects dendritic outgrowth (Fig. 5 *B* and *C*). As extension of quaternary branches toward the hypodermis is critical for FLP sensory function (35), we also quantified the FLP quaternary branch extension angle from the tertiary branch (Fig. 5*D*). V30M TTR animals had quaternary branches that bent backward toward tertiary branches more often than non-TTR control and T119M TTR animals (Fig. 5*E* and *SI Appendix*, Table S3). These data show that sensory endings do not extend fully and in some cases nearly reverse in V30M TTR animals. To test whether these phenotypes were due to developmental defects, we first surveyed the number of quaternary branches in the last larval L4 stage, when FLP quaternary branching is finalizing its development (35). The number of FLP quaternary dendritic branches was lower in L4 non-TTR control larvae than in non-TTR control day-1 adults, showing that quaternary branches are still being added as control animals develop (Fig. 5*C* and *SI Appendix*, Fig. S7*A*). Expression of V30M TTR or T119M TTR resulted in a higher number of quaternary branches in L4 animals than in control animals (*SI Appendix*, Fig. S7*A*). However, the number of branches in T119M TTR L4 larvae as they grew to day-1 adults was similar to those of non-TTR controls, whereas V30M TTR animals continued adding quaternary branches as they transitioned to day-1 adults (Fig. 5*C*). Thus, expression of V30M TTR resulted in ectopic branching in young-adult animals compared with L4 larvae. No significant differences in quaternary FLP branch angle in L4 larvae were observed in non-TTR control, V30M TTR, and T119M TTR transgenic animals, demonstrating that these morphological defects were not developmental (*SI Appendix*, Fig. S7*B* and Table S4).

We next tested whether expression of V30M TTR without the signal sequence (ΔSS) in FLP neurons with the *des-2* promoter (36) could drive the TTR nociception-sensing defects (Fig. 4). Nociception was not impaired in day-1 *des-2p*::V30MΔSS TTR animals (Fig. 4*B*), suggesting that V30M TTR expression in FLP neurons is not sufficient to impair nociception.

To test whether V30M TTR toxicity affects other neurons, we evaluated a subcellular phenotype in ALM, a set of mechanosensory neurons involved in soft-touch sensing (37). As mitochondria are critical for neuronal function, and their altered dynamics have been shown to be a key early pathological feature of most neurodegenerative diseases (38), we imaged and quantitated the size of these organelles inside ALM axons. Mitochondrial length was significantly decreased in V30M TTR animals compared with non-TTR control and T119M animals (*SI Appendix*, Fig. S8). These data suggest that secreted V30M TTR is not specifically toxic to sensory pain-sensing neurons but is also toxic to those involved in mechanosensation. Taken together, our data show that V30M TTR proteotoxicity impairs neuronal function in a cell-nonautonomous manner by targeting pathways that regulate the proper structure and function of pain-sensing and mechanosensory neurons.

TTR Clearance by Distal Cells Exacerbates TTR Proteotoxicity in Neurons.

Our data show that TTR tetramers secreted from the body-wall muscle into the body cavity are taken up by coelomocytes (Fig. 2). As coelomocytes are lysosomal-degradative cells (28), we reasoned that if TTR was degraded in coelomocytes, then modulation of coelomocyte-mediated TTR degradation would affect the level of TTR proteotoxicity. To first test if TTR was degraded in coelomocytes, we genetically ablated these cells by crossing the TTR transgenic animals to a strain expressing a diphtheria toxin mutant, DT-A(E148D), under a coelomocyte-specific promoter and measured TTR levels (28). We confirmed the absence or significant reduction of coelomocytes in DT-A(E148D) animals (*SI Appendix*, Fig. S9 *A* and *B* and Table S5). Previous studies showed that ablation of coelomocytes resulted in the accumulation of fluid-phase markers in the body cavity due to a lack of uptake and degradation (28). To test for coelomocyte ablation in TTR; DT-A strains, we injected the body cavity with soluble A680-fluorescent dextran (3,000 MW) and immediately treated them with **CMPD5** (10 μM) to convert native TTR to TTR-(**CMPD5**)$_2$ tetrameric conjugates, as described above (Fig. 2 *B* and *C*). A680-dextran as well as TTR–(**CMPD5**)$_2$ conjugates accumulated in coelomocytes in non–DT-A animals but accumulated throughout the body cavity in TTR; DT-A animals, suggesting that muscle-secreted TTR (WT TTR, V30M TTR and T119M TTR) was normally taken up from the body cavity and degraded in these cells (Fig. 6*A* and *SI Appendix*, Fig. S9 *C* and *F*). Neither non-TTR control animals nor D18G TTR; DT-A animals treated with **CMPD5** produced any significant TTR**–**(**CMPD5**)$_2$ conjugate signal (*SI Appendix*, Fig. S9 *E* and *D*). Next, to test whether ablation of coelomocytes resulted in decreased TTR degradation, we characterized TTR protein levels in animals with and without coelomocytes. Western blots of the soluble and insoluble TTR fractions of lysates from TTR; DT-A age-synchronized animals showed that adult 5-d-old animals without coelomocytes had increased TTR

protein levels compared with animals with coelomocytes (Fig. 6*B*). This shows that ablation of coelomocytes resulted in a significant decrease in TTR degradation and in the accumulation of higher levels of TTR tetramers and insoluble TTR in the body cavity of aging animals.

Next, to determine whether decreasing TTR tetramer degradation cell nonautonomously increased TTR proteotoxicity in neurons, we tested for thermal avoidance in V30M TTR; DT-A animals. A significantly higher percentage of the V30M; DT-A animals (22 ± 2%; *n* = 43) failed to respond to noxious heat (class IV) compared with non-TTR control; DT-A (9.1 ± 2.5%; *n* = 12) or V30M TTR animals with coelomocytes (10 ± 0.6%; *n* = 41). Thus, reduced TTR degradation resulted in enhanced TTR neuronal defects (Fig. 6*C* and *SI Appendix*, Table S6).

To test whether the higher number of nonresponsive V30M; DT-A animals correlated with an increase in the amount of NN V30M TTR oligomers, we measured NN TTR oligomer load via ELISA, as described above (Fig. 3*D*). The NN TTR oligomer aggregate load was significantly increased in the soluble fraction of lysates of day-1 and day-5 adult V30M TTR; DT-A animals compared with that of V30M TTR animals (Fig. 6*D*). These data suggest that the additional impairment of neuronal nociception in V30M TTR; DT-A animals correlated with the increased soluble TTR tetramers and oligomers (Fig. 6 *A* and *B*). No significant increase in the amount of insoluble NN TTR oligomers was observed in V30M TTR; DT-A animals compared with V30M TTR animals, suggesting that soluble NN oligomers could be responsible for the heightened thermal-avoidance defect in animals without coelomocytes. Taken together, these data show that removal of degradative cells distal to the original site of V30M TTR expression can increase TTR tetramer levels throughout the body cavity by decreasing TTR protein turnover. These results suggest that enhanced TTR degradation at distal sites could ameliorate neuronal TTR phenotypes.

Reduction or Small Molecule Stabilization of Native TTR Levels Improves TTR-Mediated Locomotion Impairments and Decreases Oligomeric Aggregate Load.

As neurons or possibly muscles are affected in our models, we next assessed whether expressing V30M TTR led to movement impairments. Expression of V30M TTR resulted in impaired locomotion as measured by decreased displacement and velocities compared with non-TTR controls, and TTR RNAi rescued this phenotype (Fig. 7 *A* and *B* and *SI Appendix*, Fig. S4). These motility defects could be the result of impaired muscle and/or neuronal function (39, 40). To test whether V30M TTR motility could be affected as a result of muscle dysfunction, we performed TTR RNAi in the D18G strain in which we observed no evidence of TTR secretion (Fig. 2*C*). One-day-old D18G TTR animals exhibited a pronounced uncoordinated (Unc) phenotype, which was

rescued by RNAi against TTR (Fig. 7 *C* and *D*). These data suggest that D18G TTR proteotoxicity affects proteostasis in the muscle and results in its malfunction, although muscle morphology appeared unaffected (Fig. 2*A* and *SI Appendix*, Fig. S2). Thus, expression of V30M TTR could result in defects in locomotion due to TTR cell-autonomous impairment of muscle function, but this merits further scrutiny.

Next, we tested whether stabilizing TTR pharmacologically would ameliorate the TTR-dependent Unc phenotype. To stabilize the native TTR tetramer quaternary structure, we treated V30M TTR animals with **CMPD5**. In addition to being fluorogenic upon binding to and reacting with TTR (Fig. 2 *B* and *C*), **CMPD5** affords a hyperstable tetramer, which ameliorates FAP by preventing aggregation, similar to tafamidis (8, 30). We chose **CMPD5** as the kinetic stabilizer instead of tafamidis because **CMPD5** exhibits better solubility (41). Since V30M TTR oligomers were detected in day-1 adult animals (Fig. 3*C*), we initially treated L1, L3, L4, and day-1 animals with various concentrations of **CMPD5** to establish a therapeutic dose. We determined that 10 μM applied to L3 larvae produced a response without toxicity (Fig. 7*E* and *SI Appendix*, Fig. S11*A*). **CMPD5**-treated L3 V30M TTR larvae assessed at day 2 of adulthood exhibited significantly restored locomotion (51.3% rescue of mean speed) compared with nontreated animals (Fig. 7 *F* and *G*). These data show that *C. elegans* FAP models respond to treatment with a pharmacological kinetic stabilizer to ameliorate TTR-dependent phenotypes, likely as a result of the stabilization of TTR tetramers, as demonstrated in human FAP patient serum (31).

To test whether the rescued locomotion phenotype following treatment with **CMPD5** was the result of a decrease in the TTR oligomeric aggregate load, we measured NN TTR levels by ELISA in lysates of day-2 V30M TTR animals with or without **CMPD5**. We observed a significant reduction in NN V30M TTR levels only in the soluble fractions of V30M TTR strains without coelomocytes (*SI Appendix*, Fig. S11*C*), which we earlier showed had significantly increased NN TTR oligomer levels (Fig. 6*D*). These data suggest that the rescue of the locomotion phenotype with **CMPD5** could result from a decrease in the soluble NN TTR oligomer pool. Taken together, our data show that preventing TTR aggregation, either by reducing TTR levels via RNAi or by slowing tetramer dissociation with a kinetic stabilizer (i.e., **CMPD5**), can rescue TTR-mediated locomotion defects, showing that the locomotion phenotype results from TTR aggregation.

DISCUSSION

A Model to Study Cell-Nonautonomous Proteostatic Mechanisms for Modulating Aggregate-Prone Toxicity.

Previous *C. elegans* proteinopathy models expressing human disease-linked aggregation-prone proteins specifically in the body-wall muscle, neurons, or intestine exhibited uniquely cell-autonomous tissue-specific toxicity (1). These included degenerative disease models expressing amyloid beta (Aβ) (29), poly-glutamine expansion proteins (42, 43), α-synuclein (44), WT or mutant prion protein (45), various tau variants (46), TDP-43 (47), an Ig light chain (48), and α1-antitrypsin (49). Recent observations in cell-culture models and mice have demonstrated that proteotoxicity by misfolded proteins in AD, PD, amyotrophic lateral sclerosis, Huntington's disease, and the prion diseases also appear to have cell-nonautonomous components that involve damage of tissues or cells other than those expressing the aggregation-prone, disease-associated proteins (50–52). However, the cell-nonautonomous pathways of neurodegeneration remain incompletely understood for all human amyloid diseases, in part due to the lack of models that faithfully recapitulate *in trans* toxicity. *C. elegans* have been used previously to model and characterize the cell-nonautonomous role of neuronal signaling in the impairment and restoration of proteostasis across tissues. Specifically, null mutations in *unc-30*, a transcription factor that regulates the synthesis of the inhibitory neurotransmitter GABA, caused the premature appearance of polyQ35 aggregates and an imbalance in proteostasis of postsynaptic muscle cells (53). Moreover, down-regulation of neuronally expressed *gei-11* (54), a Myb-family factor that regulates L-type AChR, increased cholinergic receptor activity at the neuromuscular junction and suppressed toxicity and protein misfolding in postsynaptic muscle cells, suggesting an effect of cholinergic signaling on muscle homeostasis (55). In addition, cell-to-cell spreading of protein aggregates has been modeled previously in *C. elegans* by expressing the cytosolic Sup35 prion NM domain from yeast in the body-wall muscle (56). Also, human α-synuclein aggregates in *C. elegans* were shown to transfer between neurons (57). Thus, these promising transgenic models could contribute to elucidating cell-nonautonomous mechanisms as well as the effects of cell-to-cell transfer of aggregate-prone toxicity, which remain unclear for all human aggregate- and spread-prone misfolding proteins.

In the TTR amyloid diseases, cell-nonautonomous toxicity is the default mechanism, thus affording the possibility to study mechanisms of toxicity directly *in trans*. The TTR models studied herein recapitulate TTR cell-nonautonomous neurotoxicity and show clear cell-nonautonomous disease model phenotypes in *C. elegans*. Our model (Fig. 8) posits that disease-prone WT TTR and V30M

TTR tetramers are secreted from the muscle into the body cavity where they are endocytosed by coelomocytes for degradation, a process that competes with NN TTR oligomer generation (i.e., misfolding and aggregation). Increases in NN V30M TTR oligomers correlate with compromised FLP sensory neuronal structure and function, as well as with locomotion defects, although other aggregated TTR structures could also contribute. D18G TTR was not efficiently secreted from the muscle, forming intracellular aggregates and exhibiting strong paralysis. We hypothesize that an overloaded ERAD system was unable to degrade D18G TTR in the muscle, demonstrating that TTR toxicity could also act cell autonomously.

The presence of protein aggregates in neurodegenerative diseases is a key indicator of disrupted organismal proteostasis (58, 59). Since increasing the NN V30M TTR oligomer load by inhibiting cell-nonautonomous TTR degradation by coelomocyte ablation significantly exacerbated the nociceptive defect in V30M TTR animals, our studies suggest that the NN V30M TTR oligomers contributed to the degenerative phenotype (Fig. 8). A conclusion from our study is that adjusting TTR tetramer concentration both cell autonomously (by RNAi to decrease TTR mRNA in the muscle) and cell nonautonomously (by coelomocyte ablation) can modulate cell-nonautonomous TTR proteotoxicity. Moreover, TTR tetramer kinetic stabilization by a small molecule reduced TTR oligomers and rescued V30M-mediated locomotion defects (Fig. 7 and *SI Appendix*, Fig. S11). These data suggest that *C. elegans* TTR models recapitulated human TTR aggregation pathways, as RNAi and kinetic stabilizers slow or stop degeneration in humans. The notion that protein-aggregate formation and proteostasis can be modulated by altering the levels of aggregate precursors in either the TTR-secreting cells or in distal cells primarily responsible for TTR degradation could provide avenues for possible therapeutic interventions. As coelomocyte degradation is autophagosomal (60), our data suggest that modulating autophagic activity cell nonautonomously could regulate TTR tetramer and oligomer levels and reduce NN TTR-mediated neurotoxicity. The liver, muscle, and skin have been shown to be the major sites of TTR degradation in rats, with no detectable degradation occurring in nervous tissue (61). Thus, the activation of autophagy or analogous lysosomal degradation mechanisms in these tissues should be considered as a strategy for treating the TTR amyloidoses and other amyloid diseases.

Cell-Nonautonomous Impairment of Neuronal Structure and Function by Toxic Oligomeric TTR.

In this study, we modeled V30M TTR-associated FAP cell-nonautonomous neurotoxicity, a feature not recapitulated in previously published *Drosophila* or murine models (22–24). Consistent with the observed defects in nociceptive sensing, extracellular V30M TTR resulted in defective FLP

dendritic branch extension and in ectopic branching that appeared to be due to degenerative processes rather than developmental defects. As nociceptive sensing was only partially impaired in V30M TTR animals, it is possible that TTR proteotoxicity primarily impaired FLP function, whereas AFD, the other neurons responsible for nociception (30, 32), were less affected; however, this needs to be evaluated further. Putative sensory neuron selectivity would suggest a specific TTR-targeting mechanism. However, V30M TTR toxicity appeared not to be selective for nociceptive neurons, as we observed defective subcellular phenotypes in mechanosensory neurons (mitochondrial size). The extent of putative *in trans* deficits in other neurons merits future investigation.

It is unclear whether TTR toxicity is imparted via direct neuronal internalization of TTR, but previous *in vitro* studies showed that TTR can be endocytosed into sensory neurons (62, 63). Our data show that animals expressing V30M TTR inside FLP neurons have a normal nociceptive response, demonstrating that TTR expression inside neurons may not be sufficient to drive toxicity. Thus, unknown extracellular pathways could mediate the effects of TTR toxicity. Another possibility is that V30M TTR could internalize in other neurons and drive toxicity in FLP sensory neurons via direct or indirect neuron-to-neuron interactions. In either case, our data point toward neuronal toxicity occurring as a result of cell-nonautonomous mechanisms, as nociception was not affected in the nonsecreting D18G TTR animals.

The observed cell-nonautonomous neuronal phenotypes of V30M TTR animals suggest that affected neurons experienced increased cell-nonautonomous proteostatic stress and a heightened stress response. How a TTR-mediated proteotoxic cell-nonautonomous stress response might be regulated remains unknown. Importantly, *in trans* mechanisms have been shown to play a role in the regulation of stress response pathways in *C. elegans* and mammals (64–67). At the organismal level in *C. elegans*, the heat-shock response (HSR) is regulated in somatic nonneuronal tissues by the AFD thermosensory neurons, which, in addition to regulating nociception, also normally modulate responses to ambient temperature to adjust thermotaxis (68). While it is unknown whether AFD function is compromised in V30M TTR animals, it is possible, because this neuron is involved in nociception (34), that a putative defective AFD function could result in an impaired HSR. If this response is impaired in V30M TTR animals, the ability of this neuron to mount an HSR could lead to the misregulation of organismal-level proteostasis. Interestingly, mutations affecting AFD function (*tax-4*, *gcy-8*, and *gcy-23*) both impair the ability to mount an HSR and display a diminished nociceptive response (68).

TTR toxicity also resulted in overbranching dendritic morphology. Notably, previous studies showed that, upon aging, the *C. elegans* nervous system exhibits significant age-dependent ectopic branching rather than neuronal cell death (69, 70). The underlying mechanisms of age-dependent aberrant ectopic branches in WT animals in these earlier studies are still unclear, but these features correlated with the age-related deterioration of synaptic structure and function. Indeed, early-disease pathology in humans is characterized by neuronal alterations, including significant dendritic pathology (71), that precede cell death. Thus, the *C. elegans* dendritic arborization phenotypes observed herein correlate with age-dependent neuronal deterioration and are already apparent in young-adult TTR animals. Thus, the models presented here seem poised to facilitate the elucidation of the mechanisms of TTR aggregation-dependent neurodegeneration. Moreover, these models could be key for scrutinizing the basis of tissue tropism in the TTR amyloidoses, e.g., neuronal versus cardiac degeneration. Due to its analogy to the vertebrate heart, the rhythmic contractile activity of the pharynx in the transgenic *C. elegans* TTR models could be used to characterize the basis of TTR cardiac tissue toxicity in TTR cardiomyopathies, as accomplished previously in other amyloidosis models (48). The ability to probe for tissue-specific mechanisms of toxicity and do genetic screens in *C. elegans* should help identify the genetic and molecular pathways by which peripheral tissues, including heart or sensory neurons, are selectively impaired in the TTR amyloidoses.

MATERIAL AND METHODS

Detailed methods and a complete list of strains and constructs used in this study are provided in *SI Appendix*, *SI Materials and Methods*.

Native PAGE Gel Analysis for Detection of TTR Oligomers.

Soluble lysate and the insoluble pellet were obtained from synchronized *C. elegans* as described in *SI Appendix*, *SI Materials and Methods*. The samples were resolved on Novex NativePAGE 3–12% Bis-Tris protein gels (Invitrogen) and probed with the MDX102 antibody against oligomeric TTR after transfer to a nitrocellulose membrane. Validation of antibodies used in this assay is reported in *SI Appendix*, *SI Materials and Methods* under *Antibodies Against Oligomeric TTR* (*SI Appendix*, Fig. S3 *A* and *B*).

Quantification of NN TTR Levels *in vitro* by ELISA.

NN TTR levels were quantitated using a sandwich ELISA developed by Misfolding Diagnostics, Inc. (patent WO2014/124334A2). Validation of antibodies used in this assay is reported in *SI Appendix*, *SI Materials and Methods* under *Antibodies Against Oligomeric TTR* (*SI Appendix*, Fig. S3 *A* and *B*). The lysates were obtained as mentioned above. Each sample used in the assay contained 2.4 µg of the total protein. A misfolded form of recombinant TTR protein was used to generate the standard curve.

Thermal-Avoidance Assay for Nociception.

The thermal-avoidance assay was done on day-1 adult animals, and their response to noxious heat was scored in one of the four categories, as published previously (*SI Appendix*, *SI Materials and Methods*) (33).

Locomotion Assay and Worm-Tracking Analysis.

Individual day-2 adult animals' movement trajectories were recorded for a duration of 40 s using a Stemi 508 microscope (Zeiss) with a SwiftCam2 camera and imaging software (Swift). All movies were analyzed using the wrMTrck plugin for ImageJ to obtain average speed and representative tracks of each of the trajectories (*SI Appendix*, *SI Materials and Methods*) (72).

ACKNOWLEDGMENTS

We thank J. Genereux, C. Monteiro, J. Chen, Y. Eisele, and G. Dendle (The Scripps Research Institute) for assistance with UPLC experiments and providing recombinant TTR; C. Link (University of Colorado at Boulder), C. Bargmann (The Rockefeller University), H. Fares (University of Arizona), and the Caenorhabditis Genetics Center for strains; S. Srinivasan (The Scripps Research Institute) and M. Hansen (Sanford Burnham Prebys Medical Discovery Institute) for reagents; S. Wolff and P. Frankino (University of California, Berkeley) for preliminary analyses; and M. Hansen, M. Petrascheck, C. Fearns, L. Wiseman, and members of the S.E.E. laboratory for advice and critical feedback on the manuscript. This work was supported in part by NIH-National Institute on Aging Grant R01AG049483, by the Glenn Foundation for Medical Research Glenn Award for Research in Biological Mechanisms of Aging, by a New Scholar in Aging Award from the Lawrence Ellison Foundation, and by Baxter Family Foundation awards (to S.E.E.); and by NIH-National Institute of Diabetes and Digestive and Kidney Disease Grant DK046335 (to J.W.K.). K.M. and E.R.G. were supported by the George E. Hewitt Foundation for Medical Research. M.A.-F. was supported by Fundação para a Ciência e Tecnologia Fellowship SFRH/BD/101352/2014, and J.F.P. was supported by the Swedish Research Council. V.P. is funded by NIH Grant R01 AG 050653. F.K.O. was supported by a graduate student fellowship from the Developmental Studies Hybridoma Bank.

REFERENCES

1. Nussbaum-Krammer CI, Morimoto RI. *Caenorhabditis elegans* as a model system for studying non-cell-autonomous mechanisms in protein-misfolding diseases. Dis Model Mech. 2014;7:31–39.

2. Goedert M, Falcon B, Clavaguera F, Tolnay M. Prion-like mechanisms in the pathogenesis of tauopathies and synucleinopathies. Curr Neurol Neurosci Rep. 2014;14:495.

3. Holmgren G, et al. Biochemical effect of liver transplantation in two Swedish patients with familial amyloidotic polyneuropathy (FAP-met30) Clin Genet. 1991;40:242–246.

4. Blake CC, Geisow MJ, Oatley SJ, Rérat B, Rérat C. Structure of prealbumin: Secondary, tertiary and quaternary interactions determined by Fourier refinement at 1.8 A. J Mol Biol. 1978;121:339–356.

5. Monaco HL, Rizzi M, Coda A. Structure of a complex of two plasma proteins: Transthyretin and retinol-binding protein. Science. 1995;268:1039–1041.

6. Bartalena L, Robbins J. Variations in thyroid hormone transport proteins and their clinical implications. Thyroid. 1992;2:237–245.

7. Coelho T, et al. A strikingly benign evolution of FAP in an individual found to be a compound heterozygote for two TTR mutations: TTR MET 30 and TTR MET 119. J Rheumatol. 1993;20:179.

8. Johnson SM, Connelly S, Fearns C, Powers ET, Kelly JW. The transthyretin amyloidoses: From delineating the molecular mechanism of aggregation linked to pathology to a regulatory-agency-approved drug. J Mol Biol. 2012;421:185–203.

9. Schonhoft JD, et al. Peptide probes detect misfolded transthyretin oligomers in plasma of hereditary amyloidosis patients. Sci Transl Med. 2017;9:eaam7621.

10. Saraiva MJ, Costa PP, Birken S, Goodman DS. Presence of an abnormal transthyretin (prealbumin) in Portuguese patients with familial amyloidotic polyneuropathy. Trans Assoc Am Physicians. 1983;96:261–270.

11. Eisele YS, et al. Targeting protein aggregation for the treatment of degenerative diseases. Nat Rev Drug Discov. 2015;14:759–780.

12. Olzscha H, et al. Amyloid-like aggregates sequester numerous metastable proteins with essential cellular functions. Cell. 2011;144:67–78.

13. Escusa-Toret S, Vonk WIM, Frydman J. Spatial sequestration of misfolded proteins by a dynamic chaperone pathway enhances cellular fitness during stress. Nat Cell Biol. 2013;15:1231–1243.

14. Voisine C, Pedersen JS, Morimoto RI. Chaperone networks: Tipping the balance in protein folding diseases. Neurobiol Dis. 2010;40:12–20.

15. Caughey B, Lansbury PT. Protofibrils, pores, fibrils, and neurodegeneration: Separating the responsible protein aggregates from the innocent bystanders. Annu Rev Neurosci. 2003;26:267–298.

16. Sekijima Y, et al. The biological and chemical basis for tissue-selective amyloid disease. Cell. 2005;121:73–85.

17. Saraiva MJ. Transthyretin mutations in health and disease. Hum Mutat. 1995;5:191–196.

18. Coelho T, Maurer MS, Suhr OB. THAOS–The Transthyretin Amyloidosis Outcomes Survey: Initial report on clinical manifestations in patients with hereditary and wild-type transthyretin amyloidosis. Curr Med Res Opin. 2013;29:63–76.

19. Hammarström P, et al. D18G transthyretin is monomeric, aggregation prone, and not detectable in plasma and cerebrospinal fluid: A prescription for central nervous system amyloidosis? Biochemistry. 2003;42:6656–6663.

20. Vidal R, et al. Meningocerebrovascular amyloidosis associated with a novel transthyretin mis-sense mutation at codon 18 (TTRD 18G) Am J Pathol. 1996;148:361–366.

21. Westermark P, Sletten K, Johansson B, Cornwell GG., 3rd Fibril in senile systemic amyloidosis is derived from normal transthyretin. Proc Natl Acad Sci USA. 1990;87:2843–2845.

22. Buxbaum JN. Animal models of human amyloidoses: Are transgenic mice worth the time and trouble? FEBS Lett. 2009;583:2663–2673.

23. Berg I, Thor S, Hammarström P. Modeling familial amyloidotic polyneuropathy (Transthyretin V30M) in Drosophila melanogaster. Neurodegener Dis. 2009;6:127–138.

24. Pokrzywa M, Dacklin I, Hultmark D, Lundgren E. Misfolded transthyretin causes behavioral changes in a Drosophila model for transthyretin-associated amyloidosis. Eur J Neurosci. 2007;26:913–924.

25. Jiang X, Kelly JW, Chapman J. 2014. US Patent WO2014124334A2.

26. Sousa MM, Cardoso I, Fernandes R, Guimarães A, Saraiva MJ. Deposition of transthyretin in early stages of familial amyloidotic polyneuropathy: Evidence for toxicity of nonfibrillar aggregates. Am J Pathol. 2001;159:1993–2000.

27. Choi S, Connelly S, Reixach N, Wilson IA, Kelly JW. Chemoselective small molecules that covalently modify one lysine in a non-enzyme protein in plasma. Nat Chem Biol. 2010;6:133–139.

28. Fares H, Greenwald I. Genetic analysis of endocytosis in Caenorhabditis elegans: Coelomocyte uptake defective mutants. Genetics. 2001;159:133–145.

29. Link CD. Expression of human beta-amyloid peptide in transgenic Caenorhabditis elegans. Proc Natl Acad Sci USA. 1995;92:9368–9372.

30. Baranczak A, et al. A fluorogenic aryl fluorosulfate for intraorganellar transthyretin imaging in living cells and in Caenorhabditis elegans. J Am Chem Soc. 2015;137:7404–7414.

31. Rappley I, et al. Quantification of transthyretin kinetic stability in human plasma using subunit exchange. Biochemistry. 2014;53:1993–2006.

32. Adamla F, Ignatova Z. Somatic expression of unc-54 and vha-6 mRNAs declines but not pan-neuronal rgef-1 and unc-119 expression in aging Caenorhabditis elegans. Sci Rep. 2015;5:10692.

33. Wittenburg N, Baumeister R. Thermal avoidance in Caenorhabditis elegans: An approach to the study of nociception. Proc Natl Acad Sci USA. 1999;96:10477–10482.

34. Liu S, Schulze E, Baumeister R. Temperature- and touch-sensitive neurons couple CNG and TRPV channel activities to control heat avoidance in Caenorhabditis elegans. PLoS One. 2012;7:e32360.

35. Albeg A, et al. C. elegans multi-dendritic sensory neurons: Morphology and function. Mol Cell Neurosci. 2011;46:308–317.

36. Treinin M, Gillo B, Liebman L, Chalfie M. Two functionally dependent acetylcholine subunits are encoded in a single Caenorhabditis elegans operon. Proc Natl Acad Sci USA. 1998;95:15492–15495.

37. Chalfie M, Sulston J. Developmental genetics of the mechanosensory neurons of Caenorhabditis elegans. Dev Biol. 1981;82:358–370.

38. Gao J, et al. Abnormalities of mitochondrial dynamics in neurodegenerative diseases. Antioxidants. 2017;6:E25.

39. Morley JF, Brignull HR, Weyers JJ, Morimoto RI. The threshold for polyglutamine-expansion protein aggregation and cellular toxicity is dynamic and influenced by aging in *Caenorhabditis elegans*. Proc Natl Acad Sci USA. 2002;99:10417–10422.

40. Wang J, et al. An ALS-linked mutant SOD1 produces a locomotor defect associated with aggregation and synaptic dysfunction when expressed in neurons of *Caenorhabditis elegans*. PLoS Genet. 2009;5:e1000350.

41. Grimster NP, et al. Aromatic sulfonyl fluorides covalently kinetically stabilize transthyretin to prevent amyloidogenesis while affording a fluorescent conjugate. J Am Chem Soc. 2013;135:5656–5668.

42. Brignull HR, Morley JF, Morimoto RI. The stress of misfolded proteins: C. elegans models for neurodegenerative disease and aging. Adv Exp Med Biol. 2007;594:167–189.

43. Parker JA, Holbert S, Lambert E, Abderrahmane S, Néri C. Genetic and pharmacological suppression of polyglutamine-dependent neuronal dysfunction in Caenorhabditis elegans. J Mol Neurosci. 2004;23:61–68.

44. Lakso M, et al. Dopaminergic neuronal loss and motor deficits in *Caenorhabditis elegans*overexpressing human α-synuclein. J Neurochem. 2003;86:165–172.

45. Park KW, Li L. Cytoplasmic expression of mouse prion protein causes severe toxicity in *Caenorhabditis elegans*. Biochem Biophys Res Commun. 2008;372:697–702.

46. Hannan SB, Dräger NM, Rasse TM, Voigt A, Jahn TR. Cellular and molecular modifier pathways in tauopathies: The big picture from screening invertebrate models. J Neurochem. 2016;137:12–25.

47. Ash PE, et al. Neurotoxic effects of TDP-43 overexpression in C. elegans. Hum Mol Genet. 2010;19:3206–3218.

48. Diomede L, et al. A Caenorhabditis elegans-based assay recognizes immunoglobulin light chains causing heart amyloidosis. Blood. 2014;123:3543–3552.

49. Cummings EE, et al. Deficient and null variants of SERPINA1 are proteotoxic in a Caenorhabditis elegans model of α1-antitrypsin deficiency. PLoS One.2015;10:e0141542.

50. Ilieva H, Polymenidou M, Cleveland DW. Non-cell autonomous toxicity in neurodegenerative disorders: ALS and beyond. J Cell Biol. 2009;187:761–772.

51. Brundin P, Melki R, Kopito R. Prion-like transmission of protein aggregates in neurodegenerative diseases. Nat Rev Mol Cell Biol. 2010;11:301–307.

52. Marchetto MC, et al. Non-cell-autonomous effect of human SOD1 G37R astrocytes on motor neurons derived from human embryonic stem cells. Cell Stem Cell. 2008;3:649–657.

53. Garcia SM, Casanueva MO, Silva MC, Amaral MD, Morimoto RI. Neuronal signaling modulates protein homeostasis in Caenorhabditis elegans post-synaptic muscle cells. Genes Dev. 2007;21:3006–3016.

54. Silva MC, et al. A genetic screening strategy identifies novel regulators of the proteostasis network. PLoS Genet. 2011;7:e1002438.

55. Silva MC, Amaral MD, Morimoto RI. Neuronal reprograming of protein homeostasis by calcium-dependent regulation of the heat shock response. PLoS Genet. 2013;9:e1003711.

56. Nussbaum-Krammer CI, Park KW, Li L, Melki R, Morimoto RI. Spreading of a prion domain from cell-to-cell by vesicular transport in Caenorhabditis elegans. PLoS Genet. 2013;9:e1003351.

57. Tyson T, et al. Novel animal model defines genetic contributions for neuron-to-neuron transfer of α-synuclein. Sci Rep. 2017;7:7506.

58. Balch WE, Morimoto RI, Dillin A, Kelly JW. Adapting proteostasis for disease intervention. Science. 2008;319:916–919.

59. Hartl FU, Bracher A, Hayer-Hartl M. Molecular chaperones in protein folding and proteostasis. Nature. 2011;475:324–332.

60. Sun T, Wang X, Lu Q, Ren H, Zhang H. CUP-5, the *C. elegans* ortholog of the mammalian lysosomal channel protein MLN1/TRPML1, is required for proteolytic degradation in autolysosomes. Autophagy. 2011;7:1308–1315.

61. Makover A, et al. Plasma transthyretin. Tissue sites of degradation and turnover in the rat. J Biol Chem. 1988;263:8598–8603.

62. Sousa MM, Saraiva MJ. Internalization of transthyretin. Evidence of a novel yet unidentified receptor-associated protein (RAP)-sensitive receptor. J Biol Chem. 2001;276:14420–14425.

63. Fleming CE, Mar FM, Franquinho F, Saraiva MJ, Sousa MM. Transthyretin internalization by sensory neurons is megalin mediated and necessary for its neuritogenic activity. J Neurosci. 2009;29:3220–3232.

64. Blake MJ, Udelsman R, Feulner GJ, Norton DD, Holbrook NJ. Stress-induced heat shock protein 70 expression in adrenal cortex: An adrenocorticotropic hormone-sensitive, age-dependent response. Proc Natl Acad Sci USA. 1991;88:9873–9877.

65. Fawcett TW, Sylvester SL, Sarge KD, Morimoto RI, Holbrook NJ. Effects of neurohormonal stress and aging on the activation of mammalian heat shock factor 1. J Biol Chem. 1994;269:32272–32278.

66. Taylor RC, Dillin A. XBP-1 is a cell-nonautonomous regulator of stress resistance and longevity. Cell. 2013;153:1435–1447.

67. Durieux J, Wolff S, Dillin A. The cell-non-autonomous nature of electron transport chain-mediated longevity. Cell. 2011;144:79–91.

68. Prahlad V, Cornelius T, Morimoto RI. Regulation of the cellular heat shock response in Caenorhabditis elegans by thermosensory neurons. Science. 2008;320:811–814.

69. Tank EM, Rodgers KE, Kenyon C. Spontaneous age-related neurite branching in Caenorhabditis elegans. J Neurosci. 2011;31:9279–9288.

70. Toth ML, et al. Neurite sprouting and synapse deterioration in the aging Caenorhabditis elegans nervous system. J Neurosci. 2012;32:8778–8790.

71. Kweon JH, Kim S, Lee SB. The cellular basis of dendrite pathology in neurodegenerative diseases. BMB Rep. 2017;50:5–11.

72. Nussbaum-Krammer CI, Neto MF, Brielmann RM, Pedersen JS, Morimoto RI. Investigating the spreading and toxicity of prion-like proteins using the metazoan model organism *C. elegans*. J Vis Exp, 2015:52321.

FIGURES

<u>Figure 1.</u> Generation of *C. elegans* TTR models. (*A*) Schematic of TTR *C. elegans* transgenes generated in this study. The human TTR with SS and full-length WT TTR, V30M TTR, T119M TTR, and D18G TTR variants were expressed under the body-wall muscle–specific promoter *unc-54*. (*B* and *C*, *Upper*) Representative Western blots of soluble (*B*) and insoluble (*C*) fractions of lysates of day-1 (D1), day-5 (D5), and day-8 (D8) adult animals probed with antibody MDX102 against TTR. (*B* and *C, Lower*) TTR/actin ratios (mean ± SEM, *n* = 3), aligned to a representative Western blot for one experiment. The percentage difference in soluble TTR/actin ratios between the strains relative to the WT TTR levels in D1 animals are 43%, 39%, and 92% for V30M, T119M, and D18G, respectively. ctrl, control; SS, signal sequence.

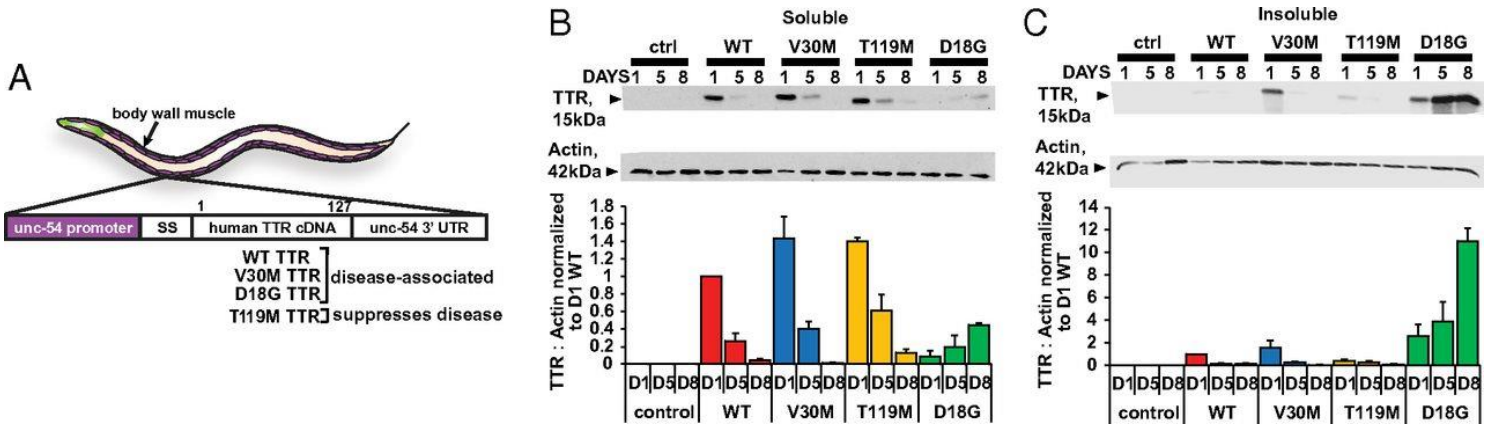

Figure 2. Differential secretion profiles of *C. elegans* TTR models. (*A*) Representative confocal IF images of adult day-1 animals stained with a polyclonal antibody against TTR (green) and phalloidin (F-actin; red). The panels at the far right show maximal intensity projections of whole animals. *Insets* in white boxes show enlargements of head regions in the adjacent column on the left. Arrowheads point to muscle cells; arrows point to the body cavity. The dotted line in the control F-actin panel outlines the contour of a single body-wall muscle cell. *Insets* in orange boxes show enlargements of aggregates. *Insets* in cyan boxes show enlargements of cell-surface TTR staining. (Scale bars: 50 μm.) (*B*) Schematic diagram of the experiment in which worms were fed **CMPD5** to detect TTR–(**CMPD5**)2 conjugates. The black box shows coelomocytes enlarged in *C*. The pharynx is shown in green. (*C*) Enlargements showing coelomocytes. Arrows point to coelomocytes. Control, *n* = 11; WT, *n* = 12; V30M, *n* = 15; T119M, *n* = 21; D18G, *n* = 23. (Scale bar: 10 μm.) DIC, differential interference contrast microscopy. See also *SI Appendix, Fig. S2*.

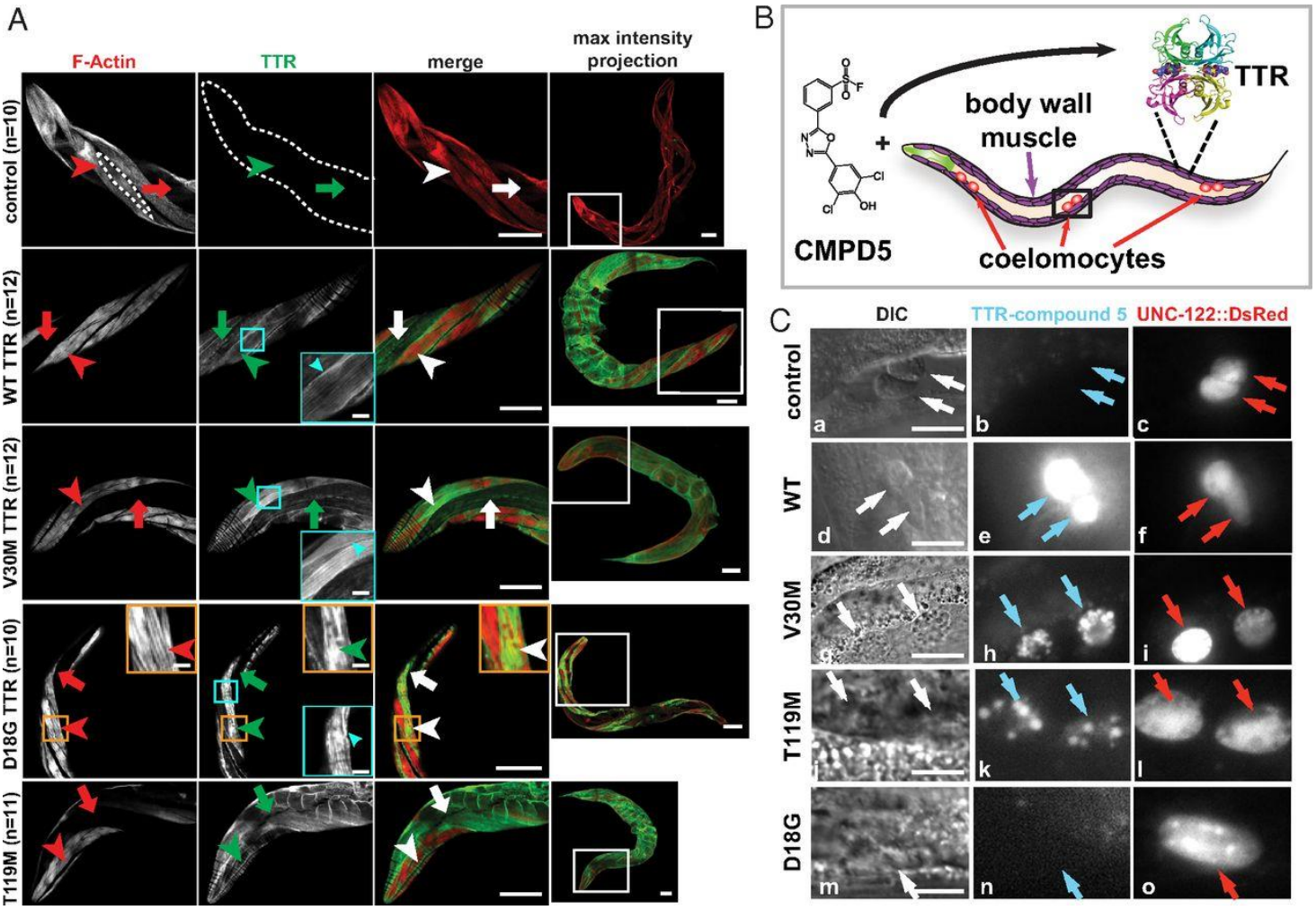

Figure 3. Soluble and insoluble oligomeric TTR aggregates in *C. elegans* TTR models. (*A, Left*) Schematic of the UPLC experiment showing the incubation of **A2** with worm lysates. (*Right*) TTR tetramer–(**A2**)2 fluorescence chromatograms from the UPLC experiment showing the TTR tetramer elution peak (red arrow) identified as TTR by comparison with recombinant TTR control (*SI Appendix*, Fig. S3*C*). AU, arbitrary units. (*B*) Quantification of TTR tetramer levels from UPLC experiments in *A*. Levels were normalized to those of adult day-1 WT TTR animals (mean ± SEM, $n = 3$). (*C*) Native gel blots of the soluble (*Left*) and insoluble (*Right*) fractions of animal lysates probed with anti-TTR MDX102 antibody. Images are representative of five replicates for day-1 samples and three replicates for day-5 samples. Loading controls are shown in *SI Appendix*, Fig. S3*D*. (*D*) NN TTR quantification by a sandwich ELISA for soluble (*Left*) and insoluble (*Right*) lysate fractions (mean ± SEM, $n = 3$). ctrl, control. See also *SI Appendix*, Fig. S3.

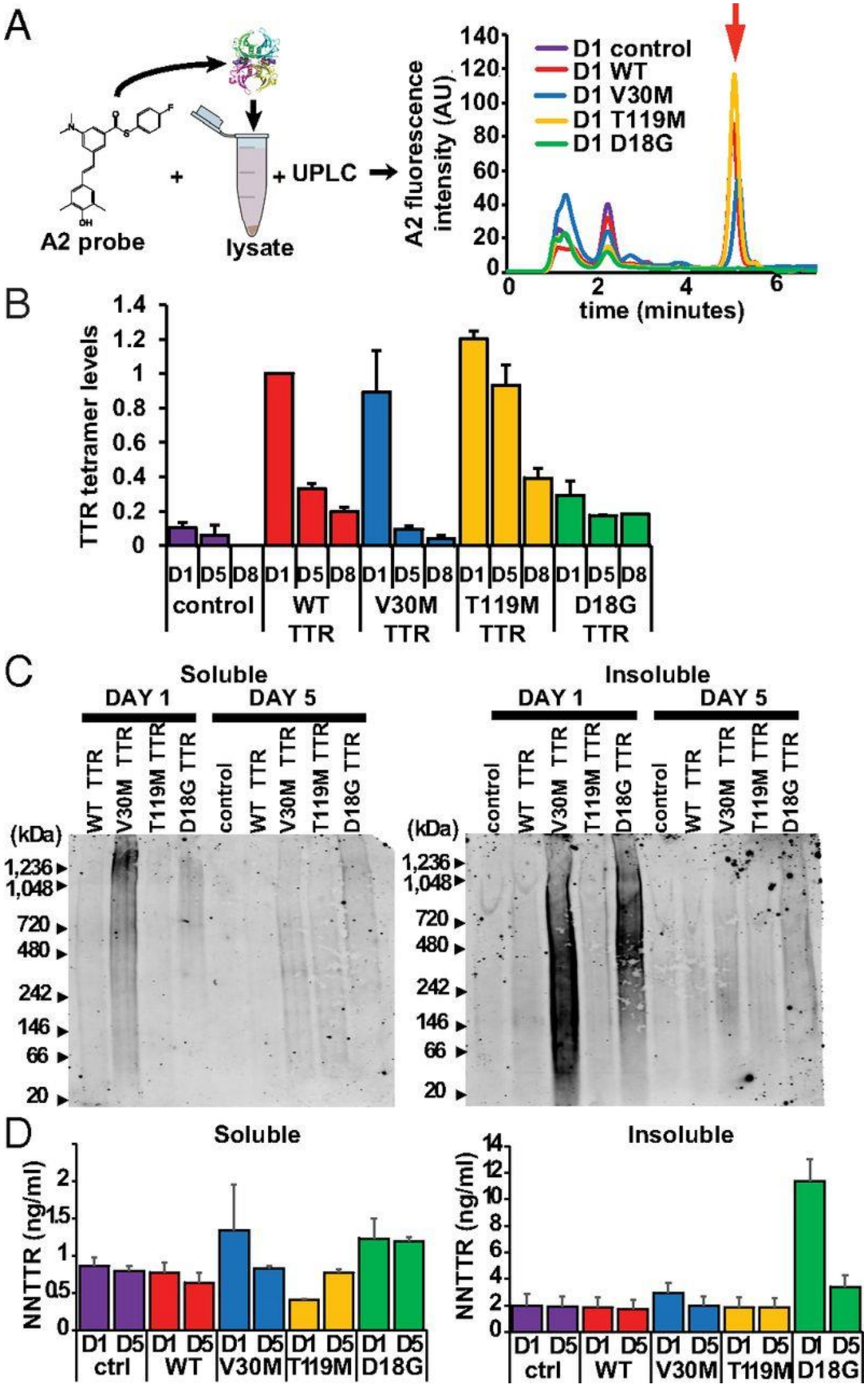
A
A2 probe
+
+ UPLC
lysate
A2 fluorescence intensity (AU)
D1 control
D1 WT
D1 V30M
D1 T119M
D1 D18G
time (minutes)
B
TTR tetramer levels
D1 D5 D8
control
WT TTR
V30M TTR
T119M TTR
D18G TTR
C
Soluble
Insoluble
DAY 1
DAY 5
control
WT TTR
V30M TTR
T119M TTR
D18G TTR
(kDa)
1,236
1,048
720
480
242
146
66
20
D
Soluble
Insoluble
NNTTR (ng/ml)
D1 D5
ctrl
WT
V30M
T119M
D18G

Figure 4. Cell-nonautonomous nociception impairments of TTR animals. (*A*) Schematic of the thermal-avoidance (nociception) assay. (*B*) Thermal-avoidance response of indicated strains. (*C*) Thermal-avoidance response of indicated strains. *unc-54p* and *des-2p* are body-wall muscle and FLP/PVD neuron promoters, respectively. Data in all graphs are representative of at least two experiments (mean ± SEM). ctrl, control; E.V., empty vector. See also *SI Appendix*, Figs. S4–S6 and Tables S1 and S2 for statistics.

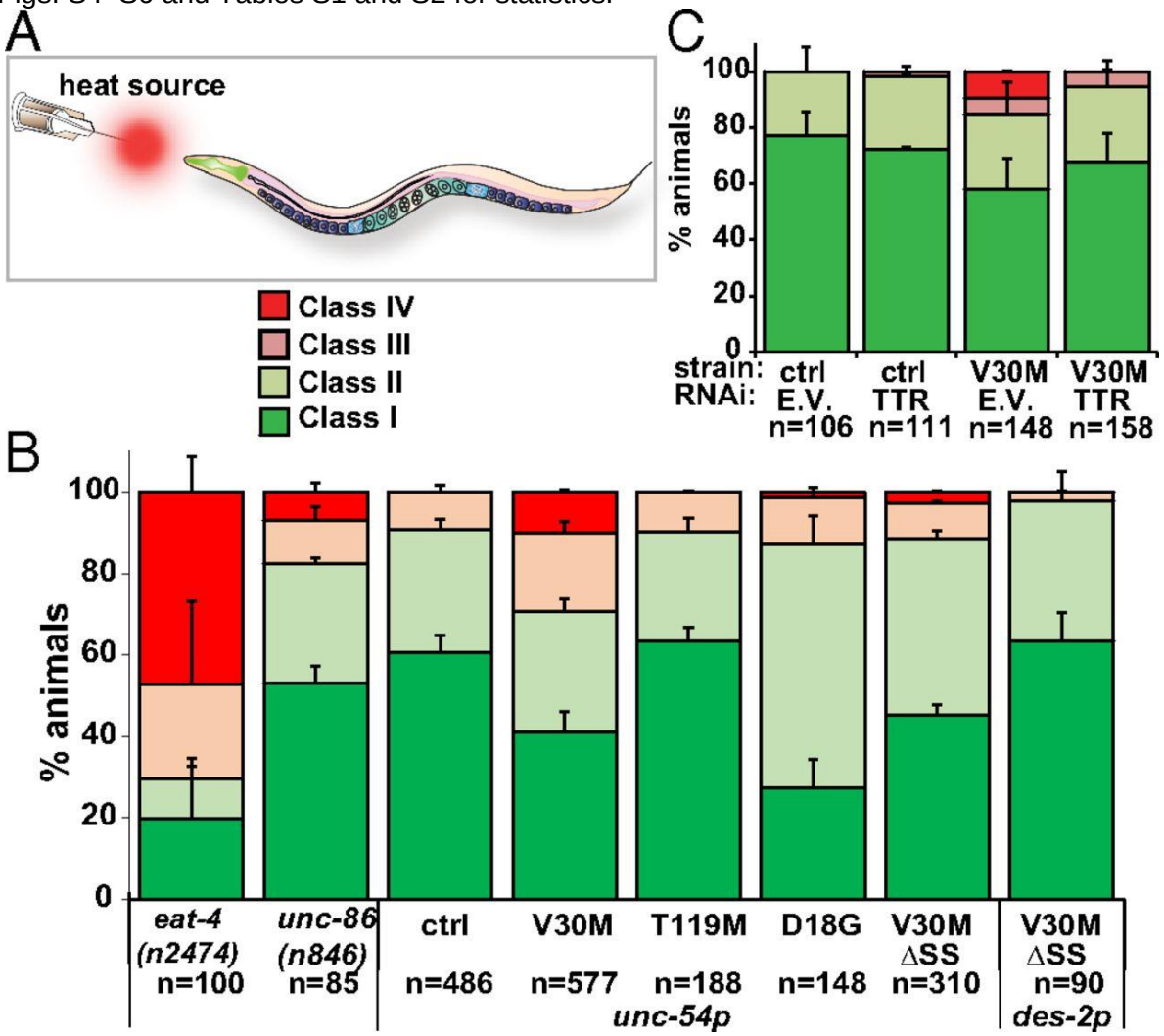

Figure 5. Defective dendritic morphology of V30M TTR sensory neurons. (*A*) Schematic of the morphology of an FLP sensory neuron. Dendrites: 1°: primary; 2°: secondary; 3°: tertiary; 4°: quaternary. (*B*) Representative confocal images of the head region of a day-1 adult animal showing the contour of FLP neurons as delineated by *des-2p*::Myristoyl::GFP with same orientation as in *A*. *Insets* show enlargements of quaternary dendritic branches. Inverted images shown. (*C*) Quantification of the FLP dendrites (mean ± SEM). *n* = 20 animals per strain. ***P* < 0.01, permutation *t* test. n.s., not significant. (*D*) Angles measured in E. (*E*) Histograms of the proportion of angular branches with a deviation greater than 0° in adult day-1 animals. **P* < 0.025; two-sample Kolmogorov–Smirnov test comparing angles of V30M TTR and control/T119M TTR. See also *SI Appendix*, Fig. S7 and Tables S3 and S4.

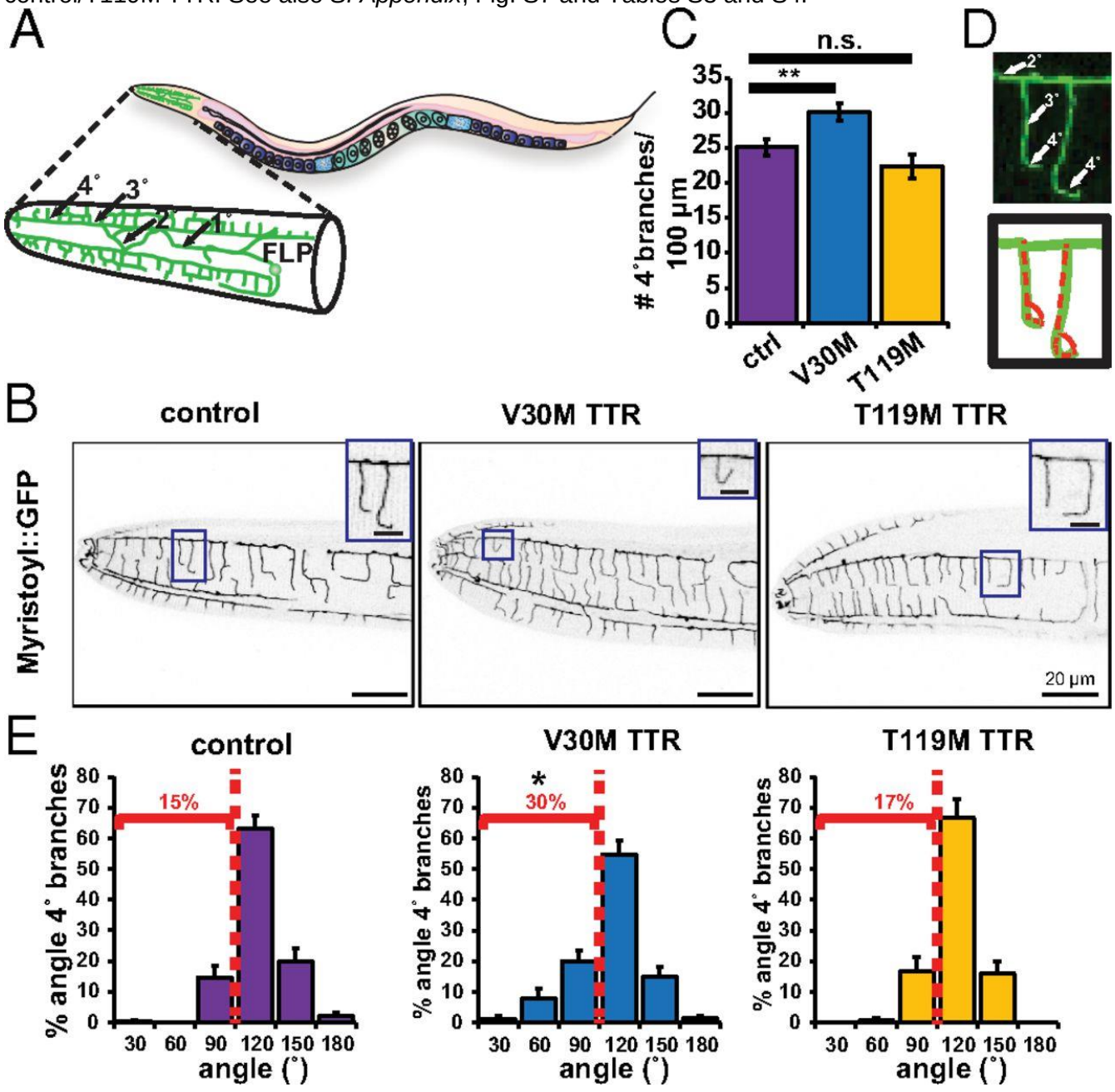

Figure 6. Inhibition of TTR degradation exacerbates TTR cell-nonautonomous neuronal proteotoxicity. (*A*) Representative images showing day-2 adult V30M TTR transgenic animals with (V30M TTR; *n* = 15) and without (V30M TTR: DT-A; *n* = 21) coelomocytes. Coelomocytes in V30M TTR animals were visualized with a UNC-122::Ds-Red marker, but V30M TTR; DT-A animals did not have the UNC-122::Ds-Red marker. Arrowheads point to representative coelomocytes. Arrows point to body cavity fluorescence. *Insets* show enlargements. (Scale bars: 200 μm.) See also *SI Appendix*, Fig. S9 and Table S5. (*B*) Soluble (*Left*) and insoluble (*Right*) TTR protein levels from lysate fractions of synchronized day-1 (D1) and day-5 (D1 and D5) animals. Exp 1: Data are the same as shown in Fig. 1 *B* and *C* for TTR: actin levels of TTR (D5) animals. Exp 2: TTR: actin levels of TTR (D1) and TTR; DT-A (D5) animals. (*C*) Thermal-avoidance response. Data are representative of at least two independent experiments (mean ± SEM). See *SI Appendix*, Fig. S10 and Table S6. ctrl, control. (*D*) NN TTR oligomer levels by a sandwich ELISA in lysates of D1 and D5 adult animals. Three human patient samples before and after tafamidis treatment were included as positive controls for this assay. Data are shown as mean ± SEM, *n* = 3 for all panels, **P* < 0.005, Student's *t* test; ctrl, control.

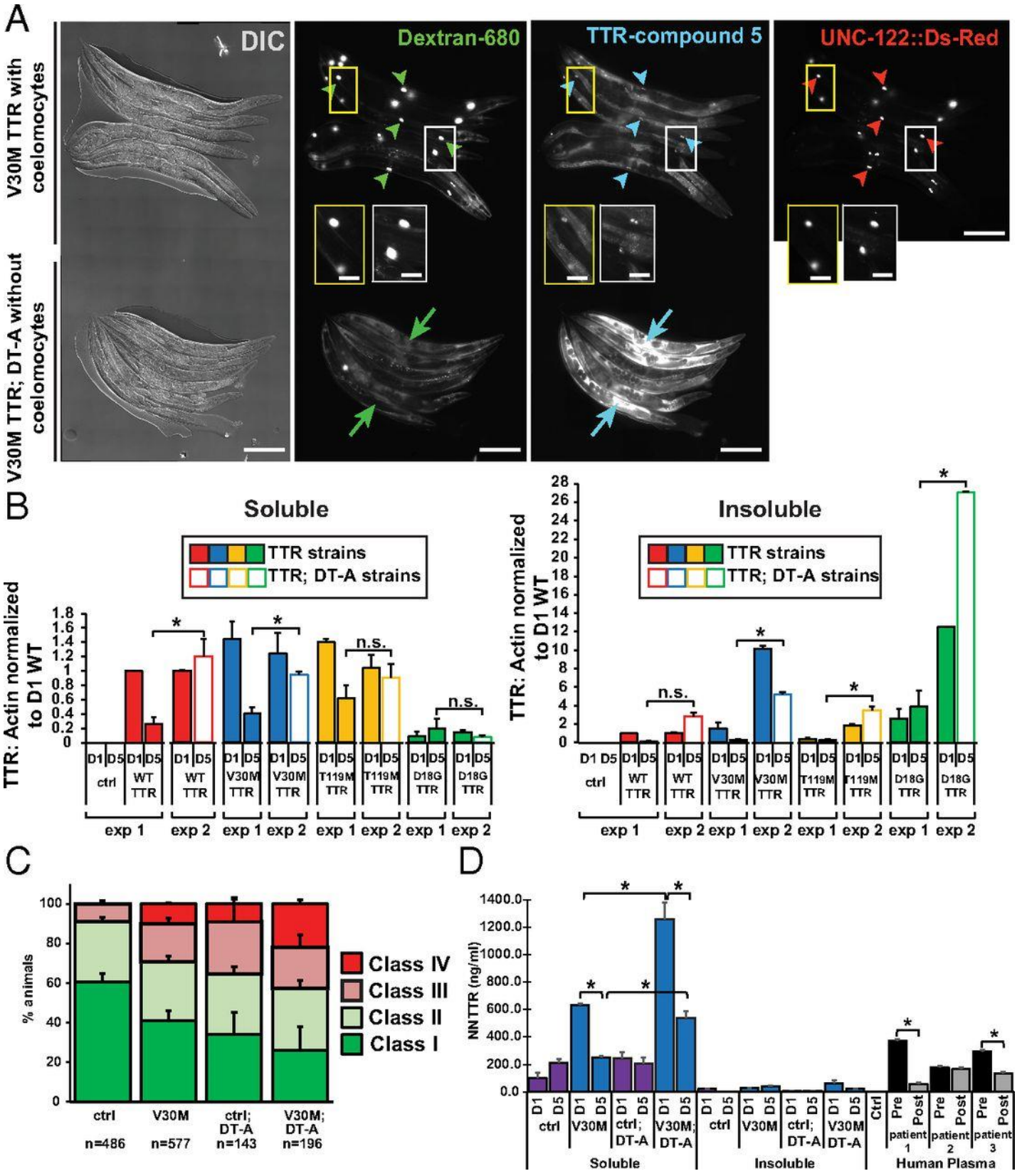
A
V30M TTR with coelomocytes
V30M TTR; DT-A without coelomocytes
DIC
Dextran-680
TTR-compound 5
UNC-122::Ds-Red
B
Soluble
Insoluble
TTR strains
TTR; DT-A strains
TTR: Actin normalized to D1 WT
ctrl
WT TTR
V30M TTR
T119M TTR
D18G TTR
exp 1
exp 2
n.s.
C
% animals
Class IV
Class III
Class II
Class I
ctrl n=486
V30M n=577
ctrl; DT-A n=143
V30M; DT-A n=196
D
NNTTR (ng/ml)
Soluble
Insoluble
Human Plasma
patient 1
patient 2
patient 3
Pre
Post

Figure 7. Reduction or stabilization of TTR levels improves TTR-mediated locomotion impairments. (*A*) Representative 40-s locomotion trajectories of adult day-1 animals quantified in *B*. The starting points for each trajectory were aligned in the middle. (*B*) Comparison of locomotion rates in the indicated strains. The number of animals analyzed is shown inside the bars. See also *SI Appendix*, Fig. S11. (*C*) Representative 40-s locomotion trajectories of the indicated strains. (*D*) Locomotion rates of the animals plotted in *C*. (*E*) Schematic of the timeline for the locomotion and **CMPD5** treatment assay. (*F*) Representative 40-s trajectories of the indicated strains. (*G*) Locomotion rates for 2-d-old strains plotted in *F*. Plots show mean ± SEM, ***P* < 0.005, ****P* < 0.001, by Student's *t* test. E.V., empty vector; n.s., not significant. (Scale bars: 2 mm.)

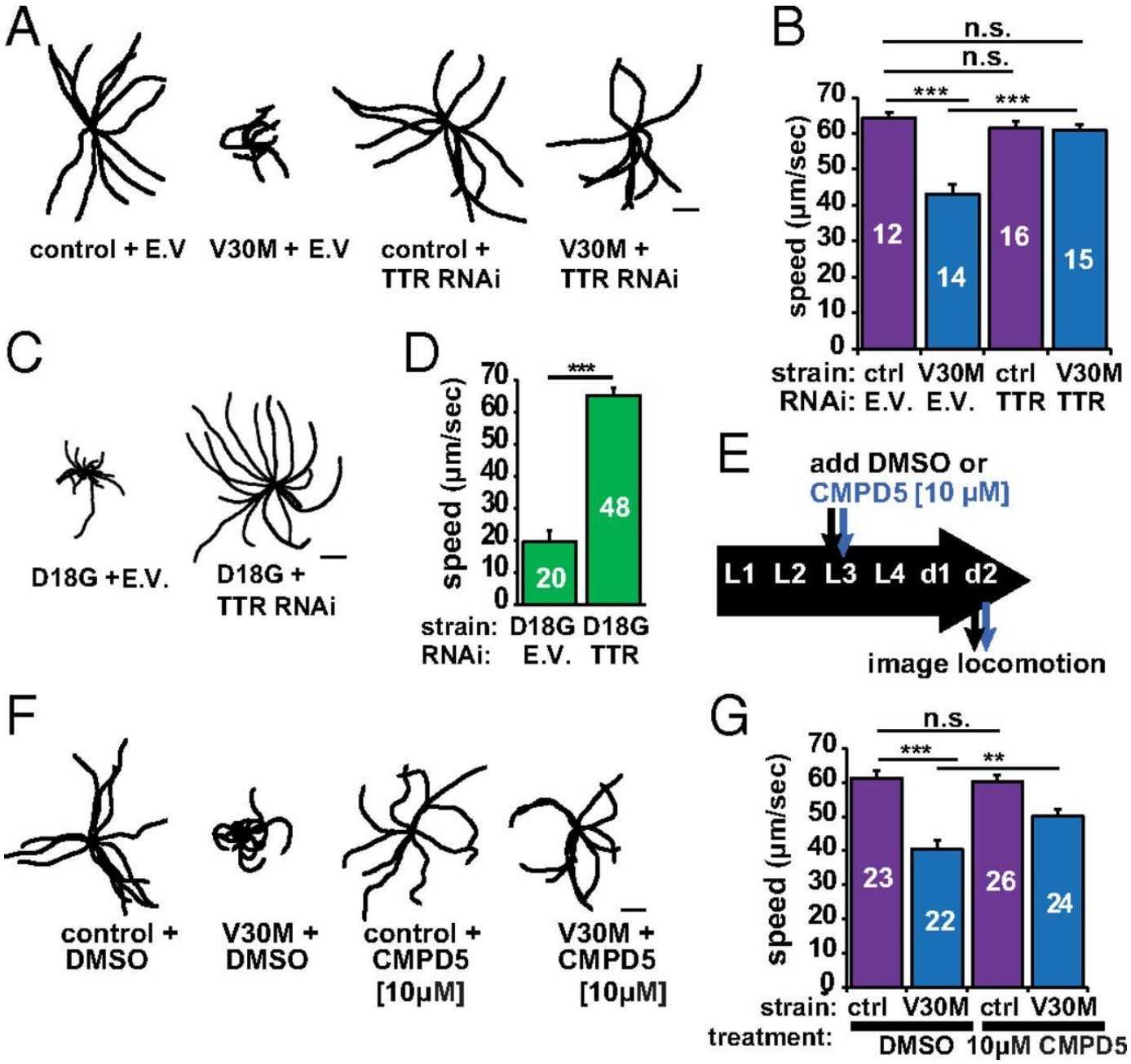

Figure 8. TTR cell-nonautonomous clearance and proteotoxicity model. (*A*) Expression of V30M TTR in the body-wall muscle results in the secretion of this variant as tetramers into the body cavity where V30M TTR is subsequently endocytosed by coelomocytes for degradation. D18G TTR remains in the muscle where it generates cell-autonomous dysfunction. TTR oligomers are generated whose presence correlates with impaired nociceptive response and with morphological abnormalities in the sensory neurons involved in this response. (*B*) Modulation of TTR-dependent cell-nonautonomous proteotoxicity can be accomplished by modifications to TTR degradation at distal sites (coelomocytes). Ablating coelomocytes results in increased TTR-dependent proteotoxicity. Reduction of TTR levels at the source cell autonomously by RNAi or nonautonomously by a small molecule (**CMPD5**) reduces TTR-dependent proteotoxicity.

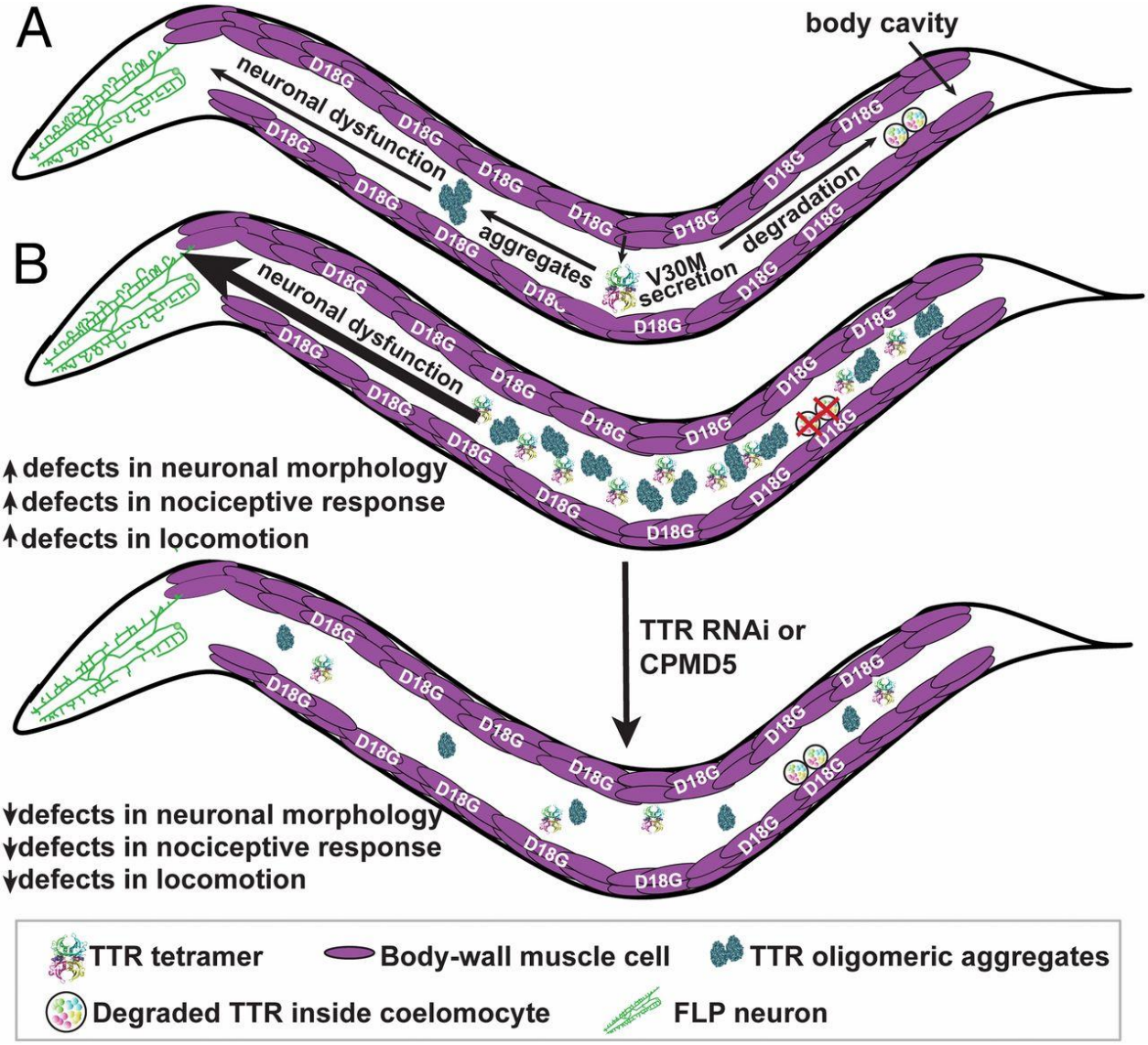

Supplementary Information

Materials and Methods

Strains and transgenes

N2 Bristol was used as the wild-type strain and standard nematode culture methods and genetics were followed as previously described (1). Nematodes were grown on NGM plates seeded with the *E. coli* strain OP50 at 15˚C or 20°C, unless otherwise specified. The strain CX11480 *kyEx3017[des-2p::myr::GFP* + *unc-122p::DsRed]* (2) was provided by C. Bargmann (Rockefeller University). Integration of *kyEx3017* was done by gamma irradiation following standard methods (3). Integrated strains were outcrossed at least 4-8 times into N2 wild-type background. The strain NP717 *unc-119(ed3); arIs37[myo-3p::ssGFP; dpy-20(+)]; cdIs32[pcc-1p::DT-A(E148D); unc-119(+) myo-2p::GFP]* (4) was provided by H. Fares (University of Arizona). The *cdIs32* transgene was isolated by outcrossing the NP717 strain at least 4 times into N2 wild-type background and selecting only for *cdIs32[pcc-1p::DT-A(E148D); unc-119(+) myo-2p::GFP]* transgene expression. The strain LG398 *geIs101[rol-6(su1006)]* was obtained from the *Caenorhabditis* Gene Center (CGC) and outcrossed 8 times before use.

<u>Generation of TTR variant constructs</u>

The following constructs were generated using standard molecular biology techniques, including quick change site directed mutagenesis using KOD-polymerase (EMD Novagen) of construct pCL10 *unc-54p::hTTR(WT*) that was generated and provided by Christopher Link (5)(University of Colorado Boulder): pSEE054 *unc-54p::hTTR(V30M*), pSEE055 *unc-54p::hTTR(D18G*), pSEE057 *unc-54p::hTTR(T119M*), pSEE106 *unc-54p::hTTR(V30M ΔSS*).

The following primers were used for site directed mutagenesis of pCL10 *unc-54p::hTTR(WT*) construct:

V30M Forward 5’-CCTGCCATCAATGTGGCCATGCATGTGTTCAGAAAGGCT-3´
V30M Reverse 5’-CAGCCTTTCTGAACACATGCATGGCCACATTGATGGCAGG-3´
D18G Forward 5’-GGTCAAAGTTCTAGGTGCTGTCCGAGGCAGTCC-3’
D18G Reverse 5’-GGACTGCCTCGGACAGCACCTAGAACTTTGACC-3’
T119M Forward 5’-CTACTCCTATTCCACCATGGCTGTCGTCACCAATC-3’
T119M Reverse 5’-GATTGGTCACGACAGCCATGGTGGAATAGGAGTAG-3’
ΔSS Forward 5’-GGCTAGCGTCGACGGTACCATGGGCCCTACGGGCACCGGTGAATC-3’
ΔSS Reverse 5’-GATTCACCGGTGCCCGTAGGGCCCATGGTACCGTCGACGCTAGCC-3’

Quick change site directed mutagenesis reactions were performed in final concentrations of reaction buffer #2 (0.12 M Tris-HCl, 10 mM KCl, 6 mM (NH4)2SO4, 0.1% Triton X-100, 0.001% BSA, pH 8.8), MgCl2 1.5 mM, dNTPs 0.2 mM (each), KOD DNA Polymerase (0.05 U µl-1), forward and reverse primers 0.4 µM, and template 5 ng µl-1. Amplification was performed by initial denaturation at 95°C for 10 minutes followed by 34 cycles consisting of a 45 second 95°C denaturation, annealing at 61°C for 45 seconds and elongation at 72°C for 90 seconds. Addition of 0.4 U µl-1 DPN1 restriction enzyme (New England Biolabs), digested the methylated template DNA during a 1-hour incubation at 37°C followed by a 20-minute heat activation at 80°C. The PCR products were purified with a QIAquick PCR Purification Kit (QIAGEN) and competent DH5α bacteria were transformed with 2 µg DNA by 30-minute incubation on ice followed by a heat shock for 90 seconds at 42°C. Positive clones were
selected on agar plates containing ampicillin (100 µg ml-1) and larger cultures were grown in LB media, and vectors were purified with QIAprep Spin Miniprep Kit a (QIAGEN) and sequenced to verify the single site mutations.

Generation of transgenic *C. elegans* strains

Germline transformation was performed as described (3) to generate two sets of TTR strains, using either the pRF4 *rol-6(su1006)* plasmid (100 ng µl-1), or *odr-1p*::RFP (100 ng µl-1) as co-injection markers (see below). To enable the characterization of thermal avoidance and of forward locomotion, as well as for the ELISA assay in Fig. 6, we used control and TTR strains carrying an *odr-1p*::RFP co-injection marker. For all other experiments the TTR strains carrying *rol-6(su1006)* co-injection marker were used. All strains were tested by western blot, and showed comparable TTR protein levels to each other (Fig. S5 and S10A). Briefly, constructs containing human WT TTR, V30M TTR, D18G TTR, or T119M TTR sequences were co-injected (100 ng µl-1) with either plasmid pRF4 *rol-6(su1006)* or plasmid *odr-1p*::RFP at a concentration of 100 ng µl-1 for each plasmid, plus 50 ng µl-1 of empty vector (E.V.) (total 250 ng µl-1 injected). Injections were performed using a Zeiss Axio Observer A1 inverted microscope (Carl Zeiss MicroImaging) connected to an Eppendorf femto jet express microinjection system (Eppendorf). Microinjection needles were made from borosilicate glass capillaries (World Precision Instruments) using a P-30 needle puller (Sutter Instruments). Injected animals were kept at 20°C and progeny were screened for either the roller phenotype or red chemosensory neurons. Since the roller phenotype was found to be temperature sensitive, the animals were always maintained

at 15°C. The extrachromosomal arrays were integrated by a dose of 3800 rad γ-irradiation(3) and outcrossed at least 4 times before use.

The following strains were generated and/or used in this study:

STRAIN NAME ABBREVIATION	STRAIN NAME	GENOTYPE	REFERENCE
control	SEE047	*geIs101[rol-6(su1006)]*	Strain first generated in Viswanathan and Guarente, 2011. Outcrossed 8X.
WT TTR	SEE037	*scrIs008[unc-54p::hTTR(WT) + rol-6]*	This study
V30M TTR	SEE034	*uthIs378[unc-54p::hTTR(V30M) + rol-6]*	This study
D18G TTR	SEE046	*uthIs352[unc-54p::hTTR(D18G) + rol-6]*	This study
T119M TTR	SEE158	*scrIs038[unc-54p::hTTR(T119M) + rol-6]*	This study
Red coelomocyte marker	SEE064	*scrIs010[des-2p::myr::GFP + unc-122p::DsRed]*	Strain first generated in Maniar *et al.*, 2012. Integrated and outcrossed 4X.
Control; Red coelomocytes marker	SEE106	*geIs101[rol-6(su1006)]*; *scrIs010[des-2p::myr::GFP + unc-122p::DsRed]*	This study
WT TTR; Red coelomocyte marker	SEE143	*scrIs006[unc-54p::hTTR(WT) + rol-6]; scrIs010[des-2p::myr::GFP + unc-122p::DsRed]*	This study
WT TTR; Red coelomocyte marker	SEE151	*scrIs008[unc-54p::hTTR(WT) + rol-6]; scrIs010[des-2p::myr::GFP + unc-122p::DsRed]*	This study
V30M TTR; Red coelomocytes	SEE145	*uthIs379[unc-54p::hTTR(V30M) + rol-6]; scrIs010[des-2p::myr::GFP + unc-122p::DsRed]*	This study
D18G TTR; Red coelomocytes	SEE141	*uthIs353[unc-54p::hTTR(D18G) + rol-6]; scrIs010[des-2p::myr::GFP + unc-122p::DsRed]*	This study
D18G TTR; Red coelomocytes	SEE222	*uthIs352[unc-54p::hTTR(D18G) + rol-6]; scrIs010[des-2p::myr::GFP + unc-122p::DsRed]*	This study
T119M TTR; Red coelomocytes	SEE223	*scrIs038[unc-54p::hTTR(T119M) + rol-6]; scrIs010[des-2p::myr::GFP + unc-122p::DsRed]*	This study
DT-A	SEE061	*cdIs32[pcc1p::DT-A(E148D)]; unc-119(+) myo-2p::GFP*	Strain first generated in Schwartz *et al.*, 2010. Outcrossed 8X.
control; DT-A	SEE079	*geIs101[rol-6(su1006)]*; *cdIs32[pcc-1p::DT-A(E148D); unc-119(+) myo-2p::GFP]*	This study

control; DT-A; red coelomocytes	SEE106	*geIs101[rol-6(su1006)]*; *cdIs32[pcc-1p::DT-A(E148D); unc-119(+) myo-2p::GFP]; scrIs010[des-2p::myr::GFP + unc-122p::DsRed]*	This study
WT TTR; DT-A	SEE080	*scrIs008[unc-54p::hTTR(WT) + rol-6]; cdIs32[pcc-1p::DT-A(E148D); unc-119(+) myo-2p::GFP]*	This study
WT TTR; DT-A	SEE120	*scrIs006[unc-54p::hTTR(WT) + rol-6]; cdIs32[pcc-1p::DT-A(E148D); unc-119(+) myo-2p::GFP]*	This study
V30M TTR; DT-A	SEE128	*uthIs378[unc-54p::hTTR(V30M) + rol-6]; cdIs32[pcc-1p::DT-A(E148D); unc-119(+) myo-2p::GFP]*	This study
T119M TTR; DT-A	SEE168	*scrIs038[unc-54p::hTTR(T119M) + rol-6]; cdIs32[pcc-1p::DT-A(E148D); unc-119(+) myo-2p::GFP]*	This study
D18G TTR; DT-A	SEE152	*uthIs353[unc-54p::hTTR(D18G) + rol-6]; cdIs32[pcc-1p::DT-A(E148D); unc-119(+) myo-2p::GFP]*	This study
D18G TTR; DT-A	SEE221	*uthIs352[unc-54p::hTTR(D18G) + rol-6]; cdIs32[pcc-1p::DT-A(E148D); unc-119(+) myo-2p::GFP]*	This study
Control	SEE109	*scrIs020[odr-1p::RFP]; scrIs010[des-2p::myr::GFP + unc-122p::DsRed]*	This study
V30M TTR	SEE130	*scrIs024[unc-54p::hTTR(V30M) + odr-1p::RFP]; scrIs010[des-2p::myr::GFP + unc-122p::DsRed]*	This study
D18G TTR	SEE115	*scrIs032[unc-54p::hTTR(D18G) + odr-1p::RFP]*	This study
control; DT-A	SEE169	*scrIs020[odr-1p::RFP]; scrIs010[des-2p::myr::GFP + unc-122::DsRed]; [cdIs32[pcc-1p::DT-A(E148D); unc-119p::myo-2p::GFP]*	This study
V30M; DT-A	SEE170	*scrIs024[unc-54p::hTTR(V30M)+odr-1p::RFP]; scrIs010[des-2p::myr::GFP+unc-122::DsRed]; cdIs32[pcc-1p::DT-A(E148D); unc-119p::myo-2p::GFP]*	This study
V30M ΔSS	SEE299	*scrEx033[unc-54p::hTTR(V30MΔSS) + odr-1p::RFP]*	This study
mtGFP	SEE045	*jsIs609[mec-7p::mtGFP + pJM23 [lin-15]]*	This study
ctrl; mtGFP	SEE110	*scrIs020[odr-1p::RFP]; jsIs609[mec-7p::mtGFP]*	This study
V30M; mtGFP	SEE148	*scrIs024[unc-54p::hTTR(V30M) + odr-1p::RFP]; jsIs609[mec-7p::mtGFP]*	This study
T119M; mtGFP	SEE329	*scrIs040[unc-54p::hTTR(T119M) + odr-1p::RFP]; jsIs609[mec-7p::mtGFP]*	This study

V30M TTR ΔSS	SEE313	*scrEx047[des-2p::hTTR(V30MΔSS) + odr-1p::RFP] + scrIs010[des-2p::myr::GFP + unc-122p::Ds-red]*	This study

mRNA extraction and quantitative reverse transcriptase (RT)-PCR

Bleached synchronized animals (~1000 to 10,000 nematodes) were grown in 50 ml Scomplete medium supplemented with 50 µg ml-1 carbenicillin, 0.1 µg ml-1 fungizone and 6 mg ml-1 (< 5000 animals) or 12 mg ml-1 (> 5000 animals) freshly prepared *E. coli* OP50. Animals were cultured in 15 cm petri dishes at 20°C. To arrest embryos prior to hatching, 5-fluoro- 2´-deoxyuridine (FUDR, Sigma) was added to a final concentration of 0.12 mM to L4 larvae animals. Animals were aged until day 1, day 5, and day 8 of adulthood, with new OP50 added (1.2 ml of 100 mg ml-1 solution) on day 5 to prevent starvation. At desired time point, animals were thoroughly washed three times in 1x M9 buffer and remove as much buffer as possible and flash freeze the samples in liquid nitrogen. RNA was extracted using the QIAzol lysis reagent (QIAGEN), followed by DNase I treatment (Sigma). mRNA was reverse transcribed using the iScript cDNA Synthesis kit (Bio-Rad). cDNA (20 ng) was used for real-time PCR amplification using the FastStart Universal SYBR Green Mastermix (Roche) and the ABS 7900HT Fast Real-Time PCR System. The relative TTR gene expression levels were determined using the Comparative CT Method. TTR gene expression levels were normalized relative to those of the following housekeeping genes: the 60S ribosomal protein L6 (*rpl-6*), and of the plasma membrane protein 3 (*pmp-3*) for each sample (internal controls).

The following primer sequences were used:

TTR Forward 5'-ATTTGCCTCTGGGAAAACCAG-3'

TTR Reverse 5'-GGCTGTGAATACCACCTCTGC-3'

rpl-6 Forward 5'-TTCACCAAGGACACTAGCG-3'

rpl-6 Reverse 5'-GACAGTCTTGGAATGTCCGA-3'

pmp-3 Forward 5'-TGGCCGGATGATGGTGTCGC-3'

pmp-3 Reverse 5'-ACGAACAATGCCAAAGGCCAGC-3'

Expression and purification of recombinant TTR and preparation of non-native TTR forms

Recombinant WT TTR, T119M TTR, D18G TTR and V30M TTR were expressed in and purified from *Escherichia coli* as described previously (7). Protein was eluted in a standard phosphate buffer (10 mM sodium phosphate (pH 7.6), 100 mM KCl, 1 mM EDTA). The molar absorptivities (ε) of TTR (73800 M−1 cm−1) tetramers in standard phosphate buffer were used to calculate TTR concentrations using the nanodrop. Non-native (NN) TTR forms were prepared

using 0.2 mg/ml monomeric (M) TTR or by incubating the same protein concentration of recombinantly-made normally folded tetrameric TTR proteins at 37˚C in 100mM pH 4.3 acetate buffer for 16 hours (8).

Antibodies against oligomeric TTR

The polyclonal MDX114 antibody, and monoclonal MDX102 and MDX108 antibodies were generated by Misfolding Diagnostics, and have been optimized for use in an ELISA assay to specifically detect non-native (NN) TTR forms that include partially unfolded or misfolded TTR monomers, and oligomeric TTR (patent WO2014/124334A2). The specificity toward NN TTR of MDX102 and MDX108 antibodies was first tested by SDS-PAGE by incubating recombinant (rec) native WT tetrameric TTR in SDS sample buffer in the absence of boiling. Rec tetrameric TTR is kinetically stable and resisted denaturation in the absence of boiling in SDS-PAGE, and was unrecognized by MDX antibodies (rec WT TTR shown in Fig. S3A, left panels). In contrast, NN monomeric (M)-TTR oligomers produced as stated above, by incubation of an engineered monomeric variant of TTR (M-TTR) at 37°C, were denatured at 25°C by unboiling SDS treatment (rec WT TTR shown in Fig. S3A, left panels), and were recognized by MDX102 in a native gel (Fig. S3A, right panel)(9). MDX114 is a rabbit polyclonal antibody that was used as the capture antibody in the ELISA assay (see below), while the MDX102 was used as the detection antibody.

Western blot analysis for quantification of total TTR protein levels

Bleached synchronized animals (~1000 to 10,000 nematodes) were grown in 50 ml Scomplete medium supplemented with 50 µg ml-1 carbenicillin, 0.1 µg ml-1 fungizone and 6 mg ml-1 (< 5000 animals) or 12 mg ml-1 (> 5000 animals) freshly prepared *E. coli* OP50. Animals were cultured in 15 cm petri dishes at 20°C. To arrest embryos prior to hatching, 5-fluoro- 2´-deoxyuridine (FUDR) was added to a final concentration of 0.12 mM to L4 larvae animals (Sigma). Animals were aged until day 1, day 5, and day 8 of adulthood, with new OP50 added (1.2 ml of 100 mg ml-1 solution) on day 5 to prevent starvation. At desired time point, animals were thoroughly washed three times in 1x PBS buffer and worm pellet was re-suspended in 300 µl cold 1x PBS supplemented with complete protease inhibitors (Roche). The approximate concentration of animals for each sample was determined by counting the number of animals in ten 10 µl drops using a dissecting scope. The animal suspension was added to a hard tissue homogenizing CK28 Precellys tube (Bertin Technologies) and subjected to Precellys-24 homogenization at 6500 x *g* for 3 x 10 sec bursts (Bertin Technologies). Sample homogenates were spun at 3000 x *g* for 15 minutes at 4°C, where the supernatant was collected as the soluble fraction and the pellet was

collected as the insoluble fraction. The insoluble pellet was re-suspended in a 10% SDS solution and boiled for 10 minutes at 95°C. Both soluble and insoluble protein fraction concentrations were determined using the Bio-Rad DC Protein Assay kit (Bio-Rad).

Samples (5-10 µg total protein) were mixed with 6x SDS loading sample buffer (20% glycerol, 12% SDS, 125 mM Tris pH 6.8) and with 100 mM DTT (Sigma), boiled for 10 minutes and loaded into the wells of a 15% SDS-Page Gel. Protein separation was performed at 150V in SDS running buffer and blotted onto a nitrocellulose membrane in transfer buffer (20 mM Tris, 150 mM glycine, 20% methanol) for 2 hours at 0.25A. Membranes were incubated in blocking solution (1X TBS with 5% non-fat milk) for 1 hour followed by an overnight incubation at 4°C with primary monoclonal antibody MDX102 against TTR (Misfolding Diagnostics, Inc.) at a 1:1000 dilution, and with a monoclonal antibody against actin (α-actinC4; MAB1501, Millipore) at a 1:4000 dilution. After three rinses in 1X TBS-T, the membrane was incubated with secondary donkey anti-mouse IRDye 800 nm conjugated antibody (LI-COR) for 1 hour at room temperature diluted 1:10,000 in blocking solution, rinsed 3 times in TBS-T, and scanned with an Odyssey infrared imager (LI-COR). Protein band intensities were measured using Image J.

Quantification of *in vitro* TTR tetramer levels

TTR tetramer levels were measured as previously described (10). Briefly, soluble protein lysates (10 µg) were incubated with the fluorogenic small molecule **A2** (10 µM final concentration, prepared in DMSO) in 1x PBS buffer. To generate a TTR tetramer standard curve, recombinant WT TTR was added to day 1 soluble non-TTR control lysate at various concentrations (serial dilution: 2 µM, 1 µM, 0.5 µM, 0.25 µM, 0.125 µM, 0.0625 µM, 0.03125 µM, 0.0156 µM, 0.00781 µM) and incubated with **A2** (10 µM) for 10-12 hours at 4°C to allow for complete covalent modification by **A2** of the two thyroxine binding sites within the TTR tetramer. A 50 µL sample was injected onto a Waters Acquity H-Class Bio-UPLC (Ultra Performance Liquid Chromatography) instrument fitted with a strong anion exchange column (Waters Corp). TTR was eluted from the column using a nonlinear gradient at a flow rate of 0.6 ml min-1 over 33 min. **A2**-modified TTR conjugate fluorescence was monitored using excitation at 328 nm with emission at 430 nm, at a sampling rate of one point per second. The TTR peak was extracted by plotting the data in excel.

Native PAGE gel analysis for detection of TTR oligomers

Soluble lysate and insoluble pellet were obtained from synchronized *C. elegans* as mentioned above in the section ‘Western blot analysis for quantification of total TTR protein levels’. The insoluble pellet was re-suspended in 50mM Tris pH8, 0.5M NaCl, 1% v/v Igepal CA630+

Protease Inhibitor to maintain the structure of the TTR proteins (11). The samples were resolved on NativePAGE™ Novex™3-12% Bis-Tris protein gels by loading 10 µg total protein and running at 150V for 90 min at room temperature. After transferring on nitrocellulose membrane, the membrane was probed with the MDX102 antibody against oligomeric TTR. Validation of antibodies used in this assay is reported above in the section 'Antibodies against oligomeric TTR' (Fig. S3A and B).

Quantification of non-native TTR levels *in vitro* by ELISA

Non-native (NN) TTR levels were quantitated using a sandwich ELISA developed by Misfolding Diagnostics, Inc. (patent WO2014/124334A2). Validation of antibodies used in this assay is reported in SI Materials and Methods under 'Antibodies against oligomeric TTR' (Fig. S3A and B). The lysates were obtained as mentioned above in the section 'Native PAGE gel analysis for detection of TTR oligomers'. Each sample containing 2.4 µg of the total protein was used in the assay. A recombinant form of misfolded TTR protein was used to generate the standard curve.

***In vivo* TTR tetramer localization with compound 5 (CMPD 5)**

Ten L4 larvae were transferred into a well of a 96-well plate containing 150 µL liquid culture media (S-complete media with 50 µg mL-1 carbenicillin, 0.1 µg mL-1 fungizone, OP50 6 mg mL-1, FUDR 0.12 mM). Animals were incubated on a nutator and overnight at 20°C. On day 1 of adulthood, **CMPD5** (0.5 µL of a 3 mM solution in DMSO, for a final concentration of 10 µM) was added to animals in culture (12). Animals were again incubated on a nutator overnight at 20 °C. On day 2 of adulthood, animals were collected and washed three times in 1 mL M9 buffer and transferred to a fresh 6 cm NGM plate prior to image analysis. For light and fluorescence microscopy, animals were mounted on 3% agar pads in 2% sodium azide buffer (prepared in 1x PBS), and covered with a coverslip. Imaging of coelomocytes was done on live animals expressing Ds-Red under the coelomocyte-specific *unc-122* promoter (13). To image the animals, we used simultaneous differential interference contrast microscopy (DIC) and epifluorescence modalities using a Nikon Ti-E Perfect Focus inverted microscope equipped with a iXon+ DU897 EM Camera, a 100X/1.49 NA oil objective and an Intensilight System M lamp. We used 340-380 nm/500-550 nm excitation and emission filters, respectively, to detect **CMPD5** fluorescence, and 545-570 nm/578-625 nm emission and excitation filters, respectively, to detect DsRed fluorescence.

Immunofluorescence

The *in vivo* localization of TTR was visualized by immunofluorescence (IF) microscopy and staining was performed following a modified protocol developed by the Loer laboratory (http://home.sandiego.edu/~cloer/loerlab/anti5htshort.html). The primary antibodies used were either the polyclonal antibody against TTR (DAKO) at a 1:100 dilution or monoclonal anti-mouse MDX102 (Misfolding Diagnostics, Inc) at a 1:100 dilution. Secondary antibodies used were Alexa647-conjugated Donkey anti-rabbit (Life Technologies) at a 1:100 dilution, or Alexa647-conjugated Donkey anti-mouse (Life Technologies) at a 1:100 dilution. To visualize the bodywall muscle, animals were incubated with Rhodamine Phalloidin (Invitrogen) at 1:10 dilution for 30 mins at RT before mounting. Whole animals were imaged using a Nikon A1R+ laser scanning confocal microscope system and a 60X/1.4 NA oil objective. The 561 nm laser was used to image Phalloidin and the 647 nm laser for imaging TTR.

Thermal avoidance assay for nociception

The thermal avoidance assay was done on day 1 adult animals and their response to noxious heat was scored in one of the 4 categories, as published before: class I: rapid withdrawal reflex, backing, and change in direction; class II: rapid withdrawal reflex with little backing; class III: slow backing; class IV: no response (14). Because the dominant roller phenotype induced by the *rol-6(su1006)* co-injection transgene interfered with this behavioral assay, we used control, TTR transgenic animals with an *odr-1p*::RFP co-injection marker. The heat source was delivered by heating a blunt 301/2-gauge needle for ~ 10 seconds in a burner and immediately placing it 1-3 mm in front of the animal when in forward motion. The following guidelines were strictly followed: The heated tip was placed in front of a single animal at a time; each animal was removed after testing to prevent re-testing; and only the initial response of the worm was recorded, i.e., animals were not re-tested. Class IV animals were moved into separate 6 cm NGM plates and were each tested with a soft touch to the nose with an eyelash to score for backing.

Analysis of FLP dendritic branching

C. elegans were picked as L4 larvae, placed in fresh NGM (+OP50) plates, and incubated at 20°C for 15 hours to allow growth into day 1 adult animals. Visualization of the branching of FLP neurons was done using a myristoyl::GFP signal under the *des-2* promoter (2). Animals were mounted in 2% sodium azide buffer (prepared in 1x PBS) on 3% agarose pads and covered with a coverslip. FLP dendritic branching was imaged using a Nikon A1R+ laser scanning confocal microscope system, a 60X/1.4 NA oil objective, and a 488 nm laser for excitation of GFP. The

number of quaternary dendritic branches per 100 µm (from the tip of the nose) were counted manually for each animal image of each strain.

Coelomocyte uptake assay of dextran

Injections into the pseudocoelom (body cavity) were performed as previously described (15). Briefly, approximately 10-15 L4 animals were transferred onto NGM (+OP50) plates and incubated overnight at 20°C. Alexa Fluor 488 3,000 MW Dextran [1 mg ml-1] (prepared in ddH2O, Invitrogen) was injected into the pseudocoelom near the pharynx, of day 1 adult animals. Injected animals were kept at 20°C on NGM (+OP50) plates overnight and Dextran- 488 fluorescence was imaged after 24 hours using epifluorescence in a Nikon Ti-E Perfect Focus inverted microscope equipped with a iXon+ DU897 EM Camera, a 100X/1.49 NA oil objective and an Intensilight System M lamp.

Quantitation of mitochondrial size in ALM neurons

L4 larvae were picked and placed in NGM (+OP50) plates at 20˚C overnight. Day 1 adults were immobilized with Polybead® Polystyrene 0.10 micron Microspheres (2.6% Solids- Latex) (Polysciences, Inc., Illinois) on ~1mm 8% agarose pads covered with a coverslip. Proximal regions of ALM neurons expressing a mitochondrial localization signal fused to GFP (mtGFP) were imaged using a Nikon Ti-E A1 confocal laser microscope system equipped with a scanning stage and Piezo-Z control, and a 60X/1.4 NA oil objective. A 488 nm laser was used for excitation of GFP. The mitochondrial length was measured using the ImageJ software and normalized by the total axonal length for each mitochondrion, expressing the values in "parts per mille" (‰) of the total axon length. Non-parametric Kruskal-Wallis with Dunn's multiple comparisons test was performed for statistical analysis.

RNA interference

Reduction of TTR transgene activity was accomplished by feeding *C. elegans* with RNAi bacterial clones expressing double-stranded RNA (dsRNA) targeting TTR. The bacterial clones were generated by amplification of a 460 bp sequence by PCR that includes the complete human TTR sequence. The primers used for the amplification were the following:

forward primer 5´-AATGAGCTCATGGCTTCTCATCGTCTGCTCCTC-3´and

reverse primer 5´- ATTAGGTTACCTCATTCCTTGGGATTGGTGACG-3´.

The sequence was purified and ligated between Sac1 and Kpn1 sites in the multiple cloning site region of the L4440 vector (plasmid 1654, Addgene) and transformed into *E. coli* HT115 with

tetracycline resistance. *E. coli* HT115 bacteria expressing RNAi were cultured in Luria-Bertani (LB) media containing 10 mg ml-1 ampicillin and spotted on NGM plates containing 100 µg ml-1 carbenicillin. RNAi production was induced with addition of 100 mM IPTG placed directly on the bacterial lawn of each plate. Animals were grown on new plates seeded with RNAi expressing bacteria for two generations prior to analysis. Lysates were made by picking animals into 300 µl cold PBS and lysed as described above (”Western blot analysis for quantification of total TTR protein levels”). Day 2 adult animals were recorded as mentioned below (”Locomotion assay and worm tracking analysis”).

Locomotion assay and worm tracking analysis

Animals were maintained at 22°C for multiple generations on NGM + OP50 seeded plates. Because the dominant roller phenotype induced by the rol-6(su1006) co-injection transgene interfered with this behavioral assay, we examined control, TTR transgenic animals with an *odr-1p*::RFP co-injection marker. L3 larvae were picked onto 150 µl liquid culture medium (S-complete media with 50 µg ml-1 carbenicillin, 0.1 µg ml-1 fungizone and 6 mg ml-1 OP50) in a 96-well plate and incubated at 22°C. To arrest embryos prior to hatching, 0.12 mM FUDR was added to each well when larvae reached the L4 stage. Individual day 2 adult animals were placed in an unseeded 35 mm plate for 40 minutes, then transferred to a new unseeded 35 mm plate and their movement trajectories recorded for a duration of 40 seconds using the Stemi 508 microscope (Zeiss) with SwiftCam2 camera and imaging software (Swift). All videos were analyzed using wrMTrck plugin for ImageJ to obtain average speed and representative tracks of each of the trajectories (16). All locomotion assays including the tracking analysis were performed blind.

Compound 5 (CMPD5) treatment for locomotion assay

Thirty L3 larvae were picked into 150 µl liquid culture medium (S-complete media with 50 µg ml-1 carbenicillin, 0.1 µg ml-1 fungizone and 6 mg ml-1 OP50) in a 96-well plate and incubated at 22°C. Animals were fed **CMPD5** (10 µM) or DMSO (concentration) starting at the L3 stage through to day 1 of adulthood. At day 1, animals were transferred onto NGM (+OP50) plates (containing 10 µM **CMPD5** or 0.3% DMSO). Day 2 adult animals were assessed for locomotion as mentioned above.

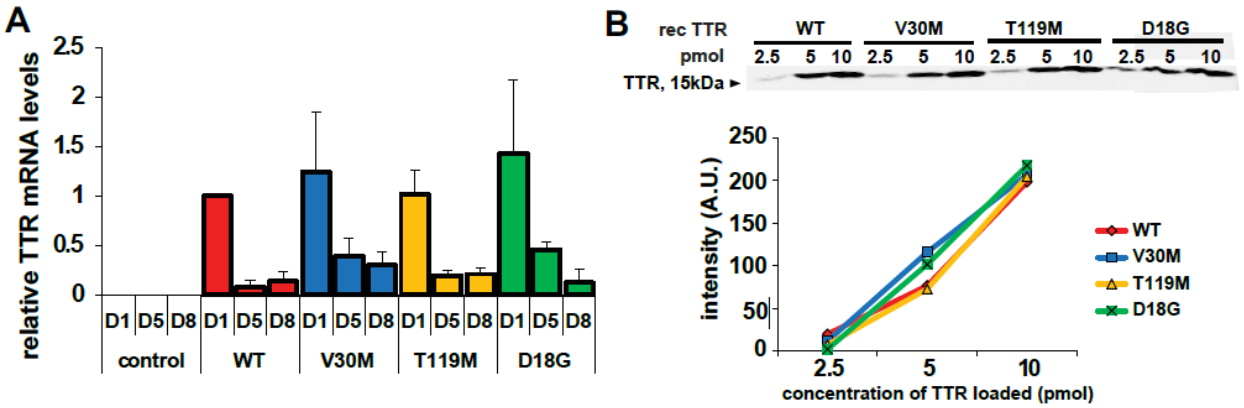

Fig. S1. Messenger RNA levels and TTR antibodies in transgenic *C. elegans* strains, Related to Fig. 1. (A) Quantitative real-time PCR analysis of synchronized adult day 1 (D1), 5 (D5), and 8 (D8) mRNA levels. TTR gene expression levels were compared to that of 60S ribosomal protein L6 (*rpl-6*) mRNA, and to the plasma membrane protein 3 (*pmp-3*) mRNA, and normalized to D1 WT TTR. Data is from two biological samples for each condition (n = 3 technical replicates, mean ± s.e.m.). The percentage difference of relative TTR mRNA levels between the strains with respect to the WT TTR D1 are 24%, 2% and 43% for V30M, T119M and D18G, respectively. (B) Top panel: Western blot of recombinant TTR protein probed with MDX102 antibody against TTR. Bottom panel: TTR protein levels are plotted as fluorescence intensity, against loaded protein amount to show linear antibody detection of TTR protein amount. Blot is representative of 2 biological replicates.

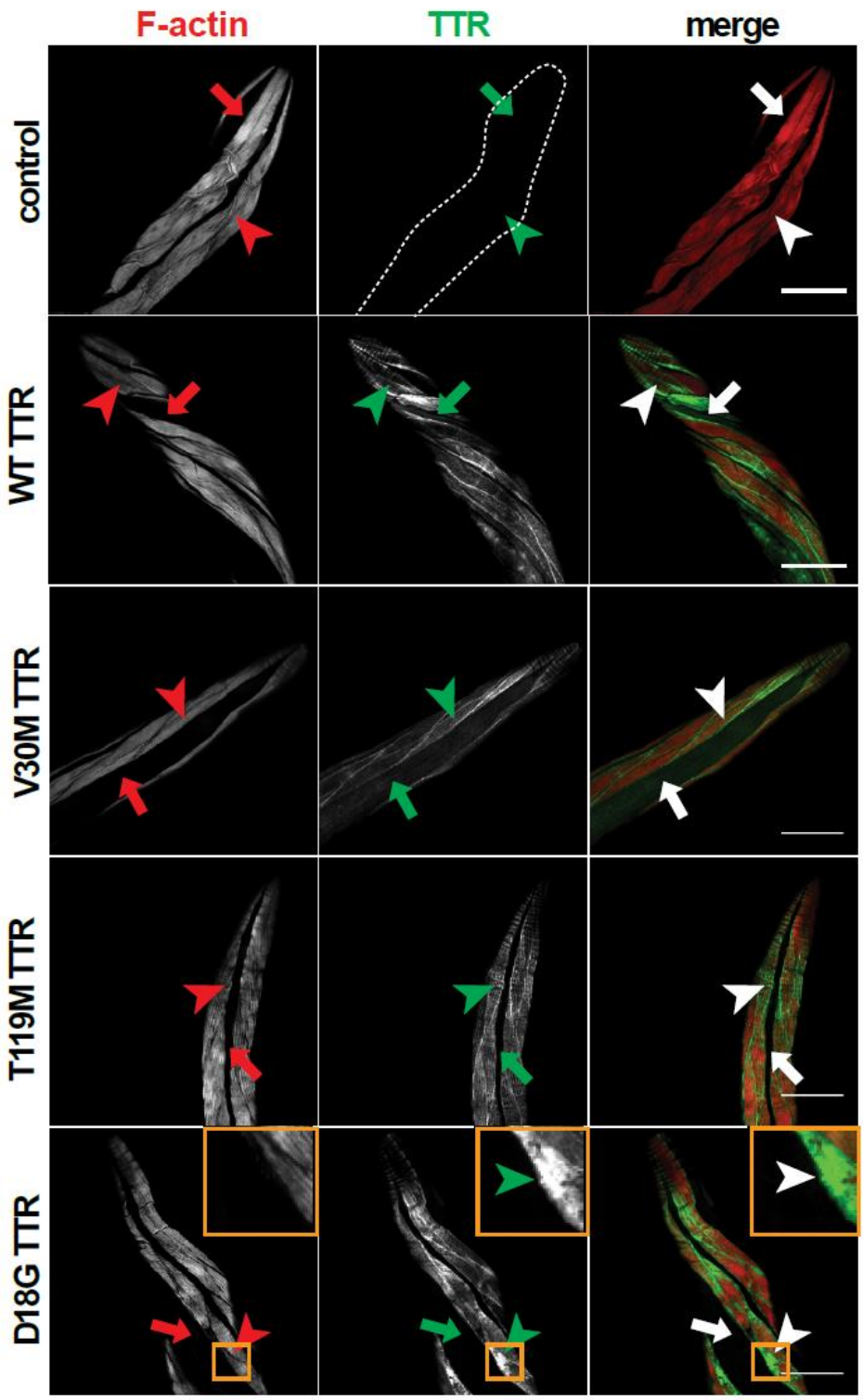

Fig. S2. Immunofluorescence (IF) of TTR transgenic animals with a non-native TTR specific antibody, Related to Fig. 2. Representative confocal images of the head region of animals stained with antibody MDX102 against oligomeric TTR (green), and with phalloidin (Factin; red). Control n=6, WT TTR n=11, V30M TTR n=10, T119M TTR n=10, D18G TTR n=6. Arrowheads point to muscle cells; arrows point to the body cavity. Insets inside D18G TTR panel shows enlargement of aggregates. Scale bars = 50μm.

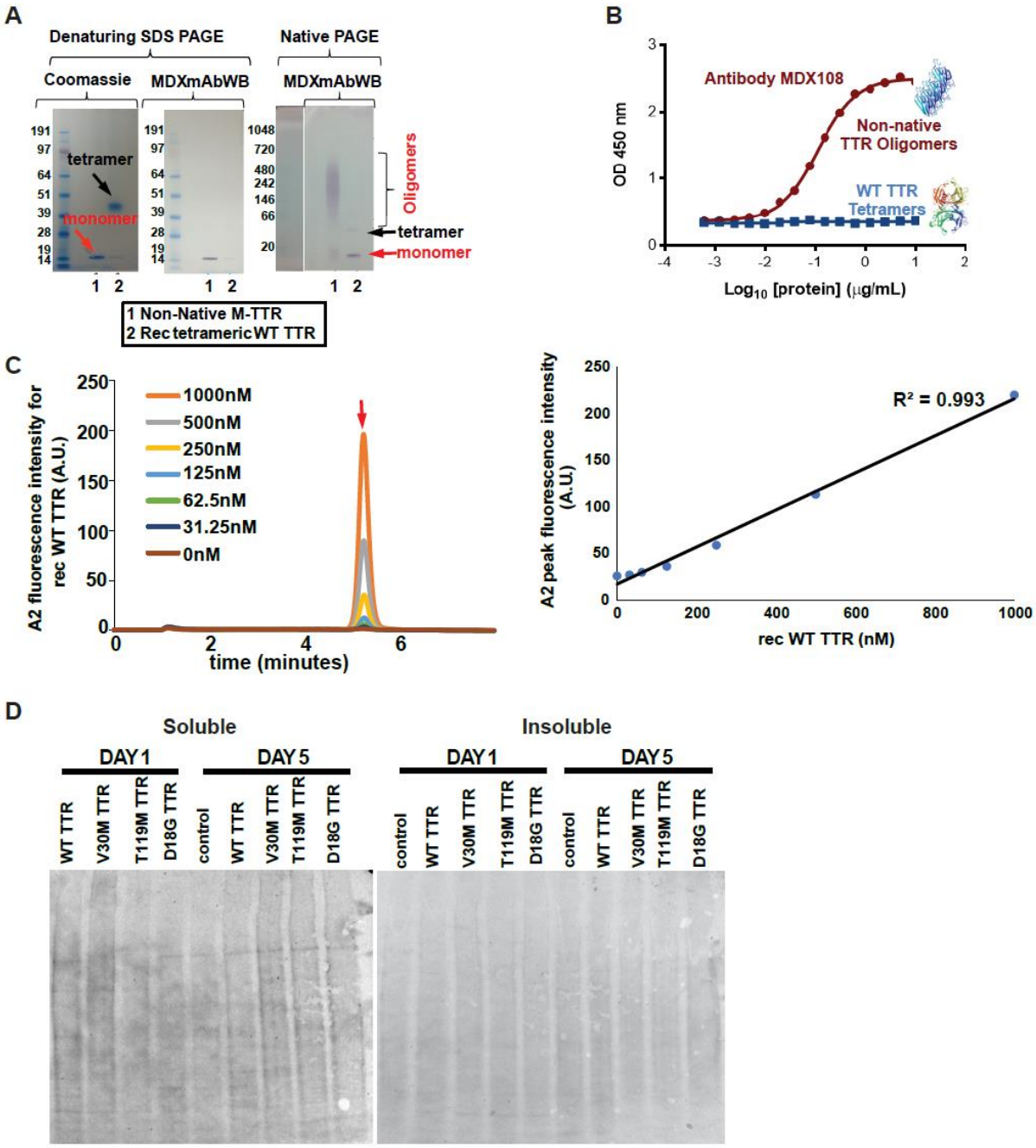

Fig. S3. Generation of soluble and insoluble TTR and oligomeric aggregates in transgenic *C. elegans* strains, Related to Fig. 3. (A) SDS-and Native-PAGE gels showing specificity of antibody MDX108 for recombinant (rec) non-native TTR monomer and oligomers of M-TTR, but not for rec WT TTR tetramer that is kinetically stable in a non-boiled SDS buffer. WB = western blot. (B) ELISA binding affinities of the MDX108 antibody to native WT TTR and to non-native TTR. (C) Left panel: UPLC chromatogram of the TTR tetramer-(**A2**)2 conjugate peak for various amounts of recombinant WT TTR tetramer. Red arrow points to eluted recombinant TTR tetramers. Right panel: standard linear regression curve for quantification of the TTR tetramer-(**A2**)2 conjugate peak heights in top panel. This standard curve was used to determine the amount of TTR tetramer in lysates. (D) Ponceau S staining of soluble and insoluble samples run on the native gels showing total equivalent protein loading.

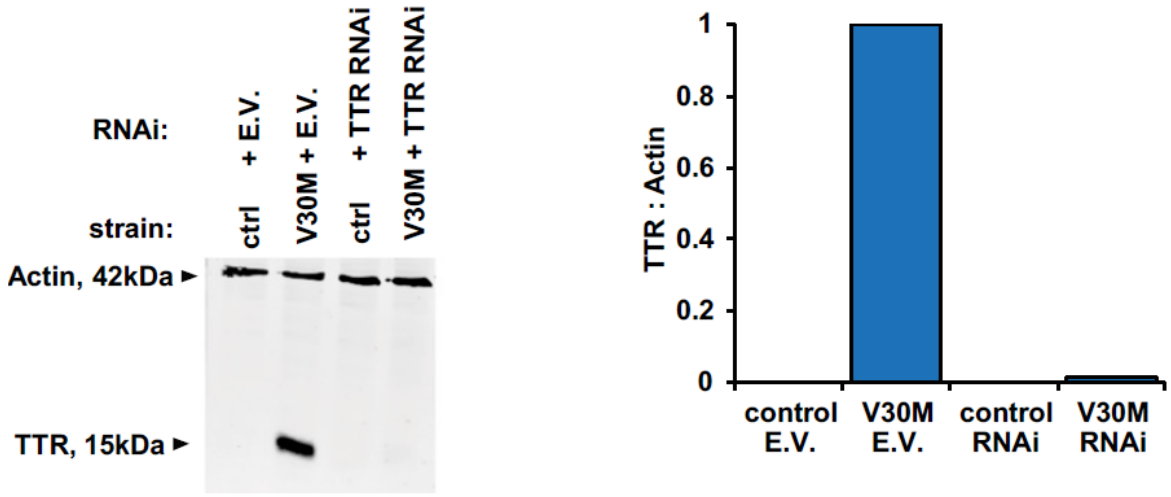

Fig. S4. RNAi treatment of V30M TTR transgenic animals, Related to Fig. 4. Western blot (left) and quantification of Western blot (right) of lysates of control and V30M TTR transgenic animals fed either with control bacteria (E.V. – empty vector) or with bacteria expressing dsRNA against TTR (TTR RNAi). Membrane was probed with the monoclonal MDX102 antibody against TTR.

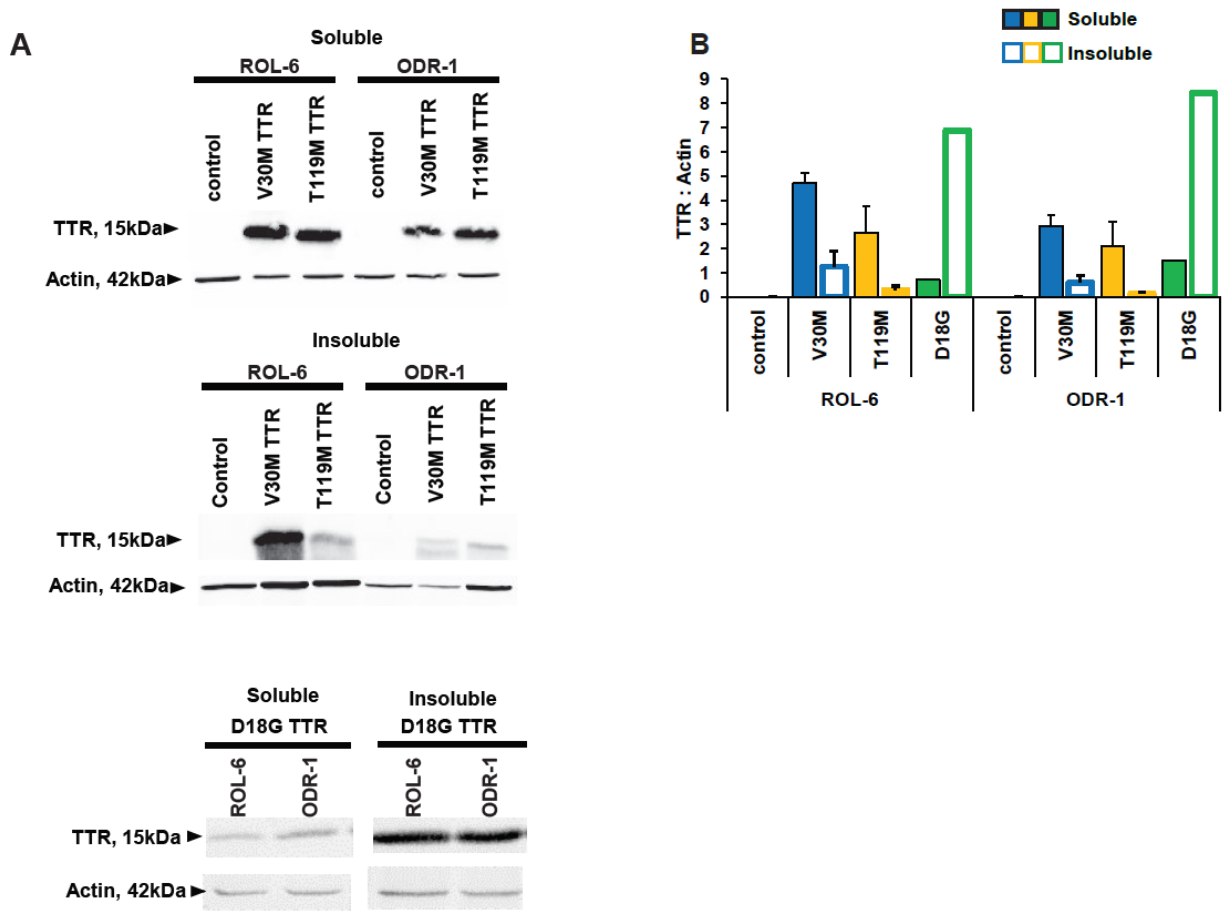

Fig. S5. Newly generated *C. elegans* strains for the characterization of nociception, locomotion, and neuronal mitochondrial morphology phenotypes, Related to Fig. 4, and Fig. 7. Analyses of nociception and neuronal mitochondrial morphology were performed on strains that had *odr-1p*::RFP instead of ROL-6 co-injection markers to avoid the rolling phenotype of *rol-6(su1006)* animals. (A) Western blot comparing TTR levels in soluble and insoluble fractions in TTR strains that were generated with *rol-6(su1006)* versus *odr-1p*::RFP as co-injection markers. Membranes were probed with the monoclonal MDX102 antibody against TTR. Images are representative of 2 independent experiments. (B) Quantification of the TTR : Actin ratio of the samples shown in (A) (mean + s.e.m.).

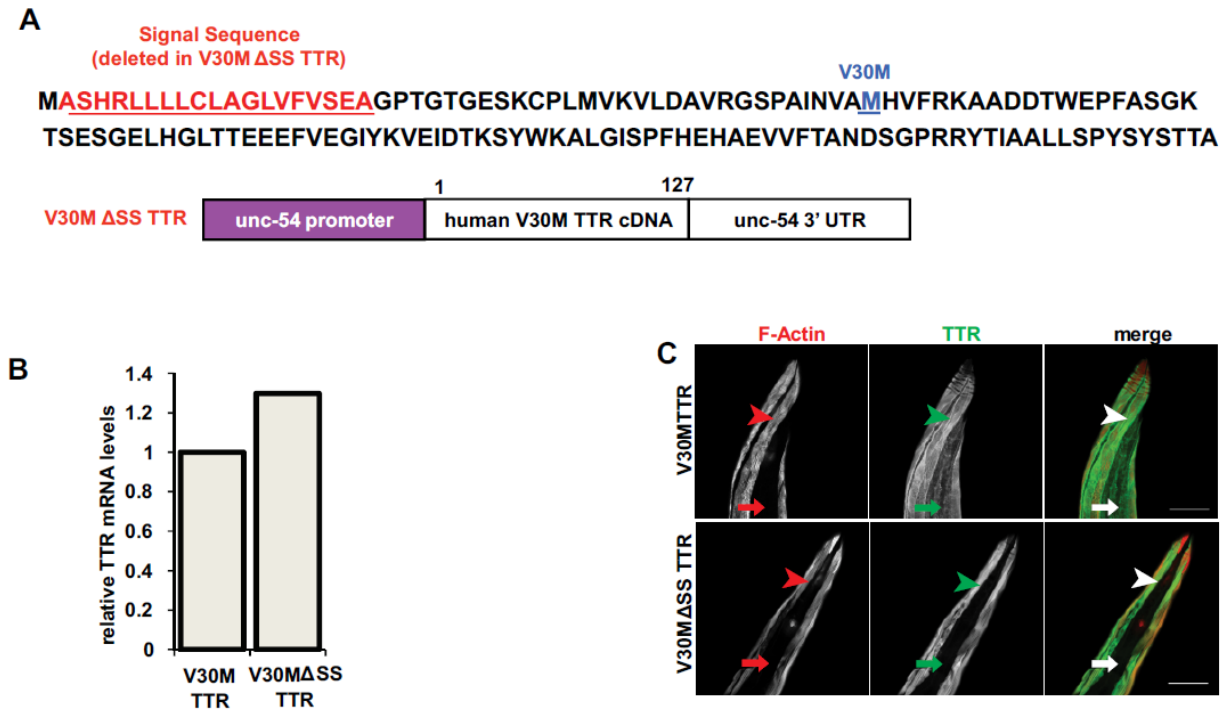

Fig. S6. Characterization of V30M ΔSS TTR animals lacking the TTR signal sequence (SS), Related to Fig. 4. (A) Top panel: TTR protein sequence showing the signal sequence (red) that was deleted in the V30M ΔSS TTR transgenic strain. Bottom panel: Schematic of the construct expressed in the V30M ΔSS TTR transgenic animal. (B) Messenger RNA levels as measured by quantitative real-time PCR analysis of synchronized day 1 V30M TTR; *odr-1p*::RFP, and of V30M ΔSS TTR; *odr-1p*::RFP transgenic animals. TTR gene expression levels were normalized relative to the 60S ribosomal protein L6 (*rpl-6*) mRNA, or to the plasma membrane protein 3 (*pmp-3*) mRNA, and normalized to day 1 V30M TTR levels. (C) Representative confocal immunofluorescence (IF) images of the head region of day 1 TTR transgenic animals stained with polyclonal antibody against TTR (green) and phalloidin (F-actin; red). n > 5 per strain. Arrowheads point to muscle cells; arrows point to the body cavity. Scale bar = 50μm.

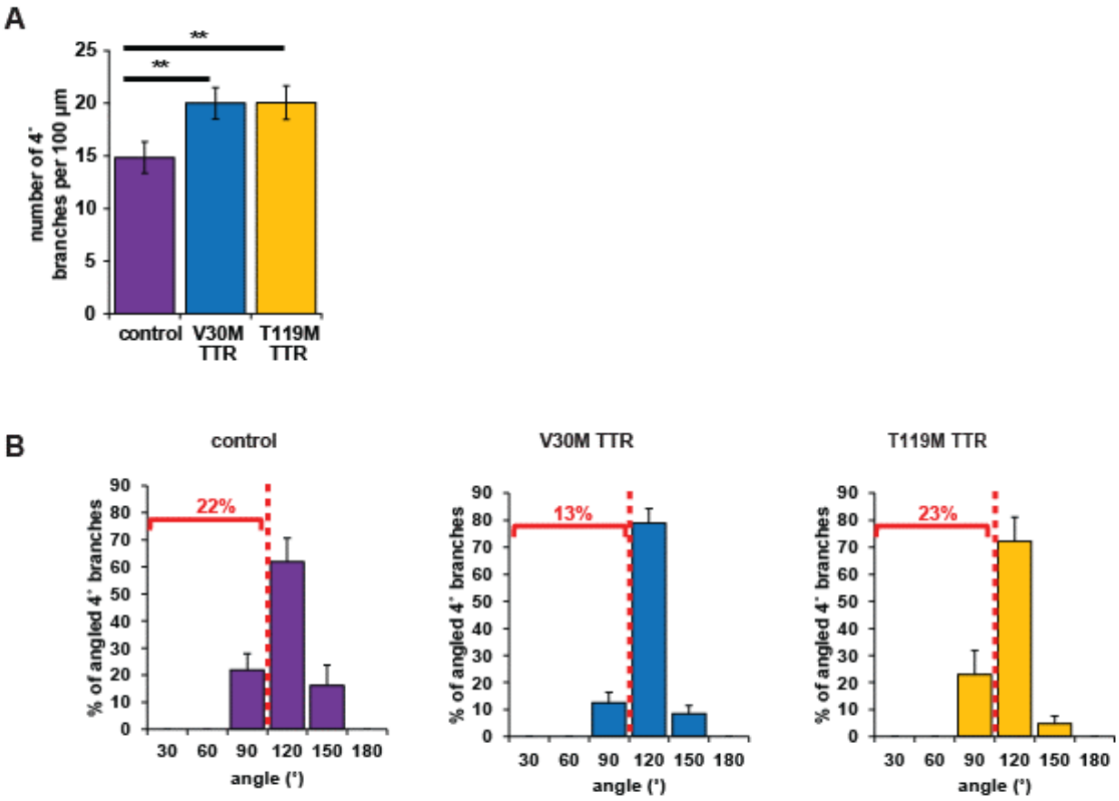

Fig. S7. FLP dendritic branching defects in L4 larval TTR transgenic animals, Related to Fig. 5. (A) Quantification of number of FLP 4˚ dendritic branches per animal in 100 µm starting from the tip of the head (mean ± s.e.m.). n=20 animals per strain. **p<0.01 by permutation ttest. (B) Histograms showing the proportion of angular branches with a deviation angle greater than 0˚ in L4 larvae, as measured in Fig. 5D. The two-sample Kolmogorov-Smirnov test showed no significant differences between the strains.

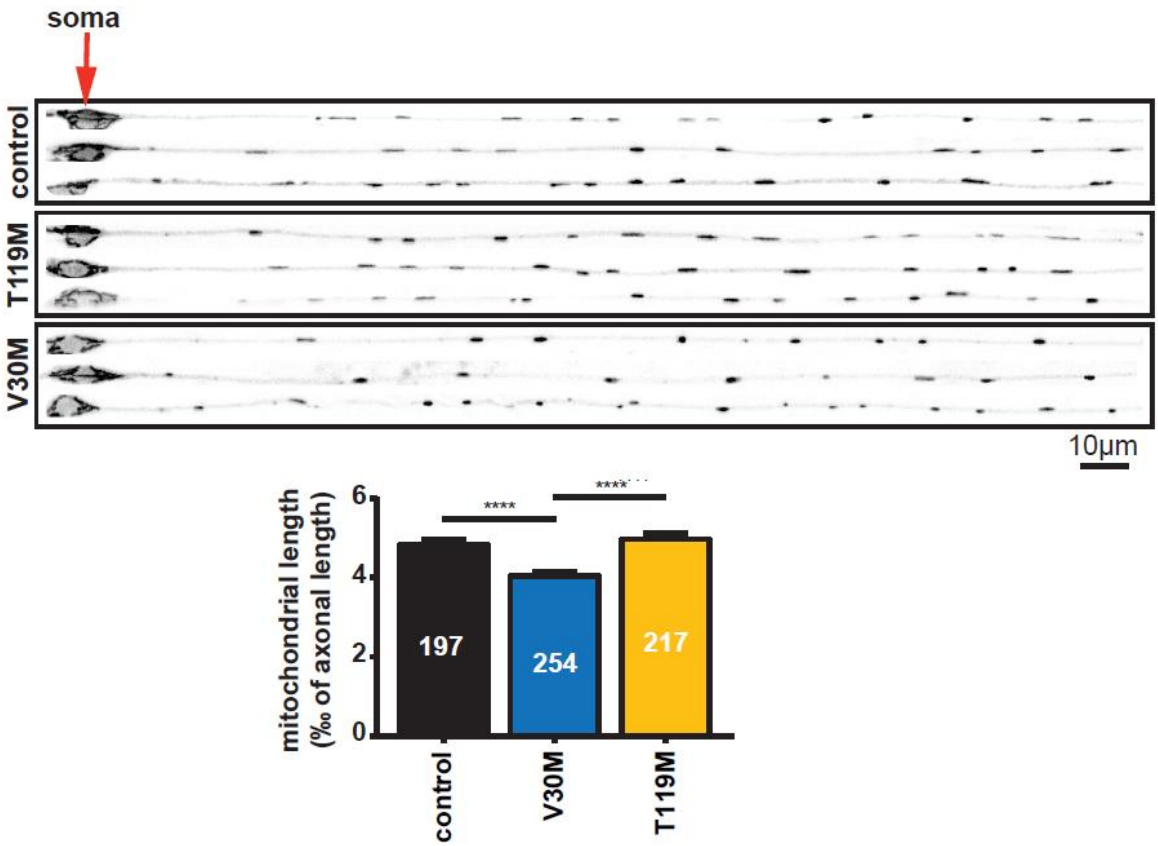

Fig. S8. Neuronal mitochondria morphology phenotypes, Related to Fig. 5. Top panels: confocal fluorescence images of the proximal region of three straightened and aligned ALM axons, expressing a mitochondrial localization sequence::GFP (MLS::GFP) fusion. Position of cell bodies is indicated by red arrow. Bottom panel: mean ± SEM of mitochondrial length in ALM axons of day 1 adult animals. The length is expressed in "parts per mille" (‰) of the total axon length. The numbers of mitochondria analyzed for each strain are indicated inside each bar. The number of axons analyzed are the following: ncontrol = 9, nT119M = 11, nV30M = 11. Non-parametric Kruskal-Wallis with Dunn's multiple comparisons tests were performed for statistical analyses. ****$p<0.0001$.

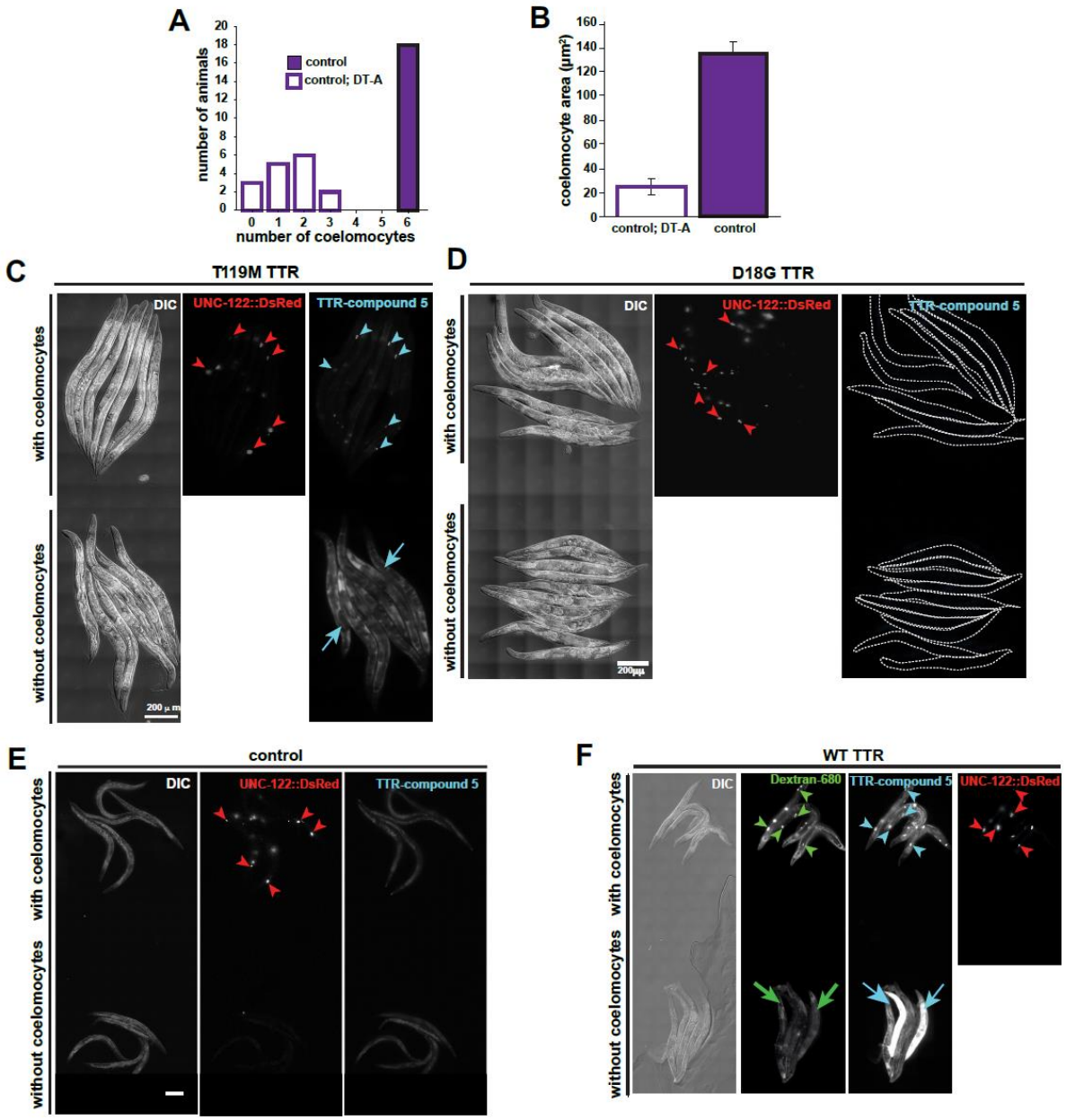

Fig. S9. Characterization of the formation and activity of coelomocytes after genetic ablation by a diphtheria-toxin (DT-A) mutation in TTR strains, Related to Fig. 6. (A) Coelomocytes counts scored with UNC-122::DsRed marker. (B) Area of coelomocytes (control ncoelomocytes = 32; for DT-A ncoelomocytes = 23). (C-F) Representative image of day 2 adult animals. Control n= 11, control; DT-A n= 5, WT n= 12, WT; DT-A n= 13, T119M = 21, T119M; DT-A n = 19, D18G = 23, D18G; DT-A n= 24. Animals were injected in the body cavity with Dextran-680 (if indicated) and fed with fluorogenic **CMPD5**. Coelomocytes were visualized with UNC- 122::Ds-Red. Arrowheads indicate position of representative coelomocytes in focus. Arrows point to body cavity fluorescence of corresponding molecule in DT-A animals. Animals without coelomocytes were not crossed to the UNC-122::Ds-Red marker strain (except control; DT-A animals).

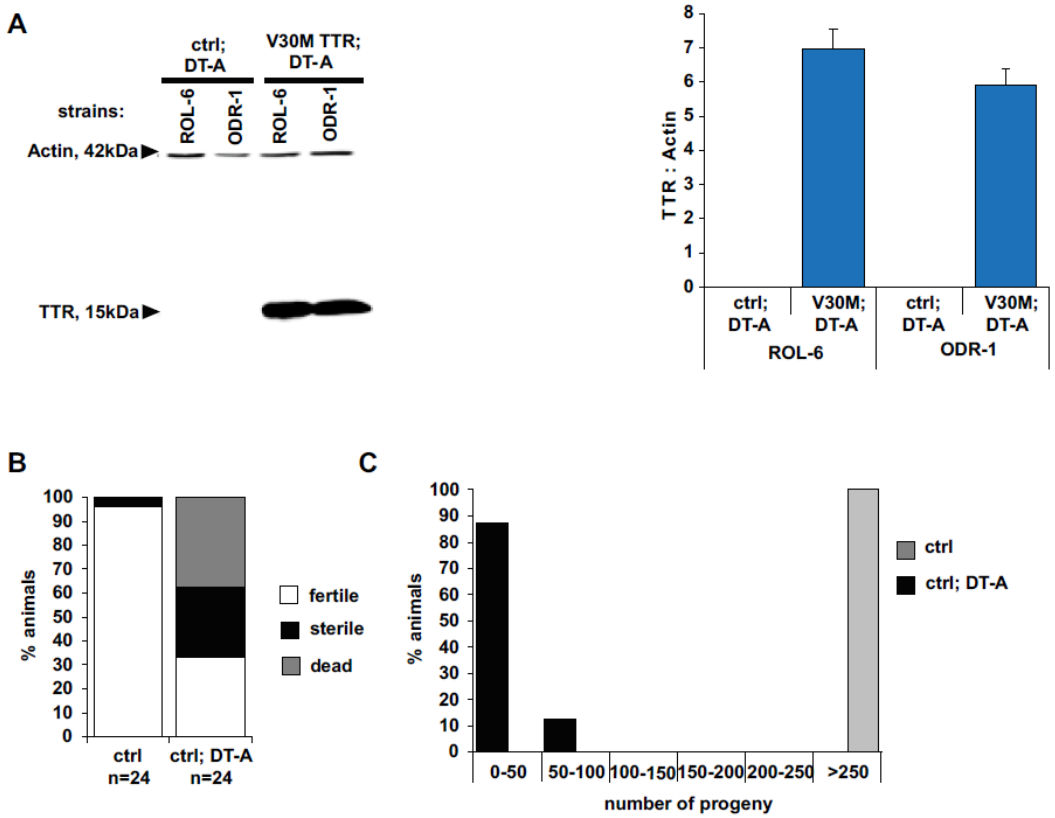

Fig. S10. Characterization of TTR protein expression levels, and viability of transgenic animals with and without coelomocytes, Related to Fig. 6. (A) Western blot (left) and quantification (right) (mean + s.e.m.) of TTR protein levels in the soluble lysates of control and V30M TTR strains without coelomocytes (DT-A) that were generated with *rol-6(su1006)* versus *odr-1p*::RFP as co-injection markers. Membranes were probed with the monoclonal MDX102 antibody against TTR. Images are representative of 2 independent experiments. (B) Viability and fecundity analyses of animals singled out as L1s and scored as young adults (day 1 adulthood) for fertility, sterility, and viability. (C) Percentage (brood size) of animals that hatched and developed at least until the L3 larval stage from fertile parents in (B); ctrl n = 8; ctrl; DT-A n = 23, ctrl = control. The observed reduction in nociception in the control; DT-A strains in Fig. 6C could be due to the generalized toxicity exhibited as a reduction in brood size and the number of viable and fertile animals compared to control animals.

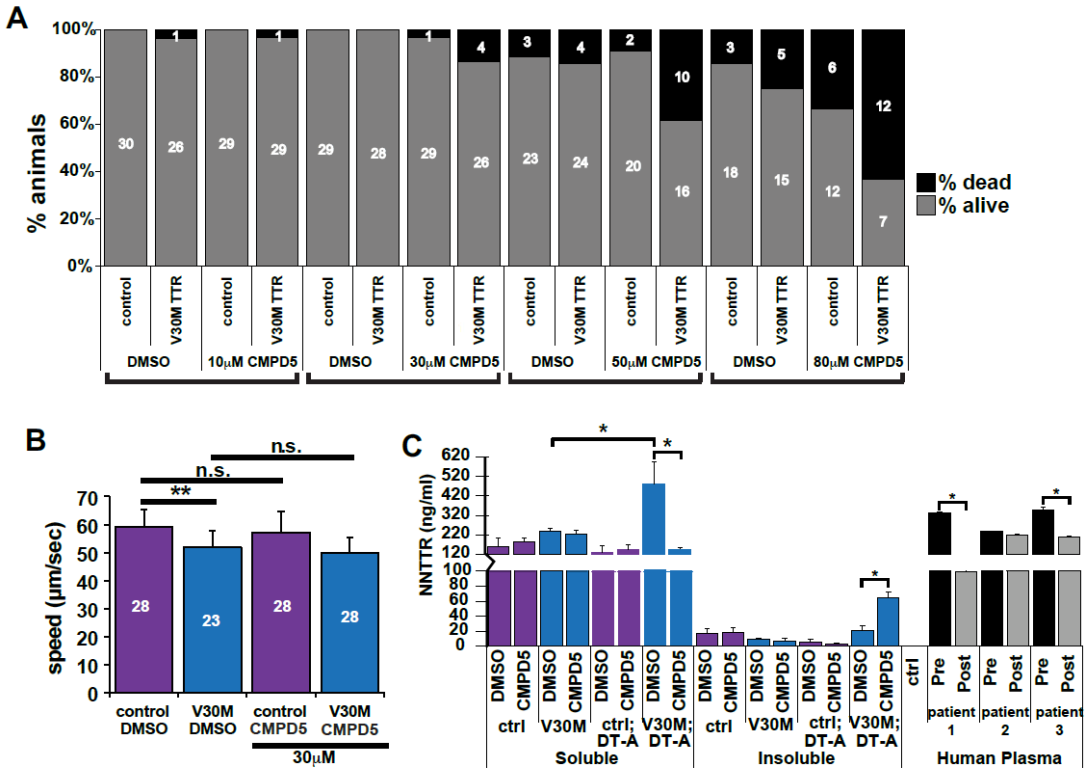

Fig. S11. Toxicity assay of V30M TTR animals treated with CMPD5, Related to Fig. 7. (A) Percentage of animals dead or alive after treatment with the same volume of vehicle (DMSO) and/or increasing concentrations of **CMPD5.** Animals were treated in liquid culture from L3 to adult day 1 and were scored on day 2 of adulthood. Brackets indicate experimental conditions with the same concentration of DMSO. (B) Locomotion rates for adult day 2 strains treated with 30 μM **CMPD5** and DMSO. Numbers of animals analyzed for each strain are shown inside bars. Plot is representative of 1 experiment (mean ± s.e.m., * $p < 0.005$, by Student's t-test). (C) Quantification of non-native (NN) TTR oligomer levels by a sandwich ELISA assay from lysates of day 2 TTR animals, and treated or not with **CMPD5** at the L3 larval stage. Data plotted shows mean ± s.e.m., n=3, * $p < 0.005$, by Student's t-test. Three human patient samples pre- and post-tafamidis treatment were included as positive controls for this assay. ctrl = control.

Table S1: Quantification of nociception defect in day 1 adult TTR transgenic animals.
[a]Student t-test.

		% animals displaying no avoidance response (Class IV)	Total # animals	# replicates	Difference from control[a]	Difference from V30M TTR[a]
eat-4(n2474)		47 ± 8.6	100	2	*** p<0.0001	-
unc-86(n846)		7 ± 2.2	85	2	*** p<0.0001	-
control		0	486	6	-	*** p<0.0001
unc-54p	**V30M TTR**	10 ± 0.6	577	6	*** p<0.0001	-
	T119M TTR	0	188	3	n.s.	*** p<0.0001
	D18G TTR	1.3 ± 1.3	148	2	*** p<0.0001	*** p<0.0003
	V30M ΔSS TTR	2.6 ± 0.5	310	3	*** p<0.0001	*** p<0.0003
des-2p	**V30M ΔSS TTR**	0	90	2	-	*** p<0.0001

Table S2: Quantification of nociception defect in day 1 adult TTR transgenic animals treated with RNAi against TTR.
[a]Student t-test.

	% animals displaying no avoidance response (Class IV)	Total # animals	# replicates	Difference from control[a]	Difference from V30M TTR[a]
control + E.V.	0	106	2	-	*** p<0.0001
control + TTR RNAi	0	111	2	n.s.	*** p<0.0001
V30M TTR + E.V.	9.5 ± 0.4	148	2	*** p<0.0001	-
V30M TTR + TTR RNAi	0	158	2	n.s.	*** p<0.0001

Table S3: Quantification of 4° FLP dendritic branches in day 1 adult animals.

Angle	# branches in control animals (n=19)	# branches in V30M animals (n=18)	# branches in T119M animals (n=18)
0°-30°	0.4	1.2	0.0
31°-60°	0.0	7.8	0.7
61°-90°	14.7	20.0	16.7
91°-120°	63.2	54.7	66.7
121°-150°	19.7	14.9	16.0
151°-180°	2.0	1.4	0.0

Table S4: Quantification of % 4° FLP dendritic branches in L4 animals.

Angle	# branches in control animals (n=19)	# branches in V30M animals (n=19)	# branches in T119M animals (n=15)
0°-30°	0	0	0
31°-60°	0	0	0
61°-90°	21.2	12.5	22.9
91°-120°	61.8	78.9	72.2
121°-150°	16.2	8.5	4.8
151°-180°	0	0	0

Table S5: Number of coelomocytes in day 2 adult animals as quantitated using dextran uptake assays.
[a] See List of Strains above for full strain genotypes.

Strain Name	Abbreviated Strain Name[a]	# animals Injected with dextran-A488	# animals with dextran-A488 in coelomocytes after 24 hrs
SEE064	control	9	9
SEE061	DT-A	11	0
SEE079	control; DT-A	8	0
SEE080	WT TTR; DT-A	12	0
SEE128	V30M TTR; DT-A	9	0
SEE168	T119M TTR; DT-A	9	0
SEE221	D18G TTR; DT-A	18	0

Table S6: Quantification of nociception defect in day 1 adult TTR DT-A transgenic animals.
[a]Student t-test.

	% animals displaying no avoidance response (Class IV)	Total # animals	# replicates	Difference from control[a]	Difference from V30M TTR[a]
control	0	486	6	-	*** p<0.0001
V30M TTR	10 ± 0.6	577	6	*** p<0.0001	-
control; DT-A	9.1 ± 2.5	143	2	*** p<0.0001	n.s.
V30M TTR; DT-A	22 ± 2	196	2	*** p<0.0001	*** p<0.0001

REFERENCES

1. Brenner S (1974) The genetics of Caenorhabditis elegans. *Genetics* 77(1):71-94.
2. Maniar TA*, et al.* (2012) UNC-33 (CRMP) and ankyrin organize microtubules and localize kinesin to polarize axon-dendrite sorting. *Nature Neuroscience* 15(1):48-56.
3. Mello C & Fire A (1995) DNA transformation. *Methods Cell Biol* 48:451-482.
4. Schwartz MS*, et al.* (2010) Detoxification of multiple heavy metals by a half-molecule ABC transporter, HMT-1, and coelomocytes of *Caenorhabditis elegans*. *PLoS One* 5(3):e9564.
5. Link CD (1995) Expression of human beta-amyloid peptide in transgenic Caenorhabditis elegans. *Proc Natl Acad Sci U S A* 92(20):9368-9372.
6. Viswanathan M & Guarente L (2011) Regulation of *Caenorhabditis elegans* lifespan by sir-2.1 transgenes. *Nature* 477(7365):E1-2.
7. Wiseman RL, Powers ET, & Kelly JW (2005) Partitioning conformational intermediates between competing refolding and aggregation pathways: insights into transthyretin amyloid disease. *Biochemistry* 44(50):16612-16623.
8. Bourgault S, Solomon JP, Reixach N, & Kelly JW (2011) Sulfated glycosaminoglycans accelerate transthyretin amyloidogenesis by quaternary structural conversion. *Biochemistry (Mosc).* 50(6):1001-1015.
9. Jiang X*, et al.* (2001) An engineered transthyretin monomer that is nonamyloidogenic, unless it is partially denatured. *Biochemistry* 40(38):11442-11452.
10. Rappley I*, et al.* (2014) Quantification of Transthyretin Kinetic Stability in Human Plasma Using Subunit Exchange. *Biochemistry* 53(12):1993-2006.
11. Walther DM*, et al.* (2015) Widespread Proteome Remodeling and Aggregation in Aging C. elegans. *Cell* 161(4):919-932.
12. Grimster NP*, et al.* (2013) Aromatic sulfonyl fluorides covalently kinetically stabilize transthyretin to prevent amyloidogenesis while affording a fluorescent conjugate. *Journal of the American Chemical Society* 135(15):5656-5668.
13. Loria PM, Hodgkin J, & Hobert O (2004) A conserved postsynaptic transmembrane protein affecting neuromuscular signaling in Caenorhabditis elegans. *J Neurosci* 24(9):2191-2201.
14. Wittenburg N & Baumeister R (1999) Thermal avoidance in Caenorhabditis elegans: an approach to the study of nociception. *Proc Natl Acad Sci U S A* 96(18):10477-10482.
15. Fares H & Greenwald I (2001) Genetic analysis of endocytosis in Caenorhabditis elegans: coelomocyte uptake defective mutants. *Genetics* 159(1):133-145.
16. Nussbaum-Krammer CI, Neto MF, Brielmann RM, Pedersen JS, & Morimoto RI (2015) Investigating the spreading and toxicity of prion-like proteins using the metazoan model organism *C. elegans*. *Journal of visualized experiments : JoVE* (95):52321.

The goal of **Article 5** was to screen for suppressors of TTR toxicity in our *C. elegans* models of FAP (developed and reported in **Article 4**), using locomotion as the phenotype to be screened against, in order to identify novel TTR interactors and pathways that mediate TTR toxicity. To this end, we performed the first unbiased forward genetic screen to identify modifiers of TTR proteotoxicity.

Of the 37 non-sibling candidate suppressors we isolated 10 candidate mutants that suppressed the uncoordinated (Unc) locomotion phenotype of the TTR model strain. After placing the mutant suppressors in complementation groups we identified the mutation in two TTR suppressors by whole-genome sequencing.

Both mutations were validated using RNAi against the mutated gene that "restores" the Unc Val30Met TTR locomotion phenotype. Importantly, the phenotype did not change in the two TTR suppressors when fed with RNAi against the candidate gene. Additionally, both TTR suppressors rescued the defective nociception phenotype.

In summary, we validated the identity of R193.2 as a suppressor of TTR toxicity, which supports the interpretation that the impaired locomotion and the defect in noxious heat sensing observed in Val30Met animals can be rescued by knocking-down the expression of R193.2.

My specific contributions on this paper were as follows:

- Isolated the 10 best TTR suppressors;
- Sequenced the full-length TTR cDNA sequences for the 10 isolated suppressors and confirmed the TTR expression by RT-PCR and western blot;
- Placed the mutant suppressors in complementation groups;
- Prepared all the genomic samples (V30M TTR parental strain and 10 TTR suppressors) and sent them for whole-genome sequencing;
- Analyzed the whole-genome sequencing results for the sttr006 and sttr009 TTR suppressors;
- Identification and characterization of *R193.2 C. elegans* gene;
- Quantitated the motility of TTR suppressors' worms and treated with tafamidis and RNAi against TTR and R193.2.

Article 5: Genetic Modulators of Transthyretin Amyloid Disease Toxicity in *Caenorhabditis elegans* models of Familial Amyloid Polyneuropathy (FAP).

Miguel Alves-Ferreira[1,2,3,4,5]; Sylvia Neumann[1,2,3,a]; Josh Lowry[6,b]; Kayalvizhi Madhivanan[1,2,3], Nirvan Rouzbeh[1,2,3,c]; Bruce Bowerman[6]; Jeffery W. Kelly[1,7,8] and Sandra E. Encalada[1,2,3,§].

[1] Department of Molecular Medicine, Scripps Research, La Jolla, CA

[2] Department of Neuroscience, Scripps Research, La Jolla, CA

[3] Dorris Neuroscience Center, Scripps Research, La Jolla, CA

[4] UnIGENe, IBMC – Institute for Molecular and Cell Biology; i3S – Instituto de Investigação e Inovação em Saúde, Universidade do Porto, Portugal;

[5] ICBAS - Instituto Ciências Biomédicas Abel Salazar, Universidade do Porto, Portugal;

[6] Institute of Molecular Biology, University of Oregon, Eugene, Oregon 97403.

[7]Department of Chemistry, The Scripps Research Institute, La Jolla, CA 92037.

[8]The Skaggs Institute for Chemical Biology, The Scripps Research Institute, La Jolla, CA 92037

[a] Present address: Department of Biological Chemistry, University of California Los Angeles, Los Angeles, CA 90095, USA

[b] Present address: Department of Human Genetics, University of Utah School of Medicine, Salt Lake City, UT 84112.

[c] Present address: Department of Biomedical and Pharmaceutical Sciences, University of Montana, Missoula, MT 59812.

[§] To whom correspondence should be addressed. E-mail: encalada@scripps.edu; Phone: +1-858-784-9681.

In preparation

SUMMARY

Familial Amyloid Polyneuropathy (FAP) is a neurodegenerative disease affecting peripheral nerves, which results in loss of pain- and thermo-sensation. Though the causal gene has been identified as transthyretin (*TTR*) and V30M the most frequent disease-causing variant, the mechanisms of TTR-mediated neuronal dysfunction are unknown.

We generated *C. elegans* models of FAP by expressing human TTR. These animals exhibit patient relevant phenotypes, including loss of pain-sensation and uncoordinated (Unc) locomotion.

Animals treated with small molecules used in human therapies to stabilize TTR, or with RNAi against TTR, rescued both phenotypes. As these interventions show limited promise in human patients, the goal of this study was to identify novel FAP targets by identifying TTR interactors leading to neurotoxicity.

We performed the first unbiased forward genetic screen in V30M TTR *C. elegans* line to identify suppressors of the TTR. We isolated 37 non-sibling candidate suppressors of the Unc phenotype exhibited by this model. Two TTR suppressors that corresponded to the same complementation group present a different missense mutation in *R193.2* gene.

These suppressors of TTR toxicity pathways results in a rescue of the Unc phenotype, but also in a reversal in the defect in noxious heat sensing of V30M TTR animals. Thus, we hypothesize that R193.2 could be involved in TTR neuronal-dependent toxicity pathways, but this needs to be further investigated.

INTRODUCTION

Transthyretin (TTR) is a thyroxine and retinol-binding protein that is readily secreted from the liver and is deposited extracellularly around nerves and in other distal tissues, leading to proteotoxicity [1-4]. Point mutations in TTR that cause misfolding and aggregation of the protein have been associated with several amyloid diseases, including the autosomal dominant lethal Familial Amyloid Polyneuropathy (FAP) [5]. The most common FAP-associated mutation is V30M TTR, in which patients' exhibit a severe gastrointestinal, genitourinary and cardiovascular autonomic dysfunction associated with a sensory neuropathy with loss of pain [6].

The TTR-mediated pathways by which neuronal dysfunction occurs, are unknown. Furthermore, it is not clear whether TTR interactions with other proteins play a significant role in proteotoxicity, or whether such interactions could also provide protective effects in neurons [7]. The role of TTR dysfunction in FAP has been investigated using transgenic mouse and Drosophila models expressing the V30M mutation, however, these models did not exhibit cell non-autonomous features [8]. *C. elegans* the was first multicellular organism to have its whole-genome sequenced and about 83% of the *C. elegans* proteome has homologous genes in humans [9], proving to be thus a powerful animal model for genetic studies and contributing to a better comprehension of the gene-gene interaction in many of the major neurodegenerative diseases [10, 11].

Previously, we generated *C. elegans* models of FAP which overexpresses human V30M TTR that recapitulate critical features of human FAP disease, including cell non-autonomous neuronal proteotoxicity leading specifically to impairment in locomotion (Uncoordinated, [Unc]) and behavioral nociception-sensing impairments [12]. Thus, coupled with its powerful genetics and genomics, short lifespan, and transparency for direct in vivo imaging, this *C. elegans* model is an ideal organism for the study of the role of protein dysfunction in age-dependent neurodegeneration.

Here we present the first forward genetic screen in *C. elegans* V30M TTR model to investigate novel proteins that interact with TTR and contribute to neuronal proteotoxicity. We further validated the potential of forward genetic screen by combining the results with proteotoxicity behavioral assays. The TTR pathways of toxicity are unknown, but the discovery of novel genes involved in TTR toxic pathways will provide insights into the mechanisms of neuronal dysfunction in FAP, and also into possible therapies for treating this disease.

MATERIAL AND METHODS

C. elegans Strains

All strains were handled and maintained followed as previously described [13]. N2 Bristol was used as the wild-type strain. V30M TTR strain [scrIs024[unc-54p::hTTR(V30M) + odr-1p::RFP]; scrIs010[des-2p::myr::GFP + unc-122p::DsRed]] and non-TTR control strain scrIs020[odr-1p::RFP]; scrIs010[des-2p::myr::GFP + unc-122p::DsRed] were generated using standard molecular biology techniques as described in Madhivanan K., et al [12]. Nematodes were grown on Nematode growth media (NGM) plates seeded with the E. coli strain OP50 at 20°C.

EMS Mutagenesis

We selected V30M TTR strains taking advantage of their locomotion defects to perform a forward genetic suppressor screen. Mutagenesis was performed using standard *C. elegans* ethyl methanesulfonate (EMS) methodology [14]. Briefly, adult P0 *C. elegans* were mutagenized using 50 mM EMS, which induces one mutant every 2500 mutagenized P0 gametes. Mutagenized P0 animals were plated onto 10 cm plates at a density of 30 animals per plate. Animals were allowed to lay about 2-5 eggs/animal in order to obtain around 100 F1 animals per plate. These allowed developing to adult animals and laid about 20 eggs/animal resulting in about 2000 F2 animals per plate of which one quarter carried homozygous mutations. Approximately, 125,000 F2 generation homozygous progeny were screened for suppressors of Unc phenotype (wild-type locomotion) and isolated onto fresh plates to produce F3 animals that were scored for wild-type locomotion as well. Each candidate suppressor was back-crossed to V30M TTR animals and selected for wild-type locomotion phenotype in order to remove unrelated mutations. Candidate suppressors were placed in complementation groups.

Genotyping

To verify DNA changes and variant confirmations we performed a polymerase chain reaction (PCR) followed by Sanger sequencing (Eton Bioscience Inc., San Diego, CA, USA). *C. elegans* in lysis buffer (1M KCl, 1MTris pH 8.2, 1m MgCl2, 0.10% NP-40, 0.50% Tween 20, 0.01% gelatin, 10 mg/ml proteinase K) were flash frozen in liquid nitrogen followed by incubation at 65°C 1 hour and proteinase was inactivated by incubation at 95°C 15 minutes. The lysate DNA templates were then added to a PCR master mix containing 8 µL water, 4 µL 10X PCR buffer, 2 µL 25 mM MgCl2, 0.5 µL 10 µM primers, 0.5 µL 10 mM dNTPs, and 0.1 µL Taq. The following primers were designed to amplify the DNA targeted regions:

V30M TTR Forward 5'-CTTCTCATCGTCTGCTCCTC-3'

V30M TTR Reverse 5'-TTCCTTGGGATTGGTGACGAC-3'
sttr006 R193.2 Forward 5'-TCCTCAACTTCACCGCTTATC-3'
sttr006 R193.2 Reverse 5'-GAGCAGATGTGTAACCTCCAA-3'
sttr009 R193.2 Forward 5'- AGCCTTGTCAGAGTAATTGGG-3'
sttr009 R193.2 Reverse 5'-GAAGATCAGCTCAGCGTAGAAG-3'

mRNA extraction and quantitative reverse transcriptase (RT)-PCR

RNA was extracted from flash frozen worm samples grown in liquid culture medium (D1 in biological duplicates) using the QIAzol lysis reagent (cat no. 79306, QIAGEN), followed by DNase I treatment (cat no. AMPD1, Sigma). mRNA was reverse transcribed using the iScript cDNA Synthesis kit (cat no. 170-8841, Bio-Rad). 20ng of cDNA was used for real-time PCR amplification using the FastStart Universal SYBR Green Mastermix (cat no. 04913850001, Roche) and the ABS 7900HT Fast Real-Time PCR System. The relative *TTR* and *R193.2* gene expression levels were determined using the Comparative CT Method. *TTR* and *R193.2* gene expression levels were normalized relatively to the 60S ribosomal protein L6 (rpl-6) and to the plasma membrane protein 3 (pmp-3) in the same sample (internal control). Measurements were performed from two biological samples per condition (n=3 technical replicates, ± SEM). The following primer sequences were used:
TTR Forward 5'-ATTTGCCTCTGGGAAAACCAG-3'
TTR Reverse 5'-GGCTGTGAATACCACCTCTGC-3'
R193.2 Forward 5'- ACGCTTGGATCGTCATCTTC -3'
R193.2 Reverse 5'- TAGAGCCGAGGGAGTCATATT -3'
rpl-6 Forward 5'-TTCACCAAGGACACTAGCG-3'
rpl-6 Reverse 5'-GACAGTCTTGGAATGTCCGA-3'
pmp-3 Forward 5'-TGGCCGGATGATGGTGTCGC-3'
pmp-3 Reverse 5'-ACGAACAATGCCAAAGGCCAGC-3'

Western blot analysis for quantification of total TTR protein levels

Bleached synchronized animals (~1000 to 10,000 nematodes) were grown in 50 ml S-complete medium supplemented with 50 µg ml-1 carbenicillin and 0.1 µg ml-1 fungizone and 6 mg ml-1 (< 5000 animals) or 12 mg ml-1 (> 5000 animals) freshly prepared E. coli OP50. Animals were cultured in 15 cm petri dishes at 20°C. To arrest embryos prior to hatching, 5-fluoro- 2´-deoxyuridine (FUDR) was added to a final concentration of 0.12 mM to L4 larvae animals (Sigma). At day 1 of adulthood, *C. elegans* were thoroughly washed three times in 1x PBS buffer and worm

pellet was re-suspended in 300 µl cold 1x PBS supplemented with complete protease inhibitors (Roche). The approximate concentration of animals for each sample was determined by counting the number of animals in ten 10 µl drops using a dissecting scope. The animal suspension was added to a hard tissue homogenizing CK28 Precellys tube (Bertin Technologies) and subjected to Precellys-24 homogenization at 6500 x g for 3 x 10 sec bursts (Bertin Technologies). Sample homogenates were re-suspended in a 10% SDS solution and boiled for 10 minutes at 95°C. Protein fraction concentrations were determined using the Bio-Rad DC Protein Assay kit (Bio-Rad).

Samples (5-10 µg total protein) were mixed with 6x SDS loading sample buffer (20% glycerol, 12% SDS, 125 mM Tris pH 6.8) and with 100 mM DTT (Sigma), boiled for 10 minutes and loaded into the wells of a 15% SDS-Page Gel gel. Protein separation was performed at 150V in SDS running buffer and blotted onto a nitrocellulose membrane in transfer buffer (20 mM Tris, 150 mM glycine, 20% methanol) for 2 hours at 0.25A. Membranes were incubated in blocking solution (1X TBS with 5% non-fat milk) for 1 hour followed by an overnight incubation at 4°C with primary monoclonal antibody MDX102 against TTR (Misfolding Diagnostics, Inc.) at a 1:1000 dilution, and with a monoclonal antibody against actin (α-actinC4; MAB1501, Millipore) at a 1:4000 dilution. After three rinses in 1X TBS-T the membrane was incubated with secondary donkey anti-mouse IRDye 800 nm conjugated antibody (LI-COR) for 1 hour at room temperature diluted 1:10000 in blocking solution, rinsed 3 times in TBS-T, and scanned with an Odyssey infrared imager (LI-COR). Protein band intensities were measured using Image J. The ratio of TTR to Actin band intensities were normalized to V30M TTR animals. Experiments were done for n = 3 biological replicates.

Whole-Genome Sequencing and Data Analysis

Genomic DNA from TTR suppressors was isolated with the Gentra Puregene Tissue Kit (Qiagen) following the manufacturer's supplementary protocol. DNA quantification was achieved using Qubit dsDNA HS assay in Qubit®2.0 Fluorometer (Life Technologies, CA, USA). The DNA from each animal was subjected to whole-genome sequencing on an Illumina HiSeq 4000 sequencing platform using paired-end 150-nucleotide reads.

The Galaxy platform was used to analyze genome sequences, obtain map data, and find mutations as previously described [15]. Briefly, the sequencing reads were first mapped to the WS241 version of the *C. elegans* genome and duplicate read pairs were then removed from further

analyses using the Bowtie2 [16]. GATK tools [17] were used for alignment quality control and for variant detection and analysis, in combination with CloudpMap[15], snpEff [18], and Bedtools [19]. By subtracting the variants in the parental strain (V30M TTR) and among the mutant strains, we determined unique variants for TTR suppressors.

RNAi feeding

Reduction of *R193.2* gene activity was accomplished by feeding *C. elegans* with RNAi bacterial clones obtained from the Ahringer library [20]. L4440 plasmid in HT115 bacteria (empty vector) was used as the RNAi control. RNAi experiments were performed at 20ºC.

E. coli HT115 bacteria expressing RNAi and empy vector were cultured in Luria-Bertani (LB) media containing 10 mg ml-1 ampicillin and spotted on NGM plates containing 100 µg ml-1 carbenicillin. RNAi production was induced with addition of 100 mM IPTG placed directly on the bacterial lawn of each plate. Animals were grown on new plates RNAi expressing bacteria for two generations prior to analysis. Lysates were made by picking animals into 300 µl cold PBS and lysed as described above (”Western blot analysis for quantification of total TTR protein levels”). Day 2 adult animals were recorded as mentioned below “Locomotion assay and worm tracking analysis”.

Locomotion assay and worm tracking analysis

Prior to locomotion assay, *C. elegans* were maintained at 22°C for multiple generations without starvation on NGM (+OP50) seeded plates. Individual day 2 adult animals were placed in an unseeded 35 mm plate for 40 minutes, then transferred to a new unseeded 35 mm plate and their movement trajectories recorded for a duration of 40 seconds using the Stemi 508 microscope (Zeiss) with SwiftCam2 camera and imaging software (Swift). All videos were analyzed using wrMTrck plugin for ImageJ to obtain average speed and representative tracks of each of the trajectories [21]. For clarity, tracks were traced in Adobe Illustrator CS6 and aligned to ensure the starting point of each worm was stacked. All locomotion assays including the tracking analysis were performed blind. Experiments were performed for n = 3 biological replicates.

Thermal avoidance assay for nociception

Thirty L4 *C. elegans* were picked onto 6 cm NGM (+OP50) plates and placed at 22˚C overnight. The thermal avoidance assay was done on D1 adult *C. elegans* and their response to noxious heat was scored in one of the 4 categories, as indicated in Wittenburg *et al.*, 1999 [22]: class I,

rapid withdrawal reflex, backing, and change in direction; class II: rapid withdrawal reflex with little backing; class III: slow backing; class IV: no response. The heat source was a blunt 301/2-gauge needle heated for at least 10 seconds in a burner and immediately placed 3-5 mm in front of the animal as it was in forward motion. The following guidelines were strictly followed: the heated tip was placed in front of a single animal at a time. Each animal was removed after testing to prevent re-testing. Only the initial response of the worm was recorded, i.e., animals were not re-tested. Experiments were done for 3 biological replicates.

Statistical analyses

Statistical comparisons of data were performed using unpaired, two-tailed Student's t-test. Quantitative data were expressed as mean ± standard deviation. Statistical significance was established for *p < 0.05, **p < 0.01, ***p < 0.001.

RESULTS

Phenotypic Characterization of V30M TTR strains

We generated *C. elegans* transgenic lines carrying V30M TTR mutation expressed under the body wall muscle unc-54 promoter (Fig. 1A). At room temperature, V30M TTR transgenic animals displayed an impaired locomotion (Unc) phenotype. This phenotype was neither observed in wild-type animals (N2 strain) nor in non-TTR control animals (scrIs020[odr-1p::RFP]; scrIs010[des-2p::myr::GFP + unc-122p::DsRed]). In the locomotion assay, V30M TTR animals had a mean speed 43.04 um/s at Day 1 of adulthood while non-TTR animals showed a mean speed 64.14 um/s (P<0.001). Animals treated with small molecules used in human therapies to stabilize TTR, or with RNAi against TTR, rescued the Unc phenotype, suggesting that the locomotion phenotype was TTR-dependent [12]. Taken together, these features make this *C. elegans* TTR model highly suitable for a forward genetic screen.

Identifying the causal mutations in V30M TTR animals using a whole-genome sequencing

The first unbiased forward genetic EMS mutagenesis screen in *C. elegans* FAP models to identify modifiers of TTR proteotoxicity was conducted, utilizing the Unc phenotype that V30M TTR *C. elegans* exhibit, to screen for suppressors of Unc.

Following mutagenesis of V30M TTR parental *C. elegans* by EMS, we screened approximately 125,000 F2 generation homozygous mutants covering about 30% of the *C. elegans* genome (Fig.

1B). From the screening we isolated at least 37 non-sibling candidate suppressors of the Unc phenotype exhibited by V30M TTR *C. elegans*. These animals were allowed to produce further progeny, which retained the wild-type locomotion phenotype.

We selected ten mutants which exhibited a suppression of the Unc phenotype. These alleles were named sttr001 through sttr010 (suppressors of TTR) (Fig. 1C). We sequenced the full-length TTR cDNA sequences and for the ten isolated suppressors, all of them only showed the V30M mutation in the human *TTR* gene. This observation suggests that there are other mutation(s) elsewhere in the genome which are able to rescue the Unc phenotype. Also, we confirmed that TTR is expressed in suppressor alleles by RT-PCR and western-blot (Fig. 1D), indicating that these suppressor alleles do not silence TTR expression both at mRNA and protein levels. Thus, suppression of the phenotype does not appear to be due to the lack of TTR expression in *C. elegans*.

Complementation analysis showed that the sttr004/sttr007 and sttr006/sttr009 were in the same complementation group, i.e., were alleles of the same gene. To identify the mutations, we performed whole-genome sequencing of the ten isolated suppressors and identified unique variants in each strain, using the CloudMap pipeline (Minevich *et al.* 2012). Other alleles isolated from this screen will be described elsewhere. These variants were confirmed by Sanger sequencing and their absence was also confirmed in the parental strain animals (Fig. 2 A, B).

R193.2 is an uncharacterized *C. elegans* gene with conserved SEA and WFA domains

The sttr006 and sttr009 strains contained a missense mutation in the R193.2 exon 21 and 3, respectively (Fig. 2 A, B). *R193.2* gene encodes an uncharacterized protein in *C. elegans* that is expressed in the intestine and germ line and predicted to localize at membrane [23, 24]. sttr009 is predicted to affect the SEA domain in the R193.2 protein (Fig. 2 B). R193.2 also has four von Willebrand A (VWA) domains. These domains have been implicated in multiprotein complexes; cell adhesion; regulating or binding carbohydrate side chains and proteolytic activity [25-27].

RNAi against R193.2 rescues the Unc phenotype

To test whether the suppression of TTR proteotoxicity in V30M animals was the result of a mutation in the *R193.2* gene, we reduced the function of R193.2 via RNAi. The R193.2 mRNA silencing effectiveness of RNAi was confirmed by real-time RT-PCR (data not shown). V30M TTR *C. elegans* fed with bacteria harboring dsRNA targeting the *R193.2* gene significantly increased the mean speed of locomotion compared to animals expressing V30M TTR sequence strain fed

with bacteria carrying empty vector L4440 (31.63 vs 45.07 um/sec; P<0.001) (Fig. 3). Additionally, both suppressors strains treated with a control RNAi (empty vector) and RNAi against R193.2 showed a similar mean speed (38.1 vs 37.73 for sttr006 and 42.68 vs 42.01um/sec for sttr009; P>0.05) (Fig. 3). Thus, the wild-type locomotion phenotype did not change in the two TTR suppressors fed with RNAi against the candidate gene. These data suggest that these two alleles exerted a similar effect on the R193.2 protein to the effect of RNAi treatment and were sufficient to suppress the Unc phenotype. Collectively, we validated the identity of R193.2 as a suppressor of TTR toxicity, which supports the interpretation that the impaired locomotion observed in these animals can be rescued by knocking-down the expression of R193.2.

TTR suppressors rescue defective sensory nociception phenotype exhibited by V30M TTR transgenic animals

TTR transgenic *C. elegans* also show behavioral nociception-sensing impairments that correlated with increased aggregation propensity of V30M TTR [12]. We hypothesized that the suppressors identified also rescue the nociception defect phenotype. To test whether R193.2 mutants suppress the proteotoxicity in the sensory pain-sensing neurons, we measured the reflex-like escape reaction of suppressor strains using a thermal-avoidance assay that measures nociception. We found a significant reduction in TTR suppressor animals that were unresponsive to noxious heat (class IV) (0.56% and 0%, sttr006 and sttr009, respectively), compared to V30M TTR animals (5.26%) (Fig. 4). These findings show that *R193.2* gene seems to play a role in the TTR mechanism, which when knocked-down reduces sensation to pain.

DISCUSSION

Here, we identified R193.2 as a suppressor of TTR toxicity pathways. Specifically, mutation of R193.2 resulted in a rescue of the Unc phenotype observed in V30M TTR animals, but also in a reversal in the defect in noxious heat sensing of V30M TTR animals, which has been previously shown to be dependent on the function of two head neurons [22, 28]. Thus, we hypothesize that R193.2 could be involved in TTR neuronal-dependent toxicity pathways, but this needs to be further investigated.

There are many ways to identify components that function in a specific genetic pathway and thus unravel part of the mechanisms. In an unbiased modifier screening, after mutagenesis, the mutant selection could focus on the search for genes that either enhance (worsen) or suppress (ameliorate) a well-characterized phenotypic defect. Our animal model showed that aggregation

of TTR leads to cell-nonautonomous proteotoxicity, i.e., degeneration of tissues which do not synthesize TTR. This proteotoxicity is expressed phenotypically in *C. elegans* as movement defects and a compromised response to noxious heat, which has been described as a response to pain sensation [12]. However, the mechanisms by which cellular dysfunction and tissue degeneration occur remain poorly understood.

The suppression of V30M TTR phenotypes in sttr006 and sttr009 animals carrying missense mutations in *R193.2* gene, combined with the rescue of the Unc phenotype by RNAi R193.2 knock-down validate the specificity of our approach. Notably, the same mutated gene was identified in both suppressors, but not in parental strain animals.

R193.2 is an uncharacterized *C. elegans* gene, comprising 37 exons located at chromosome X. Encodes a 1897 amino acid protein annotated as integral component of membrane, i.e., inferred from electronic annotation to have at least some part of peptide sequence (helical or beta-stranded domain) embedded in the hydrophobic region of the membrane (GO:0016021) [29, 30]. Based on expression studies, R193.2 is enriched in the intestine and germ line, through RNA sequencing and microarray approaches [23, 24].

R193.2 mRNA levels changed significantly in both lin-4 and lin-14 mutants [31]. LIN-14 act as a DNA binding transcriptional regulator and is down-regulated as a result of translational repression by the microRNA product of lin-4 [32]. Under those circumstances, *R193.2* gene could be a transcriptional target and consequently regulated by LIN-14 at stage-specific expression in the nucleus. It was also demonstrated that R193.2 is involved in regulation of heme homeostasis, since *R193.2* gene was upregulated under 4 μM heme concentration [33]. Recently, R193.2 protein was pinpointed as modified by small ubiquitin-related modifier (SUMO) in *C. elegans* in normal growth conditions and upon stress [34].

R193.2 encodes a protein with strong sequence similarity to an evolutionarily highly conserved SEA and VWA domains (Fig. 2 B). Named after the first three proteins in which it was identified, Sea urchin sperm; Enterokinase and Agrin, SEA domain is an extracellular domain associated glycoproteins and it is located between amino acid 65 and 166 of R193.2 protein. Akhavan et al, reported a proteolytic activity for SEA domain in addition to already proposed function of regulating or binding carbohydrate side chains [26, 27]. The SEA domains are encountered in mucins, transmembrane serine proteases, perlecan and dystroglycan. In mucins, a transmembrane

glycoproteins contain typically 110-residue SEA domains located next to the membrane and auto-proteolysis releases these molecules from the cell surface [35].

A number of human diseases arise from mutations in SEA domains, such as congenital myasthenic syndromes characterized by impaired neuromuscular transmission, mostly resulting from mutations affecting neuromuscular junction proteins [36]. In vitelliform macular dystrophies, structural modeling indicates that mutation in *IMPG1* gene destabilizes the SEA domain [37]. In another interphotoreceptor matrix proteoglycan, IMPG2 wild-type protein is targeted to the plasma membrane while mutant SEA domain appears to be trapped in the ER resulting in autosomal-recessive retinitis pigmentosa [38]. Iron-refractory iron deficiency anemia (IRIDA) is caused by mutations within SEA domain of the transmembrane serine protease TMPRSS6 that may affect the proper folding of SEA domain and as a consequence lead to structural destabilization [39].

The other predicted domain in R193.2 is a VWA domain, a well-characterized domain found in *C. elegans* extracellular matrix (ECM) [25, 40] proteins, integrin receptors, but are also found in auxiliary subunits of voltage-gated calcium channels [25]. It is an important domain for protein-protein interactions, cell adhesion and signaling in extracellular matrix proteins. R193.2 protein carry two conserved metal ion-dependent adhesion site (MIDAS) motif within VWA domain, which is often involved in ligand binding [25]. Proteins containing VWA domain binds selectively to collagen and laminin, suggesting a role in basement membrane matrix adhesion [41].

Several genetic disorders have been associated with mutations in VWA domains, namely juvenile hyaline fibromatosis and infantile systemic hyalinosis in CMG2 [42]; musculoskeletal diseases in collagen genes [43] and hereditary cerebellar ataxia in VWA3B [44]. Importantly, genetic defects within the CLCA1 VWA domain act as a modifier gene in cystic fibrosis patients with meconium ileus [45], suggesting the possible role of this domain in modifying the course of the disease caused by other primary disease-causing genes. Despite there are no obvious homologs of R193.2 to proteins in humans, the Basic Local Alignment Search Tool (BLAST) identified a limited homology to collagen type VI in humans, likely due to the presence of VWA domains that are representative of these proteins [46].

Albeit the function of R193.2 protein is currently unknown, to recognize their targets and protein-protein interactions as well as the presence of conserved domains is helpful to identify specific biological properties. Because this screen was not performed to saturation, it does not exclude

the possibility of other genes and pathways that repress the Unc phenotype, but it does suggest that if they exist, then they can be either rare or essential for *C. elegans* development. Furthermore, many genes can enhance a mutant phenotype, whereas only mutations in a few key regulators can suppress a mutant phenotype [47].

The specific role of R193.2 in TTR neuronal-dependent toxicity pathways are not clear. However, a plausible hypothesis is that R193.2 mediates R193.2/TTR protein–protein (e.g., receptor-ligand) interactions that may be involved in signaling of ECM proteins, such as integrins and collagens either in assembly or function of these complexes. Further studies in our *C. elegans* model and translational conformation in a mammalian system are required to address these hypotheses. Continued investigation of mutants and genes isolated in this screen and related screens in the future will allow us to better understand the factors that impact the neuronal toxicity and may well contribute to a better understanding of the pathogenic mechanisms of other neurological states.

Acknowledgements

We are grateful to Dr. M. Hansen (Sanford Burnham Prebys Medical Discovery Institute) and Dr. M. Petrascheck for providing the reagents and for advice and critical feedback on the work (The Scripps Research Institute).

M.A.-F. was supported by Fundação para a Ciência e Tecnologia Fellowship

SFRH/BD/101352/2014.

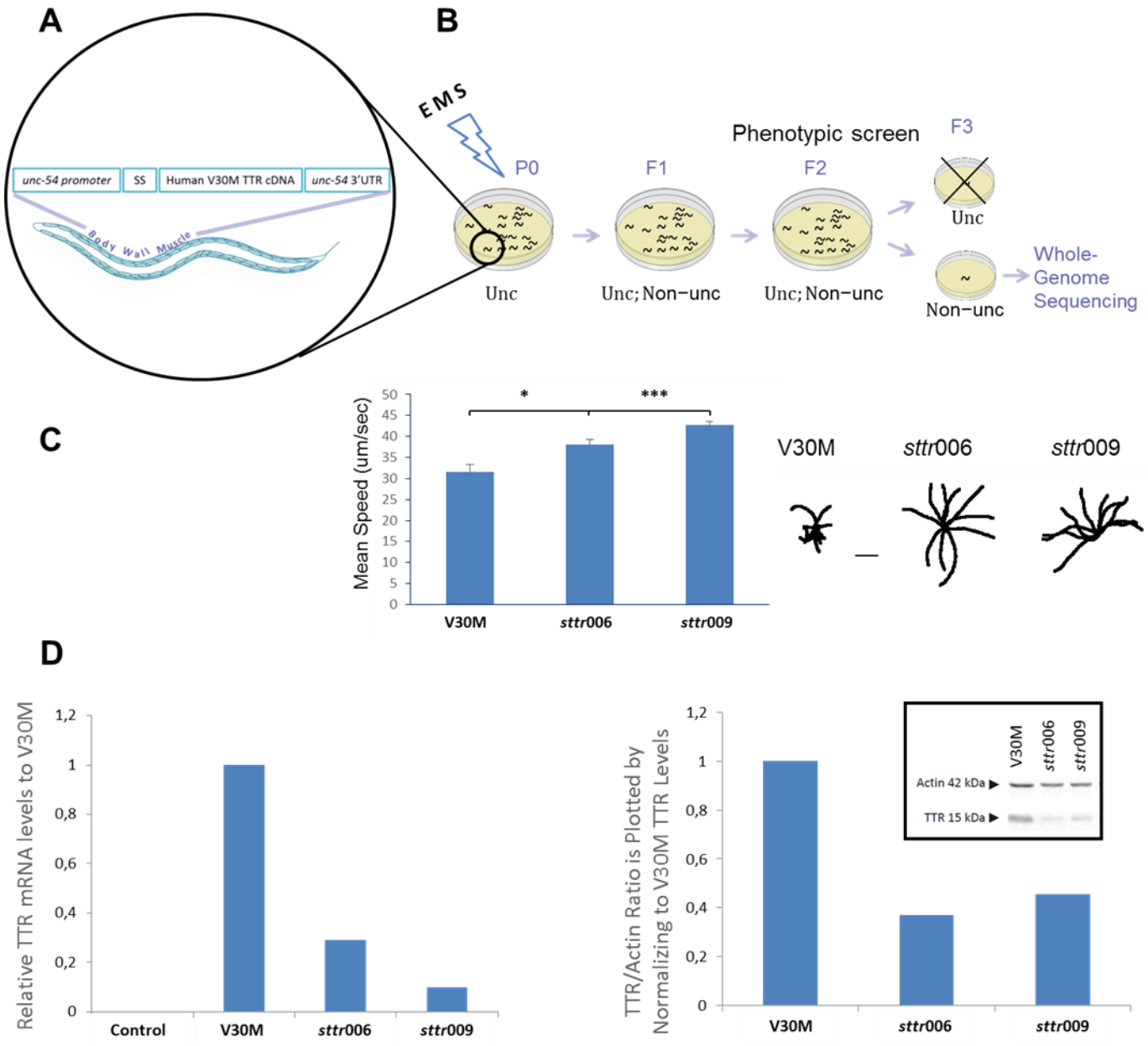

Fig. 1. Identification of suppressors of TTR (*sttr*) mutants. (A) Schematic of V30M TTR-FAP animal used in this screen. The human TTR with V30M variant was expressed under the body wall muscle *unc-54* promoter. (B) Isolation of non-sibling candidate suppressors of the Unc phenotype. Schematic of the unbiased forward genetic EMS mutagenesis screen in *C. elegans* V30M TTR-FAP models to identify modifiers of TTR proteotoxicity based on impaired locomotion (Unc) phenotype that V30M TTR *C. elegans* exhibit. See M&M for details. (C) Locomotion rates for V30M (n=24), *sttr*006 (n=20) and *sttr*009 (n=23). Plots show means ± standard deviations; *p < 0.05, ***p < 0.001, compared to V30M animals. Representative 40 seconds locomotion trajectories with starting point aligned in the middle (Scale Bar:

2000µm). (D) (left) Quantitative real-time PCR analysis of indicated strains mRNA levels. *TTR* gene expression levels were compared to 60S ribosomal protein L6 (*rpl-6*) mRNA, to the plasma membrane protein 3 (*pmp-3*) mRNA, and normalized to D1 V30M TTR. (right) Representative Western blot of TTR levels probed with antibody MDX102 against TTR and plotted the TTR/Actin ration normalized to V30M TTR levels.

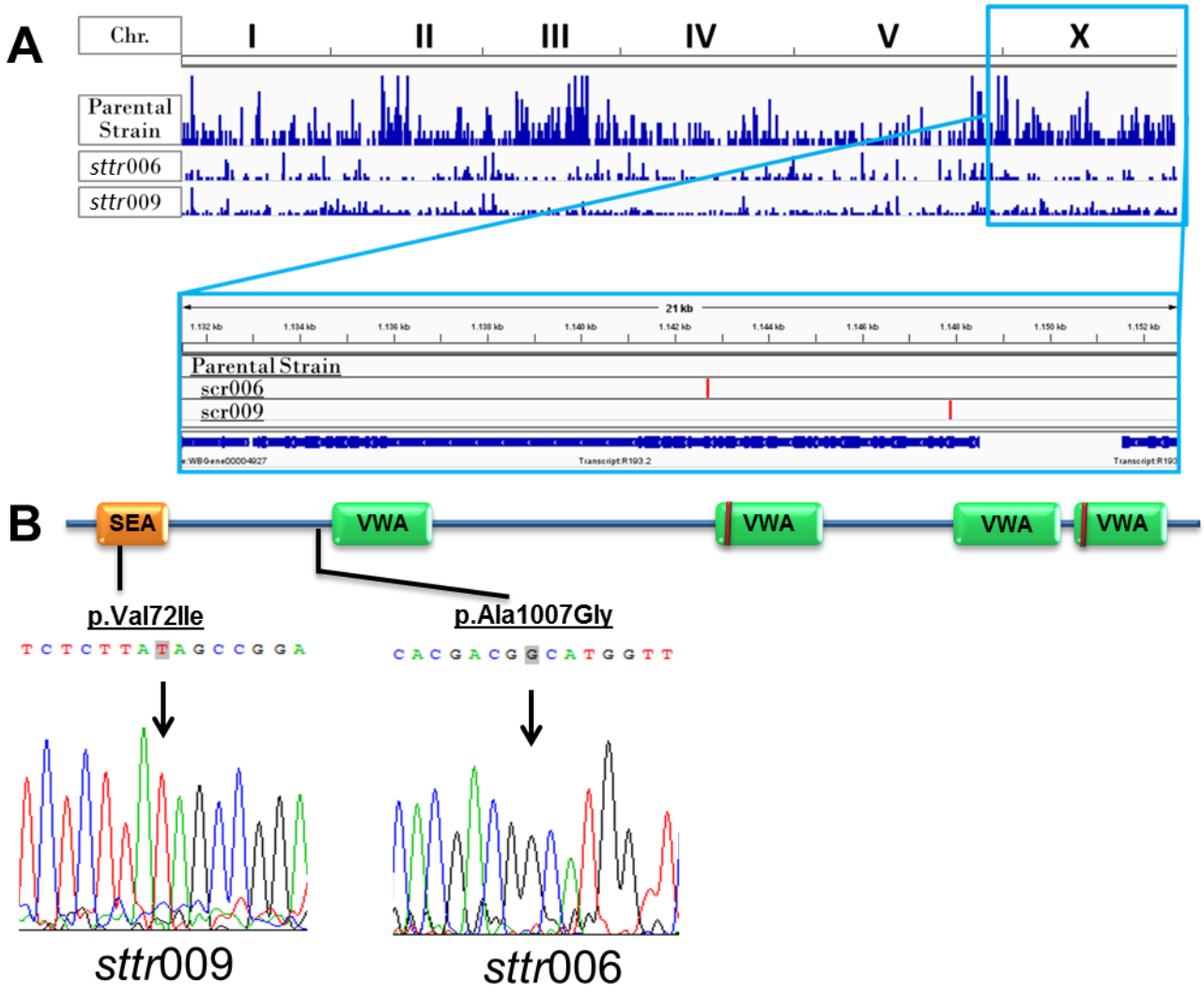

Fig. 2. R193.2 variants in *sttr*006 and *sttr*009 TTR suppressors. (A) Representative snapshot of Integrative Genomics Viewer (IGV, Broad Institute, Boston, MA) showing the aligned reads in parental strain, *sttr*006 and *sttr*009 samples exposed to EMS mutagenesis. Zoom view in *R193.2* gene showing unique variants for *sttr*006 and for *sttr*009 and the absence of variants in this gene for the parental strain (V30M TTR). (B) Schematic representation of the R193.2 protein structure showing the SEA and VWA domains. MIDAS motifs are indicated by red bar within VWA domain. The missense alterations found in *sttr*006 and *sttr*009 are indicated. Visualization of chromatogram from Sanger sequencing confirming the R193.2 variants. *sttr*006 chromatogram showing G>C variant (arrow) and *sttr*009 chromatogram showing C>T variant (arrow).

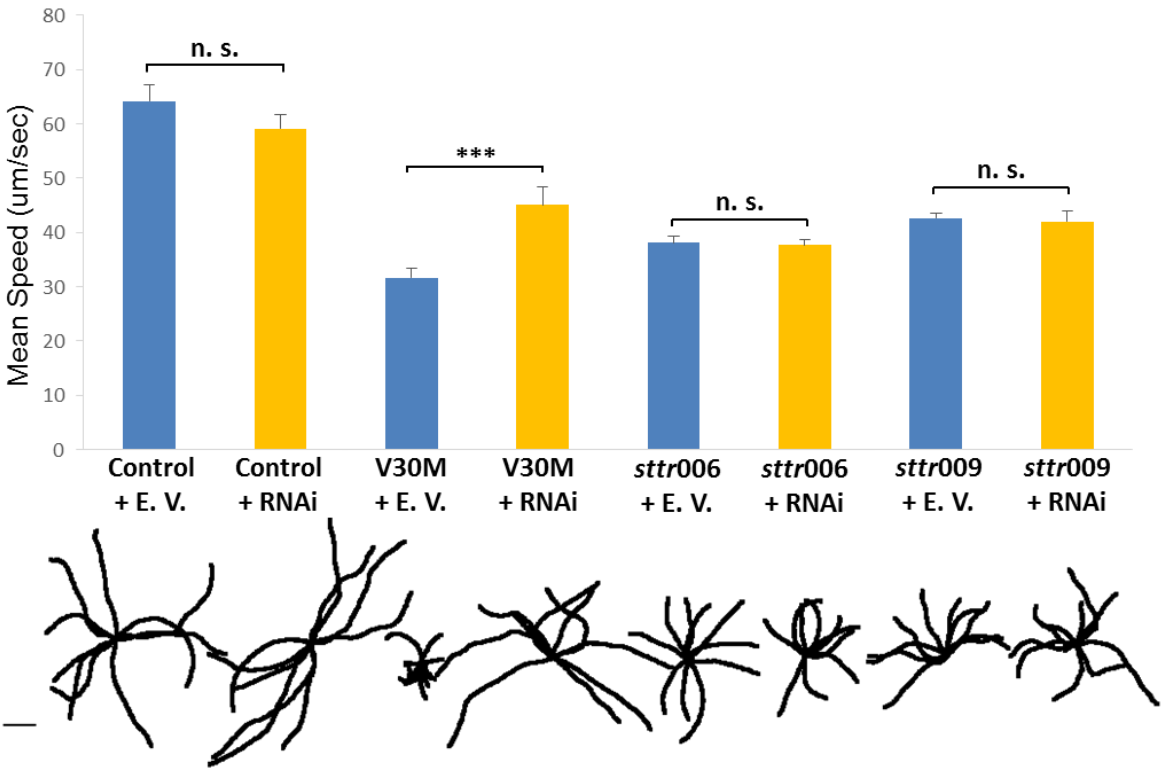

Fig. 3. R193.2 downregulation in the RNAi lines induced a statistically significant reduce of TTR toxicity in V30M TTR *C. elegans*, validating the specificity of our approach. (top) Locomotion rates for indicated strains fed with bacteria expressing an empty vector (E.V.) or dsRNA against R193.2. Control + E. V. (n=22), Control + RNAi (n=26), V30M+ E. V. (n=24), V30M + RNAi (n=24), *sttr*006+ E. V. (n=20), *sttr*006 + RNAi (n=20), *sttr*009+ E. V. (n=23), *sttr*009 + RNAi (n=21). Plots show means ± standard deviations; n.s. = not significant, ***p < 0.001. (bottom) Representative 40 seconds locomotion trajectories with starting point aligned in the middle (Scale Bar: 2000µm).

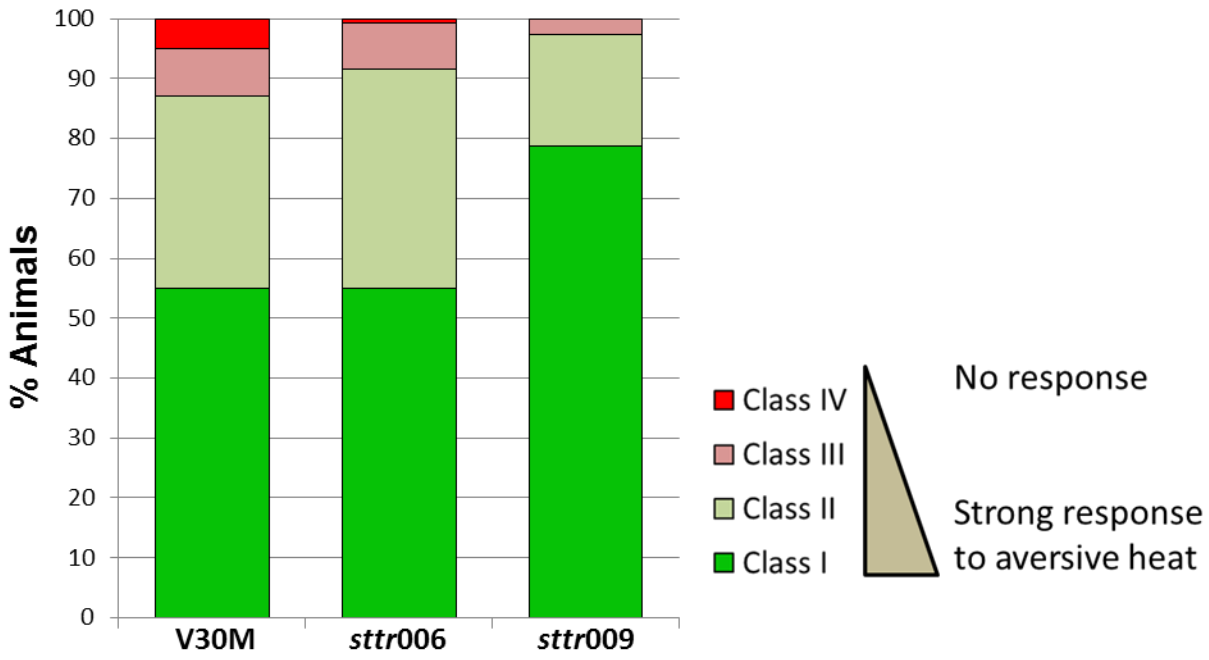

Fig. 4. Both TTR suppressors rescued the defective nociception phenotype. Thermal avoidance response of V30M TTR, *sttr*006 and *sttr*009 animals scored according to four behavioral classes. V30M TTR (n=190); *sttr*006 (n=176) and *sttr*009 (n= 179). Data represent three independent experiments.

REFERENCES

1. Monaco, H.L., M. Rizzi, and A. Coda, *Structure of a complex of two plasma proteins: transthyretin and retinol-binding protein.* Science, 1995. **268**(5213): p. 1039-41.
2. Wojtczak, A., et al., *Structures of human transthyretin complexed with thyroxine at 2.0 A resolution and 3',5'-dinitro-N-acetyl-L-thyronine at 2.2 A resolution.* Acta Crystallogr D Biol Crystallogr, 1996. **52**(Pt 4): p. 758-65.
3. Andrade, C., *A peculiar form of peripheral neuropathy; familiar atypical generalized amyloidosis with special involvement of the peripheral nerves.* Brain, 1952. **75**(3): p. 408-27.
4. Westermark, P., et al., *Fibril in senile systemic amyloidosis is derived from normal transthyretin.* Proc Natl Acad Sci U S A, 1990. **87**(7): p. 2843-5.
5. Johnson, S.M., et al., *The transthyretin amyloidoses: from delineating the molecular mechanism of aggregation linked to pathology to a regulatory-agency-approved drug.* J Mol Biol, 2012. **421**(2-3): p. 185-203.
6. Plante-Bordeneuve, V. and G. Said, *Familial amyloid polyneuropathy.* Lancet Neurol, 2011. **10**(12): p. 1086-97.
7. Richardson, S.J. and V. Cody, *Recent advances in transthyretin evolution, structure and biological functions*. 2009, Dordrecht ; New York: Springer. xiii, 360 p.
8. Buxbaum, J.N., *Animal models of human amyloidoses: are transgenic mice worth the time and trouble?* FEBS Lett, 2009. **583**(16): p. 2663-73.
9. Lai, C.H., et al., *Identification of novel human genes evolutionarily conserved in Caenorhabditis elegans by comparative proteomics.* Genome Res, 2000. **10**(5): p. 703-13.
10. Alexander, A.G., V. Marfil, and C. Li, *Use of Caenorhabditis elegans as a model to study Alzheimer's disease and other neurodegenerative diseases.* Front Genet, 2014. **5**: p. 279.
11. Dimitriadi, M. and A.C. Hart, *Neurodegenerative disorders: insights from the nematode Caenorhabditis elegans.* Neurobiol Dis, 2010. **40**(1): p. 4-11.
12. Madhivanan, K., et al., *Cellular clearance of circulating transthyretin decreases cell-nonautonomous proteotoxicity in Caenorhabditis elegans.* Proc Natl Acad Sci U S A, 2018. **115**(33): p. E7710-E7719.
13. Brenner, S., *The genetics of Caenorhabditis elegans.* Genetics, 1974. **77**(1): p. 71-94.
14. Anderson, P., *Mutagenesis.* Methods Cell Biol, 1995. **48**: p. 31-58.
15. Minevich, G., et al., *CloudMap: a cloud-based pipeline for analysis of mutant genome sequences.* Genetics, 2012. **192**(4): p. 1249-69.
16. Langmead, B. and S.L. Salzberg, *Fast gapped-read alignment with Bowtie 2.* Nat Methods, 2012. **9**(4): p. 357-9.
17. DePristo, M.A., et al., *A framework for variation discovery and genotyping using next-generation DNA sequencing data.* Nat Genet, 2011. **43**(5): p. 491-8.
18. Cingolani, P., et al., *A program for annotating and predicting the effects of single nucleotide polymorphisms, SnpEff: SNPs in the genome of Drosophila melanogaster strain w1118; iso-2; iso-3.* Fly (Austin), 2012. **6**(2): p. 80-92.
19. Quinlan, A.R. and I.M. Hall, *BEDTools: a flexible suite of utilities for comparing genomic features.* Bioinformatics, 2010. **26**(6): p. 841-2.
20. Kamath, R.S. and J. Ahringer, *Genome-wide RNAi screening in Caenorhabditis elegans.* Methods, 2003. **30**(4): p. 313-21.
21. Nussbaum-Krammer, C.I., et al., *Investigating the Spreading and Toxicity of Prion-like Proteins Using the Metazoan Model Organism C. elegans.* Jove-Journal of Visualized Experiments, 2015(95).

22. Wittenburg, N. and R. Baumeister, *Thermal avoidance in Caenorhabditis elegans: an approach to the study of nociception.* Proc Natl Acad Sci U S A, 1999. **96**(18): p. 10477-82.
23. Levin, M., et al., *Developmental milestones punctuate gene expression in the Caenorhabditis embryo.* Dev Cell, 2012. **22**(5): p. 1101-8.
24. Hashimshony, T., et al., *Spatiotemporal transcriptomics reveals the evolutionary history of the endoderm germ layer.* Nature, 2015. **519**(7542): p. 219-22.
25. Whittaker, C.A. and R.O. Hynes, *Distribution and evolution of von Willebrand/integrin A domains: widely dispersed domains with roles in cell adhesion and elsewhere.* Mol Biol Cell, 2002. **13**(10): p. 3369-87.
26. Bork, P. and L. Patthy, *The SEA module: a new extracellular domain associated with O-glycosylation.* Protein Sci, 1995. **4**(7): p. 1421-5.
27. Akhavan, A., et al., *SEA domain proteolysis determines the functional composition of dystroglycan.* FASEB J, 2008. **22**(2): p. 612-21.
28. Liu, S., E. Schulze, and R. Baumeister, *Temperature- and touch-sensitive neurons couple CNG and TRPV channel activities to control heat avoidance in Caenorhabditis elegans.* PLoS One, 2012. **7**(3): p. e32360.
29. Ashburner, M., et al., *Gene ontology: tool for the unification of biology. The Gene Ontology Consortium.* Nat Genet, 2000. **25**(1): p. 25-9.
30. *The Gene Ontology Resource: 20 years and still GOing strong.* Nucleic Acids Res, 2019. **47**(D1): p. D330-D338.
31. Hristova, M., et al., *The Caenorhabditis elegans heterochronic regulator LIN-14 is a novel transcription factor that controls the developmental timing of transcription from the insulin/insulin-like growth factor gene ins-33 by direct DNA binding.* Mol Cell Biol, 2005. **25**(24): p. 11059-72.
32. Olsen, P.H. and V. Ambros, *The lin-4 regulatory RNA controls developmental timing in Caenorhabditis elegans by blocking LIN-14 protein synthesis after the initiation of translation.* Dev Biol, 1999. **216**(2): p. 671-80.
33. Severance, S., et al., *Genome-wide analysis reveals novel genes essential for heme homeostasis in Caenorhabditis elegans.* PLoS Genet, 2010. **6**(7): p. e1001044.
34. Drabikowski, K., et al., *Comprehensive list of SUMO targets in Caenorhabditis elegans and its implication for evolutionary conservation of SUMO signaling.* Sci Rep, 2018. **8**(1): p. 1139.
35. Macao, B., et al., *Autoproteolysis coupled to protein folding in the SEA domain of the membrane-bound MUC1 mucin.* Nat Struct Mol Biol, 2006. **13**(1): p. 71-6.
36. Xi, J., et al., *Novel SEA and LG2 Agrin mutations causing congenital Myasthenic syndrome.* Orphanet J Rare Dis, 2017. **12**(1): p. 182.
37. Manes, G., et al., *Mutations in IMPG1 cause vitelliform macular dystrophies.* Am J Hum Genet, 2013. **93**(3): p. 571-8.
38. Bandah-Rozenfeld, D., et al., *Mutations in IMPG2, encoding interphotoreceptor matrix proteoglycan 2, cause autosomal-recessive retinitis pigmentosa.* Am J Hum Genet, 2010. **87**(2): p. 199-208.
39. Altamura, S., et al., *A novel TMPRSS6 mutation that prevents protease auto-activation causes IRIDA.* Biochem J, 2010. **431**(3): p. 363-71.
40. Tuckwell, D., *Evolution of von Willebrand factor A (VWA) domains.* Biochem Soc Trans, 1999. **27**(6): p. 835-40.
41. Bell, S.E., et al., *Differential gene expression during capillary morphogenesis in 3D collagen matrices: regulated expression of genes involved in basement membrane matrix assembly, cell cycle progression, cellular differentiation and G-protein signaling.* J Cell Sci, 2001. **114**(Pt 15): p. 2755-73.

42. Lacy, D.B., et al., *Crystal structure of the von Willebrand factor A domain of human capillary morphogenesis protein 2: an anthrax toxin receptor.* Proc Natl Acad Sci U S A, 2004. **101**(17): p. 6367-72.
43. Becker, A.K., et al., *A structure of a collagen VI VWA domain displays N and C termini at opposite sides of the protein.* Structure, 2014. **22**(2): p. 199-208.
44. Kawarai, T., et al., *A homozygous mutation of VWA3B causes cerebellar ataxia with intellectual disability.* J Neurol Neurosurg Psychiatry, 2016. **87**(6): p. 656-62.
45. van der Doef, H.P., et al., *Association of the CLCA1 p.S357N variant with meconium ileus in European patients with cystic fibrosis.* J Pediatr Gastroenterol Nutr, 2010. **50**(3): p. 347-9.
46. Gregorio, I., et al., *Collagen VI in healthy and diseased nervous system.* Dis Model Mech, 2018. **11**(6).
47. Jorgensen, E.M. and S.E. Mango, *The art and design of genetic screens: caenorhabditis elegans.* Nat Rev Genet, 2002. **3**(5): p. 356-69.

DISCUSSION

This thesis has crossed a long road, from families' analysis and DNA Sanger sequencing to advanced genomic technologies, resorting also to an animal model. Throughout this chapter, the most striking results will be discussed and intertwined, focusing specially in the *in silico* analysis and the in (new) pathways disclosed.

FAP belongs to a group of disorders where there is amyloid deposition, affecting the peripheral nerves in families, but they are caused by different disease-causing variants. However, even in TTR-FAP a phenotypic variability is also evident not only between different disease-associated variants but also for patients with the same disease-causing variant that display different clinical manifestations.

Variability ranges from more neurological to cardiac symptoms, a different response to different drugs, disease severity and progression, tissue specificity, age of death and AO. Our main focus was on the phenotypic variability of the TTR-FAP Val30Met individuals regarding AO.

Many hypotheses for this variability have been put forward, from environmental to genetic factors. Over time, our group has been focusing on the numerous genomic variants that are either nearby or physically separated from the disease-causing variant and that we found or confirmed to be associated with AO variability.

As our group confirmed that anticipation is a true biological phenomenon in Portuguese Val30Met TTR-FAP families[127], this supported the idea that other genetic factors in addition to Val30Met are involved in determining AO. Therefore, using a candidate-genes approach centered in families, we showed, the contribution of rare, common variants and expanded repetitive tracts in pathways related with TTR-FAP[135-137; 189]. Importantly, we demonstrated for the first time that mtDNA copy number was significantly higher in TTR-FAP Val30Met carriers than in those without it and may be associated with earlier events[141].

TTR gene sequencing - At the heart of the matter

As the various disease-causing variants are associated to a broad spectrum of symptoms, such as AO, we decided to perceive which other variants in the *TTR* gene are also present in TTR-FAP patients.

Val30Met accounts for more than 99% of the affected families in Portugal[22]. For more than thirty decades the genetic defect causing TTR-FAP is known, a valine to metionine substitution at position 30 (currently at position 50). Since then, as a monogenic autosomal dominant disorder, after identification of the TTR Val30Met variant in the index patient, diagnostic and pre-symptomatic tests were mostly Val30Met-capture (for example, by restriction fragment length

polymorphism (RFLP)), leaving aside other variants in the TTR gene. With this in mind, we sequenced all intron/exon boundaries region of the *TTR* gene (Article 1).

None of the patients studied had any other disease-causing variant, in addition to Val30Met. Although not causing disease, we identified two other missense variants: rs1800458 (p.Gly26Ser) and rs28933981 (p.Thr139Met).

rs1800458 is frequent and leads to a substitution of a glycine by a serine on position 26 (Ser6). Polyphen-2 classified this variant as benign to protein function, meaning that this variant could improve TTR transport function. The protective role of this variant has already been hypothesized before by others[13; 131], however, our results do not allow us to state that this coding variant is protective in our Val30Met patients, as it is not significantly associated with any late form of onset of symptoms. Probably rs1800458 is related with an improvement of TTR transport function, but without an effect on amyloidogenesis. This variant was also related with an increased TTR T4-binding affinity by Fitch *et al*.[13] and importantly, Jacobson, D. *et al.*[14] had suggested that rs1800458 is a neutral variant and its relative high frequency is related to its ancient origin, being widespread, not showing a selective advantage. Also, as the variant arose from a G-to-A transition at a CG dinucleotide hotspot, it may have arisen on multiple occasions[14].

rs28933981 leads to a substitution from a threonine to a methionine in position 139 (Thr119Met). Alves I. *et al.*[190] showed that compound heterozygous carriers of Val30Met/Thr119Met contain tetramers more stable than with only Val30Met. In article 1, the two Thr119Met carriers have a late AO (61 and 63 years), higher than the mean AO of their affected relatives since they belong to a family with an early-onset, so they supported the theory that the stability of the TTR molecule may be an important factor to prevent amyloidogenesis and the TTR Thr119Met may have a protective effect on pathogenic effect Val30Met[191-193].

More recently, Batista *et al.*[194] assessed the effectiveness of liver-directed vectors mediated gene delivery of Thr119Met TTR to reverse and prevent pathology in a TTR Val30Met transgenic mouse model. They concluded that inclusion of Thr119Met subunits into tetramers can exert a stabilization effect in TTR heterotetramers preventing dissociation and aggregates formation. Moreover, it was based on the characterization of this variant that one of the therapeutic lines, already approved, has been focused on the stabilization of the TTR tetramer [16; 195], even designed to mimic TTR Thr119Met[160].

Another variant found to be associated with AO is rs72922947, one of the markers used in our haplotypic analysis (Article 2), buried deep within intron 2 near the Val30Met site which is represented by the minor allele A, differentiating haplotype C from the other haplotypes that harbour the common allele G (Article 2). This variant conferred some degree of risk to early-onset

patients that once transmitted by the non-carrier parent may explain partially the early-onset observed in the offspring (Article 2, Fig. 2). Functionally, how a variant away from the extended consensus sequence of exon-intron splice junctions still acts as a phenotype modulator, remains to be answered. Several studies have come across this issue and some mechanisms have been disclosed. The growth hormone 1 (*GH1*) variant located outwith intron 4, has been associated with a reduced risk of colorectal cancer and a predisposition to osteoporosis[196; 197]. This clinical association was attributable to alleles of an additional variant in *cis* and located within either the promoter or the 3'-flanking region, which seems to be exerting a direct effect on reduced levels of circulating human growth hormone[198] Also, Do *et al*.[199] identified a risk association between childhood acute lymphoblastic leukemia and an *IRF4* intron 4+386bp variant and demonstrated a repressive effect of the variant on IRF4 promoter activity. Although these mechanisms remain unveiled for our *TTR* intronic variant, we have obtained results that provided evidence of a consequence on TFBS (which we will discuss below).

What is hidden inside the promoter region of *TTR*?

Afterwards, given the importance of DNA sequence variants within the promoter region as may change *TTR* gene expression and consequently lead to phenotypic variability, we sequenced a 2.1kb upstream region of *TTR*. In article 1, we reported fifteen variants found in the promoter region (Table 1). Using a parametric test (GEE), which is a quite powerful statistical method, we found interesting results regarding the association of some of these variants with AO, which showed that rare variants in fact seem to modulate AO variability (Article 1, Table 2). We found significant results for some rare variants that despite the heterozygous genotype appeared only once, this is in accordance with the genotypic frequencies described for European (Non-Finnish) in GnomAD. We consider that these rare variant results are equally important and should be reported, because their identification may have implications for genetic screening and personalized treatment. Interestingly, patients simultaneously carrying the minor alleles of rs3764479 and rs3764478 have a 2.22-fold susceptibility to start the symptoms before 40 years. During the last years, combinations of variants strongly associated with a multifactorial phenotype as AO have been studied, as each variant has a small effect[200]. Therefore, it is very promising that the combination of these two variants (which appear mostly together) showed a high risk for an early-AO. This approach deserves our future attention, as clusters of patient-specific variant combinations have already been found[201].

In mouse, a proximal promoter and a distal enhancer were identified in the 5'-flanking region of the *ttr* gene[202]. In humans, unlike the enhancers that have been incompletely characterized[203; 204] and, so far it is unclear and may be quite subtle; the promoter has been

reasonably explored. Over time, several studies reported that the proximal promoter region of ~2kb from the transcription start site appears to contain all the sequences required for hepatocyte-specific expression of the gene [9; 131; 202; 205-207]. For instance, Costa *et al.*[202], and Sakaki *et al.*[204] identified and confirmed several transcription factor binding sites crucial for hepatocyte-specific expression in this region, including HNF. More recently, variants located in this region have been reported to be associated with the WT and disease-causing forms of TTR[32; 131; 134].

From alleles to haplotypes - Broadening the field of view

Still focusing on *TTR* gene, in article 2, we performed a haplotype analysis covering a total of 57kb of the common variation present in the *TTR locus*, which revealed the existence of a possible modulatory *trans* effect.

Trans-modifiers may occur in any part of the genome. Soares *et al.* also reported an onset modifier downstream *TTR* locus present in the non-carrier chromosome[134], but it failed to reach statistical significance. On the contrary: (1) we found the same effect but within the TTR (FAP) *locus*; (2) we used a larger sample size; and (3) we took into account the variation within the same family, and, particularly, within and between generations.

Thus, we confirmed a possible modulatory *trans*-effect on AO, exerted by haplotype C that we found to be more frequent in early than in late-onset cases. All carriers of this haplotype received it from the non-carrier parent, i.e., together with wild-type transthyretin. The TTR tetramer is formed by four monomers, which in heterozygous patients are made up of a near-statistical distribution of Val30Met and WT subunits[208], which means both chromosomes contribute equally to the formation of heterotetramers. Important to realize is that WT TTR can also misfold into the amyloid configuration causing senile systemic amyloidosis, often associated with aging. Non-disease causing variants in WT chromosome might origin differences in the level or pattern of expression of the “normal” *TTR gene.* All things considered, it is conceivable that there is a *trans*-effect on the rate of disease pathogenesis leading to the onset of symptoms, possibly through a tetramer less stable which is more easily dissociated and transformed into amyloid.

Although some variants were not associated with AO, possibly due to its rarity, which limits the statistical power, we consider that these results are equally important and should be reported. With the fast progresses of NGS technology an increasing number of variants (potentially functional or not) are being identified. We have been witnessing the change in the paradigm of variant interpretation; a variant that nowadays is considered as a variant of uncertain/unknown significance (VUS) and, with the emergence of new studies, gains new biological features. Thus, from our point of view, reporting all the variants identified in this study is not only a scientific

contribution from an epidemiological perspective (frequency of the variant in a particular population), but also enhances the data about a variant disease-specific. In a context of VUS, to determine the implication of a certain variant provides rationale for clinicians and researchers how to interpret the genetic results that have not been fully clarified.

One of the methods adopted also in this work to explore the impact of the FAP-associated variants on the transthyretin biology was the *in silico* analysis.

TTR (post-) transcriptional regulation – *In silico* Analysis

Transcription factors binding sites (TFBS)

Briefly, *in silico* models are based on the rich databases that collect known biological data and apply a coherent framework and machine learning algorithms[209]. Together with a powerful statistical analysis, *in-silico* tools assist us in the process of understanding variant regulatory mechanisms and allow us to formulate experimentally testable hypotheses.

The analysis of non-coding regions of *TTR* gene suggests the presence of 3 non-coding variants, possibly *cis*-regulatory elements of the *TTR* gene that modulate the effect of mutations on the disease phenotype.

In article 1 and 2, unreported and very interesting results in the *in silico* analysis were found as we observed some alterations in the mechanism of splicing, TF and miRNAs binding.

TFBS analysis allowed us to estimate the probability of modulation by a variant on the expression of TTR that could drive the clinical presentation of the disease. The *TTR* gene is regulated at the transcriptional level by promoter in liver cells[210]. Non-coding variants located in the promotor region can create new TFBS, or abolish pre-existing ones, that may influence TTR expression.

In article 1, we identified two variants in promoter region that together reduce significantly AO of symptoms. Using the largest open-access database of TF-binding profiles (JASPAR) and Genotype-Tissue Expression (GTEx) project, we predicted that these variants not only may disrupt potential binding sites once occupied by transcription factors such as may create new ones (Table S1). Human transcription factors were predicted with a relative profile score threshold >80% and filtered by expression in liver. Important to highlight the hepatocyte nuclear factor 4 gamma (*HNF4G*) and HSF1, whose conservation and characterization has already been studied previously[207; 211; 212]. Hepatocyte nuclear factors (HNF-1, -3, and -4) had been described and characterized 20 years ago by Costa *et al.*[211] as liver-specific regulators and as elements in the regulation of hepatic *TTR* transcription. Additionally, *in silico* and *in vivo* analysis of

the *TTR* promoter, confirmed that human and murine *TTR* promoter regions contain the previously identified potential binding site for HNF's[212] and identified *TTR* as subject to regulation by HSF1[207]. Furthermore, a study using a mouse model expressing the human TTR Val30Met in a silenced Hsf1 background showed an earlier and increased frequency of human TTR deposits in distinct organs including the peripheral nervous system[173]. The association of several *TTR* promoter risk variants as modulators of transthyretin-related diseases potentially due to altered binding of hepatocyte transcription factors at these regulatory sites, was also speculated by Sikora *et al.*[131].

Despite the most common model for transcriptional activation suggested that TF just binds upstream of the transcription start site (promoters), it has been established that some introns contain enhancers, alternative transcription start sites, or TFBS[213]. Several hypotheses have been raised for TFs to bind introns: (1) a downstream promoter elements (that are actually downstream to transcription start site); (2) to regulate elongation or splicing and; (3) are involved in part of the transcriptional regulation of another nearby gene (e.g., acting as a distal enhancer).

Subsequently, we tried to explore the putative functional impact of rs72922947, the intronic variant associated with a decrease on mean AO of ~9 years (Article 2; Fig. 3). Three transcription factors binding sites (LM56, LM58 and LM233) were predicted to be disrupted by rs72922947. The minor allele (A) was predicted to have less affinity for all the transcription factors. However, there is scarce data about the role of these TFBS. Additionally, we verified that rs72922938, a SNP that is in linkage disequilibrium with rs72922947, may alter TP53 binding site. TP53 has been reported as a genetic modifier of AO in several types of cancer, as well as in Huntington's disease (HD), a trinucleotide repeat neurological disorder where only 50-70% of the variance in AO can be explained by the repeat size alone[214]. Polimanti *et al*.[215] identified 59 non-coding variants that may have a functional impact on the *TTR* gene, including rs72922947, however, the authors proposed that further studies are required to understand the role of this variant.

These results will enable us to obtain new hypotheses to test in further experimental investigations. Whether these variants are in fact the functional variants responsible for exerting a direct effect on *TTR* gene expression, or are instead in linkage disequilibrium with the functional SNP, is still an open question that deserves future attention. In consistency with these observations we can assume that the transcriptional mechanisms conferred by these variants are involved in FAP variability, modulating TTR course.

<u>miRNAs</u>

One paramount analysis that is important to take into account and that is being intensively studied in another neurodegenerative diseases, such as AD[216], PD[217]; Hereditary spastic

paraplegia type 31[218] and Fragile X syndrome[219], is the possible location of 3'UTR variants in miRNA target sites that could modify *TTR* expression, ultimately affecting FAP phenotype.

The presence of miRNA target sites in 3'UTR of *TTR* gene had already been studied as was cited before[32; 220]. Although they have used some miRNA target prediction software different from the ones we used, we concluded that the usage of these programs should be done with a critical view, because they can reveal different results according to the algorithms and the thresholds used. To minimize false positive predictions we set up criteria as described in the methods section of article 1, that the predicted miRNA targets should fulfil: (1) the miRNA should be present in all the prediction software, (2) be expressed in liver and (3) evolutionary conserved between species.

In Table 6, we can find miRNA target predictions for WT 3'UTR, for the polymorphic allele of rs62093482 and for the polymorphic allele of rs1053907197. Our intensive *in silico* analysis indicated that 3'UTR of *TTR* gene has miRNA binding sites for mir-200a and mir-141, in agreement with other bioinformatics analysis and confirmed with *in vitro* assays[221]. These miRNA inhibited TTR expression by directly binding to the 3′UTR of *TTR*, which is reversed by variants in the miRNA binding site[221]. Although rs62093482 and rs1053907197 variants do not affect the WT 3'UTR miRNA binding sites, these variants create new binding sites. As the miRNAs mir-1279, mir-1250 and mir-1267 are not expressed in liver and are poorly conserved between species we excluded the implication of these miRNA putative target sites in AO variation. The hsa-mir-622 is expressed in liver and, well conserved between species. Olsson *et al.*[32] proposed that the 3'UTR variant rs62093482, also present in Swedish TTR Val30Met carriers, could serve as a miRNA binding site to hsa-mir-622, possibly leading to a down regulation of mutant TTR expression, explaining the low penetrance and an increase in AO observed in the Swedish patient population. However, posterior analysis *in vitro* by Norgen *et al* to evaluate this hypothesis showed that the rs62093482 of the *TTR* gene has no effect on degrading the variant allele's expression and thus has no impact on the diminished penetrance of the Swedish patients[220]. The authors noted that the ratio of allelic variant to WT TTR in plasma was approximately the same in Swedish and Portuguese FAP patients (40% to 60%), so they concluded the hsa-mir-622 does not interfere with protein translation, is non-functional and is not involved in FAP AO variability[220]. Importantly, mir-138 binding site is conserved in several species (including non-mammals) and is expressed in the liver reinforcing the hypothesis that mir-138 should be studied *in vivo* in order to confirm these results and the hypothesis that this miRNA might play a role in TTR mechanisms capable of modulate the onset of TTR-FAP symptoms[222]. Recently, several studies have reported that differential expression of miRNAs, including mir-138, are implicated in neurodegenerative

disorders, like AD[223; 224], HD[225], schizophrenia [226; 227] and bipolar disease[227] . It was demonstrated that mir-138 is upregulated in the brains of Alzheimer's patients[224]. The involvement of miRNAs in neurodegenerative disorders point to a possible therapeutic value of these molecules. This year, two novel therapeutic drugs were approved for the treatment of FAP: Patisiran, the first siRNA-based drug approved by the US Food and Drug Administration[228] and Inotersen, an ASO[229]. As both drugs prevent production of the TTR protein by targeting its 3' UTR, is reasonable to assume that variants in this region may affect the efficiency of these drugs.

The role of Splicing

We also assessed how likely a splicing change would occur as a result of the presence of DNA variants. It is important to emphasize that some of the differences between WT and variant sequences could alter splicing either by re-directing the spliceosome or by altering the binding of auxiliary factors, such as SR proteins, exonic and intronic splicing enhancers and silencers[230].

Our results were described in Table 3, Article 1 and is important to note a possible inactivation and creation of ESEs in two missense variants. Because they are both in the coding region, we have to consider that ESEs inactivation may lead to protein-disrupting effect, but there is no evidence that ESEs creation in coding regions lead to splicing alterations. If all these variants somehow interfere with splicing machinery, consequently may result in several transcripts and thus different transthyretin proteins can be synthesized from the same *TTR* gene[231].

The role of tandem dinucleotide repeats in splicing

Dinucleotide repeats constitute another group of variants that influence splicing[232]. TTR promoter bears a tandem CA-dinucleotide repeat typically consisting of 9-10 repeats. Despite the low polymorphic propensity we found a patient with a deletion of 3 CA-repeats (CA_7). Because of their abundance, CA-dinucleotides have been related as a modifier of some genetic disorders. For example, the risk of coronary artery disease is linked to variation in the number of CA-dinucleotides in *eNOS gene;* as a result of the differences in the binding affinity of proteins involved in mRNA processing that seems to modulate the splicing efficiency and mRNA stability[233; 234]. Another key point is the efficacy of therapies that was also associated with CA-repeat length. Namely, in carcinomas, a decreased CA-repeat length improved tumor response to anti-EGFR drug therapy possibly by affecting the promoter/enhancer region and decreasing transcription efficiency[235]. In addition, other CA-dinucleotides repeat located at gene promoter regions affect both mRNA stability and gene expression, as in the following genes: IGF1[236]; cPLA2[237]; HMGA2[238] and Cyr6l[239].

We found a possible evidence of an association of AO with the different genotypes of a CA-dinucleotide repeat in TTR promoter. Based on this, we can formulate the hypothesis that the

nature of this tandem repeat in *TTR* promoter may contribute to phenotype diversity by the following mechanisms: shifting the distance between nearby *cis* sequences; affecting interactions between splicing signals and the spliceosome; perchance form secondary structures resulting in the sequestration of splicing signals; and altering the binding affinity of protein factors that alter RNA transcript processing.

To the best of our knowledge, no other studies about genetic alterations in splicing activity on *TTR* gene were made until now, except a recent association study of variants in the *TTR* gene with AD Han Chinese patients [240]. However, they only tested two variants on the *TTR* gene that can alter splicing activity. Maybe due to distinct genetic architectures between the populations, we did not find these variants in our Portuguese sample.

It is important to note that similarly with the remarkable differences found in different populations[240] there are also ethnic differences regarding allele size distribution of CA-dinucleotide repeat in *TTR* promoter found in article 1. All Swedish patients contained at least one CA_{10} allele and only two were CA_{10}/CA_{10} homozygous, contrary to our sample, where more than half were CA_{10}/CA_{10}. In our Portuguese sample, as in the French sample, homozygosity of the CA_9 allele was present. On the other hand, neither in the Swedish nor in the Japanese samples CA_9/CA_9 homozygous were found[32; 134].

Splicing and Amyloid Fibrils

One promising scenario that these splicing-related variants may be causing is the creation of the two types of amyloid fibrils: type A (a mixture of full-length and TTR fragments) and type B (only full-length TTR) fibrils[70]. However, the mechanism that results in to the formation of these two types of fibrils is still unclear. Although a mechano-enzymatic cleavage mechanism has been proposed as a mediator of transthyretin amyloid fibrillogenesis, this mechanism raises some questions to the extent that a TTR fragmented was found in material of the corpus vitreous and in the spinal cord of TTR-FAP Val30Met patients, where a mechano-enzymatic cleavage of TTR is unlikely to occur[241-243].

The correlation between fibril types and AO was also established: in general, early-onset patients showed type B fibrils while late-onset showed type A fibrils[68; 241; 244]. But, it is not always straightforward; the same amyloid fibril composition type has been found within the same family, where the AO difference reaches up to 25 years[243]. Indicating that the type of fibrils are more associated with the genetic/familial background than the AO. At the same time, two late-onset brothers displayed different fibril types among them, which lead the authors to suggest that the genes regulating TTR cleavage is situated at another location than the *TTR* gene on the

genome[243]. Hence, either genetic or epigenetic factors seem to exert an impact on amyloid fibril composition.

Genetic modifiers and Epigenetics

Another essential point is that some genetic variants may influence epigenetic signatures[245]. DNA methylation, an epigenetic mark that occurs most often on cytosines found in a CpG context, playing an important role in splicing regulation and aids the spliceosome in the process of exon definition[246]. Some studies revealed that genetic variants at CpG sites are likely to disrupt the substrate of methylation reactions by prevent the binding of CpG methyl-binding proteins[247; 248]. Indeed, if the variant is located in a region in the vicinity of CpG *loci* may affect the transcriptional silencing via differential DNA methylation and leads to a different set of spliceosomes[249; 250].

Considering these evidences, it can be concluded that the intronic variants found in this study may create or disrupt methylated CpG sites which as a consequence affects DNA methylation. Furthermore, a TFBS that overlap with differentially methylated CpG sites, associated with disruption of TF binding, may produce a functional effect that can modulate the expressiveness of the disease. Thus, coupling with our *in silico* results, this is a good hint for integrative epigenomic data analysis to be explored.

MYH11 - Thinking outside the (TTR) box

In a hereditary disorder, phenotypic manifestations are not, as has been detailed throughout this thesis, the sole result of the inherited genomic region that causes disease. On the contrary, they are rather complex, multifactorial, and the result of diverse cellular modulators, which may be located anywhere in the genome.

Here, we applied for the first time a whole-genome sequencing technology in TTR-FAP families that allowed us to study additional fixed genetic variations, spread through the human genome in addition to the inherited Val30Met TTR. We have chosen WGS over WES because we did not know whether the modifier variant would reside in known coding elements and if it is a structural variant (which is not detected in WES). Furthermore, WGS can provide uniform coverage with a higher sensitivity and lower false-positive rate of variant detection than WES[251].

Factors modifying clinical expression of inherited diseases are particularly complex and could be due to, among many other reasons, interaction of the disease-causing variant with environmental factors. One way to reduce, though not eliminate, the environmental component, is to perform the analysis within families. Moreover, as TTR-FAP is an autosomal dominant disease, intra-generational analysis sifts the alleles identical by descent in the underlying Val30Met, thus, simplifying the interpretation of the modifying variants.

Genetic anticipation is common in numerous neurodegenerative disorders (including HD and spinocerebellar ataxia) and is due to the increase in the number of repeat expansions that occurs during meiosis and gametogenesis, observed in successive generations of these families. Conversely, in diseases caused by point variants it becomes much more complicated to clarify and no general biological explanation has been found so far.

In article 3, two TTR-FAP Val30Met families with large anticipation (a ≈ difference of 40 years in AO between the grandmother and the grandchild) were whole-genome sequenced (Fig.1). After a very stringent criteria filtering, we identified *MYH11* as a modifier candidate gene in these two families with large anticipation. We cannot reject that other variants identified in these families (Table 1) may be causally connected to anticipation, but they not fulfill our filter criteria and it is challenging to predict their significance on TTR-FAP if they are not functionally tested.

MYH11 codes for the smooth muscle myosin heavy chain (SMMHC) which forms part of a myosin protein complex found in smooth muscles and, along with actin, lead to muscle contraction[252]. This group is also involved in cell movement and the transport of materials within and between cells. Structurally, myosin is organized into two pairs of light chains and two heavy chains that are encoded from the *MYH11* gene. Each heavy chain comprises a head region that binds actin, has ATPase activity and the tail domain interacts with other proteins being also responsible for cargo binding and/or dimerization of heavy chains[253]. Owing to the numerous organs containing smooth muscle cells and the wide range of myosin participation, DNA changes in *MYH11* gene can affect several pathways and are responsible for disorders as different as: colorectal cancer[254]; acute myeloid leukemia (a form of blood cancer)[255]; megacystis-microcolon-intestinal hypoperistalsis syndrome *(*severe disorder affecting the muscles that line the bladder and intestines)[256]; moyamoya-like cerebrovascular disease (a cerebral arteriopathy)[257]and familial thoracic aortic aneurysm and Aortic Dissections (one of the most severe cardiovascular conditions in adults)[258]. Mice with a homozygous deletion of *Myh11* showed several abnormalities, including abnormal intestinal movement, a FAP-relevant symptom[259].

Variant Identification

We found an arginine to glutamine substitution at position 1542 which affects the C-terminal coiled-coil region which is known to be critical for regulation of MYH11 protein, as the assembly of myosin thick filaments. Furthermore, we demonstrated that MYH11 variant is highly conserved across multiple species, validating that this variant may reside in biologically functional element (Article 3, Fig 2). Most of the thoracic aortic aneurysm causing variants are also located in the coiled-coil domain of the protein and are thought to act via a dominant-negative mechanism[260].

Based on the results of our PPI analysis, it can be argued that one of the possibilities of MYH11 modulating TTR-FAP disease expressivity is through the pathway involving ROCK2 and APP (Article 3, Fig.2). These genes are enriched in ECM organization; microtubule-based process and positive amyloid fiber formation, consistent with previous reports[261-266].

Amyloid precursor protein (APP) and its derivative, amyloid-β (Aβ) peptide, is a well-known TTR interaction partner. Genetic and biochemical studies have suggested that transthyretin is a neuroprotective protein in AD by modulating Aβ levels, a major therapeutic goal in AD. In *C. elegans* and rodent models, transthyretin can rescue behavior and pathology associated with expression of Aβ[183; 267-271]. TTR is one of the major Aβ-binding proteins and act as a neuroprotector in AD, through the sequestration of Aβ and preventing its aggregation and fibril formation[53]. Liz *et al*.[272; 273], demonstrated *in vitro* and in physiological conditions, that TTR cleave Aβ and led to inhibition and disruption of Aβ fibril formation. Likewise, altering Rho-Rock pathway through different mechanisms can alter Aβ levels[274]. Specifically, ROCK2 affects Aβ production by regulating the intracellular trafficking of APP as well as the secretion of Aβ[275]. Additionally, pharmacologic inhibition of ROCK2 diminished production of Aβ in AD mouse brain[265]. Furthermore, RhoA/ROCK pathway plays a crucial role in various biological processes, including in smooth muscle cells differentiation[276] and by an ambiguous mechanism, Aβ induced a reduction in smooth muscle[277]. ROCK2, such as MYH11, are mainly expressed in smooth muscle cells and both played an important role in vascular smooth muscle contraction, a pathway that is remodeled in response to Aβ[277; 278]. In sum up, the overlap of these genes is noteworthy and might implicate interaction with cellular functions, possibly relevant for amyloid aggregation process. Thus, on the basis of this biological evidence, we hypothesized that variants in the coiled-coil domain of MYH11 could alter its PPI properties and inevitably disturb the communication between ROCK2/APP/TTR, probably necessary for regulating the amyloid cascade formation.

So far, it is still too premature and difficult to know whether or how MYH11 gene and this pathway are in fact responsible for large anticipation. Moreover, it is highly likely that we still do not know all pathways involved in TTR pathogenesis. Thereby, extensive further functional studies are required and studies in an animal model are an added value to verify these biological activities.

C. elegans models of TTR-FAP

Several research groups tried to use the mice and *Drosophila melanogaster* as a model to study some of the transthyretin amyloidosis' mechanisms but have failed to recapitulate some of the human TTR amyloidoses phenotypes, except amyloid deposition[62]. FAP mice expressing both the WT and TTR variants showed TTR deposition in some tissues, but they never displayed a

neuropathy degenerative phenotype. *Drosophila* models of TTR amyloidoses were previously generated, expressing human WT TTR[178; 179], Leu55Pro[178] and V30M[179] variants directly in the eye, nervous system or fat body. However, these fly models showed TTR deposition and degenerative phenotypes in tissues in which the TTR was synthesized and secreted (cell-autonomous). Both animal models did not fully recapitulate human disease phenotype in which TTR is secreted from its originating tissue and aggregates onto distal tissues (cell-nonautonomous) such as the peripheral nerves resulting in polyneuropathy symptoms. Previous proteinopathy models expressing human disease-linked aggregation prone proteins have demonstrated proteotoxicity in cell-autonomous tissue-specific diseases, as AD, PD, ALS, HD, and prion diseases also appears to have cell non-autonomous components[279]. However, the cell-nonautonomous pathways of neurodegeneration remain incompletely understood, in part due to the lack of models that faithfully recapitulate in *trans* toxicity.

In article 4, we have generated and characterized *C. elegans* models of FAP that exhibit critical features of human FAP disease. With its powerful genetics and genomics, short lifespan, and transparency for direct *in vivo* imaging, the nematode *C. elegans* is an ideal model organism to explore diverse genetic and molecular pathways within the whole-organismal context. Furthermore, the conservation of disease pathways between the 959-cell *C. elegans* and higher organisms make it a simple and cost-effective system for screening compounds for drug discovery[280]. Another key point, *C. elegans* was the first multicellular organism to have its whole genome sequenced, thus proving to be a powerful animal model for genetic studies providing large-scale screenings and a better comprehension of the gene-gene interaction in many of the major neurodegenerative diseases[281; 282].

We generated *C. elegans* models of FAP overexpressing human WT TTR, V30M and the highly destabilized D18G TTR variant, which is not efficiently secreted, in the smooth body wall muscles under control of the *unc-54* promoter. We also produced a transgenic strain bearing T119M sequence which results in the formation of highly kinetically stable, non-amyloidogenic heterotetramers. (Article 4, Fig. 1A). This protective variant, as described above, allowed us to dissect the assumption that the proteotoxic phenotypes observed in the pathogenic strains were not simply the result of the overexpression of a human TTR sequence. In contrast to many other studies, we did not tag TTR with GFP or other large fluorescent proteins because TTR is a small protein and its fusion could significantly impact its folding, assembly, and/or trafficking in the early secretory pathway.

Our *C. elegans* models secreted natively folded TTR tetramers from the muscle, except for D18G TTR animals because D18G TTR was not secreted from the body wall muscle cells

(Article 4, Fig. 2). Furthermore, we detected the presence of non-native TTR oligomers in the animals expressing the disease-causing variants V30M TTR and D18G TTR, proposing that they undergo tetramer destabilization and follow the amyloidogenic cascade. These data also suggested that the highly stable T119M TTR tetramers do not dissociate and misfold into non-native TTR structures as promptly as the destabilized V30M TTR and D18G TTR disease variants.

Next, using a thermal-avoidance assay for nociception which measures the withdrawal reflex of a *C. elegans* exposed to noxious temperature stimulus, we observed a significant higher percentage of V30M TTR animals were unresponsive to noxious heat (Article 4, Fig. 4). On the other hand, T119, D18G and V30M-without signal sequence (V30M ΔSS TTR; to prevent its secretion) did not exhibit a defective thermal-avoidance responsive. Important to realize, V30M TTR animals treated with TTR RNAi, which afforded a protein knockdown of >90% (Article 4, Fig. S4) also did not exhibit a defective thermal-avoidance responsive. Altogether, these results suggested that this thermal avoidance defect is mediated by disease associated V30M TTR by a cell non-autonomous mechanism.

The defect in noxious heat sensing has been previously shown to be dependent on the function of AFD and FLP head sensory neurons, as ablation of both neurons almost completely ablated the thermal avoidance response[283; 284]. When we analyzed the dendritic morphology of FLP neurons, we beheld that the destabilizing variant V30M TTR expressing worms displayed defects in FLP dendritic branching and dendritic morphology as opposed to the control and the stabilizing variant T119M TTR worms of the same age (Article 4, Fig. 5). Despite previous *in vitro* studies showed that TTR can be endocytosed into sensory neurons[85; 285], using a transgenic line expressing V30M TTR directly in the FLP neurons (without the signal sequence and with a specific promoter) we did not observe any significant nociception impairment, demonstrating that expression of V30M TTR inside FLP neurons is not sufficient to impair nociception. Thus, unknown extracellular pathways could mediate the effects of TTR toxicity. Taken together, these data showed that V30M TTR proteotoxicity impairs neuronal function in a cell-nonautonomous manner by targeting pathways that regulate the proper structure and function of pain-sensing and mechanosensory neurons. It is also important to point out that the *C. elegans* dendritic arborization phenotypes observed herein could be a model to study TTR age-dependent neurodegeneration mechanisms.

C. elegans has a six coelomocyte cells (a macrophage-like cells) which are highly active in endocytosis and protein degradation of soluble material from the body cavity[286]. We found that WT TTR and V30M TTR tetramers are secreted from the muscle and taken up by coelomocytes. (Article 4, Fig. 2) Additionally, genetic ablation of coelomocyte cells increase V30M TTR tetramer

levels in the body cavity and greatly exacerbates V30M TTR proteotoxicity which also correlated with an increase in levels of non-native V30M TTR as opposed to the V30M TTR worms with coelomocytes, suggesting that the efficiency of V30M TTR degradation influences its toxicity. (Article 4, Fig. 6). As coelomocyte degradation is autophagosomal[287], these results demonstrate the importance of protein degradation in modulating proteotoxicity, and highlight the role of degenerative animal model to examine putative therapeutic strategies to enhance degradation to ameliorate disease. The liver, muscle, and skin have been shown to be the major sites of TTR degradation in rats, with no detectable degradation occurring in nervous tissue[288]. Thus, the activation of autophagy or analogous lysosomal degradation mechanisms in tissues where aggregation occurs (e.g. nervous tissue) should be considered as a strategy for treating TTR amyloidoses and other amyloid diseases.

The trajectory of the V30M TTR worms in comparison to control worms suggested an Unc phenotype (Article 4, Fig. 7). This resulted in a significant decrease in displacement and velocities covered by the V30M TTR worms in comparison to the non-TTR control worms. Then, we significantly rescued the abnormal motility in V30M TTR worms treated with a TTR tetramer kinetic stabilizer CMPD5 (similar to tafamidis) and reduced TTR protein levels with TTR RNAi. CMPD5 was selected instead of tafamidis since it has better solubility in the worm liquid culture media. In addition, we verified that the rescued locomotion phenotype in worms treated with CMPD5 may have been the result of a decrease in the TTR oligomeric aggregate load. Equally important were the locomotion assays with D18G worms that exhibited a pronounced Unc phenotype but were rescued by RNAi against TTR. Since this variant does not secrete TTR out of the muscle, we assume that TTR proteotoxicity affects proteostasis in the muscle and results in its malfunction, although muscle morphology appeared unaffected.

In summary, our TTR *C. elegans* model exhibited TTR aggregate formation, differential TTR variant secretion, impairment in locomotion and quantifiable cell-nonautonomous neuronal phenotypes, including pain sensation impairment and neuronal abnormalities, rendering these models suitable for a forward genetic screen to discover TTR proteotoxicity modulators.

R193.2 a suppressor of TTR

With this in mind, in Article 5 we performed the first unbiased forward genetic screen for suppressors of the TTR-mediated Unc phenotype. After performing whole-genome sequencing, we identified R193.2 mutations in two TTR suppressors that corresponded to the same complementation group. Our data suggested *R193.2* gene is a novel TTR interactor that mediates

TTR toxicity. *R193.2* gene encodes an uncharacterized protein in *C. elegans* with conserved SEA and WFA domains and predicted to localize at membrane.

The structure of SEA domains is well known and is found in a range of proteins[289]. Variants within SEA domains may affect its folding and as a consequence lead to structural destabilization. This is the case of matriptase, a protein that gets retained predominantly in the ER in conditions that alter its SEA domain normal folding[289]. Likewise, IMPG2 mutant for SEA domain appears to be trapped in the ER whereas the WT protein is targeted to the plasma membrane[290]. Taking into account these observations, it is conceivably that these mutant alleles in the TTR suppressors affects the structure of the R193.2 protein, thus preventing the proteotoxic mechanism that would develop in the presence of V30M TTR sequence, under WT R193.2 circumstances.

The other predicted domain in R193.2 is a VWA domain, a well-characterized domain important for PPI and is often involved in ligand binding [291]. Similar to MYH11, R193.2 has a domain that mediates PPI, indicating that there is a dynamic pattern of MYH11/R193.2/TTR proteins interacting with one another through their specific domains. Thus, in the future it will be important to explore the molecular relationship between these networks. Understanding R193.2 interactions gives a global view of the protein interaction network, and possibly allows to unravel the unknown protein functions. These results will also be essential to provide the *C. elegans* community with validated putative modulators of amyloid disease toxicity for future projects.

On the basis of these observations, we hypothesized that either these alleles may influence R193.2 proper folding and/or interaction proprieties or may keep R193.2 function silent in the ER and possible throughout the proteotoxicity signaling pathway. Furthermore, consistent with the observed rescue in nociceptive sensing, it is possible that R193.2 protein impairs the TTR-targeting mechanism which leads to the morphological abnormalities in the sensory neurons.

Both the uncharacterized protein R193.2 in *C. elegans* and our predicted MYH11-TTR interaction network in overall seem to be involved in the ECM pathways. R193.2 protein contains VWA domains that mediate PPI important for cell adhesion and signaling in ECM proteins, where the majority of well-characterized VWA domains are found[292].

The ECM components have been previously proposed to be involved in other diseases such as: AD[293]; diabetic peripheral neuropathy [294]; Charcot-Marie-Tooth disease type I[295] and chronic idiopathic axonal polyneuropathy (CMT1)[295]. Linkage of ECM-related proteins with amyloid TTR deposits has also long been established, as TTR aggregates and fibrils occur extracellularly in peripheral nervous system, especially in the endoneurium, where they appear close to Schwann cells and collagen fibrils[296]. Sousa *et al.*, executed microarray analysis in TTR-FAP salivary glands and nerve biopsies, showing up-regulation of the ECM remodeling genes in

different stages of disease progression[266]. Similar results were found in FAP V30M TTR-related transgenic mouse as when mice were treated with some TTR removal (e.g. doxycycline) a reduction in ECM protein levels was observed, suggesting matrix recovery[297]. Histological examination of human tissues also revealed increased expression of ECM-related proteins, in close association with TTR amyloid fibrils deposition[298]. Another key point is that TTR amyloid deposition contributes to cell and ECM damage, as explained by Lotz *et al.* after having found deposits in articular cartilage in human osteoarthritis[299]. Thus, these authors suggested that the aged and osteoarthritis cartilage ECM is characterized by several modifications that can promote TTR deposition[299].

One of the explanations for this parallel increase in the amount of the ECM-related proteins and the degree of TTR amyloid deposition might be that amyloid fibril formation induces overproduction of the ECM components (as MYH11 and R193.2 proteins) which play an important role as a scaffold for the amyloid fibril formation process, which consequently promotes further amyloid accumulation[298]. Because this screen was not performed to saturation, we do not exclude the possibility of other components in ECM or even in other pathways that repress the Unc phenotype.

Intertwining these approaches

TTR-FAP displays a clinical range that is not fully explained by the primary Val30Met TTR variant. The action of various *trans*-modifiers appears to depend also on the *cis* conditions of the Val30Met TTR, including variants within in the TTR gene. Here we demonstrated that *cis*-acting factors on TTR *locus* are reliable candidates for AO modulation. From a biological point of view, these non-coding factors are one of the most interesting categories of genetic modifiers to study, since the mechanisms by which these variants exert their effects (for example on the splicing process) are often unclear and may be quite subtle. Along with *trans*-acting TTR variants, other *trans*-acting modulators like MYH11 and R193.2 might account for the phenotype variability. Additionally, the observed *trans*-acting factors in the noncarrier parents in families with a wider range of AO is not due to consanguinity, and transmission of these factors to the proband, potentially explains the AO anticipation.

This study contributed to disclose more variants associated to TTR pathways for the genetic pool data that has been increasing in these last years. However, not all of these factors are involved in the same trait, as well as within each trait there are risks with variable weight.

Although it may appear that ‘everything but the kitchen sink’ contributes to AO variability, the truth is that there is not a single causal effect. This major effect is already carried by the TTR-FAP patients and it is caused by the Val30Met disease causing-variant itself. All other modifiers

contribute with different weights and each of these factors interacts in a complex network. A question that may be reasonably posed is: If a variant is associated with a given AO group, why is it that all patients in this group are not carriers of this variant? A possible answer lies in epistatic interactions where many modifiers may only appear when a redundant pathway cannot rescue their effects. So, we cannot look at the effect of the variant by itself but as a whole, in a genetic background. This point is well known among laboratories that use mice as the model of study, where the same mutation may show substantial variation in phenotype, from no disease to early death in some cases, depending on the strain (genetic background)[62; 300].

Nevertheless, much of what is known about genetic, cellular and molecular TTR proprieties has been determined *in vitro*, characterizing the effects of the genetic modulators of TTR pathways in a multicellular transgenic model as our TTR cell-nonautonomous *C. elegans*, will provide an invaluable tool to study TTR amyloidogenesis and proteotoxicity. Furthermore, we demonstrated that genetic screening in *C. elegans* could be used to bridge the gap between model systems and human studies, notwithstanding a translational conformation in a mammalian system is recommended.

Unfortunately, it is not always straightforward to predict the effect of a variant on the function of a gene, even when the gene knockout or even protein function is well characterized. Patient genomes contain combinations of variants that may behave in unexpected ways and many variants may only become important in the context of a particular genetic background.

Future Relevance

In the era of personal “Omics” (e.g., transcriptomics/genomics, proteomics, metabolomics), one might envisage sequencing patient genomes to reveal risk/protector factors for early-/late-onset, or to a set of more likely symptoms. We can even think about revealing a particular pathway that may be a target for treatment that could delay onset of symptoms. Because TTR-FAP proceeds inexorably to death 10-15 years after onset and because there is no preventative or cure treatment, a molecular-targeted treatment capable of delaying the onset of TTR-FAP symptoms could be of great benefit. Moreover, the identification of treatment effect modifiers has become an important issue in pharmacogenetics. Therapies that are effective in a certain subgroup of patients can be futile in others. For example, tafamidis has only demonstrated efficacy in 60% of patients, while in 40% disease has continued to progress[156].

Importantly, a better understanding the pathways of TTR proteotoxicity, including the factors that impact the AO of symptomatic FAP may well contribute to a better understanding of the pathogenic mechanisms of more common neurodegenerative states such as AD and PD, with which FAP shares some common features.

CONCLUSION

TTR-FAP is affected by numerous genomic factors that are either nearby or physically separated from the disease-causing variant, which we reported in this thesis. Some of these factors are located in the TTR *locus* and may affect the expression levels and/or TTR function; others genes directly or indirectly cross the TTR-related pathways. This genetic network interferes with the possible disease-causing mechanisms at the level of TTR expression and stability whether in terms of aggregation or, ultimately, in secondary symptomatologic mechanisms, such as the loss of temperature perception or impact on locomotion. Some of these genetic variants have largely been explored in a TTR cell-nonautonomous *C. elegans* model, while others have been directly detected in patients. We predicted that there is an entire network of genes that code for proteins and altogether regulate the TTR toxicity observed. Future research will also be necessary to determine the universality of each variant or gene and how this translates into a TTR-related mechanism.

We are confident that this study helped in the development of a useful clinical genetic and animal model that expresses the relationship between certain genetic markers and the probability that disease onset will occur by a certain age, which may be of great importance for follow-up of presymptomatic cases. Moreover, the possibility of anticipating or understanding the mechanisms that influence TTR toxicity can help in the prediction of disease progression and envisioning new therapeutic strategies.

FUTURE PERSPECTIVES

With many pieces still missing in this puzzle, our human data, in combination with *C. elegans* models, opened new lines and paths to explore in the future. Thus, it would be important to elucidate some of the hypotheses previously stated which will certainly strengthen the results presented in this thesis. As follows:

- To study *in vivo* the role of the identified miRNAs, such as the liver-expressed mir-138, to confirm its binding and involvement in TTR mechanism;
- To functionally characterize the *TTR* intronic variants, in an attempt to disentangle its potential influence upon TTR structure, function and expression;
- To carry out a chromatin immunoprecipitation (ChIP) to analyze the predicted altered TF *in vivo* models;
- To validate the potential splicing deregulation by the variants found employing mini-gene constructs and to explore the association between the splicing-affected variants and the type of fibrils (full-length or fragmented TTR) in early- and late-onset patients;
- To assess the role of epigenetic mechanisms as modifiers of AO, namely the methylation patterns interrogating each *locus* as hypo or hyper methylated on AO, disease presentation and progression;
- To include more families with large anticipation in order to continue to analyze the variants (common and rare) identified in the WGS; also monozygotic twins and discordant AO-pairs;
- To proceed to a functional validation of MYH11 protein in the TTR mechanism and confirm its potential PPI with TTR. Additionally, to explore other genes found in the PPI network;
- To create *C. elegans* models using CRISPR/Cas9 technology with the two identified mutations and also with the GFP-labeled R193.2 to continue the validation and characterization of this mutant; while we will proceed with the WGS bioinformatics analysis to identify and characterize other TTR suppressors;
- To perform a RNA-Seq to verify the differential gene expression changes in FAP patients discordant for AO;
- To derive a Polygenic Risk Scores (PRS) to measure the additive impact of FAP-associated variants on risk, frequency, and severity.

REFERENCES

1. Amyloidosis, M.i.H. http://www.amyloidosismutations.com.
2. Karathanasis, S.K., Zannis, V.I., and Breslow, J.L. (1983). Isolation and characterization of the human apolipoprotein A-I gene. Proc Natl Acad Sci U S A 80, 6147-6151.
3. Plante-Bordeneuve, V., and Said, G. (2011). Familial amyloid polyneuropathy. Lancet Neurol 10, 1086-1097.
4. Kiuru-Enari, S., and Haltia, M. (2013). Hereditary gelsolin amyloidosis. Handb Clin Neurol 115, 659-681.
5. Kiuru, S. (1992). Familial amyloidosis of the Finnish type (FAF). A clinical study of 30 patients. Acta Neurol Scand 86, 346-353.
6. Kyle, R.A. (2001). Amyloidosis: a convoluted story. Br J Haematol 114, 529-538.
7. Virchow, R. (1854). Ueber eine im Gehirn und Rückenmark des Menschen aufgefundene Substanz mit der chemischen Reaction der Cellulose. Archiv f pathol Anat 6: 135, 135-138.
8. Andrade, C. (1952). A peculiar form of peripheral neuropathy; familiar atypical generalized amyloidosis with special involvement of the peripheral nerves. Brain 75, 408-427.
9. Sasaki, H., Yoshioka, N., Takagi, Y., and Sakaki, Y. (1985). Structure of the chromosomal gene for human serum prealbumin. Gene 37, 191-197.
10. Picken, M.M., Herrera, G.A., and Dogan, A. (2015). Amyloid and Related Disorders.(Humana Press).
11. Rowczenio, D.M., Noor, I., Gillmore, J.D., Lachmann, H.J., Whelan, C., Hawkins, P.N., Obici, L., Westermark, P., Grateau, G., and Wechalekar, A.D. (2014). Online registry for mutations in hereditary amyloidosis including nomenclature recommendations. Hum Mutat 35, E2403-2412.
12. Lahuerta Pueyo, C., Aibar Arregui, M.A., Gracia Gutierrez, A., Bueno Juana, E., and Menao Guillen, S. (2019). Estimating the prevalence of allelic variants in the transthyretin gene by analysing large-scale sequencing data. Eur J Hum Genet.
13. Fitch, N.J., Akbari, M.T., and Ramsden, D.B. (1991). An inherited non-amyloidogenic transthyretin variant, [Ser6]-TTR, with increased thyroxine-binding affinity, characterized by DNA sequencing. J Endocrinol 129, 309-313.
14. Jacobson, D.R., Alves, I.L., Saraiva, M.J., Thibodeau, S.N., and Buxbaum, J.N. (1995). Transthyretin Ser 6 gene frequency in individuals without amyloidosis. Hum Genet 95, 308-312.
15. McCutchen, S.L., Lai, Z., Miroy, G.J., Kelly, J.W., and Colon, W. (1995). Comparison of lethal and nonlethal transthyretin variants and their relationship to amyloid disease. Biochemistry 34, 13527-13536.
16. Hammarstrom, P., Schneider, F., and Kelly, J.W. (2001). Trans-suppression of misfolding in an amyloid disease. Science 293, 2459-2462.
17. Almeida, M.R., Alves, I.L., Terazaki, H., Ando, Y., and Saraiva, M.J. (2000). Comparative studies of two transthyretin variants with protective effects on familial amyloidotic polyneuropathy: TTR R104H and TTR T119M. Biochem Biophys Res Commun 270, 1024-1028.
18. Terazaki, H., Ando, Y., Misumi, S., Nakamura, M., Ando, E., Matsunaga, N., Shoji, S., Okuyama, M., Ideta, H., Nakagawa, K., et al. (1999). A novel compound heterozygote (FAP ATTR Arg104His/ATTR Val30Met) with high serum transthyretin (TTR) and retinol binding protein (RBP) levels. Biochem Biophys Res Commun 264, 365-370.
19. Lim, A., Prokaeva, T., Connor, L.H., Falk, R.H., Skinner, M., and Costello, C.E. (2002). Identification of a novel transthyretin Thr59Lys/Arg104His. A case of compound heterozygosity in a Chinese patient diagnosed with familial transthyretin amyloidosis. Amyloid 9, 134-140.
20. Hawkins, P.N., Ando, Y., Dispenzeri, A., Gonzalez-Duarte, A., Adams, D., and Suhr, O.B. (2015). Evolving landscape in the management of transthyretin amyloidosis. Ann Med 47, 625-638.
21. Coelho, T., Maurer, M.S., and Suhr, O.B. (2013). THAOS - The Transthyretin Amyloidosis Outcomes Survey: initial report on clinical manifestations in patients with hereditary and wild-type transthyretin amyloidosis. Curr Med Res Opin 29, 63-76.
22. Parman, Y., Adams, D., Obici, L., Galán, L., Guergueltcheva, V., Suhr, O.B., and Coelho, T. (2016). Sixty years of transthyretin familial amyloid polyneuropathy (TTR-FAP) in Europe. Current Opinion in Neurology 29, S3-S13.
23. Saraiva, M.J., Birken, S., Costa, P.P., and Goodman, D.S. (1984). Amyloid fibril protein in familial amyloidotic polyneuropathy, Portuguese type. Definition of molecular abnormality in transthyretin (prealbumin). J Clin Invest 74, 104-119.
24. Kelly, J.W. (1996). Alternative conformations of amyloidogenic proteins govern their behavior. Curr Opin Struct Biol 6, 11-17.

25. Hammarstrom, P., Jiang, X., Hurshman, A.R., Powers, E.T., and Kelly, J.W. (2002). Sequence-dependent denaturation energetics: A major determinant in amyloid disease diversity. Proc Natl Acad Sci U S A 99 Suppl 4, 16427-16432.
26. Hammarstrom, P., Sekijima, Y., White, J.T., Wiseman, R.L., Lim, A., Costello, C.E., Altland, K., Garzuly, F., Budka, H., and Kelly, J.W. (2003). D18G transthyretin is monomeric, aggregation prone, and not detectable in plasma and cerebrospinal fluid: a prescription for central nervous system amyloidosis? Biochemistry 42, 6656-6663.
27. Sekijima, Y., Hammarstrom, P., Matsumura, M., Shimizu, Y., Iwata, M., Tokuda, T., Ikeda, S., and Kelly, J.W. (2003). Energetic characteristics of the new transthyretin variant A25T may explain its atypical central nervous system pathology. Lab Invest 83, 409-417.
28. Maurer, M.S., Hanna, M., Grogan, M., Dispenzieri, A., Witteles, R., Drachman, B., Judge, D.P., Lenihan, D.J., Gottlieb, S.S., Shah, S.J., et al. (2016). Genotype and Phenotype of Transthyretin Cardiac Amyloidosis: THAOS (Transthyretin Amyloid Outcome Survey). J Am Coll Cardiol 68, 161-172.
29. Jiang, X., Buxbaum, J.N., and Kelly, J.W. (2001). The V122I cardiomyopathy variant of transthyretin increases the velocity of rate-limiting tetramer dissociation, resulting in accelerated amyloidosis. Proc Natl Acad Sci U S A 98, 14943-14948.
30. Holmgren, G., Haettner, E., Nordenson, I., Sandgren, O., Steen, L., and Lundgren, E. (1988). Homozygosity for the transthyretin-met30-gene in two Swedish sibs with familial amyloidotic polyneuropathy. Clin Genet 34, 333-338.
31. Holmgren, G., Bergstrom, S., Drugge, U., Lundgren, E., Nording-Sikstrom, C., Sandgren, O., and Steen, L. (1992). Homozygosity for the transthyretin-Met30-gene in seven individuals with familial amyloidosis with polyneuropathy detected by restriction enzyme analysis of amplified genomic DNA sequences. Clin Genet 41, 39-41.
32. Olsson, M., Norgren, N., Obayashi, K., Plante-Bordeneuve, V., Suhr, O.B., Cederquist, K., and Jonasson, J. (2010). A possible role for miRNA silencing in disease phenotype variation in Swedish transthyretin V30M carriers. BMC Med Genet 11, 130.
33. Jacobson, D.R., Gorevic, P.D., and Buxbaum, J.N. (1990). A homozygous transthyretin variant associated with senile systemic amyloidosis: evidence for a late-onset disease of genetic etiology. Am J Hum Genet 47, 127-136.
34. Gertz, M.A., Dispenzieri, A., and Sher, T. (2015). Pathophysiology and treatment of cardiac amyloidosis. Nat Rev Cardiol 12, 91-102.
35. Merlini, G., and Westermark, P. (2004). The systemic amyloidoses: clearer understanding of the molecular mechanisms offers hope for more effective therapies. J Intern Med 255, 159-178.
36. Ines, M., Coelho, T., Conceicao, I., Duarte-Ramos, F., de Carvalho, M., and Costa, J. (2018). Epidemiology of Transthyretin Familial Amyloid Polyneuropathy in Portugal: A Nationwide Study. Neuroepidemiology 51, 177-182.
37. Schmidt, H.H., Waddington-Cruz, M., Botteman, M.F., Carter, J.A., Chopra, A.S., Hopps, M., Stewart, M., Fallet, S., and Amass, L. (2018). Estimating the global prevalence of transthyretin familial amyloid polyneuropathy. Muscle Nerve 57, 829-837.
38. Sousa, A., Coelho, T., Barros, J., and Sequeiros, J. (1995). Genetic epidemiology of familial amyloidotic polyneuropathy (FAP)-type I in Povoa do Varzim and Vila do Conde (north of Portugal). Am J Med Genet 60, 512-521.
39. Herbert, J., Wilcox, J.N., Pham, K.T., Fremeau, R.T., Jr., Zeviani, M., Dwork, A., Soprano, D.R., Makover, A., Goodman, D.S., Zimmerman, E.A., et al. (1986). Transthyretin: a choroid plexus-specific transport protein in human brain. The 1986 S. Weir Mitchell award. Neurology 36, 900-911.
40. Martone, R.L., Herbert, J., Dwork, A., and Schon, E.A. (1988). Transthyretin is synthesized in the mammalian eye. Biochem Biophys Res Commun 151, 905-912.
41. Wakasugi, S., Maeda, S., and Shimada, K. (1986). Structure and expression of the mouse prealbumin gene. J Biochem 100, 49-58.
42. Kato, M., Kato, K., Blaner, W.S., Chertow, B.S., and Goodman, D.S. (1985). Plasma and cellular retinoid-binding proteins and transthyretin (prealbumin) are all localized in the islets of Langerhans in the rat. Proc Natl Acad Sci U S A 82, 2488-2492.
43. Soprano, D.R., Herbert, J., Soprano, K.J., Schon, E.A., and Goodman, D.S. (1985). Demonstration of transthyretin mRNA in the brain and other extrahepatic tissues in the rat. J Biol Chem 260, 11793-11798.
44. Hamilton, J.A., and Benson, M.D. (2001). Transthyretin: a review from a structural perspective. Cell Mol Life Sci 58, 1491-1521.

45. Blake, C.C., Geisow, M.J., Swan, I.D., Rerat, C., and Rerat, B. (1974). Strjcture of human plasma prealbumin at 2-5 A resolution. A preliminary report on the polypeptide chain conformation, quaternary structure and thyroxine binding. J Mol Biol 88, 1-12.
46. Ingbar, S.H. (1958). Pre-albumin: a thyroxinebinding protein of human plasma. Endocrinology 63, 256-259.
47. Hagen, G.A., and Elliott, W.J. (1973). Transport of thyroid hormones in serum and cerebrospinal fluid. J Clin Endocrinol Metab 37, 415-422.
48. Monaco, H.L., Rizzi, M., and Coda, A. (1995). Structure of a complex of two plasma proteins: transthyretin and retinol-binding protein. Science 268, 1039-1041.
49. Robbins, J. (1991). Tyroid hormone transport proteins and the physiology of hormone binding.(Philadelphia: JB Lippincott Company).
50. Palha, J.A., Hays, M.T., Morreale de Escobar, G., Episkopou, V., Gottesman, M.E., and Saraiva, M.J. (1997). Transthyretin is not essential for thyroxine to reach the brain and other tissues in transthyretin-null mice. Am J Physiol 272, E485-493.
51. Fleming, C.E., Saraiva, M.J., and Sousa, M.M. (2007). Transthyretin enhances nerve regeneration. J Neurochem 103, 831-839.
52. Sousa, M.M., Berglund, L., and Saraiva, M.J. (2000). Transthyretin in high density lipoproteins: association with apolipoprotein A-I. J Lipid Res 41, 58-65.
53. Schwarzman, A.L., Gregori, L., Vitek, M.P., Lyubski, S., Strittmatter, W.J., Enghilde, J.J., Bhasin, R., Silverman, J., Weisgraber, K.H., Coyle, P.K., et al. (1994). Transthyretin sequesters amyloid beta protein and prevents amyloid formation. Proc Natl Acad Sci U S A 91, 8368-8372.
54. Santos, S.D., Lambertsen, K.L., Clausen, B.H., Akinc, A., Alvarez, R., Finsen, B., and Saraiva, M.J. (2010). CSF transthyretin neuroprotection in a mouse model of brain ischemia. J Neurochem 115, 1434-1444.
55. Brouillette, J., and Quirion, R. (2008). Transthyretin: a key gene involved in the maintenance of memory capacities during aging. Neurobiol Aging 29, 1721-1732.
56. Delliere, S., and Cynober, L. (2017). Is transthyretin a good marker of nutritional status? Clin Nutr 36, 364-370.
57. Shirahama, T., Skinner, M., Westermark, P., Rubinow, A., Cohen, A.S., Brun, A., and Kemper, T.L. (1982). Senile cerebral amyloid. Prealbumin as a common constituent in the neuritic plaque, in the neurofibrillary tangle, and in the microangiopathic lesion. Am J Pathol 107, 41-50.
58. Strittmatter, W.J., Weisgraber, K.H., Huang, D.Y., Dong, L.M., Salvesen, G.S., Pericak-Vance, M., Schmechel, D., Saunders, A.M., Goldgaber, D., and Roses, A.D. (1993). Binding of human apolipoprotein E to synthetic amyloid beta peptide: isoform-specific effects and implications for late-onset Alzheimer disease. Proc Natl Acad Sci U S A 90, 8098-8102.
59. Ghiso, J., Matsubara, E., Koudinov, A., Choi-Miura, N.H., Tomita, M., Wisniewski, T., and Frangione, B. (1993). The cerebrospinal-fluid soluble form of Alzheimer's amyloid beta is complexed to SP-40,40 (apolipoprotein J), an inhibitor of the complement membrane-attack complex. Biochem J 293 (Pt 1), 27-30.
60. Serot, J.M., Christmann, D., Dubost, T., and Couturier, M. (1997). Cerebrospinal fluid transthyretin: aging and late onset Alzheimer's disease. J Neurol Neurosurg Psychiatry 63, 506-508.
61. Velayudhan, L., Killick, R., Hye, A., Kinsey, A., Guntert, A., Lynham, S., Ward, M., Leung, R., Lourdusamy, A., To, A.W., et al. (2012). Plasma transthyretin as a candidate marker for Alzheimer's disease. J Alzheimers Dis 28, 369-375.
62. Buxbaum, J.N. (2009). Animal models of human amyloidoses: are transgenic mice worth the time and trouble? FEBS Lett 583, 2663-2673.
63. Lai, Z., Colon, W., and Kelly, J.W. (1996). The acid-mediated denaturation pathway of transthyretin yields a conformational intermediate that can self-assemble into amyloid. Biochemistry 35, 6470-6482.
64. Lashuel, H.A., Lai, Z., and Kelly, J.W. (1998). Characterization of the transthyretin acid denaturation pathways by analytical ultracentrifugation: implications for wild-type, V30M, and L55P amyloid fibril formation. Biochemistry 37, 17851-17864.
65. Quintas, A., Vaz, D.C., Cardoso, I., Saraiva, M.J., and Brito, R.M. (2001). Tetramer dissociation and monomer partial unfolding precedes protofibril formation in amyloidogenic transthyretin variants. J Biol Chem 276, 27207-27213.
66. Lim, K.H., Dasari, A.K., Hung, I., Gan, Z., Kelly, J.W., and Wemmer, D.E. (2016). Structural Changes Associated with Transthyretin Misfolding and Amyloid Formation Revealed by Solution and Solid-State NMR. Biochemistry 55, 1941-1944.
67. Gustavsson, A., Jahr, H., Tobiassen, R., Jacobson, D.R., Sletten, K., and Westermark, P. (1995). Amyloid fibril composition and transthyretin gene structure in senile systemic amyloidosis. Lab Invest 73, 703-708.

68. Ihse, E., Rapezzi, C., Merlini, G., Benson, M.D., Ando, Y., Suhr, O.B., Ikeda, S., Lavatelli, F., Obici, L., Quarta, C.C., et al. (2013). Amyloid fibrils containing fragmented ATTR may be the standard fibril composition in ATTR amyloidosis. Amyloid 20, 142-150.
69. Thylen, C., Wahlqvist, J., Haettner, E., Sandgren, O., Holmgren, G., and Lundgren, E. (1993). Modifications of transthyretin in amyloid fibrils: analysis of amyloid from homozygous and heterozygous individuals with the Met30 mutation. EMBO J 12, 743-748.
70. Bergstrom, J., Gustavsson, A., Hellman, U., Sletten, K., Murphy, C.L., Weiss, D.T., Solomon, A., Olofsson, B.O., and Westermark, P. (2005). Amyloid deposits in transthyretin-derived amyloidosis: cleaved transthyretin is associated with distinct amyloid morphology. J Pathol 206, 224-232.
71. Chiti, F., and Dobson, C.M. (2009). Amyloid formation by globular proteins under native conditions. Nat Chem Biol 5, 15-22.
72. Reixach, N., Deechongkit, S., Jiang, X., Kelly, J.W., and Buxbaum, J.N. (2004). Tissue damage in the amyloidoses: Transthyretin monomers and nonnative oligomers are the major cytotoxic species in tissue culture. Proc Natl Acad Sci U S A 101, 2817-2822.
73. Hou, X., Parkington, H.C., Coleman, H.A., Mechler, A., Martin, L.L., Aguilar, M.I., and Small, D.H. (2007). Transthyretin oligomers induce calcium influx via voltage-gated calcium channels. J Neurochem 100, 446-457.
74. Sekijima, Y., Kelly, J.W., and Ikeda, S. (2008). Pathogenesis of and therapeutic strategies to ameliorate the transthyretin amyloidoses. Curr Pharm Des 14, 3219-3230.
75. Plante-Bordeneuve, V. (2017). Transthyretin familial amyloid polyneuropathy: an update. Journal of Neurology 265, 976-983.
76. Koike, H., and Sobue, G. (2010). Diagnosis of familial amyloid polyneuropathy: wide-ranged clinicopathological features. Expert Opin Med Diagn 4, 323-331.
77. Ando, E., Ando, Y., Okamura, R., Uchino, M., Ando, M., and Negi, A. (1997). Ocular manifestations of familial amyloidotic polyneuropathy type I: long-term follow up. Br J Ophthalmol 81, 295-298.
78. Conceição, I., González-Duarte, A., Obici, L., Schmidt, H.H.J., Simoneau, D., Ong, M.-L., and Amass, L. (2016). "Red-flag" symptom clusters in transthyretin familial amyloid polyneuropathy. Journal of the Peripheral Nervous System 21, 5-9.
79. Westermark, P., Bergstrom, J., Solomon, A., Murphy, C., and Sletten, K. (2003). Transthyretin-derived senile systemic amyloidosis: clinicopathologic and structural considerations. Amyloid 10 Suppl 1, 48-54.
80. Sekijima, Y., Uchiyama, S., Tojo, K., Sano, K., Shimizu, Y., Imaeda, T., Hoshii, Y., Kato, H., and Ikeda, S. (2011). High prevalence of wild-type transthyretin deposition in patients with idiopathic carpal tunnel syndrome: a common cause of carpal tunnel syndrome in the elderly. Hum Pathol 42, 1785-1791.
81. Lim, K.H., Dasari, A.K.R., Ma, R., Hung, I., Gan, Z., Kelly, J.W., and Fitzgerald, M.C. (2017). Pathogenic Mutations Induce Partial Structural Changes in the Native beta-Sheet Structure of Transthyretin and Accelerate Aggregation. Biochemistry 56, 4808-4818.
82. Kanai, M., Raz, A., and Goodman, D.S. (1968). Retinol-binding protein: the transport protein for vitamin A in human plasma. J Clin Invest 47, 2025-2044.
83. Livrea, M.A. (2000). Vitamin A and Retinoids: An Update of Biological Aspects and Clinical Applications.(Birkhäuser Basel).
84. Sousa, M.M., Norden, A.G., Jacobsen, C., Willnow, T.E., Christensen, E.I., Thakker, R.V., Verroust, P.J., Moestrup, S.K., and Saraiva, M.J. (2000). Evidence for the role of megalin in renal uptake of transthyretin. J Biol Chem 275, 38176-38181.
85. Fleming, C.E., Mar, F.M., Franquinho, F., Saraiva, M.J., and Sousa, M.M. (2009). Transthyretin internalization by sensory neurons is megalin mediated and necessary for its neuritogenic activity. J Neurosci 29, 3220-3232.
86. Schwarzman, A.L., and Goldgaber, D. (1996). Interaction of transthyretin with amyloid beta-protein: binding and inhibition of amyloid formation. Ciba Found Symp 199, 146-160; discussion 160-144.
87. Goncalves, I., Quintela, T., Baltazar, G., Almeida, M.R., Saraiva, M.J., and Santos, C.R. (2008). Transthyretin interacts with metallothionein 2. Biochemistry 47, 2244-2251.
88. Martinho, A., Goncalves, I., Cardoso, I., Almeida, M.R., Quintela, T., Saraiva, M.J., and Santos, C.R. (2010). Human metallothioneins 2 and 3 differentially affect amyloid-beta binding by transthyretin. FEBS J 277, 3427-3436.
89. Liz, M.A., Faro, C.J., Saraiva, M.J., and Sousa, M.M. (2004). Transthyretin, a new cryptic protease. J Biol Chem 279, 21431-21438.

90. Liz, M.A., Fleming, C.E., Nunes, A.F., Almeida, M.R., Mar, F.M., Choe, Y., Craik, C.S., Powers, J.C., Bogyo, M., and Sousa, M.M. (2009). Substrate specificity of transthyretin: identification of natural substrates in the nervous system. Biochem J 419, 467-474.
91. Koide-Yoshida, S., Niki, T., Ueda, M., Himeno, S., Taira, T., Iguchi-Ariga, S.M., Ando, Y., and Ariga, H. (2007). DJ-1 degrades transthyretin and an inactive form of DJ-1 is secreted in familial amyloidotic polyneuropathy. Int J Mol Med 19, 885-893.
92. Zhou, L., Tang, X., Li, X., Bai, Y., Buxbaum, J.N., and Chen, G. (2019). Identification of transthyretin as a novel interacting partner for the delta subunit of GABAA receptors. PLoS One 14, e0210094.
93. Pullakhandam, R., Srinivas, P.N., Nair, M.K., and Reddy, G.B. (2009). Binding and stabilization of transthyretin by curcumin. Arch Biochem Biophys 485, 115-119.
94. Green, N.S., Foss, T.R., and Kelly, J.W. (2005). Genistein, a natural product from soy, is a potent inhibitor of transthyretin amyloidosis. Proc Natl Acad Sci U S A 102, 14545-14550.
95. Trivella, D.B., Bleicher, L., Palmieri Lde, C., Wiggers, H.J., Montanari, C.A., Kelly, J.W., Lima, L.M., Foguel, D., and Polikarpov, I. (2010). Conformational differences between the wild type and V30M mutant transthyretin modulate its binding to genistein: implications to tetramer stability and ligand-binding. J Struct Biol 170, 522-531.
96. Radovic, B., Mentrup, B., and Kohrle, J. (2006). Genistein and other soya isoflavones are potent ligands for transthyretin in serum and cerebrospinal fluid. Br J Nutr 95, 1171-1176.
97. Ferreira, N., Cardoso, I., Domingues, M.R., Vitorino, R., Bastos, M., Bai, G., Saraiva, M.J., and Almeida, M.R. (2009). Binding of epigallocatechin-3-gallate to transthyretin modulates its amyloidogenicity. FEBS Lett 583, 3569-3576.
98. Klabunde, T., Petrassi, H.M., Oza, V.B., Raman, P., Kelly, J.W., and Sacchettini, J.C. (2000). Rational design of potent human transthyretin amyloid disease inhibitors. Nat Struct Biol 7, 312-321.
99. Miller, S.R., Sekijima, Y., and Kelly, J.W. (2004). Native state stabilization by NSAIDs inhibits transthyretin amyloidogenesis from the most common familial disease variants. Lab Invest 84, 545-552.
100. Said, G., Ropert, A., and Faux, N. (1984). Length-dependent degeneration of fibers in Portuguese amyloid polyneuropathy: a clinicopathologic study. Neurology 34, 1025-1032.
101. Plante-Bordeneuve, V., and Kerschen, P. (2013). Transthyretin familial amyloid polyneuropathy. Handb Clin Neurol 115, 643-658.
102. Ando, Y., Coelho, T., Berk, J.L., Cruz, M.W., Ericzon, B.G., Ikeda, S., Lewis, W.D., Obici, L., Plante-Bordeneuve, V., Rapezzi, C., et al. (2013). Guideline of transthyretin-related hereditary amyloidosis for clinicians. Orphanet J Rare Dis 8, 31.
103. Koike, H., Morozumi, S., Kawagashira, Y., Iijima, M., Yamamoto, M., Hattori, N., Tanaka, F., Nakamura, T., Hirayama, M., Ando, Y., et al. (2009). The significance of carpal tunnel syndrome in transthyretin Val30Met familial amyloid polyneuropathy. Amyloid 16, 142-148.
104. Conceicao, I., Gonzalez-Duarte, A., Obici, L., Schmidt, H.H., Simoneau, D., Ong, M.L., and Amass, L. (2016). "Red-flag" symptom clusters in transthyretin familial amyloid polyneuropathy. J Peripher Nerv Syst 21, 5-9.
105. Coutinho, P., Martins da Silva, A., Lopes Lima, J., and Resende Barbosa, A. (1980). Forty years of experience with type I amyloid neuropathy. Review of 483 cases. In: Glenner GG, e Costa PP, de Freitas AF, eds Amyloid and Amyloidosis Amsterdam: Execerpta Medica,, 88-89.
106. Ando, Y., Nakamura, M., and Araki, S. (2005). Transthyretin-related familial amyloidotic polyneuropathy. Arch Neurol 62, 1057-1062.
107. Maia, L.F., Magalhaes, R., Freitas, J., Taipa, R., Pires, M.M., Osorio, H., Dias, D., Pessegueiro, H., Correia, M., and Coelho, T. (2015). CNS involvement in V30M transthyretin amyloidosis: clinical, neuropathological and biochemical findings. J Neurol Neurosurg Psychiatry 86, 159-167.
108. Rapezzi, C., Quarta, C.C., Riva, L., Longhi, S., Gallelli, I., Lorenzini, M., Ciliberti, P., Biagini, E., Salvi, F., and Branzi, A. (2010). Transthyretin-related amyloidoses and the heart: a clinical overview. Nat Rev Cardiol 7, 398-408.
109. Lobato, L., Beirao, I., Guimaraes, S.M., Droz, D., Guimaraes, S., Grunfeld, J.P., and Noel, L.H. (1998). Familial amyloid polyneuropathy type I (Portuguese): distribution and characterization of renal amyloid deposits. Am J Kidney Dis 31, 940-946.
110. Lobato, L., Beirao, I., Silva, M., Bravo, F., Silvestre, F., Guimaraes, S., Sousa, A., Noel, L.H., and Sequeiros, J. (2003). Familial ATTR amyloidosis: microalbuminuria as a predictor of symptomatic disease and clinical nephropathy. Nephrol Dial Transplant 18, 532-538.
111. Lobato, L., and Rocha, A. (2012). Transthyretin amyloidosis and the kidney. Clin J Am Soc Nephrol 7, 1337-1346.

112. Haraoka, K., Ando, Y., Ando, E., Sandgren, O., Hirata, A., Nakamura, M., Terazaki, H., Tajiri, T., Tanoue, Y., Sun, X., et al. (2002). Amyloid deposition in ocular tissues of patients with familial amyloidotic polyneuropathy (FAP). Amyloid 9, 183-189.
113. Seca, M., Ferreira, N., and Coelho, T. (2014). Vitreous Amyloidosis as the Presenting Symptom of Familial Amyloid Polyneuropathy TTR Val30Met in a Portuguese Patient. Case Rep Ophthalmol 5, 92-97.
114. Beirao, J.M., Malheiro, J., Lemos, C., Beirao, I., Costa, P., and Torres, P. (2015). Ophthalmological manifestations in hereditary transthyretin (ATTR V30M) carriers: a review of 513 cases. Amyloid 22, 117-122.
115. Sekijima, Y., Ueda, M., Koike, H., Misawa, S., Ishii, T., and Ando, Y. (2018). Diagnosis and management of transthyretin familial amyloid polyneuropathy in Japan: red-flag symptom clusters and treatment algorithm. Orphanet J Rare Dis 13, 6.
116. Sousa, A., Andersson, R., Drugge, U., Holmgren, G., and Sandgren, O. (1993). Familial amyloidotic polyneuropathy in Sweden: geographical distribution, age of onset, and prevalence. Hum Hered 43, 288-294.
117. Ikeda, S., Nakazato, M., Ando, Y., and Sobue, G. (2002). Familial transthyretin-type amyloid polyneuropathy in Japan: clinical and genetic heterogeneity. Neurology 58, 1001-1007.
118. Saporta, M.A., Zaros, C., Cruz, M.W., Andre, C., Misrahi, M., Bonaiti-Pellie, C., and Plante-Bordeneuve, V. (2009). Penetrance estimation of TTR familial amyloid polyneuropathy (type I) in Brazilian families. Eur J Neurol 16, 337-341.
119. Munar-Ques, M., Saraiva, M.J., Viader-Farre, C., Zabay-Becerril, J.M., and Mulet-Ferrer, J. (2005). Genetic epidemiology of familial amyloid polyneuropathy in the Balearic Islands (Spain). Amyloid 12, 54-61.
120. Reines, J.B., Vera, T.R., Martin, M.U., Serra, H.A., Campins, M.M., Millan, J.M., Lezaun, C.G., and Cruz, M.R. (2014). Epidemiology of transthyretin-associated familial amyloid polyneuropathy in the Majorcan area: Son Llatzer Hospital descriptive study. Orphanet J Rare Dis 9, 29.
121. Sousa A. (1995). A variabilidade fenotípica da Polineuropatia Amiloidótica Familiar: um estudo de genética quantitativa em Portugal e na Suécia. Dissertation for the Doctoral degree in biomedical sciences, genetic speciality, submitted to Instituto de Ciências Biomédicas Abel Salazar, University of Porto.
122. Coelho, T., Sousa, A., Lourenco, E., and Ramalheira, J. (1994). A study of 159 Portuguese patients with familial amyloidotic polyneuropathy (FAP) whose parents were both unaffected. J Med Genet 31, 293-299.
123. Sequeiros, J., and Saraiva, M.J. (1987). Onset in the seventh decade and lack of symptoms in heterozygotes for the TTRMet30 mutation in hereditary amyloid neuropathy-type I (Portuguese, Andrade). Am J Med Genet 27, 345-357.
124. Drugge, U., Andersson, R., Chizari, F., Danielsson, M., Holmgren, G., Sandgren, O., and Sousa, A. (1993). Familial amyloidotic polyneuropathy in Sweden: a pedigree analysis. J Med Genet 30, 388-392.
125. Tashima, K., Ando, Y., Tanaka, Y., Uchino, M., and Ando, M. (1995). Change in the age of onset in patients with familial amyloidotic polyneuropathy type I. Intern Med 34, 748-750.
126. Soares, M., Buxbaum, J., Sirugo, G., Coelho, T., Sousa, A., Kastner, D., and Saraiva, M.J. (1999). Genetic anticipation in Portuguese kindreds with familial amyloidotic polyneuropathy is unlikely to be caused by triplet repeat expansions. Hum Genet 104, 480-485.
127. Lemos, C., Coelho, T., Alves-Ferreira, M., Martins-da-Silva, A., Sequeiros, J., Mendonca, D., and Sousa, A. (2014). Overcoming artefact: anticipation in 284 Portuguese kindreds with familial amyloid polyneuropathy (FAP) ATTRV30M. J Neurol Neurosurg Psychiatry 85, 326-330.
128. Conceicao, I., and De Carvalho, M. (2007). Clinical variability in type I familial amyloid polyneuropathy (Val30Met): comparison between late- and early-onset cases in Portugal. Muscle Nerve 35, 116-118.
129. Soares, M.L., Coelho, T., Sousa, A., Batalov, S., Conceicao, I., Sales-Luis, M.L., Ritchie, M.D., Williams, S.M., Nievergelt, C.M., Schork, N.J., et al. (2005). Susceptibility and modifier genes in Portuguese transthyretin V30M amyloid polyneuropathy: complexity in a single-gene disease. Hum Mol Genet 14, 543-553.
130. Dardiotis, E., Koutsou, P., Zamba-Papanicolaou, E., Vonta, I., Hadjivassiliou, M., Hadjigeorgiou, G., Cariolou, M., Christodoulou, K., and Kyriakides, T. (2009). Complement C1Q polymorphisms modulate onset in familial amyloidotic polyneuropathy TTR Val30Met. J Neurol Sci 284, 158-162.
131. Sikora, J.L., Logue, M.W., Chan, G.G., Spencer, B.H., Prokaeva, T.B., Baldwin, C.T., Seldin, D.C., and Connors, L.H. (2015). Genetic variation of the transthyretin gene in wild-type transthyretin amyloidosis (ATTRwt). Hum Genet 134, 111-121.
132. Polimanti, R., Di Girolamo, M., Manfellotto, D., and Fuciarelli, M. (2013). Functional variation of thetransthyretingene among human populations and its correlation with amyloidosis phenotypes. Amyloid 20, 256-262.

133. Iorio, A., De Lillo, A., De Angelis, F., Di Girolamo, M., Luigetti, M., Sabatelli, M., Pradotto, L., Mauro, A., Mazzeo, A., Stancanelli, C., et al. (2017). Non-coding variants contribute to the clinical heterogeneity of TTR amyloidosis. European Journal of Human Genetics 25, 1055-1060.
134. Soares, M.L., Coelho, T., Sousa, A., Holmgren, G., Saraiva, M.J., Kastner, D.L., and Buxbaum, J.N. (2004). Haplotypes and DNA sequence variation within and surrounding the transthyretin gene: genotype-phenotype correlations in familial amyloid polyneuropathy (V30M) in Portugal and Sweden. Eur J Hum Genet 12, 225-237.
135. Santos, D., Coelho, T., Alves-Ferreira, M., Sequeiros, J., Mendonca, D., Alonso, I., Lemos, C., and Sousa, A. (2016). Variants in RBP4 and AR genes modulate age at onset in familial amyloid polyneuropathy (FAP ATTRV30M). Eur J Hum Genet 24, 756-760.
136. Santos, D., Coelho, T., Alves-Ferreira, M., Sequeiros, J., Mendonca, D., Alonso, I., Lemos, C., and Sousa, A. (2017). Familial amyloid polyneuropathy in Portugal: New genes modulating age-at-onset. Ann Clin Transl Neurol 4, 98-105.
137. Dias, A., Santos, D., Coelho, T., Alves-Ferreira, M., Sequeiros, J., Alonso, I., Sousa, A., and Lemos, C. (2019). C1QA and C1QC modify age-at-onset in familial amyloid polyneuropathy patients. Ann Clin Transl Neurol
138. Abreu-Silva, J. (2017). Modulators of phenotypic variability in Familial Amyloid Polyneuropathy (TTR-FAP Val30Met). Master, University of Porto.
139. Bonaiti, B., Olsson, M., Hellman, U., Suhr, O., Bonaiti-Pellie, C., and Plante-Bordeneuve, V. (2010). TTR familial amyloid polyneuropathy: does a mitochondrial polymorphism entirely explain the parent-of-origin difference in penetrance? Eur J Hum Genet 18, 948-952.
140. Olsson, M., Hellman, U., Plante-Bordeneuve, V., Jonasson, J., Lang, K., and Suhr, O.B. (2009). Mitochondrial haplogroup is associated with the phenotype of familial amyloidosis with polyneuropathy in Swedish and French patients. Clin Genet 75, 163-168.
141. Santos, D., Santos, M.J., Alves-Ferreira, M., Coelho, T., Sequeiros, J., Alonso, I., Oliveira, P., Sousa, A., Lemos, C., and Grazina, M. (2017). mtDNA copy number associated with age of onset in familial amyloid polyneuropathy. J Neurol Neurosurg Psychiatry.
142. Iorio, A., De Angelis, F., Di Girolamo, M., Luigetti, M., Pradotto, L., Mauro, A., Manfellotto, D., Fuciarelli, M., and Polimanti, R. (2015). Most recent common ancestor of TTR Val30Met mutation in Italian population and its potential role in genotype-phenotype correlation. Amyloid 22, 73-78.
143. Zaros, C., Genin, E., Hellman, U., Saporta, M.A., Languille, L., Wadington-Cruz, M., Suhr, O., Misrahi, M., and Plante-Bordeneuve, V. (2008). On the origin of the transthyretin Val30Met familial amyloid polyneuropathy. Ann Hum Genet 72, 478-484.
144. Leal, C. (2018). Tracking the origin of Val30Met mutation in Familial Amyloid Polyneuropathy (TTR-FAP) within different Portuguese regions Master, Universidade do Porto, Porto.
145. Adams, D., Suhr, O.B., Hund, E., Obici, L., Tournev, I., Campistol, J.M., Slama, M.S., Hazenberg, B.P., and Coelho, T. (2016). First European consensus for diagnosis, management, and treatment of transthyretin familial amyloid polyneuropathy. Curr Opin Neurol 29 Suppl 1, S14-26.
146. Plante-Bordeneuve, V. (2014). Update in the diagnosis and management of transthyretin familial amyloid polyneuropathy. J Neurol 261, 1227-1233.
147. Cortese, A., Vegezzi, E., Lozza, A., Alfonsi, E., Montini, A., Moglia, A., Merlini, G., and Obici, L. (2017). Diagnostic challenges in hereditary transthyretin amyloidosis with polyneuropathy: avoiding misdiagnosis of a treatable hereditary neuropathy. J Neurol Neurosurg Psychiatry 88, 457-458.
148. Holmgren, G., Steen, L., Ekstedt, J., Groth, C.G., Ericzon, B.G., Eriksson, S., Andersen, O., Karlberg, I., Norden, G., Nakazato, M., et al. (1991). Biochemical effect of liver transplantation in two Swedish patients with familial amyloidotic polyneuropathy (FAP-met30). Clin Genet 40, 242-246.
149. Furtado, A., Tome, L., Oliveira, F.J., Furtado, E., Viana, J., and Perdigoto, R. (1997). Sequential liver transplantation. Transplant Proc 29, 467-468.
150. Bolte, F.J., Schmidt, H.H., Becker, T., Braun, F., Pascher, A., Klempnauer, J., Schmidt, J., Nadalin, S., Otto, G., and Barreiros, A.P. (2013). Evaluation of domino liver transplantations in Germany. Transpl Int 26, 715-723.
151. Adams, D., Cauquil, C., and Labeyrie, C. (2017). Familial amyloid polyneuropathy. Current Opinion in Neurology 30, 481-489.
152. Niemietz, C., Chandhok, G., and Schmidt, H. (2015). Therapeutic Oligonucleotides Targeting Liver Disease: TTR Amyloidosis. Molecules 20, 17944-17975.
153. Adams, D., Gonzalez-Duarte, A., O'Riordan, W.D., Yang, C.-C., Ueda, M., Kristen, A.V., Tournev, I., Schmidt, H.H., Coelho, T., Berk, J.L., et al. (2018). Patisiran, an RNAi Therapeutic, for Hereditary Transthyretin Amyloidosis. New England Journal of Medicine 379, 11-21.

154. Niemietz, C., Chandhok, G., and Schmidt, H. (2015). Therapeutic Oligonucleotides Targeting Liver Disease: TTR Amyloidosis. Molecules 20, 17944-17975.
155. Benson, M.D., Waddington-Cruz, M., Berk, J.L., Polydefkis, M., Dyck, P.J., Wang, A.K., Planté-Bordeneuve, V., Barroso, F.A., Merlini, G., Obici, L., et al. (2018). Inotersen Treatment for Patients with Hereditary Transthyretin Amyloidosis. New England Journal of Medicine 379, 22-31.
156. Coelho, T., Maia, L.F., Martins da Silva, A., Waddington Cruz, M., Plante-Bordeneuve, V., Lozeron, P., Suhr, O.B., Campistol, J.M., Conceicao, I.M., Schmidt, H.H., et al. (2012). Tafamidis for transthyretin familial amyloid polyneuropathy: a randomized, controlled trial. Neurology 79, 785-792.
157. Coelho, T., Maia, L.F., da Silva, A.M., Cruz, M.W., Plante-Bordeneuve, V., Suhr, O.B., Conceicao, I., Schmidt, H.H., Trigo, P., Kelly, J.W., et al. (2013). Long-term effects of tafamidis for the treatment of transthyretin familial amyloid polyneuropathy. J Neurol 260, 2802-2814.
158. Coelho, T., Ines, M., Conceicao, I., Soares, M., de Carvalho, M., and Costa, J. (2018). Natural history and survival in stage 1 Val30Met transthyretin familial amyloid polyneuropathy. Neurology 91, e1999-e2009.
159. Berk, J.L., Suhr, O.B., Obici, L., Sekijima, Y., Zeldenrust, S.R., Yamashita, T., Heneghan, M.A., Gorevic, P.D., Litchy, W.J., Wiesman, J.F., et al. (2013). Repurposing diflunisal for familial amyloid polyneuropathy: a randomized clinical trial. JAMA 310, 2658-2667.
160. Miller, M., Pal, A., Albusairi, W., Joo, H., Pappas, B., Haque Tuhin, M.T., Liang, D., Jampala, R., Liu, F., Khan, J., et al. (2018). Enthalpy-Driven Stabilization of Transthyretin by AG10 Mimics a Naturally Occurring Genetic Variant That Protects from Transthyretin Amyloidosis. J Med Chem 61, 7862-7876.
161. Hosoi, A., Su, Y., Torikai, M., Jono, H., Ishikawa, D., Soejima, K., Higuchi, H., Guo, J., Ueda, M., Suenaga, G., et al. (2016). Novel Antibody for the Treatment of Transthyretin Amyloidosis. J Biol Chem 291, 25096-25105.
162. Sevigny, J., Chiao, P., Bussiere, T., Weinreb, P.H., Williams, L., Maier, M., Dunstan, R., Salloway, S., Chen, T., Ling, Y., et al. (2017). Addendum: The antibody aducanumab reduces Abeta plaques in Alzheimer's disease. Nature 546, 564.
163. Obici, L., Cortese, A., Lozza, A., Lucchetti, J., Gobbi, M., Palladini, G., Perlini, S., Saraiva, M.J., and Merlini, G. (2012). Doxycycline plus tauroursodeoxycholic acid for transthyretin amyloidosis: a phase II study. Amyloid 19 Suppl 1, 34-36.
164. Cardoso, I., Martins, D., Ribeiro, T., Merlini, G., and Saraiva, M.J. (2010). Synergy of combined doxycycline/TUDCA treatment in lowering Transthyretin deposition and associated biomarkers: studies in FAP mouse models. J Transl Med 8, 74.
165. Teng, M.H., Yin, J.Y., Vidal, R., Ghiso, J., Kumar, A., Rabenou, R., Shah, A., Jacobson, D.R., Tagoe, C., Gallo, G., et al. (2001). Amyloid and nonfibrillar deposits in mice transgenic for wild-type human transthyretin: a possible model for senile systemic amyloidosis. Lab Invest 81, 385-396.
166. Ueda, M., Ando, Y., Hakamata, Y., Nakamura, M., Yamashita, T., Obayashi, K., Himeno, S., Inoue, S., Sato, Y., Kaneko, T., et al. (2007). A transgenic rat with the human ATTR V30M: a novel tool for analyses of ATTR metabolisms. Biochem Biophys Res Commun 352, 299-304.
167. Sasaki, H., Tone, S., Nakazato, M., Yoshioka, K., Matsuo, H., Kato, Y., and Sakaki, Y. (1986). Generation of transgenic mice producing a human transthyretin variant: a possible mouse model for familial amyloidotic polyneuropathy. Biochem Biophys Res Commun 139, 794-799.
168. Yamamura, K., Wakasugi, S., Maeda, S., Inomoto, T., Iwanaga, T., Uehira, M., Araki, K., Miyazaki, J., and Shimada, K. (1987). Tissue-specific and developmental expression of human transthyretin gene in transgenic mice. Dev Genet 8, 195-205.
169. Yi, S., Takahashi, K., Naito, M., Tashiro, F., Wakasugi, S., Maeda, S., Shimada, K., Yamamura, K., and Araki, S. (1991). Systemic amyloidosis in transgenic mice carrying the human mutant transthyretin (Met30) gene. Pathologic similarity to human familial amyloidotic polyneuropathy, type I. Am J Pathol 138, 403-412.
170. Araki, S., Yi, S., Murakami, T., Watanabe, S., Ikegawa, S., Takahashi, K., and Yamarnura, K. (1994). Systemic amyloidosis in transgenic mice carrying the human mutant transthyretin (Met 30) gene. Pathological and immunohistochemical similarity to human familial amyloidotic polyneuropathy, type I. Mol Neurobiol 8, 15-23.
171. Nagata, Y., Tashiro, F., Yi, S., Murakami, T., Maeda, S., Takahashi, K., Shimada, K., Okamura, H., and Yamamura, K. (1995). A 6-kb upstream region of the human transthyretin gene can direct developmental, tissue-specific, and quantitatively normal expression in transgenic mouse. J Biochem 117, 169-175.
172. Sousa, M.M., Fernandes, R., Palha, J.A., Taboada, A., Vieira, P., and Saraiva, M.J. (2002). Evidence for early cytotoxic aggregates in transgenic mice for human transthyretin Leu55Pro. Am J Pathol 161, 1935-1948.

173. Santos, S.D., Fernandes, R., and Saraiva, M.J. (2010). The heat shock response modulates transthyretin deposition in the peripheral and autonomic nervous systems. Neurobiol Aging 31, 280-289.
174. Ito, S., and Maeda, S. (2009). Mouse Models of Transthyretin Amyloidosis. In: Richardson SJ, Cody V (eds) Recent Advances in Transthyretin Evolution, Structure and Biological Functions, 261-280.
175. Cardoso, I., and Saraiva, M.J. (2006). Doxycycline disrupts transthyretin amyloid: evidence from studies in a FAP transgenic mice model. FASEB J 20, 234-239.
176. Panayiotou, E., Papacharalambous, R., Antoniou, A., Christophides, G., Papageorgiou, L., Fella, E., Malas, S., and Kyriakides, T. (2016). Genetic background modifies amyloidosis in a mouse model of ATTR neuropathy. Biochem Biophys Rep 8, 48-54.
177. Li, X., Lyu, Y., Shen, J., Mu, Y., Qiang, L., Liu, L., Araki, K., Imbimbo, B.P., Yamamura, K.I., Jin, S., et al. (2018). Amyloid deposition in a mouse model humanized at the transthyretin and retinol-binding protein 4 loci. Lab Invest 98, 512-524.
178. Pokrzywa, M., Dacklin, I., Hultmark, D., and Lundgren, E. (2007). Misfolded transthyretin causes behavioral changes in a Drosophila model for transthyretin-associated amyloidosis. Eur J Neurosci 26, 913-924.
179. Berg, I., Thor, S., and Hammarstrom, P. (2009). Modeling familial amyloidotic polyneuropathy (Transthyretin V30M) in Drosophila melanogaster. Neurodegener Dis 6, 127-138.
180. Andersson, K., Pokrzywa, M., Dacklin, I., and Lundgren, E. (2013). Inhibition of TTR aggregation-induced cell death--a new role for serum amyloid P component. PLoS One 8, e55766.
181. Saelices, L., Pokrzywa, M., Pawelek, K., and Eisenberg, D.S. (2018). Assessment of the effects of transthyretin peptide inhibitors in Drosophila models of neuropathic ATTR. Neurobiol Dis 120, 118-125.
182. Iakovleva, I., Begum, A., Pokrzywa, M., Walfridsson, M., Sauer-Eriksson, A.E., and Olofsson, A. (2015). The flavonoid luteolin, but not luteolin-7-O-glucoside, prevents a transthyretin mediated toxic response. PLoS One 10, e0128222.
183. Link, C.D. (1995). Expression of human beta-amyloid peptide in transgenic Caenorhabditis elegans. Proc Natl Acad Sci U S A 92, 9368-9372.
184. Tsuda, Y., Yamanaka, K., Toyoshima, R., Ueda, M., Masuda, T., Misumi, Y., Ogura, T., and Ando, Y. (2018). Development of transgenic Caenorhabditis elegans expressing human transthyretin as a model for drug screening. Sci Rep 8, 17884.
185. Ueda, M., Ageyama, N., Nakamura, S., Nakamura, M., Chambers, J.K., Misumi, Y., Mizuguchi, M., Shinriki, S., Kawahara, S., Tasaki, M., et al. (2012). Aged vervet monkeys developing transthyretin amyloidosis with the human disease-causing Ile122 allele: a valid pathological model of the human disease. Lab Invest 92, 474-484.
186. Nakamura, S., Okabayashi, S., Ageyama, N., Koie, H., Sankai, T., Ono, F., Fujimoto, K., and Terao, K. (2008). Transthyretin amyloidosis and two other aging-related amyloidoses in an aged vervet monkey. Vet Pathol 45, 67-72.
187. Chambers, J.K., Kanda, T., Shirai, A., Higuchi, K., Ikeda, S., and Une, Y. (2010). Senile systemic amyloidosis in an aged savannah monkey (Cercopithecus aethiops) with tenosynovial degeneration. J Vet Med Sci 72, 657-659.
188. Macintyre, G., Bailey, J., Haviv, I., and Kowalczyk, A. (2010). is-rSNP: a novel technique for in silico regulatory SNP detection. Bioinformatics 26, i524-530.
189. Santos, D., Coelho, T., Alves-Ferreira, M., Sequeiros, J., Mendonca, D., Alonso, I., Sousa, A., and Lemos, C. (2019). Large normal alleles of ATXN2 decrease age at onset in transthyretin familial amyloid polyneuropathy Val30Met patients. Ann Neurol 85, 251-258.
190. Longo Alves, I., Hays, M.T., and Saraiva, M.J. (1997). Comparative stability and clearance of [Met30]transthyretin and [Met119]transthyretin. Eur J Biochem 249, 662-668.
191. Lobato, L., BeirÃ£o, I., Monteiro, P., Saraiva, M. J. M., Coelho, T., & Sousa, A. (1996). Epidemiology and genetic analysis in patients with familial amyloid polyneuropathy (FAP) type i and end-stage renal disease: Can we predict kidney involvement? Neuromusc Disord 6.
192. Coelho, T., Chorão, R., Sousa, A., Alves, I., Torres, M.F., and Saraiva, M.J.M. (1996). Compound heterozygotes of transthyretin Met30 and transthyretin Met119 are protected from the devastating effects of familial amyloid polyneuropathy. Neuromuscular Disorders 6, S20.
193. Hammarstrom, P., Wiseman, R.L., Powers, E.T., and Kelly, J.W. (2003). Prevention of transthyretin amyloid disease by changing protein misfolding energetics. Science 299, 713-716.
194. Batista, A.R., Gianni, D., Ventosa, M., Coelho, A.V., Almeida, M.R., Sena-Esteves, M., and Saraiva, M.J. (2014). Gene therapy approach to FAP: in vivo influence of T119M in TTR deposition in a transgenic V30M mouse model. Gene Ther.

195. Palhano, F.L., Leme, L.P., Busnardo, R.G., and Foguel, D. (2009). Trapping the monomer of a non-amyloidogenic variant of transthyretin: exploring its possible use as a therapeutic strategy against transthyretin amyloidogenic diseases. J Biol Chem 284, 1443-1453.
196. Le Marchand, L., Donlon, T., Seifried, A., Kaaks, R., Rinaldi, S., and Wilkens, L.R. (2002). Association of a common polymorphism in the human GH1 gene with colorectal neoplasia. J Natl Cancer Inst 94, 454-460.
197. Dennison, E.M., Syddall, H.E., Rodriguez, S., Voropanov, A., Day, I.N., and Cooper, C. (2004). Polymorphism in the growth hormone gene, weight in infancy, and adult bone mass. J Clin Endocrinol Metab 89, 4898-4903.
198. Millar, D.S., Horan, M., Chuzhanova, N.A., and Cooper, D.N. (2010). Characterisation of a functional intronic polymorphism in the human growth hormone (GH1) gene. Hum Genomics 4, 289-301.
199. Do, T.N., Ucisik-Akkaya, E., Davis, C.F., Morrison, B.A., and Dorak, M.T. (2010). An intronic polymorphism of IRF4 gene influences gene transcription in vitro and shows a risk association with childhood acute lymphoblastic leukemia in males. Biochim Biophys Acta 1802, 292-300.
200. Fang, G., Haznadar, M., Wang, W., Yu, H., Steinbach, M., Church, T.R., Oetting, W.S., Van Ness, B., and Kumar, V. (2012). High-order SNP combinations associated with complex diseases: efficient discovery, statistical power and functional interactions. PLoS One 7, e33531.
201. Mellerup, E., and Moller, G.L. (2017). Combinations of Genetic Variants Occurring Exclusively in Patients. Comput Struct Biotechnol J 15, 286-289.
202. Costa, R.H., Lai, E., and Darnell, J.E., Jr. (1986). Transcriptional control of the mouse prealbumin (transthyretin) gene: both promoter sequences and a distinct enhancer are cell specific. Mol Cell Biol 6, 4697-4708.
203. Martinho, A., Santos, C.R., and Goncalves, I. (2013). A distal estrogen responsive element upstream the cap site of human transthyretin gene is an enhancer-like element upon ERalpha and/or ERbeta transactivation. Gene 527, 469-476.
204. Sakaki, Y., Yoshioka, K., Tanahashi, H., Furuya, H., and Sasaki, H. (1989). Human transthyretin (prealbumin) gene and molecular genetics of familial amyloidotic polyneuropathy. Mol Biol Med 6, 161-168.
205. Sparkes, R.S., Sasaki, H., Mohandas, T., Yoshioka, K., Klisak, I., Sakaki, Y., Heinzmann, C., and Simon, M.I. (1987). Assignment of the prealbumin (PALB) gene (familial amyloidotic polyneuropathy) to human chromosome region 18q11.2-q12.1. Hum Genet 75, 151-154.
206. Li, X., Masliah, E., Reixach, N., and Buxbaum, J.N. (2011). Neuronal production of transthyretin in human and murine Alzheimer's disease: is it protective? J Neurosci 31, 12483-12490.
207. Wang, X., Cattaneo, F., Ryno, L., Hulleman, J., Reixach, N., and Buxbaum, J.N. (2014). The systemic amyloid precursor transthyretin (TTR) behaves as a neuronal stress protein regulated by HSF1 in SH-SY5Y human neuroblastoma cells and APP23 Alzheimer's disease model mice. J Neurosci 34, 7253-7265.
208. Sekijima, Y., Wiseman, R.L., Matteson, J., Hammarstrom, P., Miller, S.R., Sawkar, A.R., Balch, W.E., and Kelly, J.W. (2005). The biological and chemical basis for tissue-selective amyloid disease. Cell 121, 73-85.
209. Kel A, Kel-Margoulis O, Borlack J, Tchekmenev D, Wingender E, and J., B. (2005). Databases and tools for in silico analysis of regulation of gene expression.(Handbook of Toxicogenomics).
210. Wang, Z., and Burke, P.A. (2010). Hepatocyte nuclear factor-4alpha interacts with other hepatocyte nuclear factors in regulating transthyretin gene expression. FEBS J 277, 4066-4075.
211. Costa, R.H., Van Dyke, T.A., Yan, C., Kuo, F., and Darnell, J.E., Jr. (1990). Similarities in transthyretin gene expression and differences in transcription factors: liver and yolk sac compared to choroid plexus. Proc Natl Acad Sci U S A 87, 6589-6593.
212. Drewes, T., Senkel, S., Holewa, B., and Ryffel, G.U. (1996). Human hepatocyte nuclear factor 4 isoforms are encoded by distinct and differentially expressed genes. Mol Cell Biol 16, 925-931.
213. Wei, C.L., Wu, Q., Vega, V.B., Chiu, K.P., Ng, P., Zhang, T., Shahab, A., Yong, H.C., Fu, Y., Weng, Z., et al. (2006). A global map of p53 transcription-factor binding sites in the human genome. Cell 124, 207-219.
214. Langbehn, D.R., Brinkman, R.R., Falush, D., Paulsen, J.S., and Hayden, M.R. (2004). A new model for prediction of the age of onset and penetrance for Huntington's disease based on CAG length. Clin Genet 65, 267-277.
215. Polimanti, R., Di Girolamo, M., Manfellotto, D., and Fuciarelli, M. (2014). In silico analysis of TTR gene (coding and non-coding regions, and interactive network) and its implications in transthyretin-related amyloidosis. Amyloid 21, 154-162.
216. Lukiw, W.J. (2007). Micro-RNA speciation in fetal, adult and Alzheimer's disease hippocampus. Neuroreport 18, 297-300.
217. Wang, G., van der Walt, J.M., Mayhew, G., Li, Y.J., Zuchner, S., Scott, W.K., Martin, E.R., and Vance, J.M. (2008). Variation in the miRNA-433 binding site of FGF20 confers risk for Parkinson disease by overexpression of alpha-synuclein. Am J Hum Genet 82, 283-289.

218. Sethupathy, P., and Collins, F.S. (2008). MicroRNA target site polymorphisms and human disease. Trends Genet 24, 489-497.
219. Duan, R., and Jin, P. (2006). Identification of messenger RNAs and microRNAs associated with fragile X mental retardation protein. Methods Mol Biol 342, 267-276.
220. Norgren, N., Hellman, U., Ericzon, B.G., Olsson, M., and Suhr, O.B. (2012). Allele specific expression of the transthyretin gene in swedish patients with hereditary transthyretin amyloidosis (ATTR V30M) is similar between the two alleles. PLoS One 7, e49981.
221. Saha, S., Chakraborty, S., Bhattacharya, A., Biswas, A., and Ain, R. (2017). MicroRNA regulation of Transthyretin in trophoblast differentiation and Intra-Uterine Growth Restriction. Sci Rep 7, 16548.
222. Eskildsen, T., Taipaleenmaki, H., Stenvang, J., Abdallah, B.M., Ditzel, N., Nossent, A.Y., Bak, M., Kauppinen, S., and Kassem, M. (2011). MicroRNA-138 regulates osteogenic differentiation of human stromal (mesenchymal) stem cells in vivo. Proc Natl Acad Sci U S A 108, 6139-6144.
223. Wang, X., Tan, L., Lu, Y., Peng, J., Zhu, Y., Zhang, Y., and Sun, Z. (2015). MicroRNA-138 promotes tau phosphorylation by targeting retinoic acid receptor alpha. FEBS Lett 589, 726-729.
224. Cogswell, J.P., Ward, J., Taylor, I.A., Waters, M., Shi, Y., Cannon, B., Kelnar, K., Kemppainen, J., Brown, D., Chen, C., et al. (2008). Identification of miRNA changes in Alzheimer's disease brain and CSF yields putative biomarkers and insights into disease pathways. J Alzheimers Dis 14, 27-41.
225. Lee, S.T., Chu, K., Im, W.S., Yoon, H.J., Im, J.Y., Park, J.E., Park, K.H., Jung, K.H., Lee, S.K., Kim, M., et al. (2011). Altered microRNA regulation in Huntington's disease models. Exp Neurol 227, 172-179.
226. Mellios, N., and Sur, M. (2012). The Emerging Role of microRNAs in Schizophrenia and Autism Spectrum Disorders. Front Psychiatry 3, 39.
227. Moreau, M.P., Bruse, S.E., David-Rus, R., Buyske, S., and Brzustowicz, L.M. (2011). Altered microRNA expression profiles in postmortem brain samples from individuals with schizophrenia and bipolar disorder. Biol Psychiatry 69, 188-193.
228. Alnylam, P.I. (2018). Onpattro (patisiran) lipid complex injection, for intravenous use: US prescribing information. . In. (http://www.fda.gov/, .
229. EU., E.M.A.-E. (2018). Tegsedi International non-proprietary name: inotersen. Assessment report. . In. (
230. Cartegni, L., Chew, S.L., and Krainer, A.R. (2002). Listening to silence and understanding nonsense: exonic mutations that affect splicing. Nat Rev Genet 3, 285-298.
231. Breitbart, R.E., Nguyen, H.T., Medford, R.M., Destree, A.T., Mahdavi, V., and Nadal-Ginard, B. (1985). Intricate combinatorial patterns of exon splicing generate multiple regulated troponin T isoforms from a single gene. Cell 41, 67-82.
232. Hefferon, T.W., Groman, J.D., Yurk, C.E., and Cutting, G.R. (2004). A variable dinucleotide repeat in the CFTR gene contributes to phenotype diversity by forming RNA secondary structures that alter splicing. Proc Natl Acad Sci U S A 101, 3504-3509.
233. Hui, J., Reither, G., and Bindereif, A. (2003). Novel functional role of CA repeats and hnRNP L in RNA stability. RNA 9, 931-936.
234. Hui, J., Stangl, K., Lane, W.S., and Bindereif, A. (2003). HnRNP L stimulates splicing of the eNOS gene by binding to variable-length CA repeats. Nat Struct Biol 10, 33-37.
235. Saridaki, Z., Georgoulias, V., and Souglakos, J. (2010). Mechanisms of resistance to anti-EGFR monoclonal antibody treatment in metastatic colorectal cancer. World J Gastroenterol 16, 1177-1187.
236. Rietveld, I., Janssen, J.A., Hofman, A., Pols, H.A., van Duijn, C.M., and Lamberts, S.W. (2003). A polymorphism in the IGF-I gene influences the age-related decline in circulating total IGF-I levels. Eur J Endocrinol 148, 171-175.
237. Wu, T., Ikezono, T., Angus, C.W., and Shelhamer, J.H. (1994). Characterization of the promoter for the human 85 kDa cytosolic phospholipase A2 gene. Nucleic Acids Res 22, 5093-5098.
238. Borrmann, L., Seebeck, B., Rogalla, P., and Bullerdiek, J. (2003). Human HMGA2 promoter is coregulated by a polymorphic dinucleotide (TC)-repeat. Oncogene 22, 756-760.
239. Wang, B., Ren, J., Ooi, L.L., Chong, S.S., and Lee, C.G. (2005). Dinucleotide repeats negatively modulate the promoter activity of Cyr61 and is unstable in hepatocellular carcinoma patients. Oncogene 24, 3999-4008.
240. Xiang, Q., Bi, R., Xu, M., Zhang, D.F., Tan, L., Zhang, C., Fang, Y., and Yao, Y.G. (2017). Rare Genetic Variants of the Transthyretin Gene Are Associated with Alzheimer's Disease in Han Chinese. Mol Neurobiol 54, 5192-5200.
241. Oshima, T., Kawahara, S., Ueda, M., Kawakami, Y., Tanaka, R., Okazaki, T., Misumi, Y., Obayashi, K., Yamashita, T., Ohya, Y., et al. (2014). Changes in pathological and biochemical findings of systemic tissue

sites in familial amyloid polyneuropathy more than 10 years after liver transplantation. J Neurol Neurosurg Psychiatry 85, 740-746.
242. Sandgren, O., Westermark, P., and Stenkula, S. (1986). Relation of vitreous amyloidosis to prealbumin. Ophthalmic Res 18, 98-103.
243. Suhr, O.B., Wixner, J., Anan, I., Lundgren, H.E., Wijayatunga, P., Westermark, P., and Ihse, E. (2019). Amyloid fibril composition within hereditary Val30Met (p. Val50Met) transthyretin amyloidosis families. PLoS One 14, e0211983.
244. Ihse, E., Ybo, A., Suhr, O., Lindqvist, P., Backman, C., and Westermark, P. (2008). Amyloid fibril composition is related to the phenotype of hereditary transthyretin V30M amyloidosis. J Pathol 216, 253-261.
245. Hachiya, T., Furukawa, R., Shiwa, Y., Ohmomo, H., Ono, K., Katsuoka, F., Nagasaki, M., Yasuda, J., Fuse, N., Kinoshita, K., et al. (2017). Genome-wide identification of inter-individually variable DNA methylation sites improves the efficacy of epigenetic association studies. NPJ Genom Med 2, 11.
246. Oberdoerffer, S. (2012). A conserved role for intragenic DNA methylation in alternative pre-mRNA splicing. Transcription 3, 106-109.
247. Hellman, A., and Chess, A. (2010). Extensive sequence-influenced DNA methylation polymorphism in the human genome. Epigenetics Chromatin 3, 11.
248. Gertz, J., Varley, K.E., Reddy, T.E., Bowling, K.M., Pauli, F., Parker, S.L., Kucera, K.S., Willard, H.F., and Myers, R.M. (2011). Analysis of DNA methylation in a three-generation family reveals widespread genetic influence on epigenetic regulation. PLoS Genet 7, e1002228.
249. Shilpi, A., Bi, Y., Jung, S., Patra, S.K., and Davuluri, R.V. (2017). Identification of Genetic and Epigenetic Variants Associated with Breast Cancer Prognosis by Integrative Bioinformatics Analysis. Cancer Inform 16, 1-13.
250. Jones, P.A., and Baylin, S.B. (2002). The fundamental role of epigenetic events in cancer. Nat Rev Genet 3, 415-428.
251. Belkadi, A., Bolze, A., Itan, Y., Cobat, A., Vincent, Q.B., Antipenko, A., Shang, L., Boisson, B., Casanova, J.L., and Abel, L. (2015). Whole-genome sequencing is more powerful than whole-exome sequencing for detecting exome variants. Proc Natl Acad Sci U S A 112, 5473-5478.
252. Milewicz, D.M., Guo, D.C., Tran-Fadulu, V., Lafont, A.L., Papke, C.L., Inamoto, S., Kwartler, C.S., and Pannu, H. (2008). Genetic basis of thoracic aortic aneurysms and dissections: focus on smooth muscle cell contractile dysfunction. Annu Rev Genomics Hum Genet 9, 283-302.
253. Krendel, M., and Mooseker, M.S. (2005). Myosins: tails (and heads) of functional diversity. Physiology (Bethesda) 20, 239-251.
254. Alhopuro, P., Phichith, D., Tuupanen, S., Sammalkorpi, H., Nybondas, M., Saharinen, J., Robinson, J.P., Yang, Z., Chen, L.Q., Orntoft, T., et al. (2008). Unregulated smooth-muscle myosin in human intestinal neoplasia. Proc Natl Acad Sci U S A 105, 5513-5518.
255. Liu, P., Tarle, S.A., Hajra, A., Claxton, D.F., Marlton, P., Freedman, M., Siciliano, M.J., and Collins, F.S. (1993). Fusion between transcription factor CBF beta/PEBP2 beta and a myosin heavy chain in acute myeloid leukemia. Science 261, 1041-1044.
256. Gauthier, J., Ouled Amar Bencheikh, B., Hamdan, F.F., Harrison, S.M., Baker, L.A., Couture, F., Thiffault, I., Ouazzani, R., Samuels, M.E., Mitchell, G.A., et al. (2015). A homozygous loss-of-function variant in MYH11 in a case with megacystis-microcolon-intestinal hypoperistalsis syndrome. Eur J Hum Genet 23, 1266-1268.
257. Keylock, A., Hong, Y., Saunders, D., Omoyinmi, E., Mulhern, C., Roebuck, D., Brogan, P., Ganesan, V., and Eleftheriou, D. (2018). Moyamoya-like cerebrovascular disease in a child with a novel mutation in myosin heavy chain 11. Neurology 90, 136-138.
258. Khau Van Kien, P., Wolf, J.E., Mathieu, F., Zhu, L., Salve, N., Lalande, A., Bonnet, C., Lesca, G., Plauchu, H., Dellinger, A., et al. (2004). Familial thoracic aortic aneurysm/dissection with patent ductus arteriosus: genetic arguments for a particular pathophysiological entity. Eur J Hum Genet 12, 173-180.
259. Morano, I., Chai, G.X., Baltas, L.G., Lamounier-Zepter, V., Lutsch, G., Kott, M., Haase, H., and Bader, M. (2000). Smooth-muscle contraction without smooth-muscle myosin. Nat Cell Biol 2, 371-375.
260. Zhu, L., Vranckx, R., Khau Van Kien, P., Lalande, A., Boisset, N., Mathieu, F., Wegman, M., Glancy, L., Gasc, J.M., Brunotte, F., et al. (2006). Mutations in myosin heavy chain 11 cause a syndrome associating thoracic aortic aneurysm/aortic dissection and patent ductus arteriosus. Nat Genet 38, 343-349.
261. Poirel, H., Radford-Weiss, I., Rack, K., Troussard, X., Veil, A., Valensi, F., Picard, F., Guesnu, M., Leboeuf, D., Melle, J., et al. (1995). Detection of the chromosome 16 CBF beta-MYH11 fusion transcript in myelomonocytic leukemias. Blood 85, 1313-1322.

262. Gu, W., Hong, X., Le Bras, A., Nowak, W.N., Issa Bhaloo, S., Deng, J., Xie, Y., Hu, Y., Ruan, X.Z., and Xu, Q. (2018). Smooth muscle cells differentiated from mesenchymal stem cells are regulated by microRNAs and suitable for vascular tissue grafts. J Biol Chem 293, 8089-8102.
263. Rossetti, S., Anauo, M.J., and Sacchi, N. (2017). MiR-221-regulated KIT level by wild type or leukemia mutant RUNX1: a determinant of single myeloblast fate decisions that - collectively - drives or hinders granulopoiesis. Oncotarget 8, 85783-85793.
264. Henderson, B.W., Gentry, E.G., Rush, T., Troncoso, J.C., Thambisetty, M., Montine, T.J., and Herskowitz, J.H. (2016). Rho-associated protein kinase 1 (ROCK1) is increased in Alzheimer's disease and ROCK1 depletion reduces amyloid-beta levels in brain. J Neurochem 138, 525-531.
265. Herskowitz, J.H., Feng, Y., Mattheyses, A.L., Hales, C.M., Higginbotham, L.A., Duong, D.M., Montine, T.J., Troncoso, J.C., Thambisetty, M., Seyfried, N.T., et al. (2013). Pharmacologic inhibition of ROCK2 suppresses amyloid-beta production in an Alzheimer's disease mouse model. J Neurosci 33, 19086-19098.
266. Sousa, M.M., do Amaral, J.B., Guimaraes, A., and Saraiva, M.J. (2005). Up-regulation of the extracellular matrix remodeling genes, biglycan, neutrophil gelatinase-associated lipocalin, and matrix metalloproteinase-9 in familial amyloid polyneuropathy. FASEB J 19, 124-126.
267. Stein, T.D., and Johnson, J.A. (2002). Lack of neurodegeneration in transgenic mice overexpressing mutant amyloid precursor protein is associated with increased levels of transthyretin and the activation of cell survival pathways. J Neurosci 22, 7380-7388.
268. Choi, S.H., Leight, S.N., Lee, V.M., Li, T., Wong, P.C., Johnson, J.A., Saraiva, M.J., and Sisodia, S.S. (2007). Accelerated Abeta deposition in APPswe/PS1deltaE9 mice with hemizygous deletions of TTR (transthyretin). J Neurosci 27, 7006-7010.
269. Buxbaum, J.N., Ye, Z., Reixach, N., Friske, L., Levy, C., Das, P., Golde, T., Masliah, E., Roberts, A.R., and Bartfai, T. (2008). Transthyretin protects Alzheimer's mice from the behavioral and biochemical effects of Abeta toxicity. Proc Natl Acad Sci U S A 105, 2681-2686.
270. Alemi, M., Silva, S.C., Santana, I., and Cardoso, I. (2017). Transthyretin stability is critical in assisting beta amyloid clearance- Relevance of transthyretin stabilization in Alzheimer's disease. CNS Neurosci Ther 23, 605-619.
271. Alemi, M., Gaiteiro, C., Ribeiro, C.A., Santos, L.M., Gomes, J.R., Oliveira, S.M., Couraud, P.O., Weksler, B., Romero, I., Saraiva, M.J., et al. (2016). Transthyretin participates in beta-amyloid transport from the brain to the liver--involvement of the low-density lipoprotein receptor-related protein 1? Sci Rep 6, 20164.
272. Silva, C.S., Eira, J., Ribeiro, C.A., Oliveira, A., Sousa, M.M., Cardoso, I., and Liz, M.A. (2017). Transthyretin neuroprotection in Alzheimer's disease is dependent on proteolysis. Neurobiol Aging 59, 10-14.
273. Liz, M.A., Leite, S.C., Juliano, L., Saraiva, M.J., Damas, A.M., Bur, D., and Sousa, M.M. (2012). Transthyretin is a metallopeptidase with an inducible active site. Biochem J 443, 769-778.
274. Zhou, Y., Su, Y., Li, B., Liu, F., Ryder, J.W., Wu, X., Gonzalez-DeWhitt, P.A., Gelfanova, V., Hale, J.E., May, P.C., et al. (2003). Nonsteroidal anti-inflammatory drugs can lower amyloidogenic Abeta42 by inhibiting Rho. Science 302, 1215-1217.
275. Lai, A.Y., and McLaurin, J. (2018). Rho-associated protein kinases as therapeutic targets for both vascular and parenchymal pathologies in Alzheimer's disease. J Neurochem 144, 659-668.
276. Parmacek, M.S. (2007). Myocardin-related transcription factors: critical coactivators regulating cardiovascular development and adaptation. Circ Res 100, 633-644.
277. Hald, E.S., Timm, C.D., and Alford, P.W. (2016). Amyloid Beta Influences Vascular Smooth Muscle Contractility and Mechanoadaptation. J Biomech Eng 138.
278. Wan, L., Huang, J., Ni, H., and Yu, G. (2018). Screening key genes for abdominal aortic aneurysm based on gene expression omnibus dataset. BMC Cardiovasc Disord 18, 34.
279. Ilieva, H., Polymenidou, M., and Cleveland, D.W. (2009). Non-cell autonomous toxicity in neurodegenerative disorders: ALS and beyond. Journal of Cell Biology 187, 761-772.
280. Kaletta, T., and Hengartner, M.O. (2006). Finding function in novel targets: C. elegans as a model organism. Nat Rev Drug Discov 5, 387-398.
281. Alexander, A.G., Marfil, V., and Li, C. (2014). Use of Caenorhabditis elegans as a model to study Alzheimer's disease and other neurodegenerative diseases. Front Genet 5, 279.
282. Dimitriadi, M., and Hart, A.C. (2010). Neurodegenerative disorders: insights from the nematode Caenorhabditis elegans. Neurobiol Dis 40, 4-11.
283. Wittenburg, N., and Baumeister, R. (1999). Thermal avoidance in Caenorhabditis elegans: an approach to the study of nociception. Proc Natl Acad Sci U S A 96, 10477-10482.

284. Liu, S., Schulze, E., and Baumeister, R. (2012). Temperature- and touch-sensitive neurons couple CNG and TRPV channel activities to control heat avoidance in Caenorhabditis elegans. PLoS One 7, e32360.
285. Sousa, M.M., and Saraiva, M.J. (2001). Internalization of transthyretin. Evidence of a novel yet unidentified receptor-associated protein (RAP)-sensitive receptor. J Biol Chem 276, 14420-14425.
286. Fares, H., and Greenwald, I. (2001). Genetic analysis of endocytosis in Caenorhabditis elegans: coelomocyte uptake defective mutants. Genetics 159, 133-145.
287. Sun, T., Wang, X., Lu, Q., Ren, H., and Zhang, H. (2011). CUP-5, the C. elegans ortholog of the mammalian lysosomal channel protein MLN1/TRPML1, is required for proteolytic degradation in autolysosomes. Autophagy 7, 1308-1315.
288. Makover, A., Moriwaki, H., Ramakrishnan, R., Saraiva, M.J., Blaner, W.S., and Goodman, D.S. (1988). Plasma transthyretin. Tissue sites of degradation and turnover in the rat. J Biol Chem 263, 8598-8603.
289. Nonboe, A.W., Krigslund, O., Soendergaard, C., Skovbjerg, S., Friis, S., Andersen, M.N., Ellis, V., Kawaguchi, M., Kataoka, H., Bugge, T.H., et al. (2017). HAI-2 stabilizes, inhibits and regulates SEA-cleavage-dependent secretory transport of matriptase. Traffic 18, 378-391.
290. Bandah-Rozenfeld, D., Collin, R.W., Banin, E., van den Born, L.I., Coene, K.L., Siemiatkowska, A.M., Zelinger, L., Khan, M.I., Lefeber, D.J., Erdinest, I., et al. (2010). Mutations in IMPG2, encoding interphotoreceptor matrix proteoglycan 2, cause autosomal-recessive retinitis pigmentosa. Am J Hum Genet 87, 199-208.
291. Whittaker, C.A., and Hynes, R.O. (2002). Distribution and evolution of von Willebrand/integrin A domains: widely dispersed domains with roles in cell adhesion and elsewhere. Mol Biol Cell 13, 3369-3387.
292. Tuckwell, D. (1999). Evolution of von Willebrand factor A (VWA) domains. Biochem Soc Trans 27, 835-840.
293. Ariga, T., Miyatake, T., and Yu, R.K. (2010). Role of proteoglycans and glycosaminoglycans in the pathogenesis of Alzheimer's disease and related disorders: amyloidogenesis and therapeutic strategies--a review. J Neurosci Res 88, 2303-2315.
294. Hill, R. (2009). Extracellular matrix remodelling in human diabetic neuropathy. J Anat 214, 219-225.
295. Palumbo, C., Massa, R., Panico, M.B., Di Muzio, A., Sinibaldi, P., Bernardi, G., and Modesti, A. (2002). Peripheral nerve extracellular matrix remodeling in Charcot-Marie-Tooth type I disease. Acta Neuropathol 104, 287-296.
296. Coimbra, A., and Andrade, C. (1971). Familial amyloid polyneuropathy: an electron microscope study of the peripheral nerve in five cases. II. Nerve fibre changes. Brain 94, 207-212.
297. Cardoso, I., Brito, M., and Saraiva, M.J. (2008). Extracellular matrix markers for disease progression and follow-up of therapies in familial amyloid polyneuropathy V30M TTR-related. Dis Markers 25, 37-47.
298. Misumi, Y., Ando, Y., Ueda, M., Obayashi, K., Jono, H., Su, Y., Yamashita, T., and Uchino, M. (2009). Chain reaction of amyloid fibril formation with induction of basement membrane in familial amyloidotic polyneuropathy. J Pathol 219, 481-490.
299. Akasaki, Y., Reixach, N., Matsuzaki, T., Alvarez-Garcia, O., Olmer, M., Iwamoto, Y., Buxbaum, J.N., and Lotz, M.K. (2015). Transthyretin deposition in articular cartilage: a novel mechanism in the pathogenesis of osteoarthritis. Arthritis Rheumatol 67, 2097-2107.
300. Carlson, G.A., Borchelt, D.R., Dake, A., Turner, S., Danielson, V., Coffin, J.D., Eckman, C., Meiners, J., Nilsen, S.P., Younkin, S.G., et al. (1997). Genetic modification of the phenotypes produced by amyloid precursor protein overexpression in transgenic mice. Hum Mol Genet 6, 1951-1959.